ASSESSMENT OF RIVERBED CHANGE DUE TO THE OPERATION OF A SERIES OF GATES IN A NATURAL RIVER

A Thesis

by

ZOOHO KIM

Submitted to the Office of Graduate Studies of
Texas A&M University
in partial fulfillment of the requirements for the degree of

MASTER OF SCIENCE

Approved by:

Chair of Committee,	Vijay P. Singh
Committee Members,	Ralph A. Wurbs
	Patricia K. Smith
Head of Department,	Stephen W. Searcy

May 2013

Major Subject: Biological Agricultural Engineering

ABSTRACT

Changes in the bed of Geum River (L=130 km from Daechung regulation dam to Geum River estuarial bank) in South Korea were predicted using the 1-D HEC-RAS model and the 2-D CCHE2D model. Three movable weirs have been installed and dredging has been carried out in Geum River under the Four Major Rivers Restoration Project (2009-2012).

Inflow data of sub basins were calibrated with daily runoff data generated by PRMS based on a hydrologic unit map. To determine the gate opening height for maintaining the management water level, unsteady analysis was performed using HEC-RAS. Thereafter, long-term riverbed changes through quasi-unsteady analysis were simulated for 20 years. In order to investigate the effect of movable weirs, sediment analysis was done for three cases of gate opening: case 1 is fully close, case 2 is fully open, and case 3 is regulating gates by the operating rule. Also, short-term riverbed changes were predicted with CCHE2D for 11 days in the problem area, depending on the results of 1-D model, and the effect of dikes was examined.

In future, gate operation and structural methods such as dikes must be in step with each other in order to manage sediment and rivers in an ecofriendly manner.

TABLE OF CONTENTS

LIST OF FIGURES

LIST OF TABLES

1. INTRODUCTION

The utilizable volume of water resources in South Korea is only 27 % of the available total and the annual average precipitation of South Korea is 1,341 mm which is more than the 880 mm world average, but the total amount of water available per capita in a year is approximately 13 % of the world average. The flow variation in Korea is large. About 2/3 of the annual rainfall occurs during the rainy season (June-September). Floods and droughts often occur and are being accentuated by climate change. A lot of money has been spent on restoration than on flood amelioration. Water shortages have become common and pollution has been on the rise. To address floods, droughts, and other water-related problems, a large water resources plan entitled "The Four Major Rivers Restoration Project," was created. This project was estimated to cost $17.3 billion over the period June 2009-December 2012. The Four Major Rivers Restoration Project, shown in Figure 1, is a comprehensive, pan-governmental project. It represents the plan made by several Korean governmental ministries and a commitment to work together in order to restore 929 km of Korea's national rivers, the Han, the Nakdong, the Geum, and the Yeongsan. The project envisions dredging (450 million m^3), reinforcing old levees (620 km), construction weirs (16 sites), elevating reservoir banks (96 sites), creation of bicycle roads (1,592 km), and restoration of ecologically healthy streams. River management construction was finished in December, 2011.

The expectations of the project are classified into 5 categories: 1) mitigating water scarcity by securing abundant water resources, 2) implementing comprehensive

flood control measures, 3) improving water quality and restoring the ecosystem, 4) creating multipurpose spaces for local residents, and 5) regional development centered on rivers.

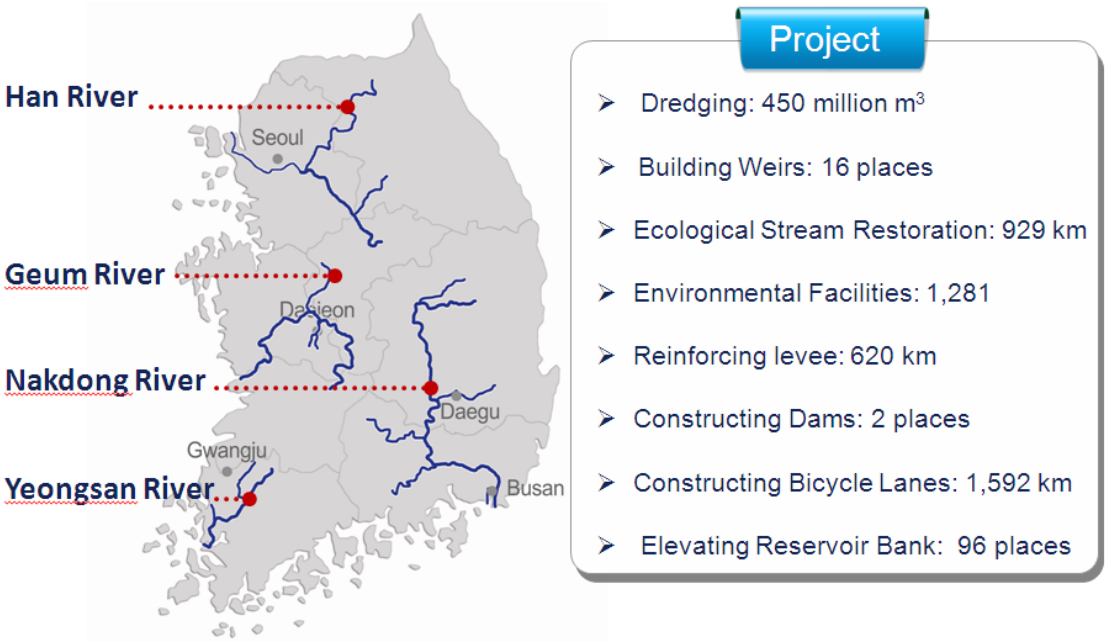

Figure 1. Map of the Four Major Rivers Restoration Project

Sediment plays an important role in maintaining the ecosystem in a river, but its effect through the project has not been fully quantified. Thus, when the project is finished, it is important to evaluate its role. In other words, analyzing the effect of the project on riverbed change and determining proper management is vital for maintaining a sound ecosystem.

Weirs installed in the project are movable weirs, as shown in Figure 2. But they have been designed to control flood damage and secure water resources. Therefore, it is

important to investigate how many movable weirs affect riverbed change, since sediment analysis is important for river management.

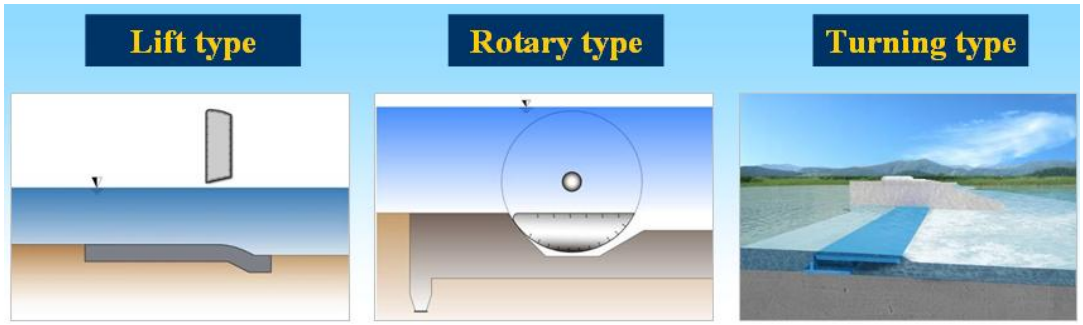

Figure 2. Movable Weirs Installed in the Four Major Rivers

In the Four Major Rivers Restoration Project, the target of the weirs is to maintain the water level to enlarge water resources through closing and opening gates without flood damage. Therefore, it is important to regulate gate opening depending on the flow situation. In this study, the actual gate operation rule was applied to unsteady analysis in HEC-RAS for managing the water level, and proper gate opening at each time step was considered to predict the riverbed change by quasi-unsteady analysis of the 1-D model and unsteady analysis of the 2-D model. HEC-RAS (1-D) model was used to predict river bed changes by gate operation. In 2008, the essential features of HEC-6 were incorporated into HEC-RAS, so one can simultaneously calculate sediment transport using hydraulic results reflecting the gate operation.

This study analyzed the long-term and short-term riverbed changes using a numerical model depending on the influence of gate operation on sediment transport in

the Geum River. The objectives of this study included: 1) predicting the riverbed change in the long term and short term through extensive dredging; 2) analyzing the effect of gate operation on river bed changes; and 3) suggesting measures to mitigate serious erosion or deposition.

To accomplish the above objectives, the following tasks were performed:

1. Collect data on geometry, sediment, rating curve, discharge & sediment loads.
2. Determine gate opening height to keep proper water level in HEC-RAS (1-D) model.
3. Predict long-term riverbed changes and analyze the impact of gate operation on sediment transport.
4. Build a mesh in the problem section due to the 1-D model results.
5. Develop the CCHE2D (2-D) model and predict short term riverbed change.
6. Suggest structural measures in problem sections for sustaining ecofriendly streams.

This study assessed quantitatively the effect of gate operation on sediment transport by predicting long term riverbed change (1D) and suggest a river management method to secure river safety (dike installation: 2D) which can be beneficial for designing a river management plan, including the ecosystem.

2. LITERATURE REVIEW

The study of riverbed change is essential for maintaining ecofriendly surroundings, such as habitat for aquatic biota. Such sediment movement is complex, because it is affected by sediment distribution, hydraulic conditions, sediment concentration, etc. As a result, numerical analyses using models has been applied for river management. Changes in river morphology also occurred because of human activities, such as dikes, dams, weirs, dredging, etc. Among these, the operation of gates directly affects riverbed change as well as flow, because gates control whether inflow and sediment pass downstream or not. In most cases, the effects of gate operation have been confined to flood control and water supply, though it plays an important role in the ecosystem. Therefore, the study of impacts of gate operation in a natural river system is important for water resources management.

2.1 Impact of sediment on habitat

One of the major issues in river management is to maintain sustainable natural ecosystems. The habitat is affected by the stability of the channel. Also, many hydraulic and geomorphologic techniques have been used for the determination of bed stability in rivers. Schwendel et al. (2010) classified major characteristics of bed stability into shear stress, substratum entrainment, erosion and deposition, bed load transport, and abrasion by suspended sediments, and assessed methods for each item. They argued that bed shear stress plays an important role in channel stability. Also, they mentioned recent

technological advances, such as acoustic and electronic sensors, active tracer particles and topographic survey methods, let observation of riverbeds be conducted in detail. Therefore, they would be beneficial for the examination of stability-biota relationships.

Bilotta et al. (2008) examined how much suspended solids (SS) affected water quality and aquatic life, in respect of the concentration of SS, the duration period of SS concentrations, the chemical ingredients of SS, and the particle-size distribution of SS. Also, they searched water quality guidelines for several of suspended solids in freshwater systems, and then they mentioned several improvements need to be done to the present guidelines. They argued that SS must be based on the turbidity records to make a meaningful correlation between SS and turbidity, also SS should be investigated, reflecting their particle-size distribution and chemical component

On the other hand, Jones et al. (2012) examined the effect of fine suspended sediments on the macro-invertebrates and concluded that it would be meaningful for the introduction of fine sediments to add to water quality guidelines.

As seen above, suspended and bedload sediment have much impact on the ecological system, and it is therefore important to predict riverbed change quantitatively for an ecofriendly water management plan.

2.2 Models for riverbed change

As computer technology has been developed, numerical models have become universal tools for investigating flow and sediment transport in open channels. One-dimensional models demand small amount of field data, and the numerical schemes,

which are needed for calculating, then let computation be more stable than two-dimensional and three-dimensional models. Two-dimensional and three-dimensional models can conduct flow analysis and sediment transport calculation in limited natural river, because of the computing time demanded and the vast of field data for calibration and verification.

Papanicolaou et al. (2008) compared the characteristics of existing 1-D, 2-D, and 3-D models. They suggested that current many models have their advantages and weakness for their applications, so sediment transport models with hydrodynamic movement would be needed.

HEC-RAS has been commonly used to address the hydraulic issues in the engineering field. The essential features of HEC-6 were incorporated into HEC-RAS in 2008, so we can simultaneously simulate the sediment transport with hydraulic results. Furthermore, HEC-RAS model provides useful user interfaces for one dimensional sediment transport modeling. HEC-RAS has assumed the quasi-unsteady flow, although a spatial and temporal lag occurs between flow movement and sediment transport rate in unsteady flow.

Hummel and Duan (2011) used HEC-RAS 4.1 model in predicting sediment transport in dry land streams in Arizona. A sediment analysis was made on the Pantano Wash and Rincon Creek which is one of its tributaries in Tucson, Arizona. Comparing the Ackers-White, Engelund-Hansen, Laursen, and Toffaleti method, they recommended that Yang's method would be most desirable for modeling rivers in a semi-arid ephemeral stream system, such as the Pantano Wash.

Noting that structural methods, including flood protection banks along the Mississippi River, have deprived the Louisiana coast of vast amount of sediment, Pereira et al. (2009) assessed sediment transport for the restoration of the Louisiana coast by HEC-RAS 4.0 and found that the Engelund-Hansen formula gave the best results when compared with the USGS field observations.

The HEC-RAS 4.1 can simulate hydraulics by various gate operations in unsteady flow and predict transport sediment due to various gate operations in quasi-unsteady flow. Therefore, it was chosen for 1-dimensional modeling for this study.

HEC-RAS is suitable for long-term riverbed change because it treats equilibrium state, though cannot explain the temporal and spatial lags between flow and sediment transport. Nonequilibrium phenomena mainly happen in natural rivers, so 2-dimensional habitat modeling treating nonequilibrium state is becoming necessary these days, because eco-hydraulic information in longitudinal and lateral dimensions in rivers and wetlands is essential for habitat evaluation, in particular in habitat restoration projects. Most analytical models for river restoration are based on hydrological and hydraulic factors, such as water depth, velocity, and shear stress for aquatic ecosystems. However, habitat suitability is also affected by many biological factors needed for living, such as water quality, temperature, and dissolved oxygen.

CCHE2D (National Center for Computational Hydroscience and Engineering's Two-Dimensional (2D) Model) is a depth-averaged 2D model for flow, sediment transport, water quality, and ecology in aquatic systems (Wu, 2004). This model was developed by National Center for Computational Hydroscience and Engineering,

University of Mississippi, and provides an integrated package which is consisted of a mesh generator (CCHE2D Mesh Generator) and a Graphical User Interface (CCHE2D-GUI). Also, many studies have shown the applicability of CCHE2D for addressing the sediment problems.

He et al. (2009) used CCHE2D model to examine how much large wood structures affected the flow, sediment transport, riverbed change, and fish surroundings in the Little Topashaw Creek (L=2 km), North Central Mississippi. Five structures made of trees were put in the study area. Habitat assessment for two fish species, blacktail shiner and largemouth bass, were conducted using before and after the large wood structure (LWS) construction and as a result of that, both fish species were increased in case of the LWS installation. In other words, LWS had a positive effect on fish habitat.

Scott and Jia (2006) demonstrated CCHD2D model capability for addressing sediment transport problems in the Mississippi (L=25 miles). The quasi-unsteady simulation in CCHE2D option was used to simulate long-term analysis. Evaluation of sedimentation in the point bar dike for a ten-year period of record flow was conducted in the Catfish point reach (L=25 miles) and the effect of a series of dikes were constructed to reduce dredging in the Redeye Crossing reach (L=5.5 miles).

2.3 Impact of gate operation

Sedimentation in rivers and reservoirs is caused by the conveyance of water and is part of the natural dynamics of alluvial river systems. Since the mobility and transport of sediments in the downstream river are directly related with the reservoir release, the

determination of optimal releases is significant in the analysis. As a result, additional bed changes can be caused from gate operation with dams.

Ding and Wang (2012) investigated the effect of operating a single floodgate on flood control and the effect of three floodgates on flood flow and sediment transport. They tested optimal flood control by a single floodgate and three floodgates in a 10 km long alluvial channel for the optimal solutions. First, only one flood gate was installed 7 km downstream. An operation through the flood water withdrawal caused the erosion on the upstream reach of the floodgate according to the increased flow by the withdrawal, as well as the deposition on its downstream according to the decrease of downstream flow. Second, they applied this system to the operation of three floodgates. When considering the results by the single floodgate, they found the regulated stages by three flood gates were more stable and the riverbed was also less altered. In other words, results showed the multiple floodgates are beneficial for the riverbed change as well as flow.

Tena et al. (2012) assessed impacts of a flushing flow from dams in the lower Ebro River (L=12 km) on the riverbed using CCHE2D. Results showed erosion happened by 30 mm, 4 km downstream of the dam and the flushing flow did not cause severe riverbed change.

Also, Nicklow and Mays (2000) developed an optimal control methodology that minimizes the change of sediment in river networks with multiple-reservoir and applied to the Yazoo River basin in northwest Mississippi.

Also, using a HEC-RAS user-defined rule operation technique, New Jersey Department of Environmental Protection (2012) evaluated the downstream effects due to the operation of the Pompton Lakes Dam Floodgate Facility in New Jersey. The floodgates on the Pompton Lake Dam are regulated to maintain an elevation in Pomton Lake. If the lake level is higher than 0.25 ft. above the set point elevation, the gates plan to be opened 0.25 ft.; if the lake level is higher than 0.5 ft. above the set point elevation, the gates are operated to be opened 0.5 ft.; if the lake level is higher than 1.0 ft. above the set point elevation, the gates are worked to be opened 1.0 ft. by the operation rule curve.

Using a HEC-RAS E.C.G (Elevation Controlled Gate) technique and a Rule Operation technique, Hwang (2010) reviewed the effect of the operation of the Chungju dam in South Korea on the water level at the main points downstream. The E.C.G. technique showed a water level lessened only in the upstream or downstream of Chungju dam, whereas the results by the rule operation technique showed a decreased water level happened at many sections of Chungju dam.

In the Lower River Murray, Australia, 10 low-level weirs were constructed in 1922-1935. The weirs were designed originally to improve the efficiency of navigation, but are now operated to maintain a constant water level. Daily stage fluctuations were caused from weir operations and a stepped gradient happened in the channel, as a result of deposition and erosion (Walker and Thoms, 1993).

When searching for many researches, it is meaningful to examine the impact of riverbed change by gates which were installed in natural rivers and maintained by certain operational rules.

2.4 Countermeasures for preventing sediment

To maintain or restore a river's habitat diversity, different nonstructural and structural approaches have been proposed. Ercan and Younis (2009) examined the prediction of bank erosion in a reach of the Sacramento River. The maximum erosion rate was predicted to be 5.6 m/year in case of no-groyne and 4.7 m/year in case of four-groyne in the right bank of the river. Therefore, he mentioned the groyne structures would be beneficial for considerably reducing bank erosion where they are located, whereas they also passed down safety of the bank erosion.

Dargahi (2008) examined how to address the sedimentation problems in the lower reach of the River Klarälven where is divided into two channels. He investigated the influence of five different river training methods, which involved water level control, groynes, guide walls, vanes and local river bed protection, through a two dimensional depth-averaged model (CCHE2D) to increase the transport sediment capacity of the west channel. He suggested that gate and the utilization of groynes or vanes were beneficial for the addressing the sediment problems. Bhuiyan et al. (2007) studied the effect of W-weir on the riverbed and anticipated it would contribute to the plan of river management. Duan and Nanda (2006) developed a two-dimensional model to assess the effect of a groyne on suspended sediment at the confluence of Kankakee and Iroquois Rivers in Illinois. They examined that short dikes at the confluence reduced the concentration of

the suspended sediment, whereas longer dikes increased the sediment concentration at the confluence because they prevented the flow movement.

In the Four Major Rivers Restoration Project, management water level is set, so gates are supposed to operate for maintaining the management water level (The Four Major Rivers Restoration Master Plan, 2009). If the water level were higher than the management water level, the land near river would be flooded. On the other hand, if the water level were lower than the management water level, the intake of water for livelihood and agricultural use would have difficulty.

Literature review shows that gate operation influences sediment deposition and transport. Therefore, it is necessary to investigate quantitatively how much gates affect sediment as well as enlarge water resources, depending on gate operation, because it is important to manage Geum River in the future.

HEC-RAS 4.1 was used to simulate long-term riverbed change in the equilibrium state, because it can control gate operation to maintain certain water level in unsteady flow and predict riverbed change in quasi-unsteady flow according to the gate opening height. Also, CCHE2D was used to predict short-term riverbed change in non-equilibrium state including dike's impact on addressing sediment problems for actually river management. Of course, it is important to operate weirs in connection with upper dam operation. But this study aims to predict riverbed changes due to gate operation focusing on the management water level.

3. DATA COLLECTION

This chapter discusses input data which are used for simulation by 1-D and 2-D models. Data on cross section, inflow, water level, structures (weirs and bridges), and Manning's coefficients are necessary for hydraulic calculations; and data on sediment size distribution, sediment discharge, and temperature are used for simulating riverbed change. Most of the data are based on the Geum River Management Basin Plan (Daejeon Regional Construction Management Administration, 2009), Four Major Rivers Restoration Project Master Plan (Ministry of Land, Transport and Maritime Affairs, 2009), and observed data (water level, flow) were obtained from the WAter Management Information System (WAMIS), as shown in Table 1.

Table 1. Input Data for Modeling

Type	Reference	Year	Administrator
Hydrologic unit map	WAMIS (http://www.wamis.go.kr)	-	Ministry of Land. Transport and Maritime Affairs
Geometric data	Geum River Management Basic Plan	2009	Daejeon Regional Construction Management Administration
Bridge	"	"	"
Weir (gates)	"	"	"
Flow data	WAMIS (http://www.wamis.go.kr)	-	Ministry of Land. Transport and Maritime Affairs
Water level	"	"	"
Manning coefficient (n)	Geum River Management Basic Plan	2009	Daejeon Regional Construction Management Administration
Bed material	Geum River Management Basic Plan Geum River Actual Design Plan	2009	Daejeon Regional Construction Management Administration
Temperature	http://www.kma.go	-	Metrological Administration

3.1 Hydrologic unit map

Geum River has a length of 398 km and a drainage area of 9,912 ㎢ and there are two multi-purpose dams (Yongdam Dam and Daechung Dam). The study watershed is about 130 km (area: 5,713 ㎢) from Daechung Regulation Dam (about 5 km downstream from Daechung Dam) to Geum Estuary. The tributary and the remaining basin inflow are necessary to calculate the total water resources of Geum River. Therefore, sub basin inflows were obtained by adjusting model values to observed data. In Korea, many hydrologic and hydraulic data are provided, based on water resources unit map in WAMIS (Water Management Information System), which is maintained by the Ministry of Land, Transport and Maritime Affairs. Geum River is composed of 78 watershed areas and 46 watershed areas are included in this study, as shown in Figure 3. Detail description of study area can be seen in Figure 4.

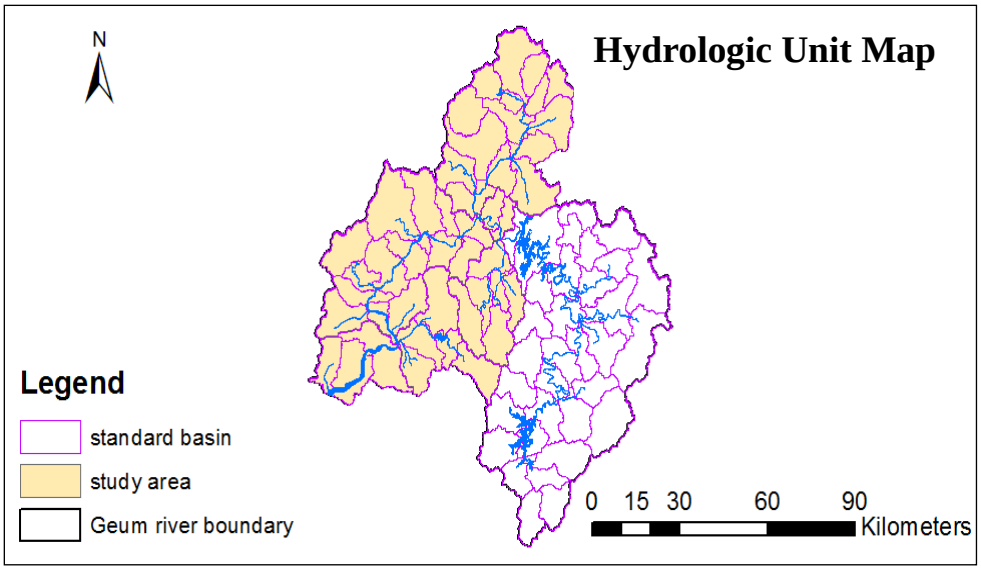

Figure 3. Hydrologic Unit Map in Geum River

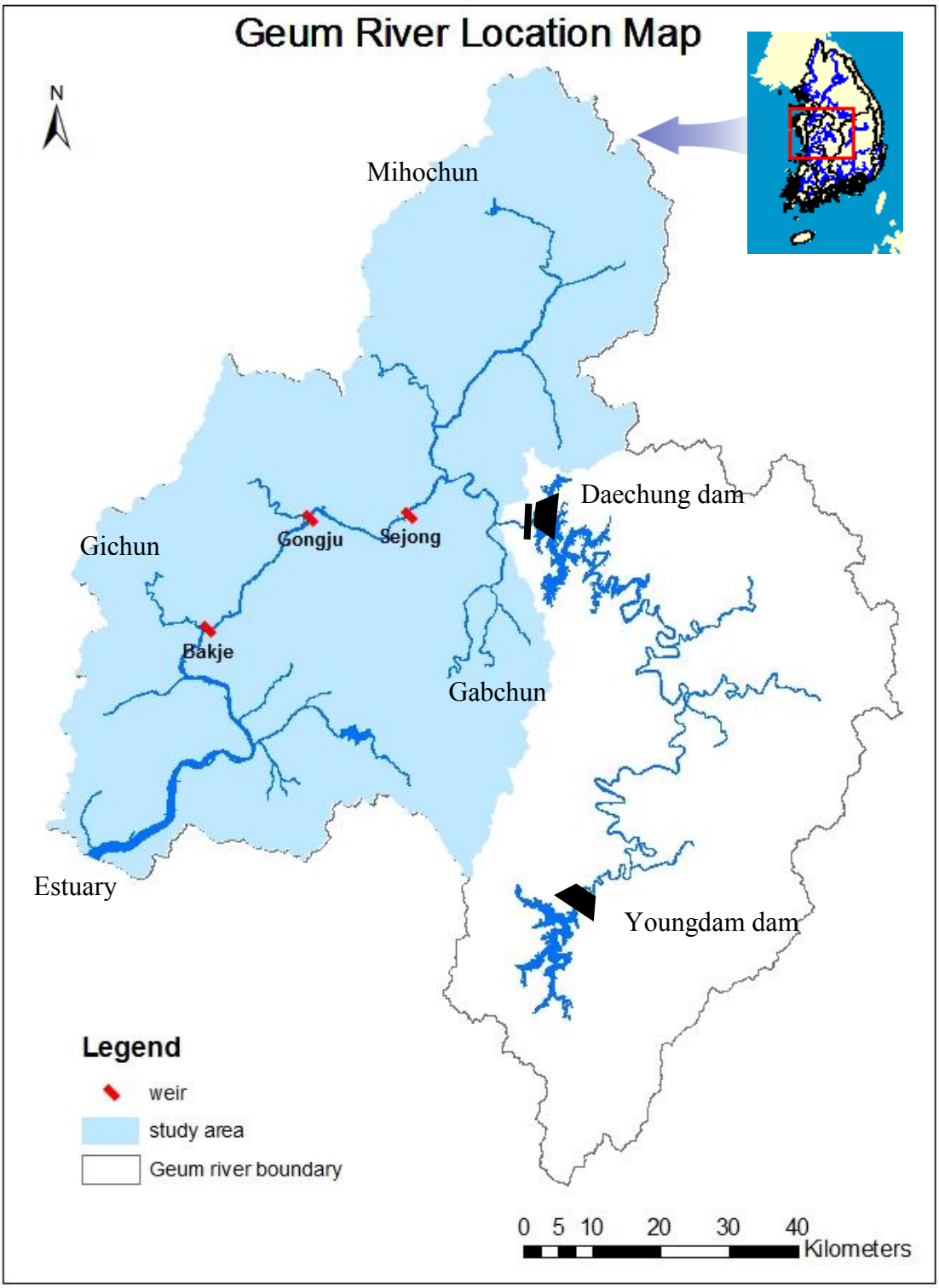

Figure 4. Location Map

3.2 Geometric data (cross section, bridge, and weir)

The length of the river is about 130 km and the spatial interval of cross section is 100~1,000 m. Two types of cross section data were used. One type is the measured data in 2008 before the Four Major Rivers Restoration Project and the other is the planned cross section after Four Major Rivers Restoration Project, as shown in Figure 5.

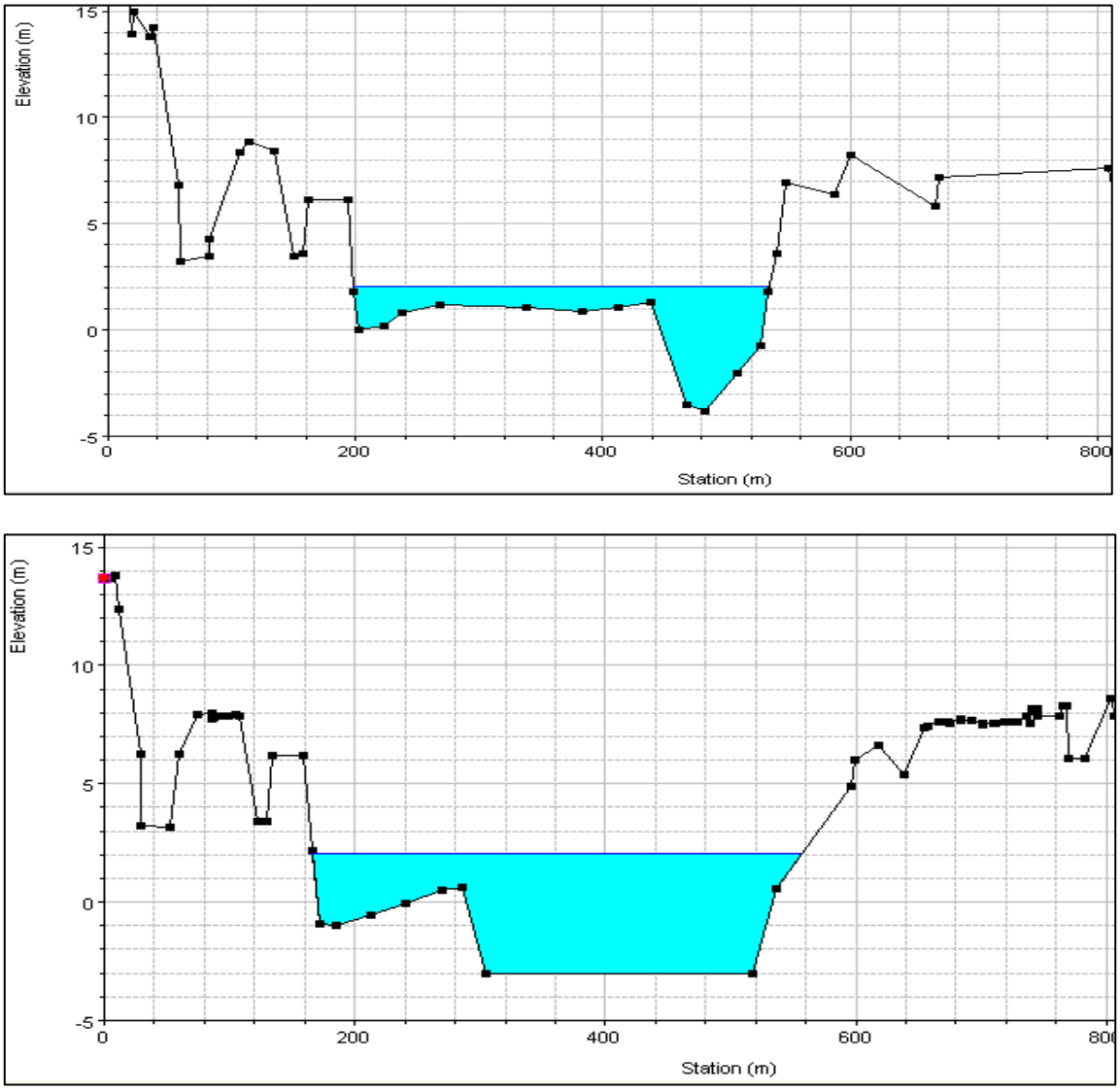

Figure 5. Cross Section of Station No. 55.32 (up: before, down: after)

There are 23 bridges in the study area, as shown in Figure 6 and 7. Though Gongju weir and Bakje weir have bridges together, it was assumed that the bridges were not installed in the weir, since HEC-RAS does not simulate simultaneously both weir and bridge.

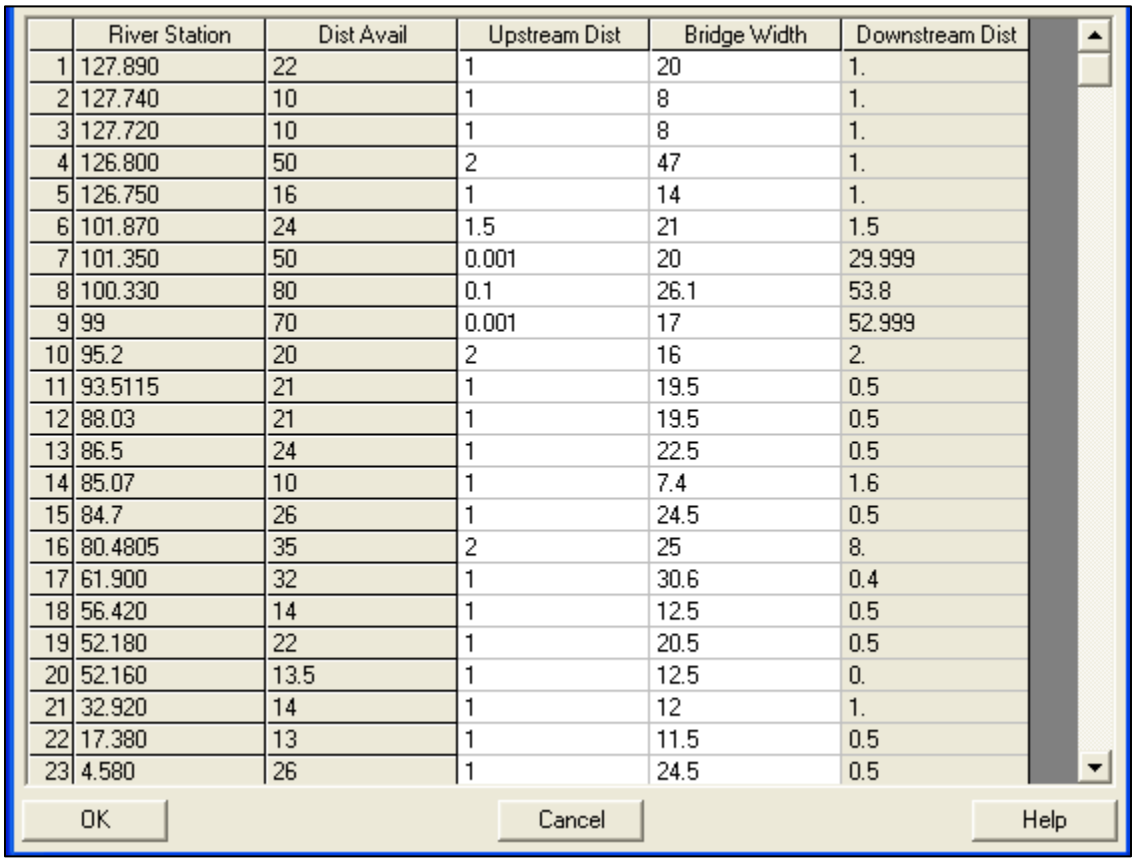

	River Station	Dist Avail	Upstream Dist	Bridge Width	Downstream Dist
1	127.890	22	1	20	1.
2	127.740	10	1	8	1.
3	127.720	10	1	8	1.
4	126.800	50	2	47	1.
5	126.750	16	1	14	1.
6	101.870	24	1.5	21	1.5
7	101.350	50	0.001	20	29.999
8	100.330	80	0.1	26.1	53.8
9	99	70	0.001	17	52.999
10	95.2	20	2	16	2.
11	93.5115	21	1	19.5	0.5
12	88.03	21	1	19.5	0.5
13	86.5	24	1	22.5	0.5
14	85.07	10	1	7.4	1.6
15	84.7	26	1	24.5	0.5
16	80.4805	35	2	25	8.
17	61.900	32	1	30.6	0.4
18	56.420	14	1	12.5	0.5
19	52.180	22	1	20.5	0.5
20	52.160	13.5	1	12.5	0.
21	32.920	14	1	12	1.
22	17.380	13	1	11.5	0.5
23	4.580	26	1	24.5	0.5

Figure 6. Location of Bridges

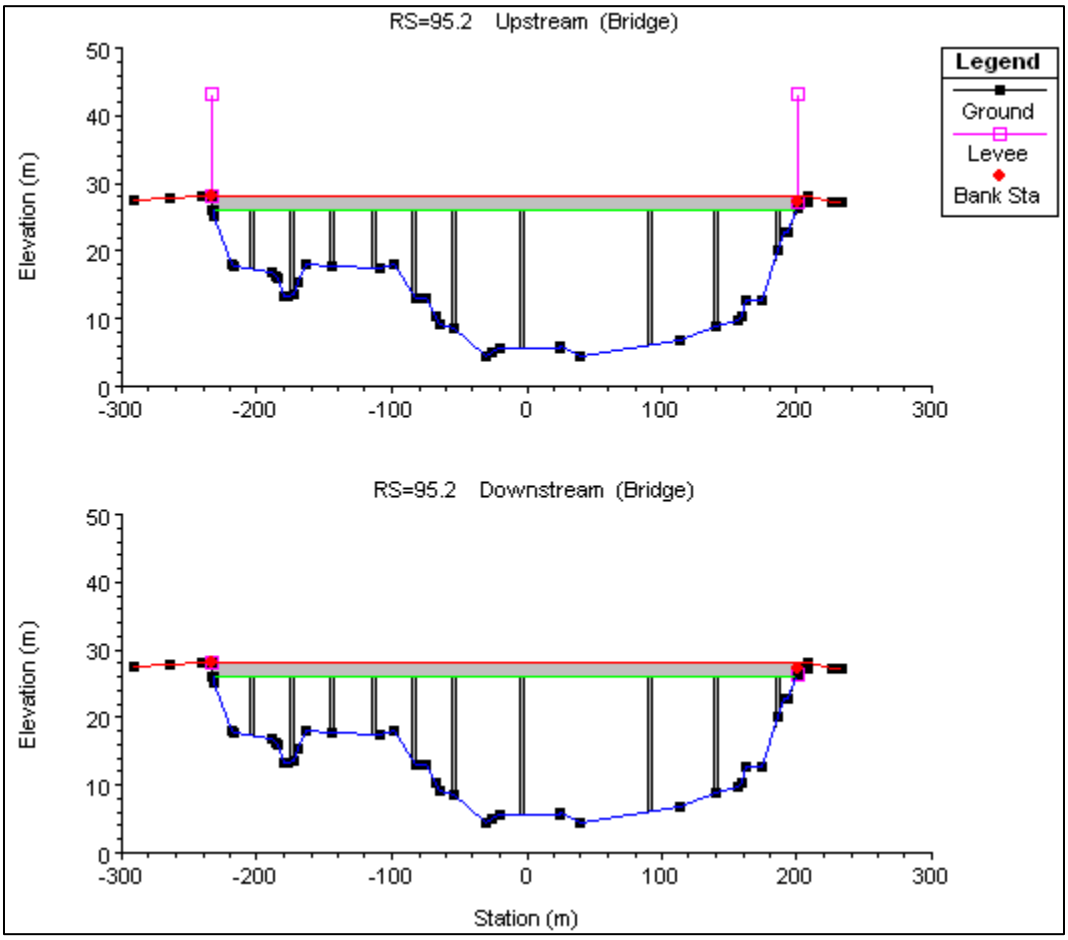

Figure 7. Example of Bridges Profiles

There are three weirs installed in Geum River. Sejong weir has flap gates, so they were applied to the “overflow in air” type. Gongju weir and Bakje weir have lifted type gates, so they were applied to “sluice” type in the HEC-RAS model, as shown in Figures 8 to10.

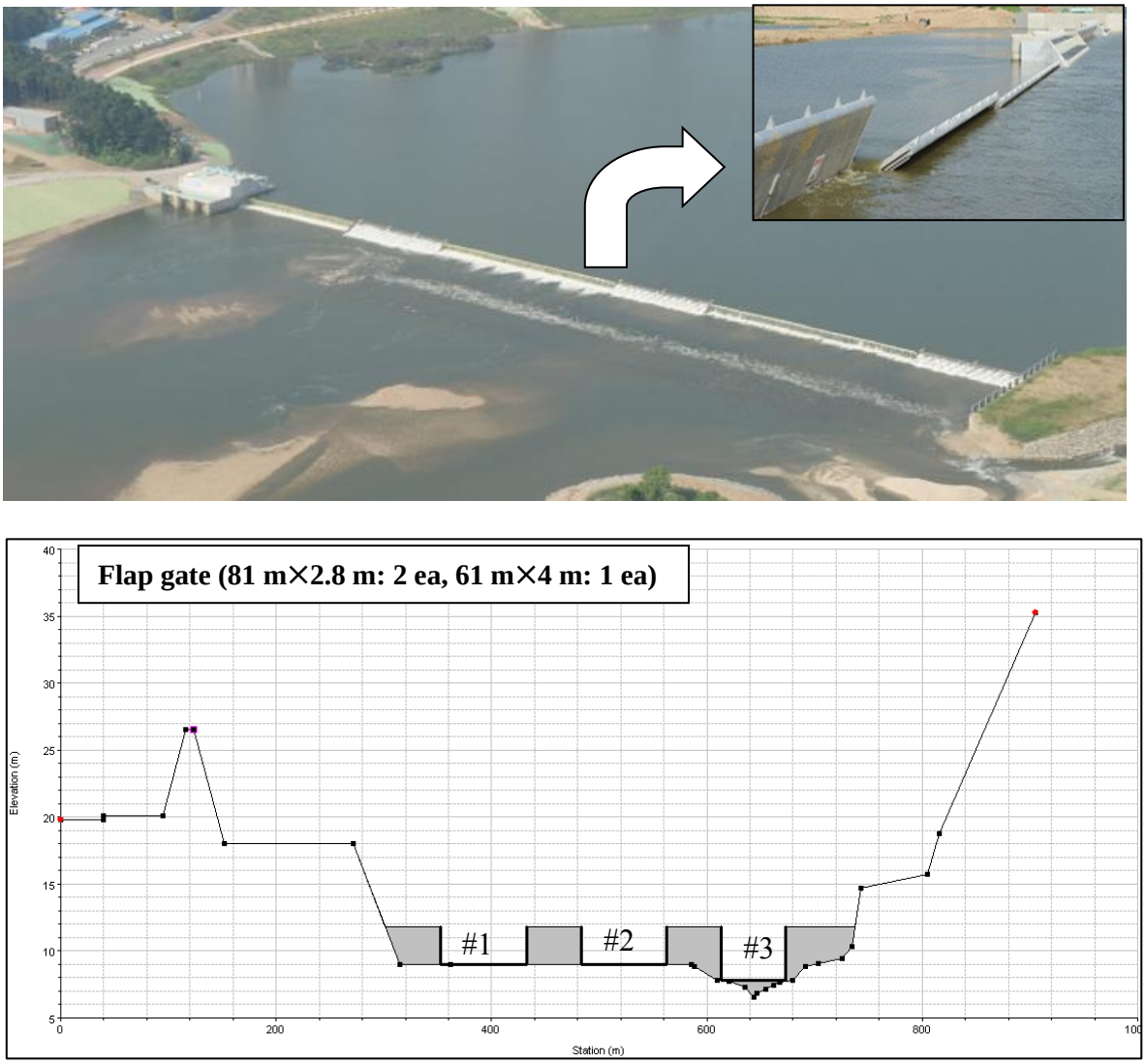

Figure 8. Input Data of Sejong Weir in HEC-RAS (Station No 100.655)

Figure 9. Input Data of Gongju Weir in HEC-RAS (Station No 81.72)

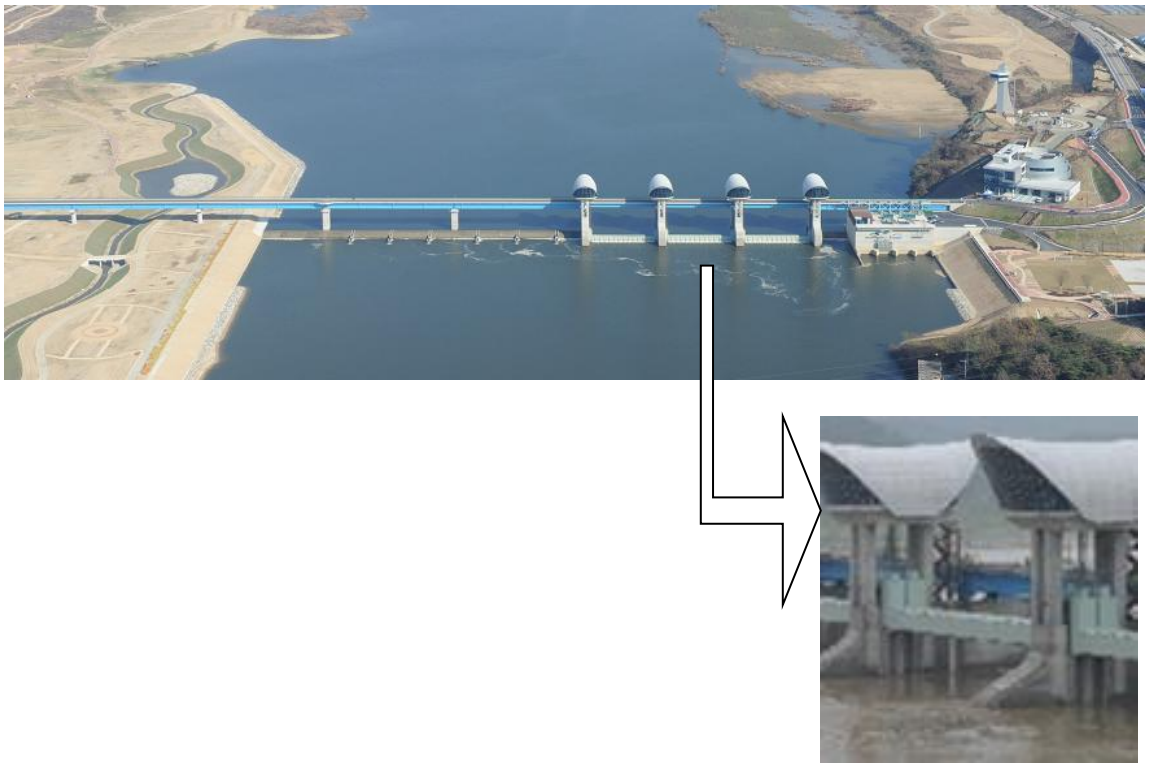

Figure 10. Input Data of Bakje Weir in HEC-RAS (Station No 58.789)

3.3 Flow data

The study area was divided into 22 sub basins, including tributary and residual watersheds based on hydrologic map. Observed flow data of Daechung Regulation Dam were used and lateral inflows were assembled through calibrating PRMS (Precipitation Runoff Modeling System) with observations from Gongju and Gyuam stations. The procedure involves the following steps:

a) collect a representative rainfall event;
b) collect runoff data based on hydrologic unit;
c) collect the stage-discharge curve and the water level of Gongju and Gyuam stations;
d) calibrate each standard basin with observations from Gongju and Gyuam stations; and
e) assemble the above data into 22 sub basins, as shown in Table 3.

Most of all, it is necessary to choose rainfall events to show the characteristics of study area well. The flow duration curve at Gongju station, which is the main control point in Geum River, was plotted, as shown in Figure 11 for recent 3 years (2006-2008) and was compared with the flow duration curve calculated for 1982-2007 in the Geum River Management Basin Plan (Daejeon Regional Construction Management Administration, 2009), as shown in Table 2. As a result, the inflow event assumed in 2006-2007 rainfall events represented the characteristics of Gongju station well. Therefore, the assumed inflow event in 2006-2007 happened repeatedly during the simulation period (20 years) in this study.

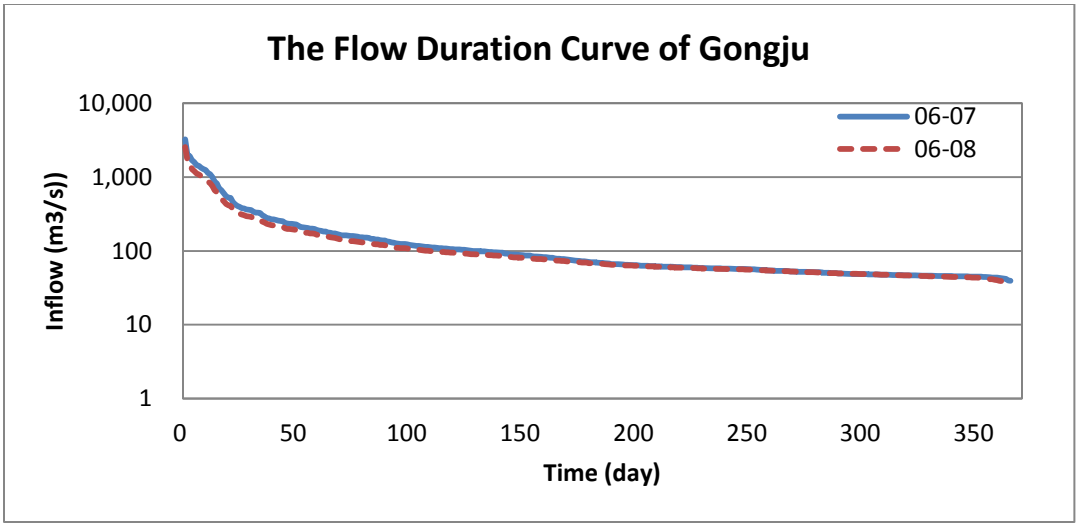

Figure 11. Flow Duration Curve at Gongju Station

Table 2. Comparison of Flow Duration at Gongju Station

unit: ㎥/s

Time	Abundant flow	Ordinary flow	Low flow	Drought flow
2006	135.10	71.70	61.60	54.40
2007	149.20	70.90	45.80	45.80
2008	79.35	68.55	53.32	47.78
Ave 06-08 (a)	121.22	70.38	53.57	49.33
Ave 06-07 (b)	142.15	71.30	53.70	50.10
Ave 82-07 (c)	144.45	79.12	53.01	34.74
(a) / (c)	83.92	88.96	101.06	141.99
(b) / (c)	98.41	90.12	101.30	144.21

Next, daily inflow data for each standard basin were collected from the long-term runoff analysis by the PRMS model by the River Basin Survey (Ministry of Land, Transport and Maritime Affairs). Flows at Gongju station were calculated using the stage-discharge curve of 2006, 2007 (Ministry of Construction & Transportation, 2006, 2007) and flows at Gyuam station were calculated from only the stage-discharge curve of 2006, because discharge measurements were not conducted in 2007. When the flow at Gyuam station (downstream) was less than that at Gongju station (upstream), the flows

at Gyuam were multiplied by 1.15 (the ratio of watershed area between both stations) times inflow at Gongju station. Results are shown in Figure 12 to 13.

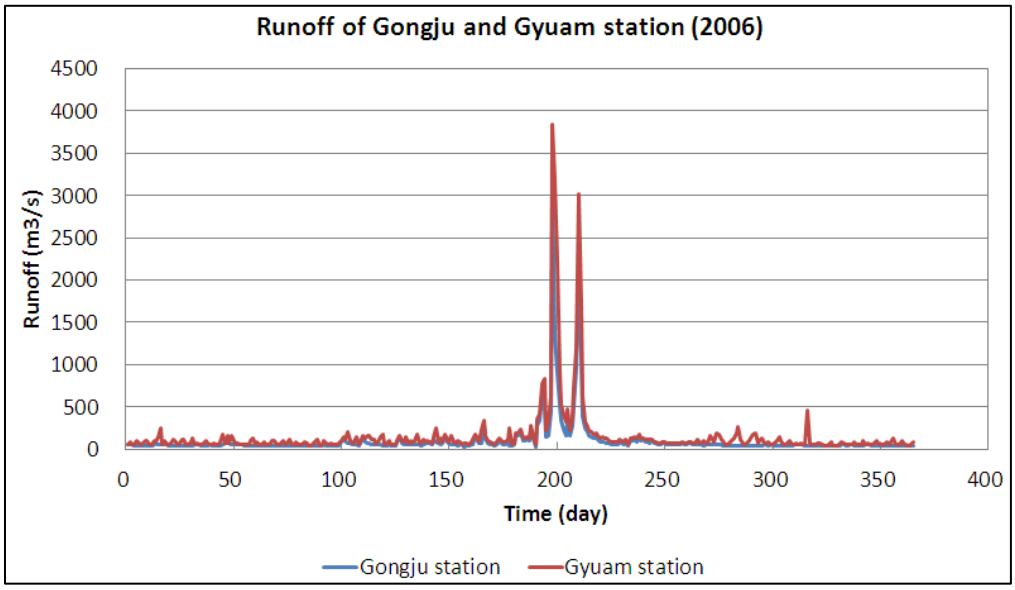

Figure 12. Runoff Data of Gongju and Gyuam Stations (2006)

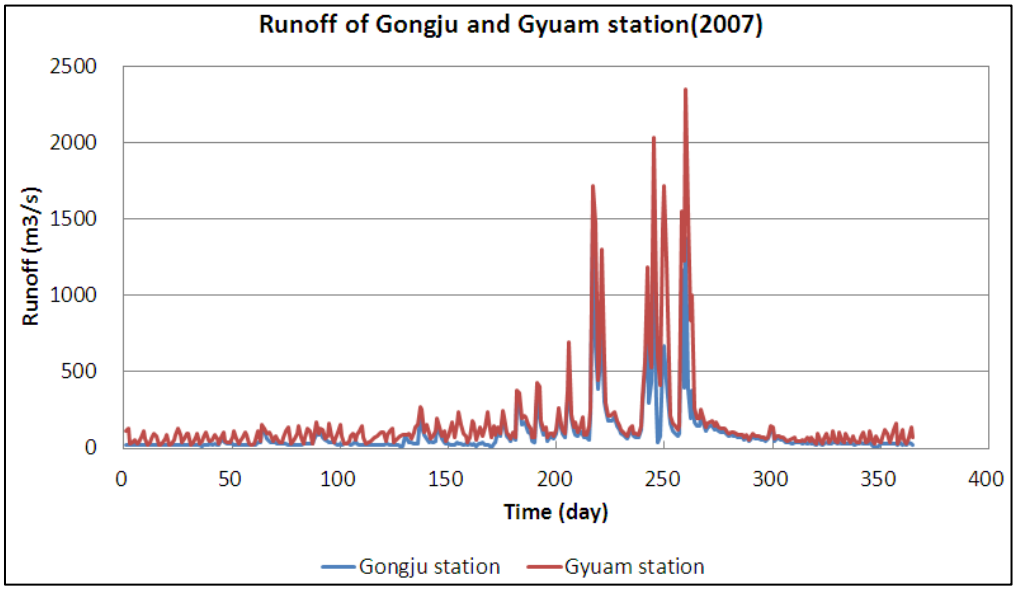

Figure 13. Runoff Data of Gongju and Gyuam Stations (2007)

To calculate lateral inflow, the study area was divided into 3 sections based on the Gongju station and Gyuam station, as shown in Figure 14.

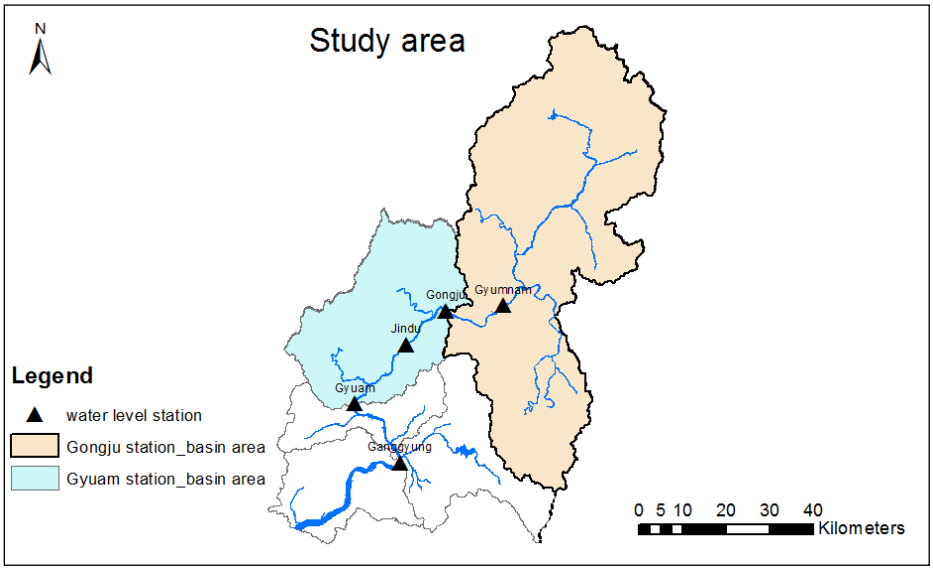

Figure 14. Basin Diagram

The value of PRMS model cannot be used directly, because the model value assumed only natural runoff without human activity, such as water supply from dam, withdrawal, etc. Therefore, those data were used as a weighing factor to calibrate with observations for obtaining the inflow of sub basin.

The inflow of sub basin upstream of Gongju station was obtained using equation (1) and the inflow between Gongju station and Gyuam station was obtained using equation (2). Downstream of Gyuam station, equation (3) was used;

$$Q_i = (Q_{Gongju} - Q_{Dam\_outflow}) \times \frac{q_i}{\sum_{i=1}^{n} q_i} \quad (1)$$

$$Q_j = (Q_{Gyuam} - Q_{Gongju} - Q_{Dam\_outflow}) \times \frac{q_j}{\sum_{j=1}^{m} q_j} \quad (2)$$

$$Q_o = \frac{Q_{Gyuam} - Q_{Dam\_outflow}}{\sum_{k=1}^{l} q_k} \times q_o \quad (3)$$

Where Qi, Qj , Q_o =the calibrated inflow of each standard basin; q_i , n=the inflow of the PRMS model and the number of standard basins upstream of Gongju station; q_j, m=the inflow of the PRMS model and the number of standard basins between Gongju and Gyuam stations; q_k, l=the inflow of the PRMS model and the number of standard basins upstream of Gyuam station; q_o=the inflow of the PRMS model downstream of Gyuam station; Q_{Gongju} , Q_{Gyuam} = the inflows of Gongju station and Gyuam station, respectively; and $Q_{Dam\_outflow}$= the outflow from Daechung Regulation Dam.

Then, each standard basin was gathered into 22 sub basins, as shown in Figure 15, Table 3. As a result, upstream and the lateral inflow data were obtained, as shown in Figures 16 to 18, and input data for HEC-RAS is shown in Figure 19.

Table 3. Details of Basin Classification

Tributary	Sta. no	Standard basin
ⓐ	125.66	300901-6
ⓑ	109.40	301002, 301101-5
ⓒ	100.28	301201, 301203
ⓓ	80.47	301206
ⓔ	57.81	301209-10
ⓕ	49.82	301212
ⓖ	38.62	301213
ⓗ	34.49	301301-5
ⓘ	1.14	301402

Residual watershed	Sta. no	Standard basin
①	130.33	300805(b)
②	124.96	301001-2
③	108.75	301202
④	98.36	301204
⑤	84.79	301205
⑥	80.19	301207-8
⑦	57.33	301211
⑧	52.17	301214(a)
⑨	49.40	301214(b)
⑩	38.22	301214(c)
⑪	33.83	301305, 301402
⑫	20.58	301401, 301403(a)
⑬	0.72	301403(b)

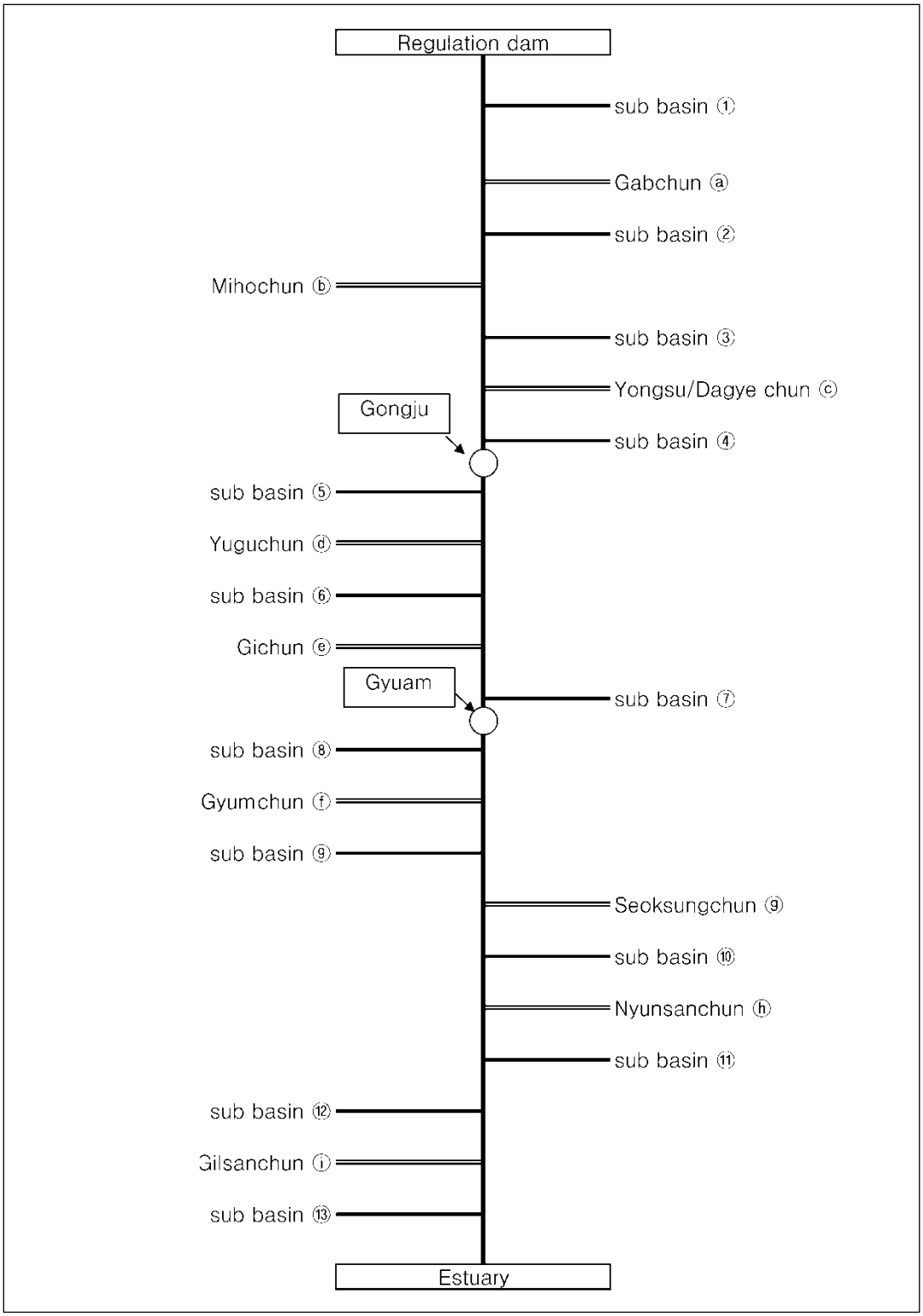

Figure 15. Tree Diagram of Basin

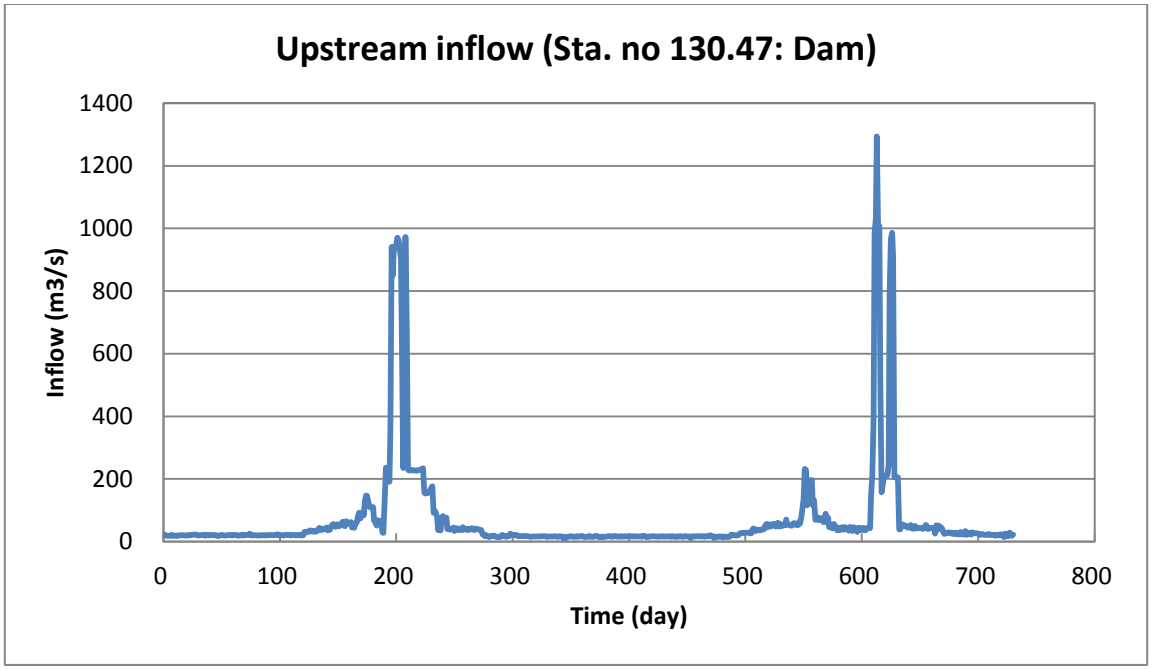

Figure 16. Upstream Boundary Condition in HEC-RAS (Daechung)

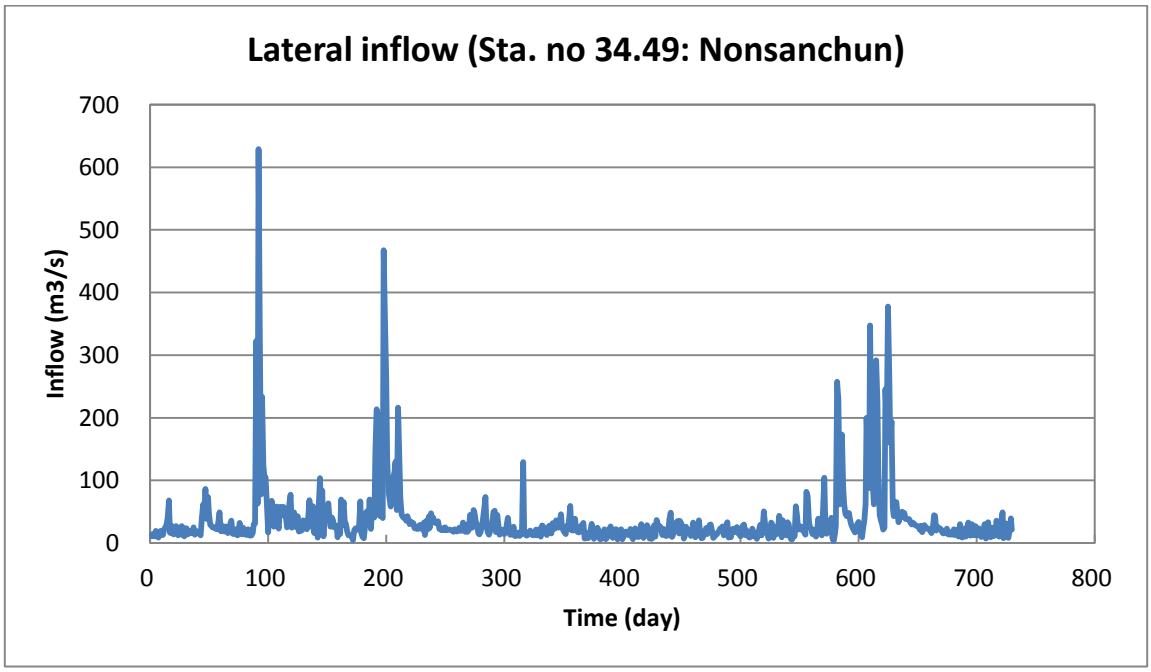

Figure 17. Lateral Boundary Condition in HEC-RAS (Residual watershed)

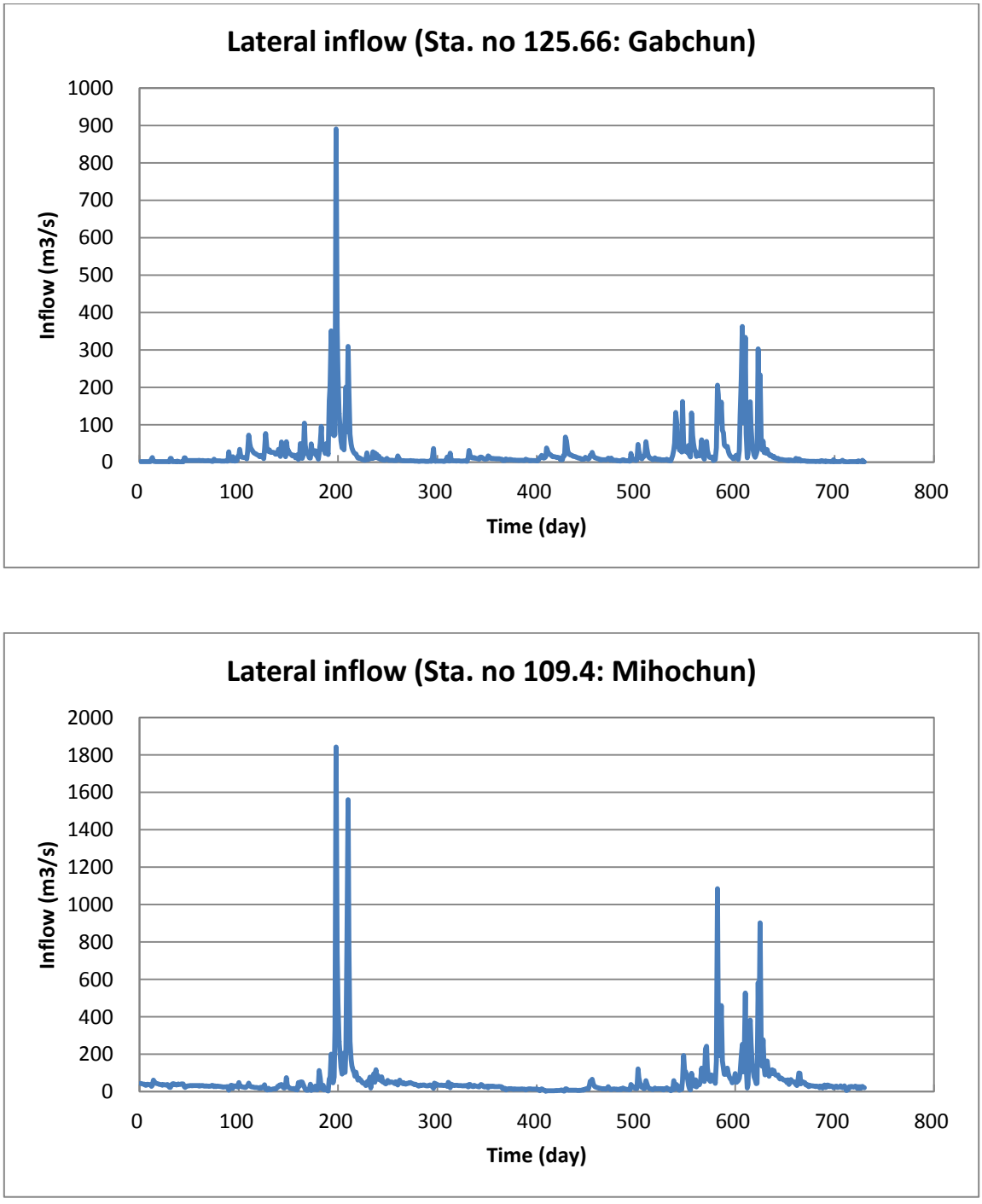

Figure 18. Lateral Boundary Condition in HEC-RAS (Tributary)

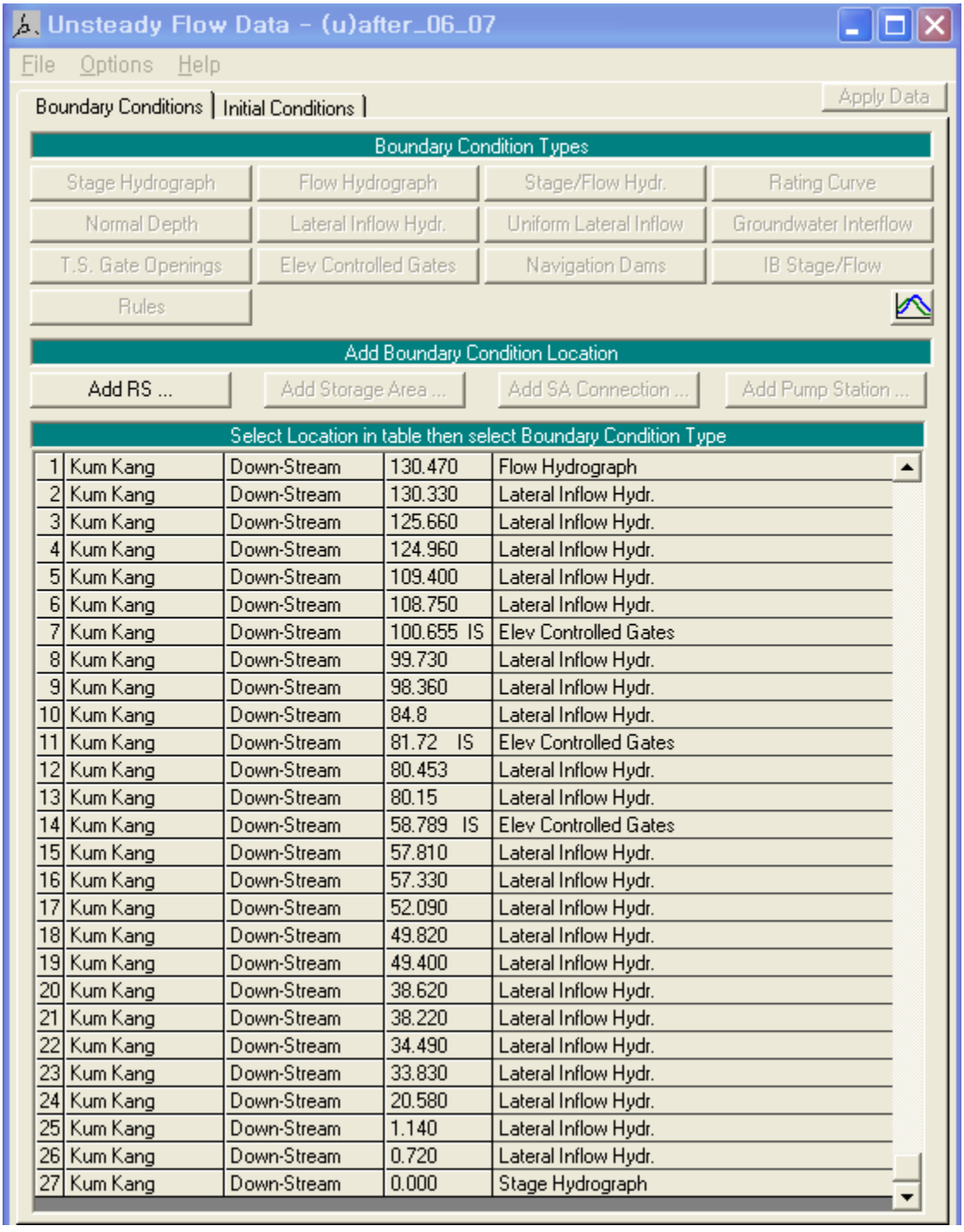

Figure 19. Inflow Data for HEC-RAS

3.4 Water level data and manning coefficient

For hydraulic analysis, the water level of the Geum River estuarial bank was used for the downstream boundary condition. The Geum River estuarial bank has a length of 1,127 m, and there are tidal gates which have a length of 600 m. The management water level is regulated differently, depending on seasons; water level is maintained by EL. (+) 2.0 m from March to June when maximum water for agricultural crops is needed and water level is kept by EL. (+) 1.0 m from July to February when there is less water usage (Daejeon Regional Construction Management Administration, 2009). Therefore, the downstream boundary condition is input, as shown in Figure 20, reflecting season change.

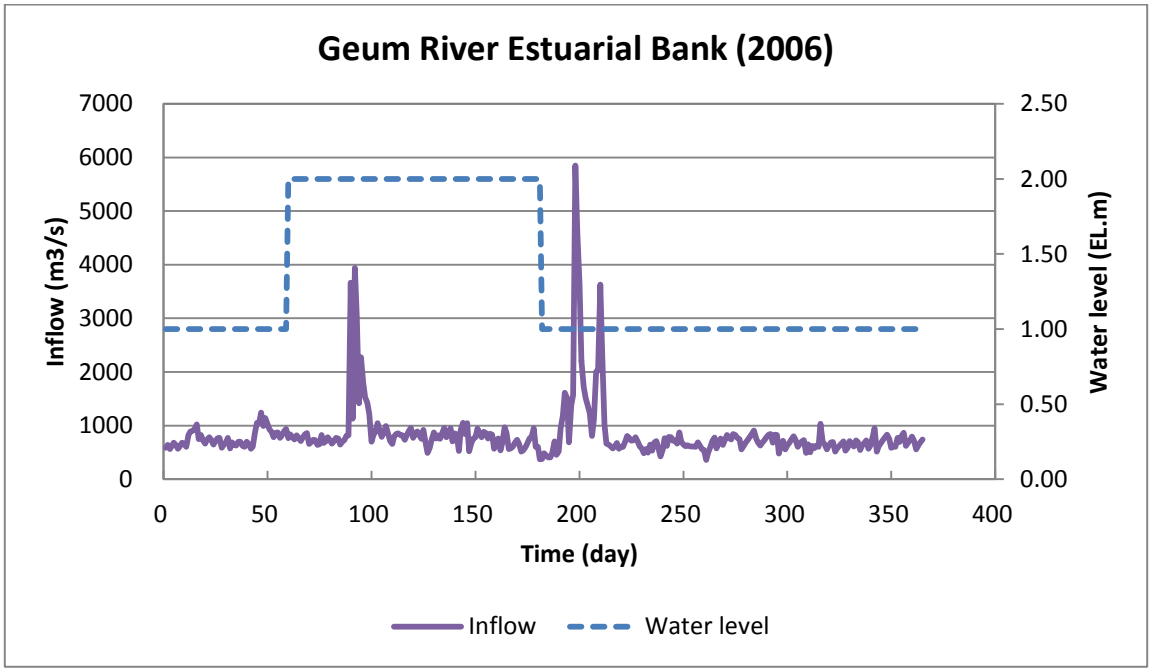

Figure 20. Downstream Boundary Condition in HEC-RAS (2006)

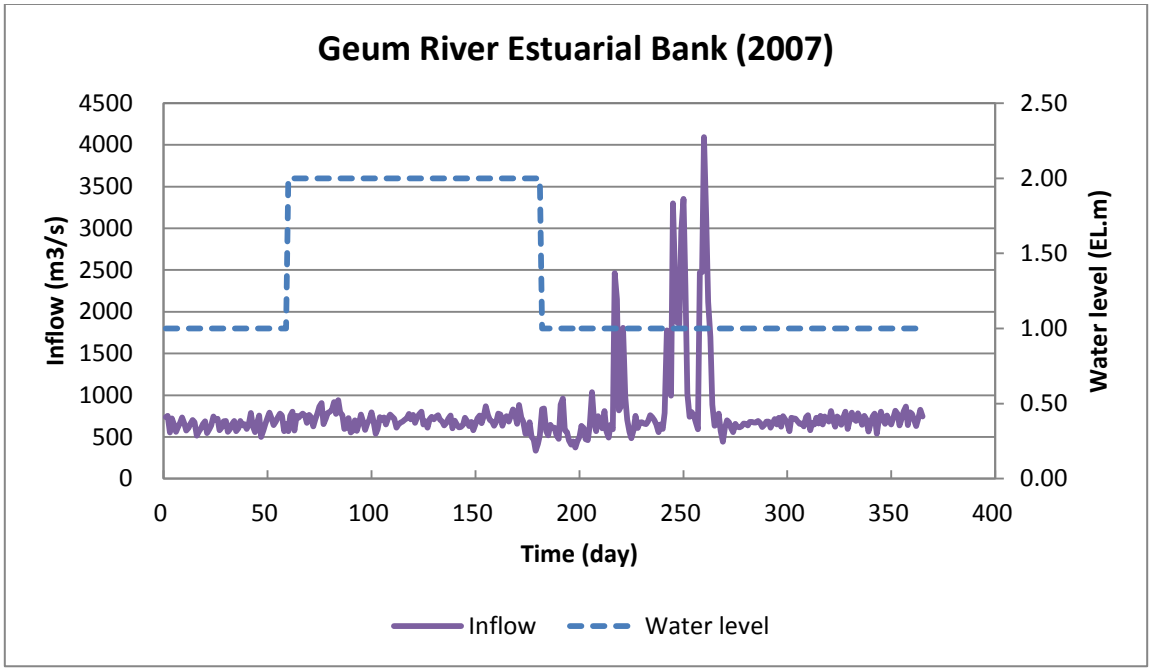

Figure 20. Downstream Boundary Condition in HEC-RAS (2007)

The Manning coefficient (n) is referenced in the Geum River Management Basic Plan (Daejeon Regional Construction Management Administration, 2009), as shown in Table 4.

Table 4. Roughness Coefficient

Section	Coefficient	Remarks
No. 0+00 ~ No. 33+830	0.025	Geum River Management Basin Plan (2009)
No. 34+490 ~ No. 56+970	0.026	
No. 57+330 ~ No. 140+470	0.027	

3.5 Gathering sediment data

Sediment size distribution and sediment inflow data are necessary to predict the riverbed change. We assumed that there was no sediment entering from Daechung Regulation Dam and the sediment entering from three tributaries (Gabchun, Mihochun, and Gichun) was suspended sediment. The bed gradation is input as particle sizes with an associated percentage value that indicates the amount of material within a sediment mixture that is finer by volume (percent finer). The standard grade class sizes are based on the American Geophysical Union (AGU) classification scale, as shown in Table 5 (USACE, 2002).

Table 5. American Geophysical Union (AGU) classifications (USACE, 2002)

Class	Sediment Material		Min (mm)	Max (mm)	Mean (mm)
1	Clay	Clay	0.002	0.004	0.003
2	Very Fine Silt	VFM	0.004	0.008	0.006
3	Fine Silt	FM	0.008	0.016	0.011
4	Medium Silt	MM	0.016	0.032	0.023
5	Coarse Silt	CM	0.032	0.0625	0.045
6	Very Fine Sand	VFS	0.0625	0.125	0.088
7	Fine Sand	FS	0.125	0.25	0.177
8	Medium Sand	MS	0.25	0.5	0.354
9	Coarse Sand	CS	0.5	1	0.707
10	Very Coarse Sand	VCS	1	2	1.41
11	Very Fine Gravel	VFG	2	4	2.83
12	Fine Gravel	FG	4	8	5.66
13	Medium Gravel	MG	8	16	11.3
14	Coarse Gravel	CG	16	32	22.6
15	Very Coarse Gravel	VCG	32	64	45.3
16	Small Cobbles	SC	64	128	90.5
17	Large Cobbles	LC	128	256	181
18	Small Boulders	SB	256	512	362
19	Medium Boulders	MB	512	1024	724
20	Large Boulders	LB	1024	2048	1448

In this study, 145 sediment data points were collected from the Geum River Management Basic Plan (Daejeon Regional Construction Management Administration, 2009) and Geum River Actual Plan Report for Lot (2009), as shown in Table 6. To overview sediment, the reach was divided into 4 sections by weirs location, as shown in Figure 21 and composition rate was plotted, as shown in Figures 22 to 25. Silt means VFM~CM and sand means VFS~VCS. Geum River was mostly made up of sand and the upstream reach dominantly consists of gravel.

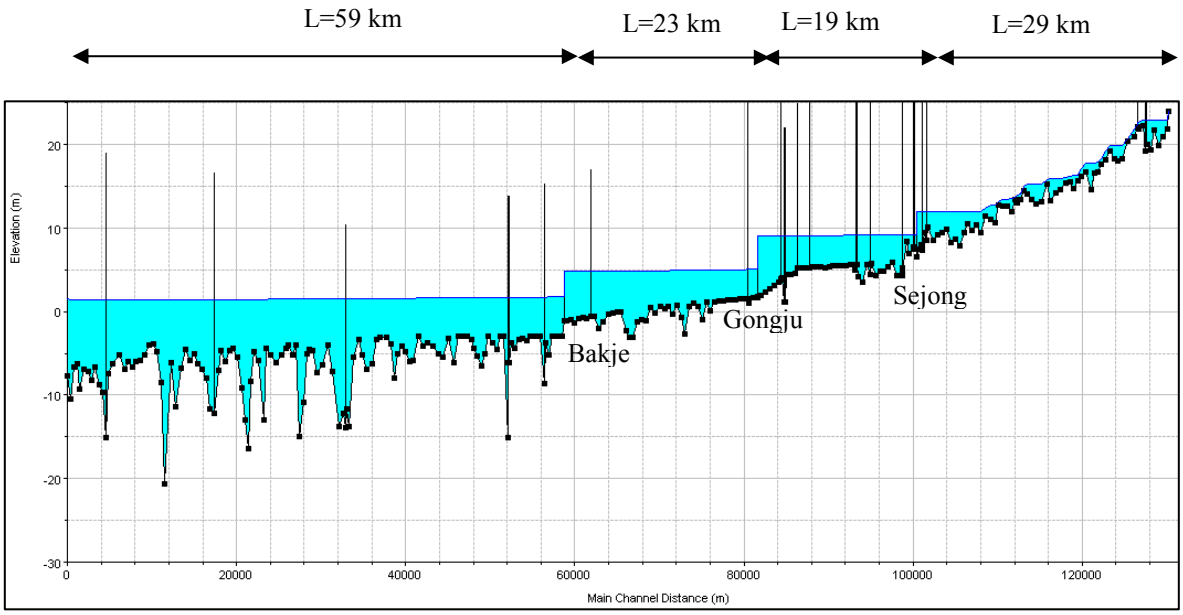

Figure 21. Division of Reach through Sediment Size Distribution

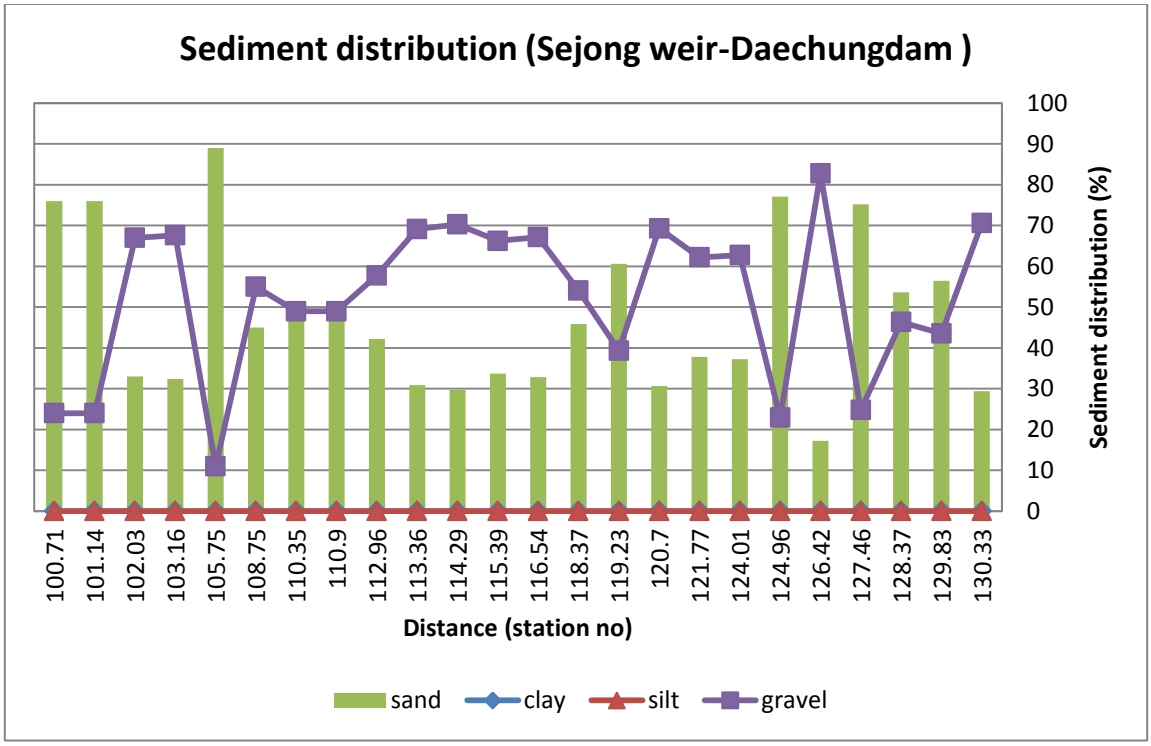

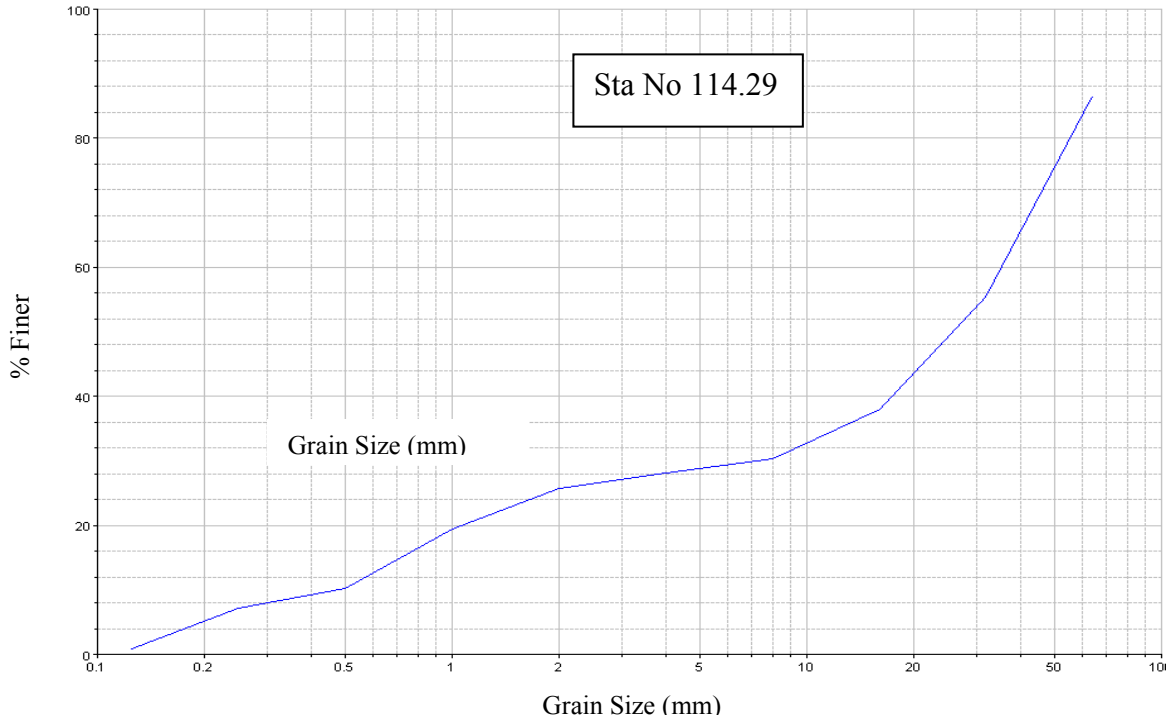

Figure 22. Sediment Size Distribution (Sejong - Daechung Regulation Dam)

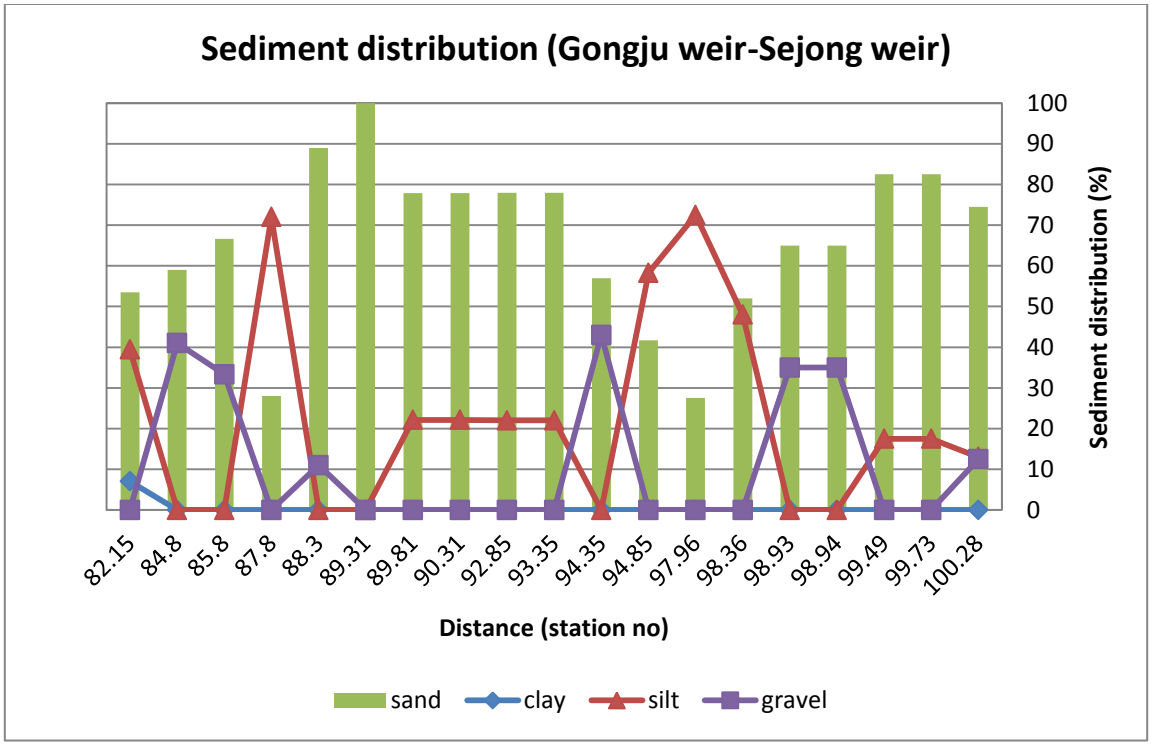

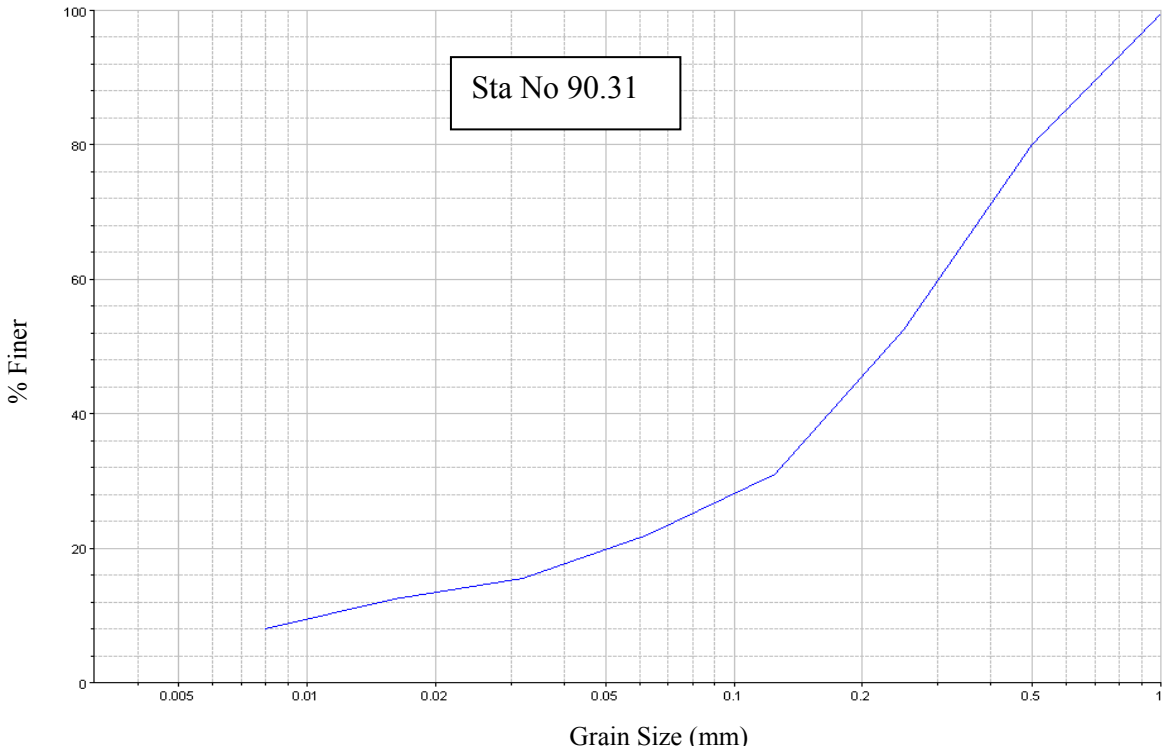

Figure 23. Sediment Size Distribution (Gongju - Sejong)

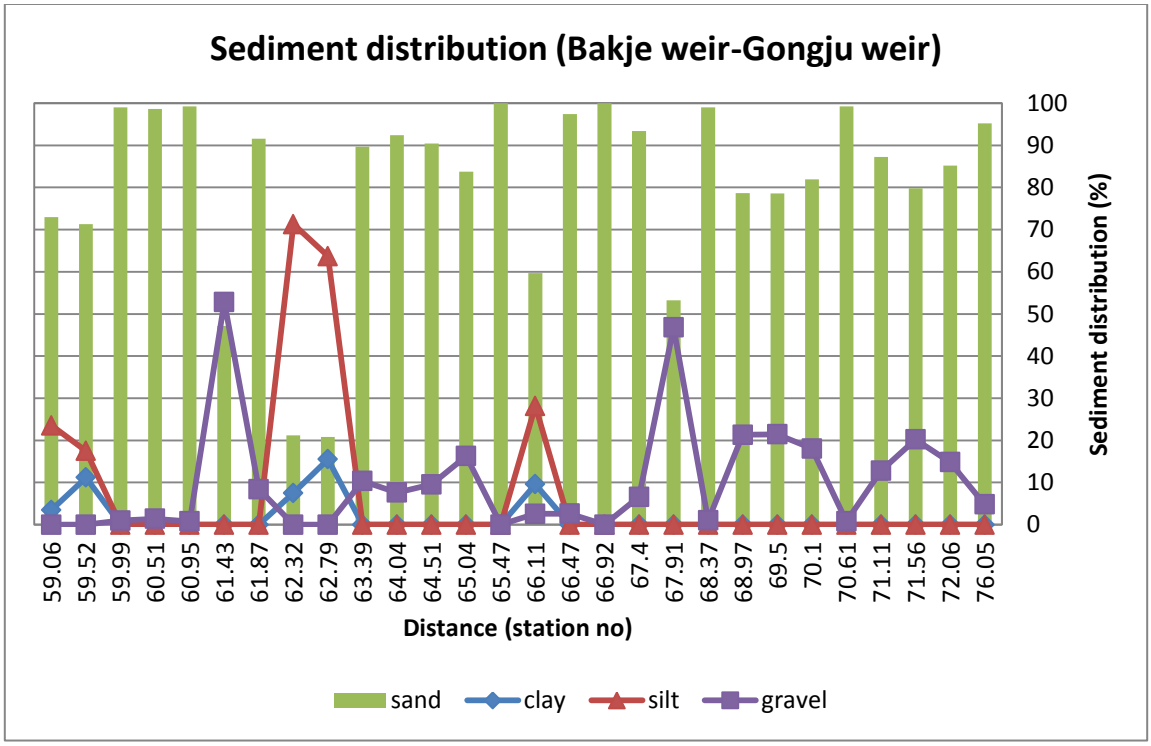

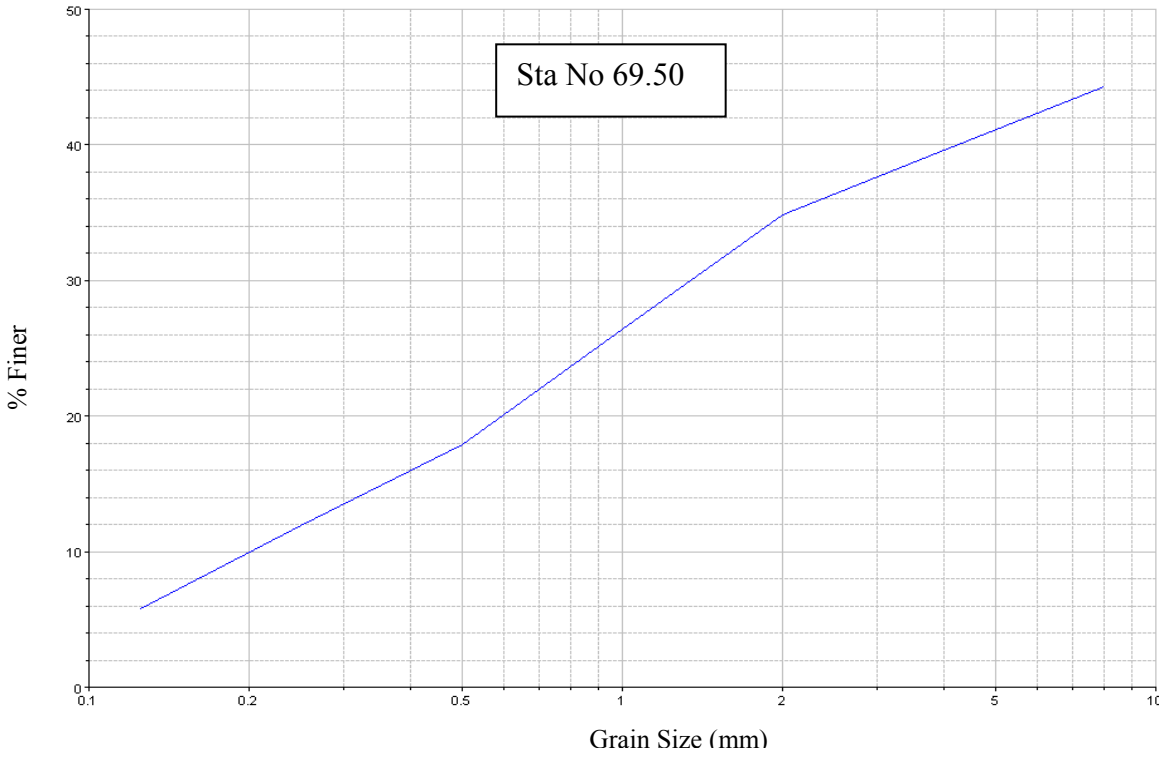

Figure 24. Sediment Size Distribution (Bakje - Gongju)

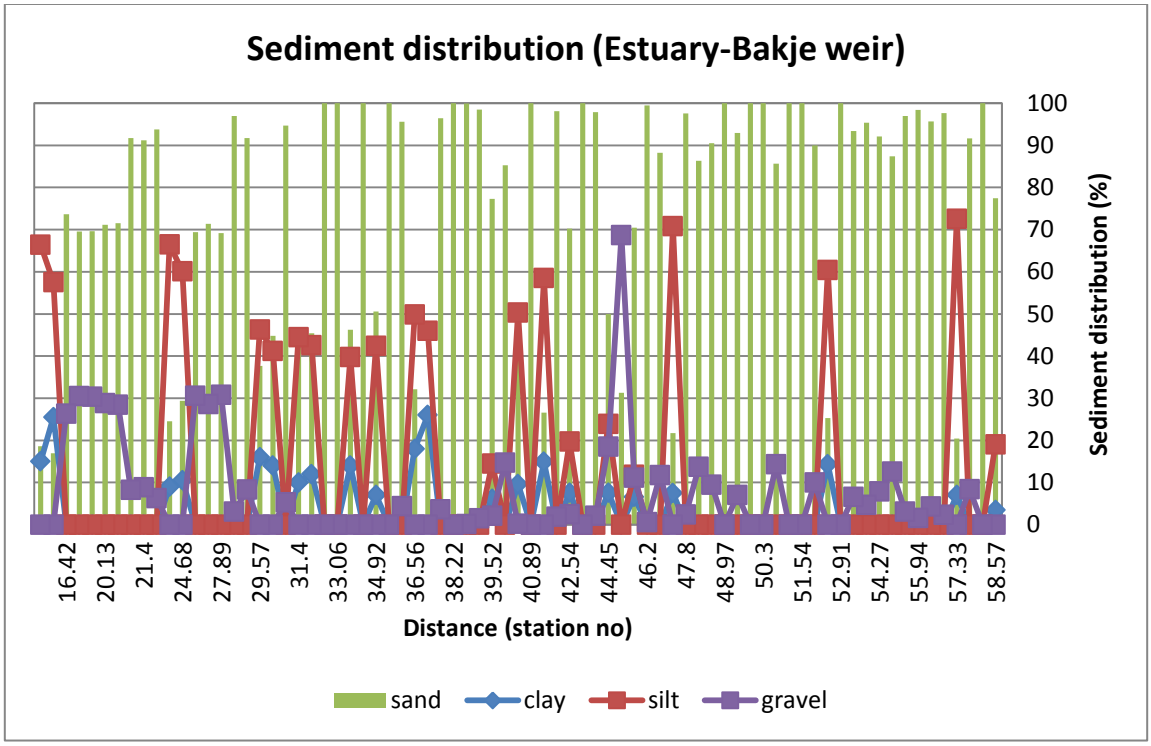

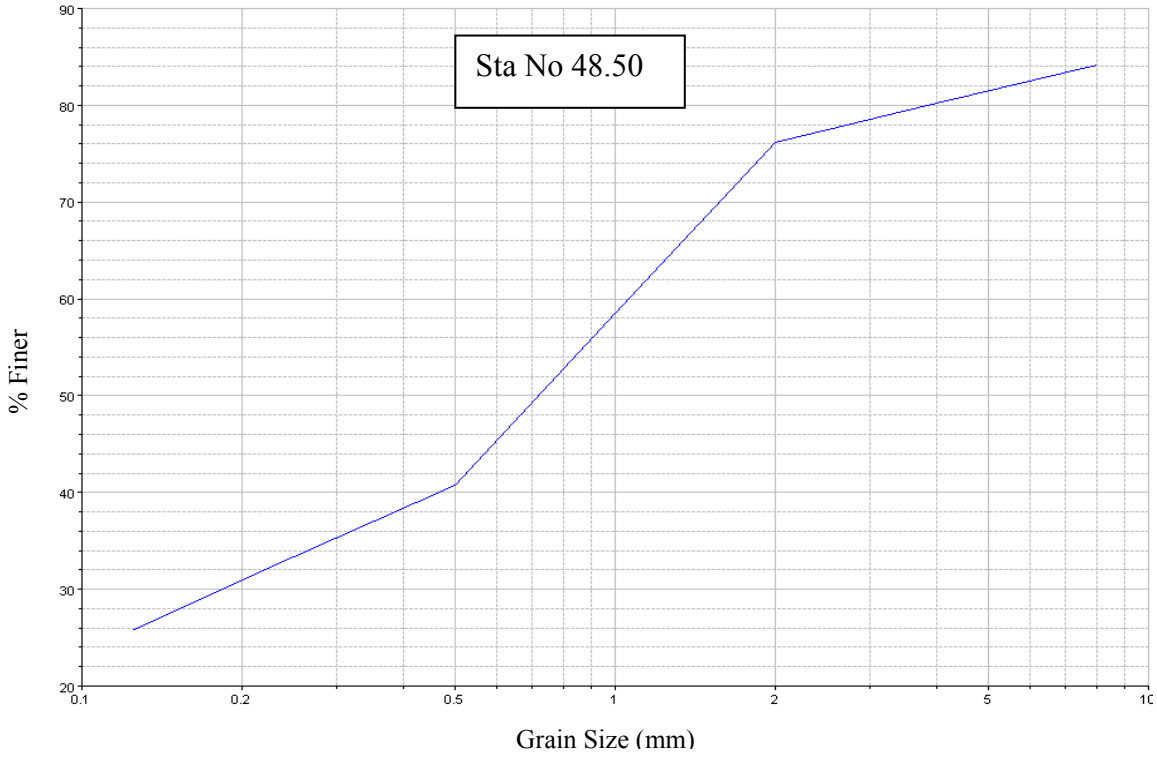

Figure 25. Sediment Size Distribution (Estuary - Bakje)

Table 6. Sediment Size Distribution

Sta. No	Finer (%)														
	1	2	3	4	5	6	7	8	9	10	11	12	13	14	15
	Clay	VFM	FM	MM	CM	VFS	FS	MS	CS	VCS	VFG	FG	MG	CG	VCG
130.33						1.7	8.2	11.4	21.1	27.5	30.4	33.2	42.1	60.5	93.5
129.83						0.6	12.2	17.9	35.3	46.8	50.7	54.5	58.7	66.6	82.9
128.37						1.6	9.9	14.0	26.4	34.7	39.4	44.1	49.9	64.7	
127.46						1.5	18.6	27.1	52.7	69.7	78.2	86.6	91.7	92.7	
126.42						0.5	3.9	5.6	10.7	14.1	18.4	22.6	32.4	50.5	81.7
124.96						9.7	24.5	31.9	54.1	68.9	72.4	75.9	82.0	89.4	
124.01						3.1	9.8	13.2	23.2	29.9	33.3	36.7	43.9	56.3	80.3
121.77						0.4	5.6	8.2	16.0	21.2	23.6	26.0	33.4	45.8	56.1
120.7						0.4	4.3	6.2	12.0	15.9	18.0	20.0	26.9	39.6	51.8
119.23						1.3	9.8	14.1	26.8	35.3	39.9	44.4	50.2	58.2	
118.37						1.0	11.1	16.1	31.2	41.3	43.8	46.2	52.6	63.7	90.0
116.54						1.0	8.0	11.4	21.9	28.8	34.3	39.8	49.1	65.0	87.7
115.39						0.8	8.3	12.1	23.3	30.8	35.7	40.5	48.1	57.8	91.3
114.29						0.9	7.1	10.2	19.5	25.7	28.1	30.4	38.0	55.3	86.5
113.36						4.1	9.7	12.5	21.0	26.6	28.9	31.1	36.8	51.7	86.2
112.96									8.0	42.0	73.0	92.0	97.5	99.5	
110.9							5.0	7.5	20.0	51.0	84.5	88.5	97.0	100.0	
110.35							5.0	7.5	20.0	51.0	84.5	88.5	97.0	100.0	
108.75									10.0	45.0	76.0	95.0	100.0		
105.75							23.0	50.0	75.0	89.0	100.0				
103.16						3.3	4.6	8.7	13.1	17.4	20.6	23.9	29.4	53.6	
102.03									9.0	32.5	56.0	89.0	94.0	98.5	
101.14							17.5	39.0	59.0	76.0	91.0	95.5	99.0	100.0	
100.71							17.5	39.0	59.0	76.0	91.0	95.5	99.0	100.0	
100.28		5.0	7.5	10.0	13.0	23.0	37.5	56.0	73.0	87.5	99.0	100.0			
99.73		7.0	8.0	12.0	17.5	26.0	50.0	80.0	99.0	100.0					
99.49		7.0	8.0	12.0	17.5	26.0	50.0	80.0	99.0	100.0					
98.94							17.0	29.0	44.0	65.0	86.0	97.0	100.0		
98.93							17.0	29.0	44.0	65.0	86.0	97.0	100.0		
98.36		19.0	27.0	37.0	48.0	62.0	76.0	90.0	99.5	100.0					
97.96		32.0	45.0	61.0	72.5	84.0	92.0	97.0	99.0	100.0					
94.85		22.0	32.0	43.0	58.0	73.0	85.0	93.0	99.5						
94.35							3.0	6.0	20.0	57.0	100.0				
93.35		9.0	12.0	17.0	22.0	30.0	54.0	82.0	100.0						
92.85		9.0	12.0	17.0	22.0	30.0	54.0	82.0	100.0						
90.31		8.0	12.5	15.5	22.0	31.0	52.5	80.0	99.5						
89.81		8.0	12.5	15.5	22.0	31.0	52.5	80.0	99.5						
89.31							36.0	75.5	100.0						

Table 6. Continued

Sta. No	Finer (%)														
	1	2	3	4	5	6	7	8	9	10	11	12	13	14	15
	Clay	VFM	FM	MM	CM	VFS	FS	MS	CS	VCS	VFG	FG	MG	CG	VCG
88.3						28.4	46.3	64.2	76.6	89.0	93.2	97.3	100.0		
87.8		30.0	46.0	57.0	72.0	87.0	95.0	98.0	100.0						
85.8							7.0	28.0	41.0	66.0	90.0	94.5	96.0	99.0	
84.8							5.0	9.0	23.0	59.0	95.0	99.0	100.0		
82.15	7.0	9.8	22.0	34.2	46.5	58.7	79.1	99.4	99.7	100.0					
76.05						4.3	30.9	57.4	76.3	95.2	97.6	100.0			
72.06						17.8	28.3	38.8	45.6	52.3	56.9	61.4			
71.56						4.8	9.1	13.3	20.9	28.4	32.0	35.6			
71.11						10.2	22.0	33.7	50.0	66.2	71.1	75.9			
70.61						1.8	17.7	33.6	66.4	99.2	99.6	100.0			
70.1						12.3	19.3	26.2	34.7	43.1	47.9	52.6			
69.5						5.8	11.9	17.9	26.4	34.8	39.6	44.3			
68.97						6.6	12.4	18.2	25.7	33.2	37.7	42.2			
68.37						1.0	16.6	32.2	65.6	99.0	99.5	100.0			
67.91						6.5	13.1	19.7	31.9	44.0	63.4	82.7			
67.4						1.6	25.7	49.8	66.8	83.7	86.7	89.6			
66.92						2.5	30.6	58.7	79.4	100.0					
66.47						3.2	22.6	42.0	69.7	97.4	98.7	100.0			
66.11	9.0	15.6	22.2	28.8	35.4	42.0	52.1	62.1	76.7	91.3	92.5	93.7			
65.47						1.9	18.9	35.8	67.9	100.0					
65.04						4.1	8.2	12.2	19.0	25.7	28.2	30.7			
64.51						4.1	10.9	17.6	28.7	39.8	41.9	44.0			
64.04						3.8	15.0	26.2	50.8	75.3	78.4	81.5			
63.39						2.4	9.3	16.1	26.3	36.4	38.5	40.6			
62.79	15.5	31.4	47.3	63.3	79.2	95.1	97.6	100.0							
62.32	7.5	25.3	43.1	61.0	78.8	96.6	98.3	100.0							
61.87						14.9	32.1	49.3	59.5	69.7	72.9	76.1			
61.43						8.4	14.0	19.6	31.5	43.3	67.6	91.8			
60.95						8.3	34.7	61.1	80.2	99.2	99.6	100.0			
60.51						4.5	27.5	50.5	74.6	98.6	99.3	100.0			
59.99						18.4	39.4	60.3	76.4	92.4	92.9	93.3			
59.52	8.3	11.5	14.8	18.0	21.3	24.5	46.4	68.2	71.2	74.1					
59.06	3.5	9.4	15.3	21.1	27.0	32.9	65.3	97.6	98.8	100.0					
58.57	3.5	8.3	13.0	17.8	22.5	27.3	61.0	94.7	97.4	100.0					
58.08						3.0	45.8	88.5	94.3	100.0					
57.81						3.7	14.6	25.5	54.4	83.2	87.0	90.8			
57.33	7.0	25.1	43.3	61.4	79.6	97.7	98.9	100.0							
56.97						4.8	22.8	40.7	68.3	95.9	97.1	98.2			
56.51						2.4	13.0	23.6	59.7	95.7	97.9	100.0			

Table 6. Continued

Sta. No	Finer (%)														
	1	2	3	4	5	6	7	8	9	10	11	12	13	14	15
	Clay	VFM	FM	MM	CM	VFS	FS	MS	CS	VCS	VFG	FG	MG	CG	VCG
55.94						21.2	38.1	54.9	76.7	98.4	99.2	100.0			
55.32						12.9	29.8	46.7	58.2	69.6	70.7	71.8			
54.73						14.4	18.5	22.6	26.7	55.6	59.6	63.6			
54.27						17.5	31.4	45.3	59.2	83.9	87.5	91.1			
53.76						8.1	18.8	29.4	40.1	69.4	71.1	72.8			
53.35						2.8	11.8	20.8	29.8	87.6	90.7	93.8			
52.91						97.3	98.0	98.7	99.4	100.0					
52.54	14.3	29.4	44.5	59.6	74.7	89.8	92.9	95.9	99.0	100.0					
52.09						4.0	8.7	13.4	18.1	79.3	83.7	88.1			
51.54						49.8	64.8	79.7	94.7	100.0					
51.22						10.7	26.5	42.2	58.0	100.0					
50.8						7.0	19.6	32.1	51.9	71.7	77.7	83.7			
50.3						39.1	65.9	92.6	96.3	100.0					
49.82						3.0	29.1	55.2	77.6	100.0					
49.4						5.1	18.2	31.3	48.7	66.0	68.5	71.0			
48.97						5.8	24.4	43.0	71.5	100.0					
48.5						25.8	33.3	40.7	58.5	76.2	80.2	84.2			
48.1						5.8	11.2	16.5	29.4	42.2	45.6	48.9			
47.8						19.7	56.7	93.6	95.6	97.6	98.8	100.0			
47.27	7.5	25.2	42.9	60.6	78.3	96.0	98.0	100.0							
46.67						14.3	20.7	27.0	42.4	57.7	61.6	65.4			
46.2						12.2	41.1	69.9	80.2	90.4	90.7	90.9			
45.65	6.6	9.6	12.5	15.5	18.4	21.4	30.0	58.3	76.1	88.9	92.8	96.6	100.0		
45.06						3.6	7.9	12.1	21.7	31.3	35.4	39.4	51.5	100.0	
44.45	7.6	13.6	19.6	25.5	31.5	37.5	51.1	66.2	74.1	81.5	84.1	86.7	91.9	100.0	
43.85						1.6	4.3	24.8	74.4	97.9	99.0	100.0			
43.29						3.8	15.0	85.5	99.9	100.0					
42.54	7.6	12.5	17.4	22.4	27.3	32.2	50.7	80.7	91.3	97.5	98.8	100.0			
41.99						1.2	2.9	45.8	87.9	98.1	98.3	98.5	100.0		
41.49	14.9	29.5	44.1	58.8	73.4	88.0	97.4	99.0	100.0						
40.89						3.2	10.8	74.8	98.7	100.0					
40.47	9.6	22.2	34.8	47.3	59.9	72.5	90.0	98.1	98.8	99.8	99.9	100.0			
40						3.0	3.4	13.2	35.6	85.3	92.3	99.2	100.0		
39.52	6.1	9.7	13.3	17.0	20.6	24.2	43.7	84.2	93.2	97.9	99.0	100.0			
39.05						2.5	5.6	41.5	91.5	98.5	99.0	100.0			
38.62						4.7	12.9	70.1	98.8	99.9	100.0	100.0			
38.22						4.5	31.4	99.7	100.0						
37.71						28.4	37.2	79.3	87.9	96.4	98.2	100.0			

Table 6. Continued

Sta. No	Finer (%)														
	1	2	3	4	5	6	7	8	9	10	11	12	13	14	15
	Clay	VFM	FM	MM	CM	VFS	FS	MS	CS	VCS	VFG	FG	MG	CG	VCG
36.56	18.0	30.5	42.9	55.4	67.8	80.3	87.0	96.3	98.2	100.0					
36						13.4	18.0	58.3	77.0	95.6	97.8	100.0			
35.37						2.9	4.3	45.6	72.8	100.0					
34.92	7.0	17.6	28.2	38.8	49.4	60.0	69.0	85.2	92.6	100.0					
34.49						3.5	5.2	50.3	75.2	100.0					
33.27	14.0	23.9	33.9	43.8	53.8	63.7	71.9	91.6	95.8	100.0					
33.06						18.4	25.0	68.5	84.3	100.0					
32.59						29.1	37.0	78.2	89.1	100.0					
32.12	12.0	22.6	33.3	43.9	54.6	65.2	73.5	92.5	96.3	100.0					
31.4	10.0	21.1	32.2	43.4	54.5	65.6	75.3	90.0	95.0	100.0					
30.83						4.1	7.2	39.5	67.1	94.7	97.4	100.0			
30.16	14.0	24.3	34.6	44.9	55.2	65.5	73.6	91.3	95.7	100.0					
29.57	16.0	27.6	39.2	50.7	62.3	73.9	81.5	94.4	97.2	100.0					
29.03						23.5	30.2	69.2	80.5	91.7	94.6	97.5	98.8	100.0	
28.29						90.8	92.3	93.9	95.4	96.9	98.5	100.0			
27.89						7.5	22.9	38.3	53.8	69.2	84.6	100.0			
27.4						14.1	28.4	42.7	57.1	71.4	85.7	100.0			
26.99						8.2	23.5	38.8	54.1	69.4	84.7	100.0			
24.68	10.5	25.5	40.5	55.6	70.6	85.6	91.6	97.5	98.8	100.0					
24.05	9.0	25.6	42.2	58.9	75.5	92.1	96.1	100.0							
21.66						81.2	84.3	87.5	90.6	93.7	96.9	100.0			
21.4						73.5	77.9	82.3	86.8	91.2	95.6	100.0			
21						75.2	79.3	83.5	87.6	91.7	95.9	100.0			
20.58						14.6	28.8	43.1	57.3	71.5	85.8	100.0			
20.13						13.5	27.9	42.3	56.8	71.2	85.6	100.0			
17.85						8.9	24.1	39.3	54.5	69.6	84.8	100.0			
16.91						8.6	23.8	39.1	54.3	69.5	84.8	100.0			
16.42						21.0	34.2	47.3	60.5	73.7	86.8	100.0			
2.45	25.5	39.9	54.3	68.6	83.0	97.4	98.7	100.0							
2.02	15.0	31.6	48.2	64.8	81.4	98.0	99.0	100.0							

In the case of sediment loads entering from tributaries; which are Gabchun, Mihochun, and Jichun, we input inflow-sediment relationship and sediment size analysis, which were obtained from the Water Resources Investigation Report (Ministry of Land, Transport and Maritime Affairs, 2010), as shown in Figure 26. Of course, when more observed data will be accumulated in future, model results will be more reliable.

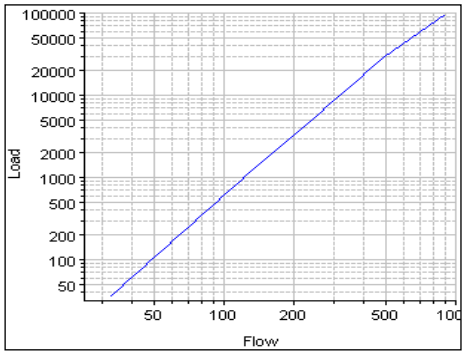

	Flow (m3/s)	32.6	137.5	218.4	492.6	900
	Total Load (tonnes/day)	36.6	1305.4	4067.4	29469	95430.3
1	Clay					
2	VFM					
3	FM					
4	MM	17.24	9.29	12.14	4.51	4.51
5	CM	37.93	10.48	7.05	9.27	9.27
6	VFS	44.83	18.33	15.38	19.85	19.85
7	FS		14.76	15.38	14.51	14.51
8	MS		21.19	23.35	18.08	18.08
9	CS		25.95	26.71	33.77	33.77
10	VCS					
11	VFG					
12	FG					
13	MG					

Gabchun

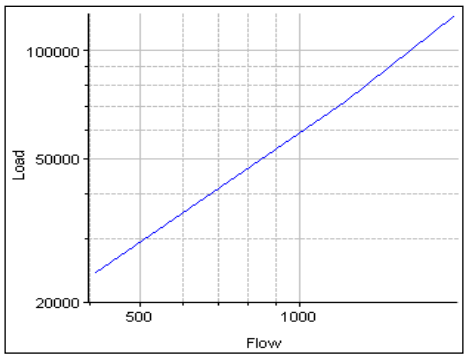

	Flow (m3/s)	410.1	1222.7	1967.4
	Total Load (tonnes/day)	24134.2	71944.3	124867.1
1	Clay			
2	VFM			
3	FM			
4	MM	10.01	11.28	10.19
5	CM	22.84	26.25	23.83
6	VFS	31.79	28.64	28.93
7	FS	12.78	11.28	13.94
8	MS	10.66	10.26	10.64
9	CS	11.92	12.28	12.47
10	VCS			
11	VFG			
12	FG			
13	MG			
14	CG			
15	VCG			
16	SC			
17	LC			
18	SR			

Mihochun

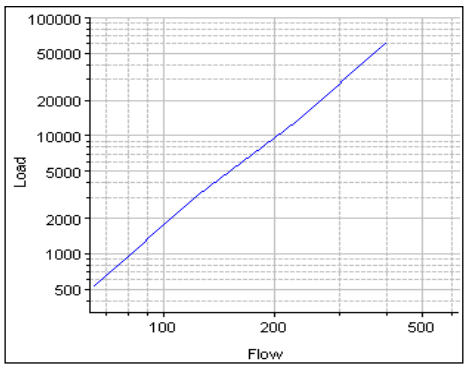

	Flow (m3/s)	64.8	123.1	228.8	400
	Total Load (tonnes/day)	530.8	3099.2	13279.4	62029.49
1	Clay				
2	VFM				
3	FM				
4	MM	10.36	9.72	9.1	9.1
5	CM	31.83	27.91	27.93	27.93
6	VFS	25.99	28.03	30.16	30.16
7	FS	11.3	11.26	10.68	10.68
8	MS	9.79	11.01	10.34	10.34
9	CS	10.73	12.07	11.77	11.77
10	VCS				
11	VFG				
12	FG				
13	MG				
14	CG				
15	VCG				
16	SC				
17	LC				
18	SR				

Jichun

Figure 26. Sediment Loads in Tributary

3.6 Temperature

Because several aspects of sediment transport mechanics, particularly fall velocity, are sensitive to water temperature, HEC-RAS requires temperature information, and only one temperature per time step can be specified for the entire model. Temperature was obtained from the Daejeon climatic observation data which represents the Geum River, as shown in Figure 27 and they have been provided in the website (http://www.kma.go.) which is managed by Korea Metrological Administration.

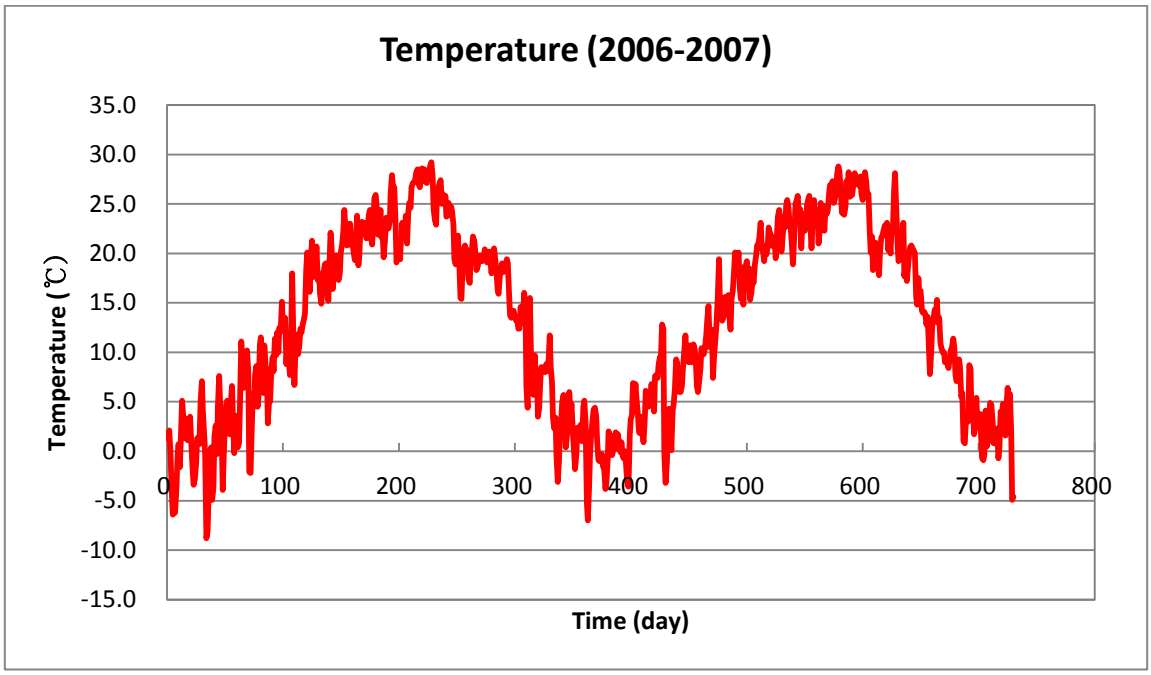

Figure 27. Temperatures in Geum River

4. METHODOLOGY

Most numerical models of sediment transport are assumed that the bed load or the total load are instantaneously in equilibrium, and then calculate the riverbed change using several of sediment transport equations. But this assumption did not explain the temporal and spatial lags. When compared with the equilibrium state, the non-equilibrium let the calculation be more stable and make the natural river properly analyze (Sanchez et al., 2011).

This study used HEC-RAS, a 1-dimensional model, and CCHE2D, 2-dimensional model. HEC-RAS calculates sediment transport capacity and then predict the riverbed change by the Exner equation. On the other hand, CCHE2D carries out a non-equilibrium sediment transport model for total sediment load. The depth-integrated convection-diffusion equation was used for the suspended load transport and the continuity equation is used for the bed load transport rate (Wu, 2001).

To calculate sediment transport, hydraulic calculation must be done in advance and then sediment analysis can be done. First, 1-D hydraulic analysis was done by HEC-RAS with input data. Then, the model output (water level) was compared with observed values at main control water level stations in the case of rainfall event (7.6-8.3.'06, 8.7-9.23.'07). Sediment change depends on the gate operation of weirs, so three scenarios were applied to the 1-D model. The first case was: gates are close fully (open: 0 %). This case mainly takes place in the drought season, and may also happen when gates may be in disorder. The second case was: gates are open fully (open: 100 %). This scenario

happens in the flood season and is meaningful when compared with the effect of sediment passing through gate operation. The last case is: gates are manipulated according to an operation rule.

The Four Major Rivers Restoration Project has set Management Water Level (MWL). When the upstream water level of a weir is higher than MWL, flood damage may happen in land near the weir. On the other hand, when the upstream water level is lower, the withdrawal of water from the river for drinking or agricultural use may be difficult. Therefore, the third scenario approximates the real situation. But the gate option can be set by the gate opening height when calculating sediment in HEC-RAS. So, the hourly gate height for keeping MWL was produced through unsteady analysis and averaged to determine daily gate height. Then, sediment analysis was simulated with daily average gate height using quasi-unsteady flow.

1-D analysis is limited to seeing the riverbed change in detail. So, we found the problem section with the 1-D model and analyzed that in detail with the 2-D model (CCHE2D) treating non-equilibrium state. In addition, the structural measure (installation dike) preventing sediment problem was investigated, as shown in Figure 28.

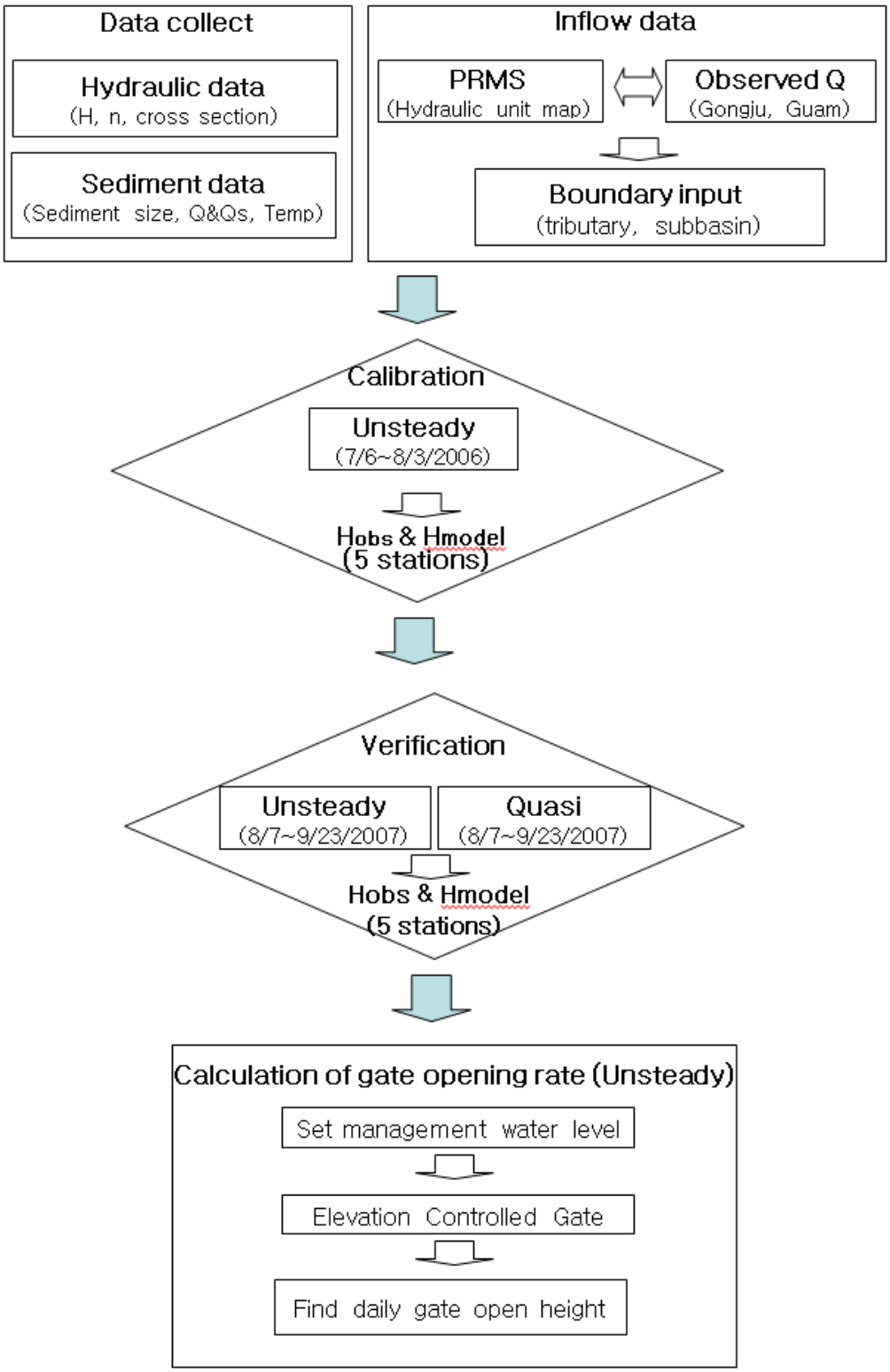

Figure 28. Procedure of Study

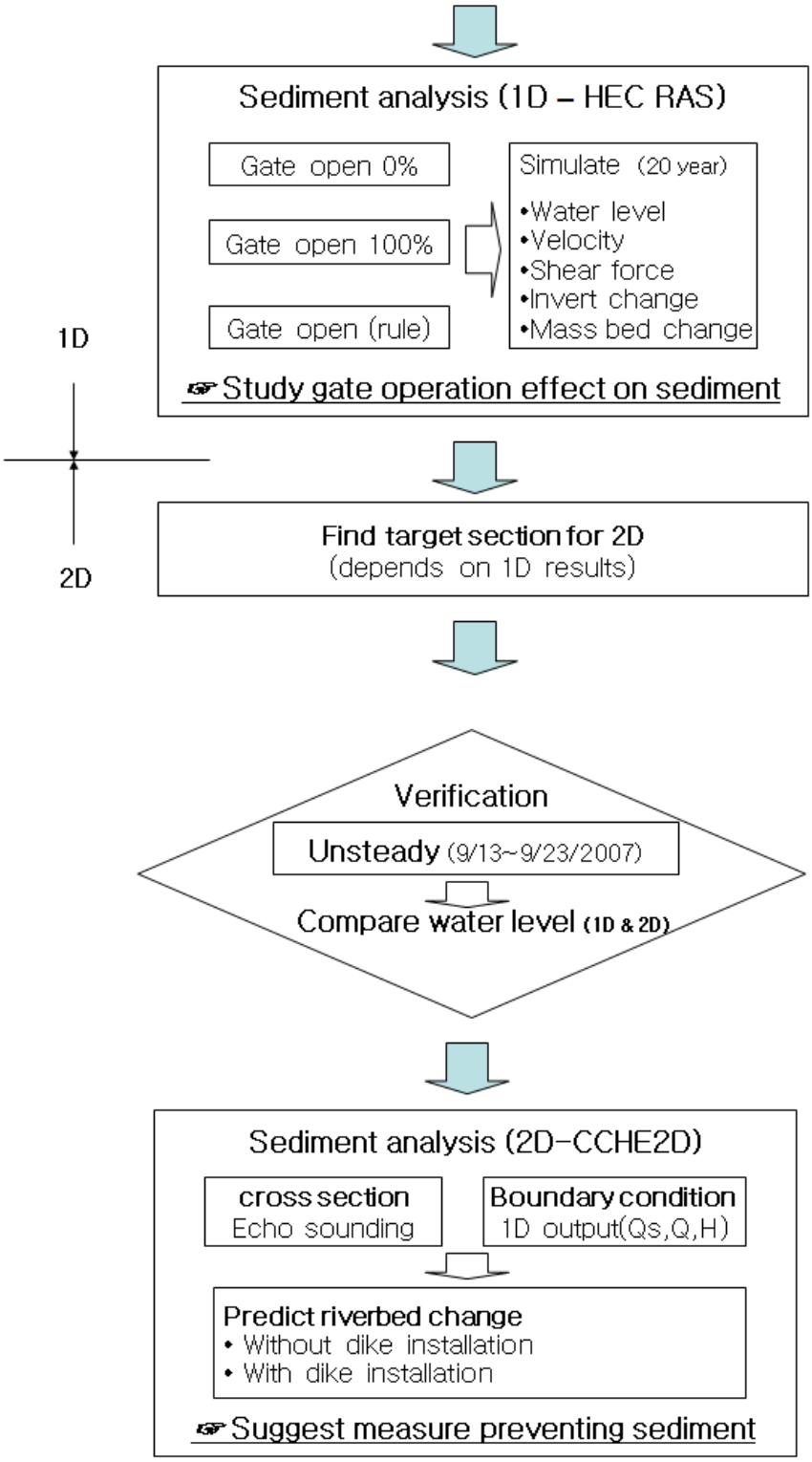

Figure 28. Continued

4.1 Development of the HEC-RAS model

The HEC-RAS 4.1 software has been developed by the United States Army Corps of Engineers Hydrology Engineering Center (HEC) for calculating and analyzing one-dimensional steady-flow, predicting water surface profiles in unsteady flow, and estimating the potential for erosion and sediment transport. The standard step method is used for steady gradually varied flow to calculate water level. Also, continuity equation (conservation of mass) and momentum equation (conservation of momentum) are used for unsteady flow analysis. The sediment continuity equation, called as Exner equation, is used for predicting sediment change over control volumes. A display using HEC-RAS in Geum River is shown in Figure 29.

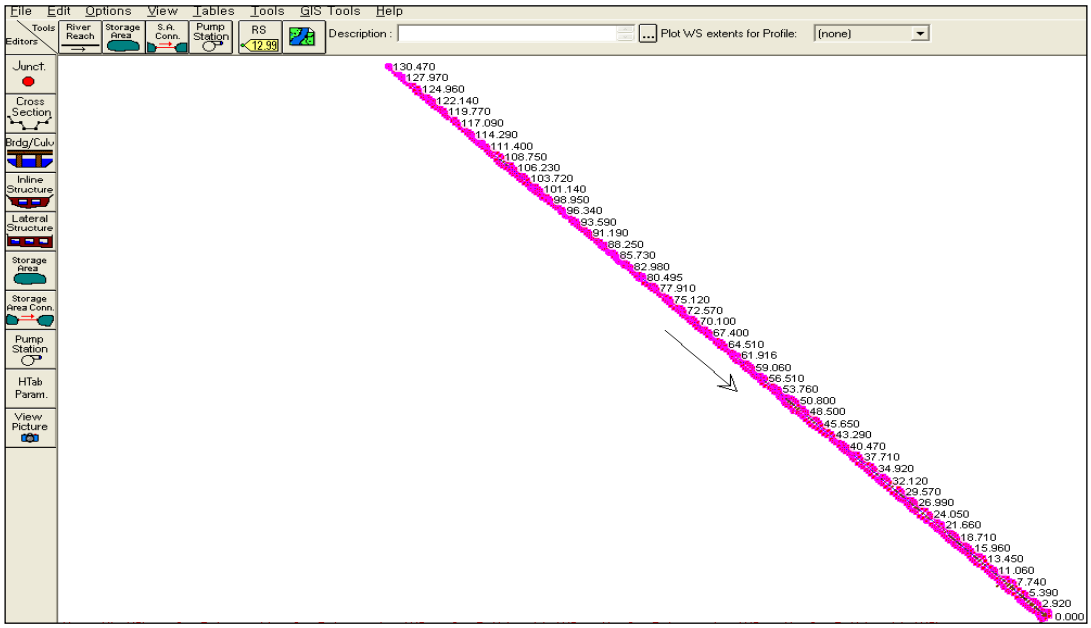

Figure 29. Main Display in HEC-RAS

In the calibration step, measured cross section data (Daejeon Regional Construction Management Administration, 2009) which was actually done in 2008 before the Four Major Rivers Restoration Project, were used assuming they were similar to cross section data of 2006 and 2007. Also, in the case of gate, Sejong weir was applied to overflow in open air, since it is a type of flap gate. Gongju and Bakje gates were applied to sluice gate, since they are a type of lifted gate, as shown in Figure 30.

(Sejong weir)

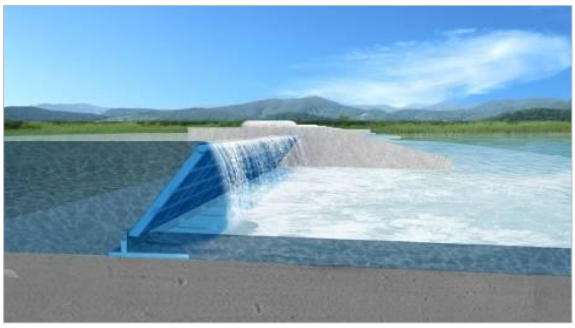

(Overflow gate)

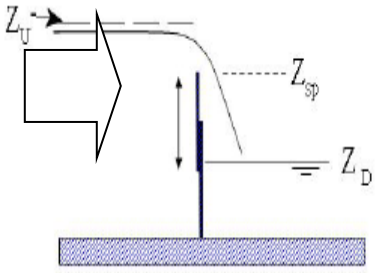

(Gongju, Bakje weir)

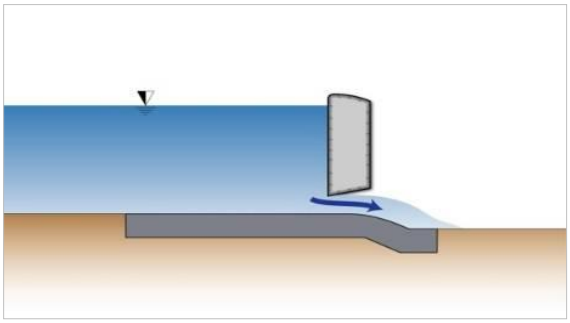

(Sluice gate)

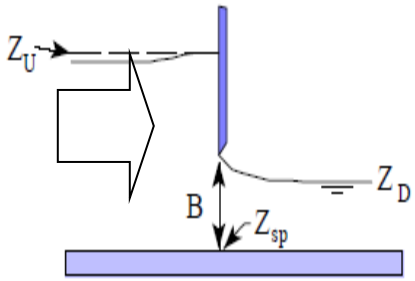

Figure 30. Gate Types in HEC-RAS

In case of sluice gate in HEC-RAS, four equations are applied to calculate discharge. First, the equation for a free flowing sluice gate is as follows:

$$Q = CWB\sqrt{2gH} \tag{4}$$

where W=the width of the gated spillway in feet, B=the height of gate opening in feet, H=the upstream energy head above the spillway crest (Zu-Zsp), and C=the coefficient of discharge. “Free Flow” means when the downstream tailwater (Z_D) do not affect the water level upstream.

Second, submergence begins to happen when the tailwater depth over the spillway divided by the headwater energy above the spillway is larger than 0.67. When a submergence of 0.8 happens, fully submerged orifice equation is applied

$$Q = CA\sqrt{2gH} \tag{5}$$

where A=the area of the gate opening, H= Zu- Z_D, and C= the coefficient of discharge.

Third, when the downstream tailwater reaches to the point at which the gate is not the condition of free flow, the transition equation between free flow and fully submerged flow is used:

$$Q = CWB\sqrt{2g3H} \tag{6}$$

where H= Zu- Z_D.

Finally, when the upstream water surface is equal to or less than the top of the gate opening, the program calculates flow as weir flow and overflow gate corresponds to this case:

$$Q = CLH^{\frac{3}{2}} \tag{7}$$

where L=the length of the spillway crest, and H=the upstream energy head above the spillway crest (Zu-Zsp).

4.1.1 Steady analysis

In steady analysis, flood data according to frequency were used as the upstream boundary condition. The flood data (up and lateral boundary condition) and water level (EL. 4.62, the downstream boundary condition) in Geum Estuary was used in Geum River Management Basic Plan (Daejeon Regional Construction Management Administration, 2009). The frequency flows of 1 dam upstream, 13 tributaries, and 6 water level stations were input, as shown in Table 7 and Gabchun, Mihochun, Yuguchun, Gichun, and Nonsanchun increase flood flow in the main river, as shown in Figure 31.

Table 7. Inflow Data in Steady Analysis in HEC-RAS

unit: ㎥/s

Type	Sta.No	Distance (m)	2yr	5yr	10yr	20yr	30yr	50yr	80yr	100yr	200yr
1	130.470	130,220	2185	3060	3660	4250	4560	4995	5385	5550	6675
2	124.960	124,710	2720	3875	4675	5455	5875	6445	6960	7175	8175
3	120.700	120,450	2740	3905	4710	5500	5925	6500	7015	7235	8225
4	108.750	108,500	4500	6055	7390	8695	9420	10340	11180	11540	12795
5	99.730	99,480	4500	6110	7460	8775	9510	10445	11295	11660	12935
6	98.360	98,110	4515	6175	7545	8875	9610	10555	11420	11790	13080
7	93.350	93,060	4515	6200	7570	8910	9650	10600	11465	11835	13130
8	84.800	84,560	4545	6295	7690	9050	9810	10780	11660	12040	13355
9	80.150	80,060	4670	6530	7985	9405	10195	11210	12130	12530	13905
10	71.110	71,110	4695	6555	8025	9450	10250	11260	12185	12580	13970
11	57.330	57,330	4900	6785	8305	9790	10620	11680	12640	13055	14490
12	52.090	52,090	4910	6790	8310	9795	10625	11680	12640	13055	14495
13	49.400	49,400	5000	6875	8420	9925	10765	11835	12810	13235	14695
14	38.220	38,220	5030	6940	8490	10010	10855	11935	12915	13340	14810
15	33.830	33,830	5305	7360	9025	10645	11550	12705	13765	14220	15790
16	24.050	24,050	5340	7440	9125	10760	11680	12845	13910	14370	15955
17	20.580	20,580	5345	7460	9145	10790	11710	12880	13945	14405	16000
18	13.450	13,450	5360	7505	9205	10860	11790	12965	14040	14505	16105
19	3.330	3,330	5365	7505	9205	10860	11790	12970	14045	14510	16115
20	0.720	720	5405	7555	9275	10945	11880	13070	14155	14625	16240

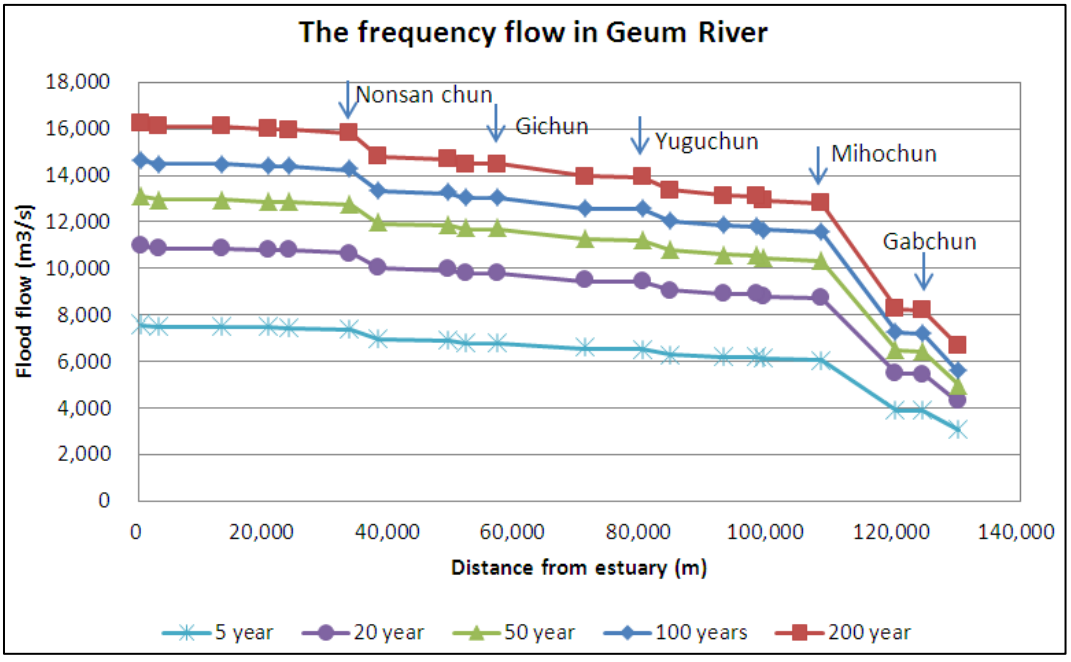

Figure 31. Frequency Flow in Geum River

4.1.2 Unsteady analysis

To calibrate the model, rainfall events in the flood season are necessary, since they include various amounts of discharge. As a result of plotting discharge values for 2006-2007, 7.6-8.7.2006 and 8.27-9.23.2007 were chosen, as shown in Figures 32 and 33.

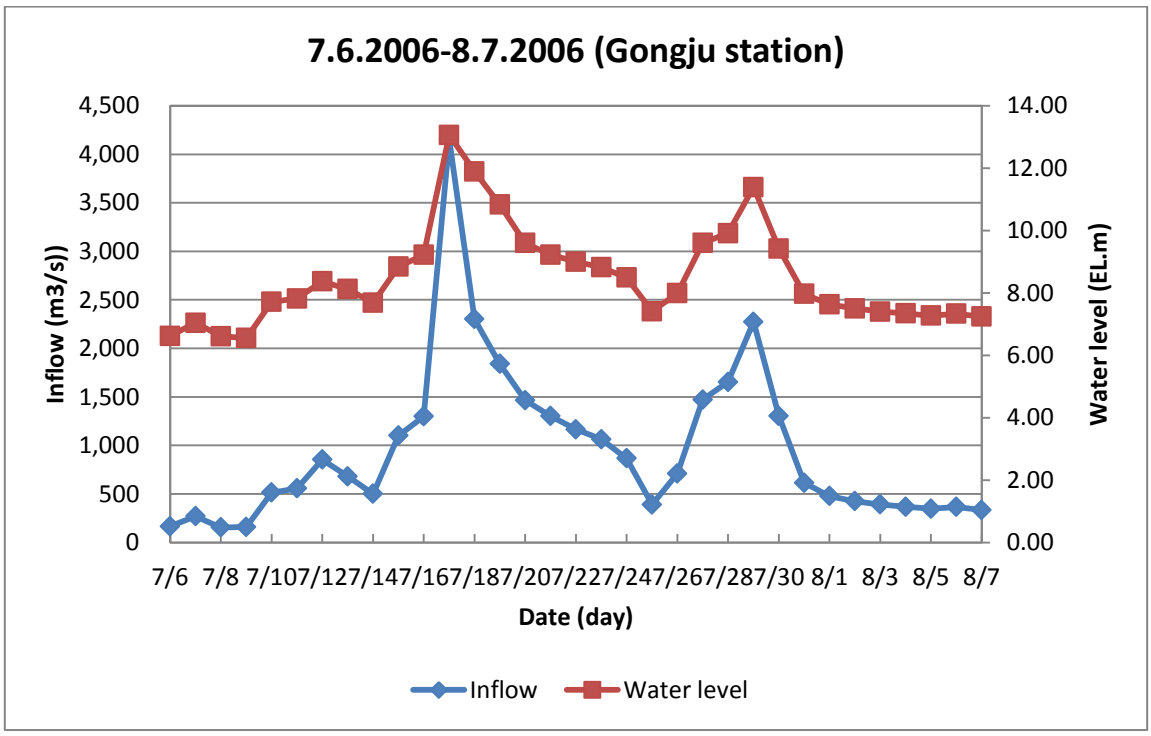

Figure 32. Flood Events in 2006

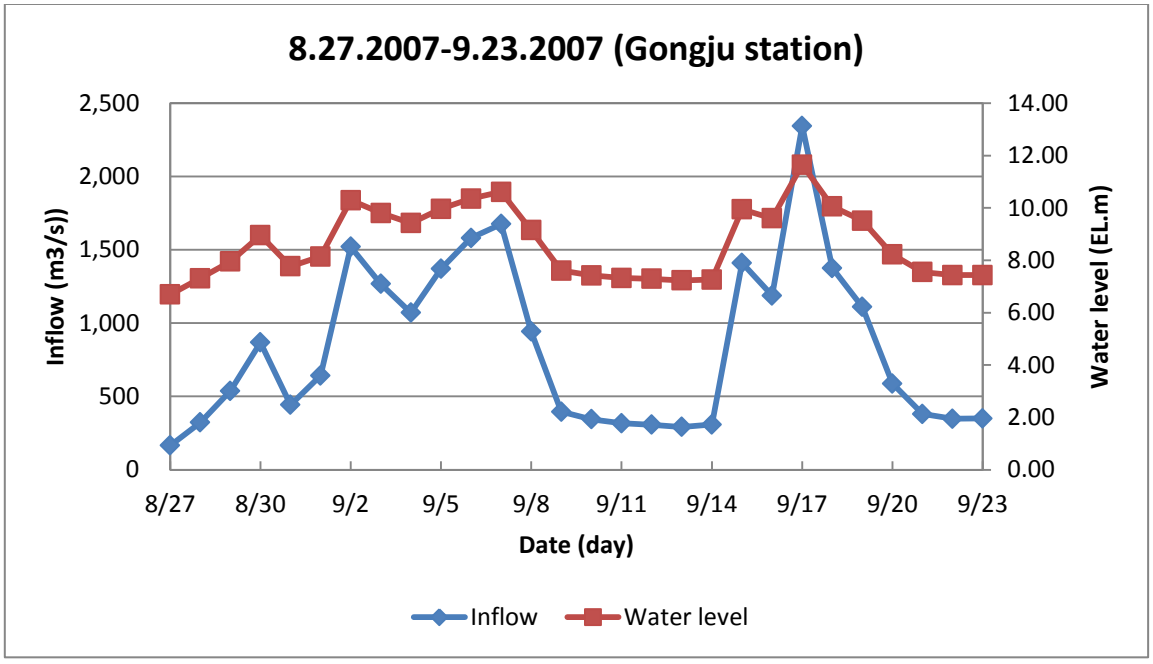

Figure 33. Flood Events in 2007

To obtain daily gate height reflecting the gate operation rule, it is necessary to set a management water level which is seen in Figure 34 (Ministry of Land, Transport and Maritime Affairs, 2009).

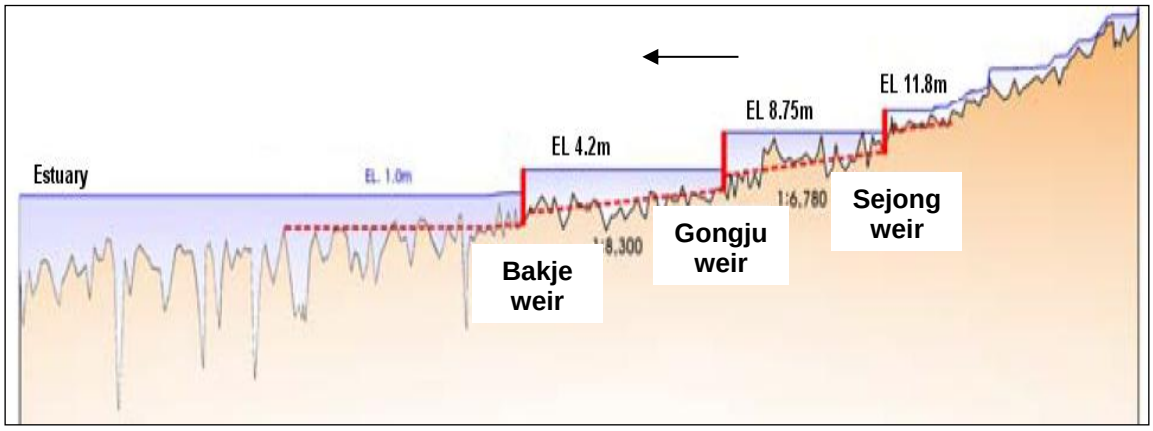

Figure 34. Management Water Level

Water level stations, located upstream of the weirs, were chosen as a reference section to monitor management water level: Sejong weir's reference section is upstream of Gyumnam station (Station No 101.882), Gongju weir's reference section is upstream of Gongju station (Station No 85.075), and Bakje's reference section is Jindu station (Station No 71.110), as shown in Figure 35. The gate opening and closing speed was set at 0.3 m/min. In unsteady analysis, computational interval must be set shortly to abruptly overcome water level. So, a 5 minute interval was input and other input data, including gate, are shown in Figure 36 to 40.

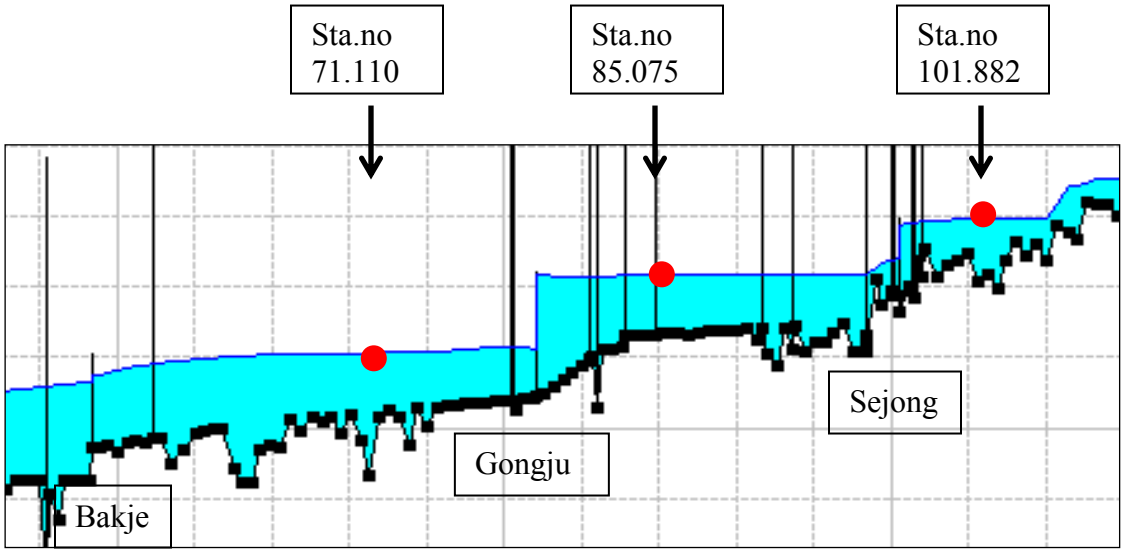

Figure 35. Reference Sections for Monitoring

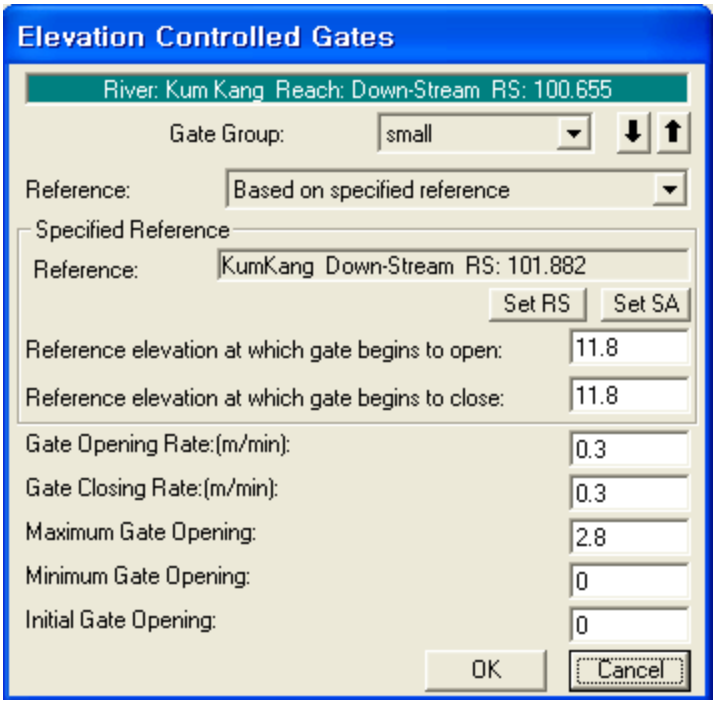

Figure 36. Gate Option in HEC-RAS (Sejong)

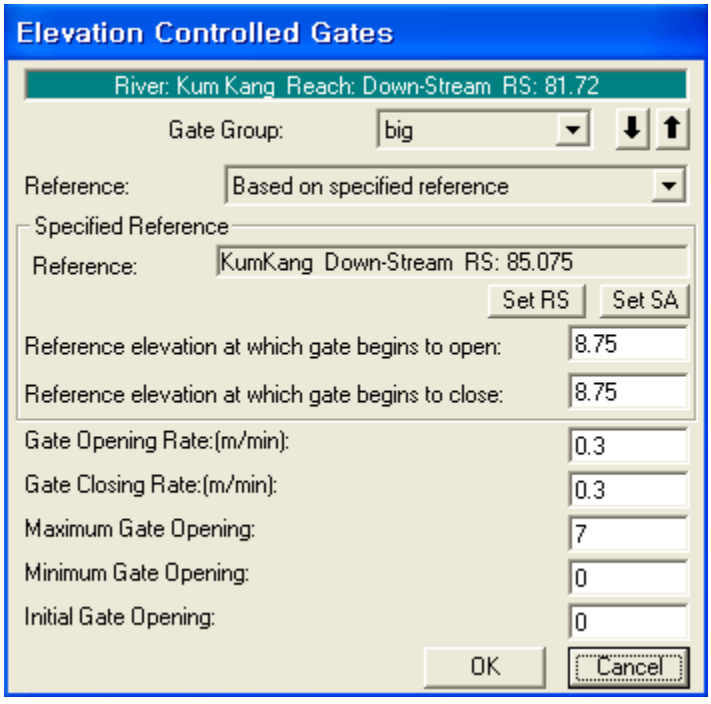

Figure 37. Gate Option in HEC-RAS (Gongju)

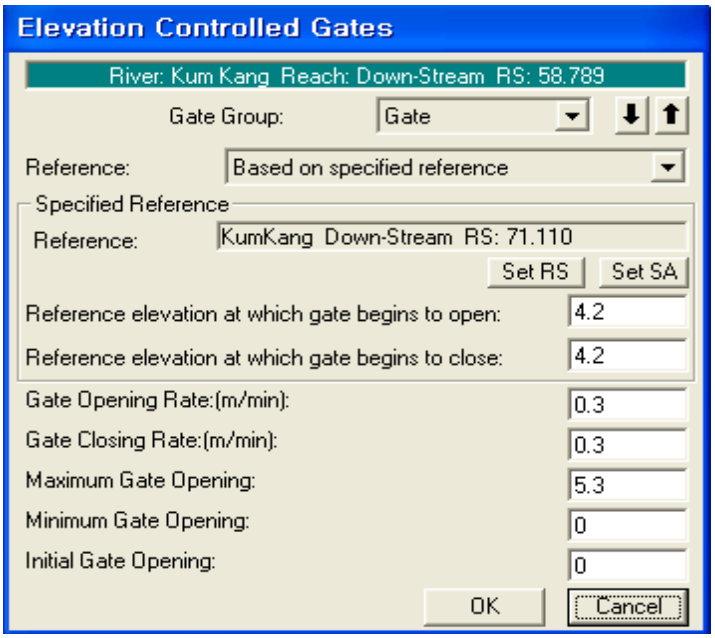

Figure 38. Gate Option in HEC-RAS (Bakje)

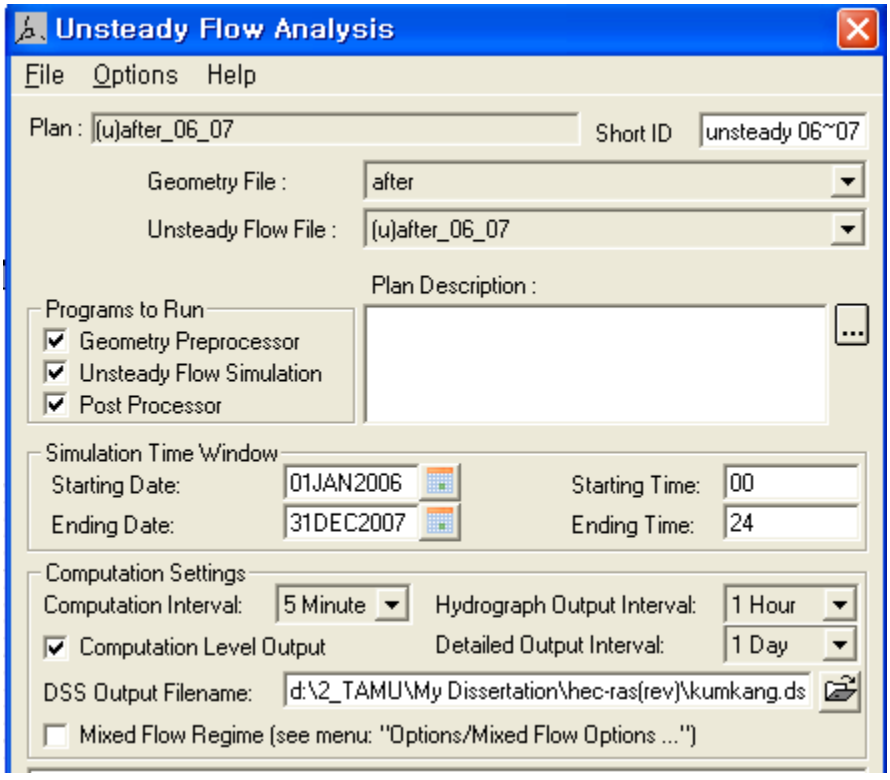

Figure 39. Unsteady Plan Data

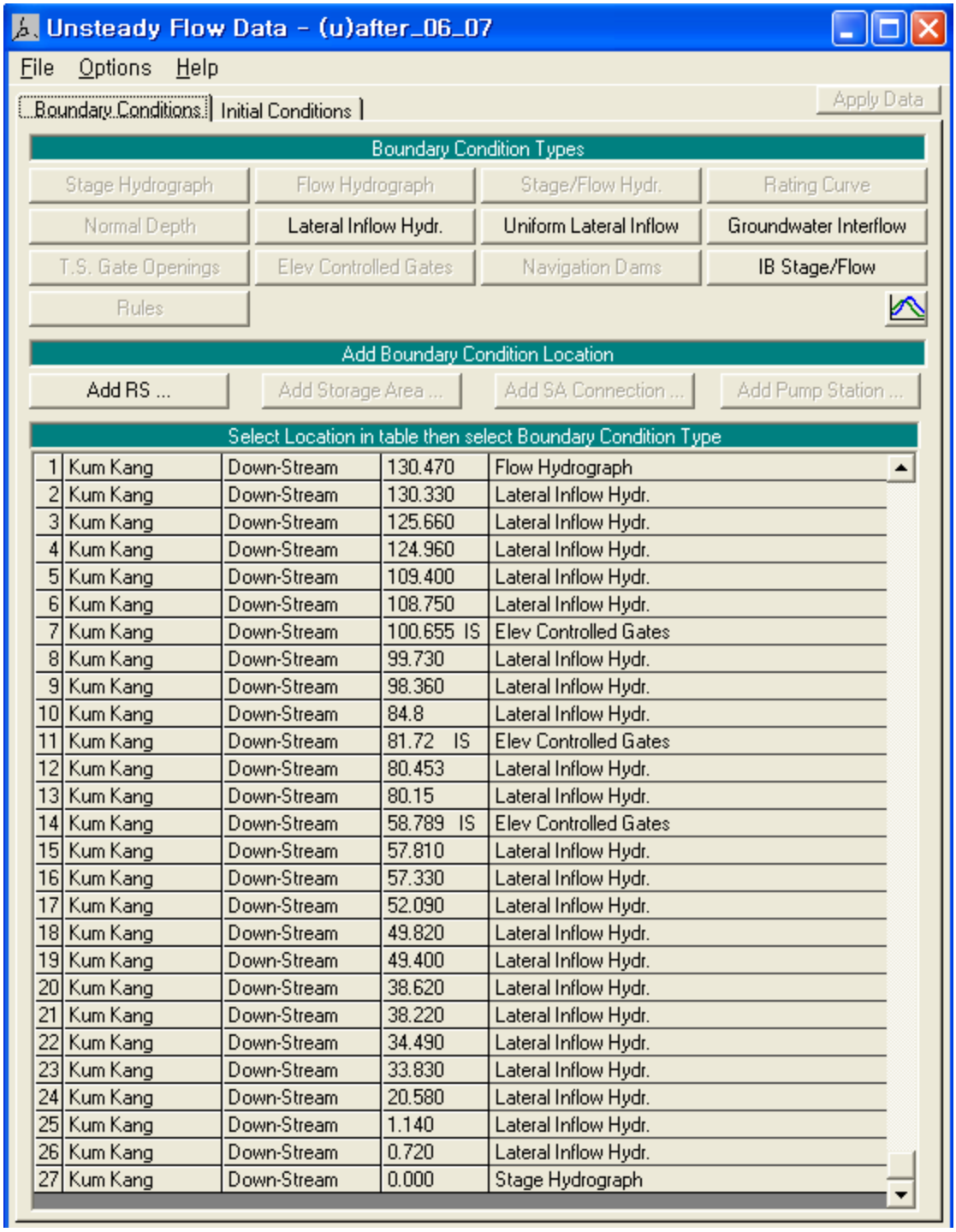

1	Kum Kang	Down-Stream	130.470	Flow Hydrograph
2	Kum Kang	Down-Stream	130.330	Lateral Inflow Hydr.
3	Kum Kang	Down-Stream	125.660	Lateral Inflow Hydr.
4	Kum Kang	Down-Stream	124.960	Lateral Inflow Hydr.
5	Kum Kang	Down-Stream	109.400	Lateral Inflow Hydr.
6	Kum Kang	Down-Stream	108.750	Lateral Inflow Hydr.
7	Kum Kang	Down-Stream	100.655 IS	Elev Controlled Gates
8	Kum Kang	Down-Stream	99.730	Lateral Inflow Hydr.
9	Kum Kang	Down-Stream	98.360	Lateral Inflow Hydr.
10	Kum Kang	Down-Stream	84.8	Lateral Inflow Hydr.
11	Kum Kang	Down-Stream	81.72 IS	Elev Controlled Gates
12	Kum Kang	Down-Stream	80.453	Lateral Inflow Hydr.
13	Kum Kang	Down-Stream	80.15	Lateral Inflow Hydr.
14	Kum Kang	Down-Stream	58.789 IS	Elev Controlled Gates
15	Kum Kang	Down-Stream	57.810	Lateral Inflow Hydr.
16	Kum Kang	Down-Stream	57.330	Lateral Inflow Hydr.
17	Kum Kang	Down-Stream	52.090	Lateral Inflow Hydr.
18	Kum Kang	Down-Stream	49.820	Lateral Inflow Hydr.
19	Kum Kang	Down-Stream	49.400	Lateral Inflow Hydr.
20	Kum Kang	Down-Stream	38.620	Lateral Inflow Hydr.
21	Kum Kang	Down-Stream	38.220	Lateral Inflow Hydr.
22	Kum Kang	Down-Stream	34.490	Lateral Inflow Hydr.
23	Kum Kang	Down-Stream	33.830	Lateral Inflow Hydr.
24	Kum Kang	Down-Stream	20.580	Lateral Inflow Hydr.
25	Kum Kang	Down-Stream	1.140	Lateral Inflow Hydr.
26	Kum Kang	Down-Stream	0.720	Lateral Inflow Hydr.
27	Kum Kang	Down-Stream	0.000	Stage Hydrograph

Figure 40. Unsteady Flow Data

After simulating unsteady analysis, hourly gate opening height was converted to daily height through averaging and we can also see gates are full open in flood season, as shown in Figure 41. In this way, results of a 2 year event (2006~2007) are shown in Figure 42 to 44 and this value was repeated for 20 years for sediment analysis.

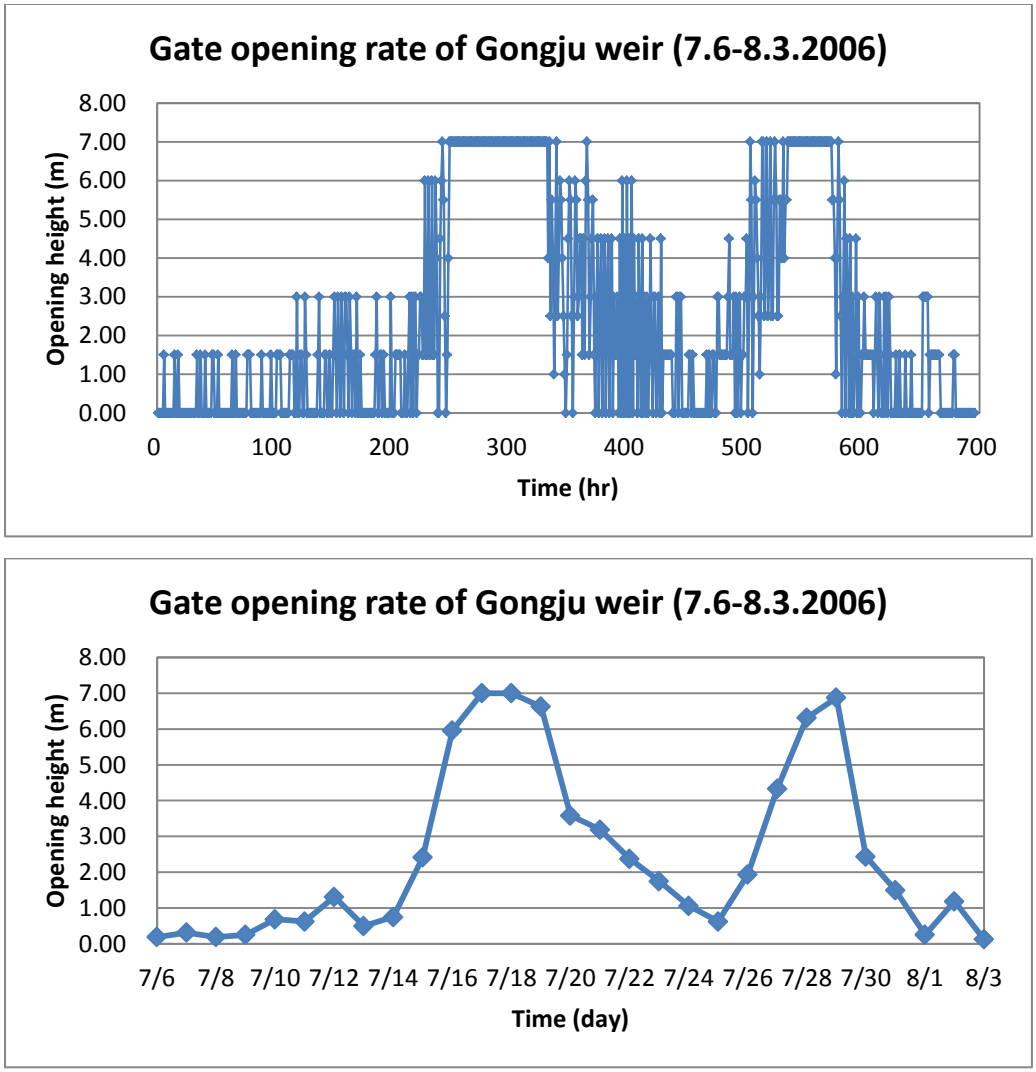

Figure 41. Gate Opening Rate of Gongju Weir (up: hourly, down: daily)

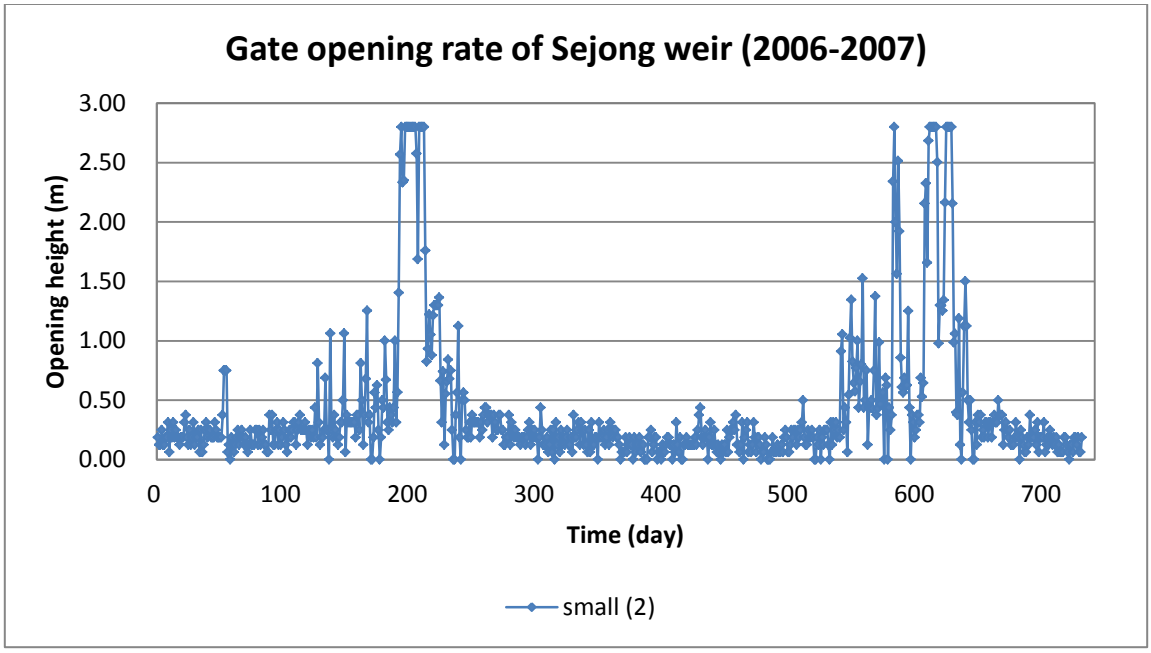

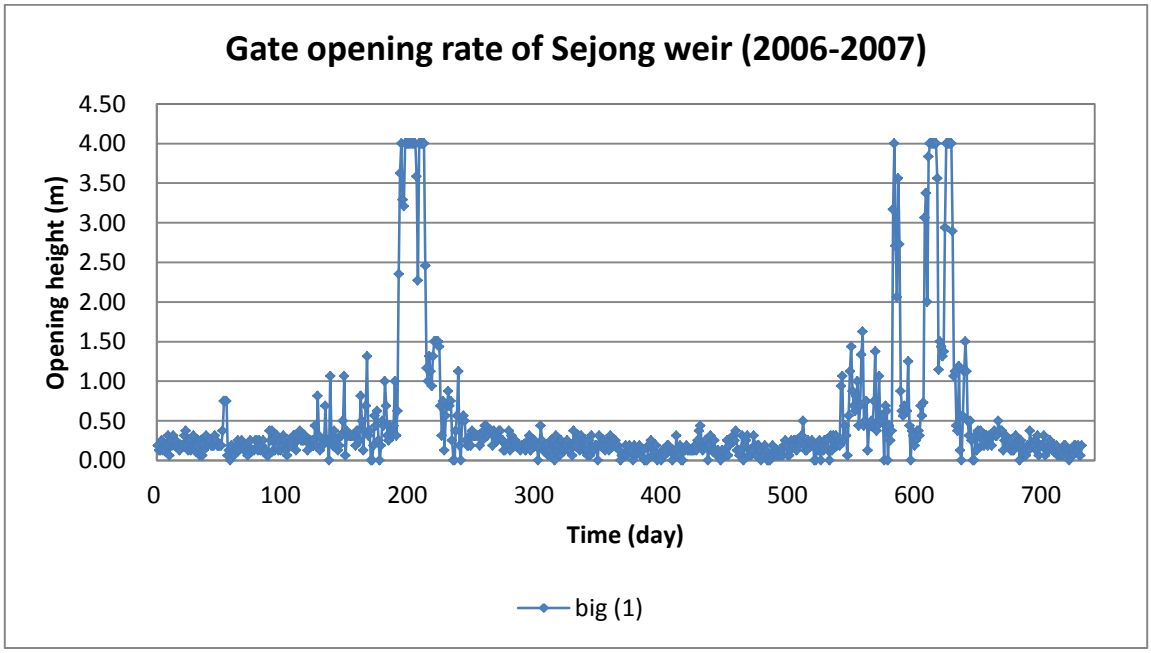

Figure 42. Gate Opening Rate of Sejong Weir (up: small gate, down: big gate)

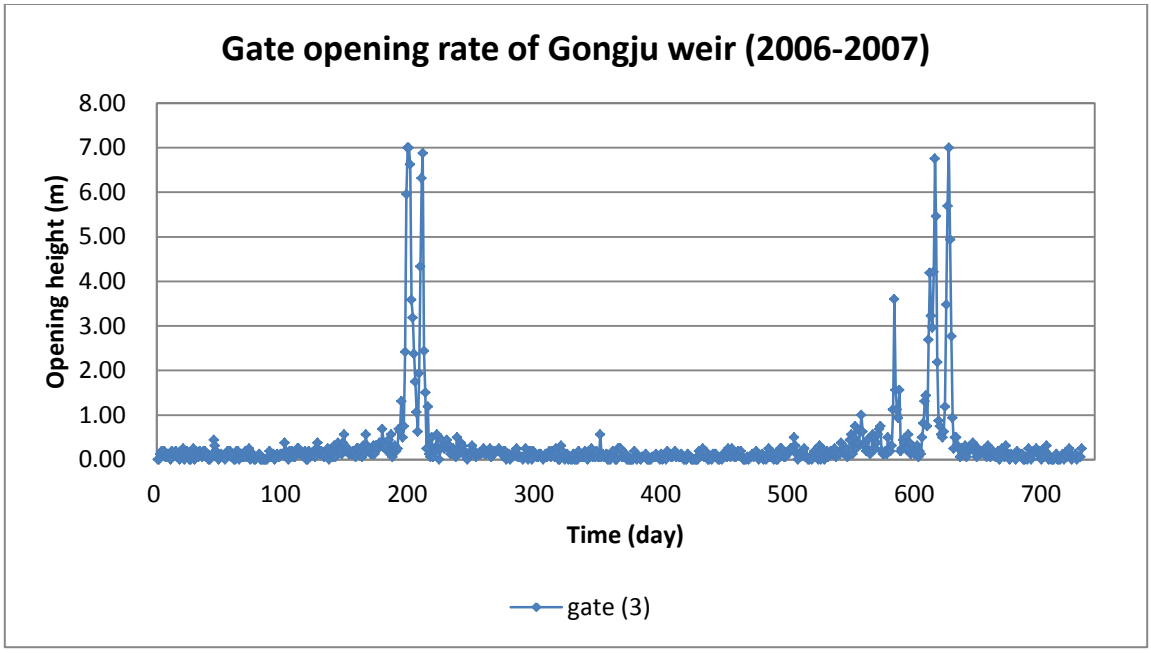

Figure 43. Gate Opening Rate of Gongju Weir

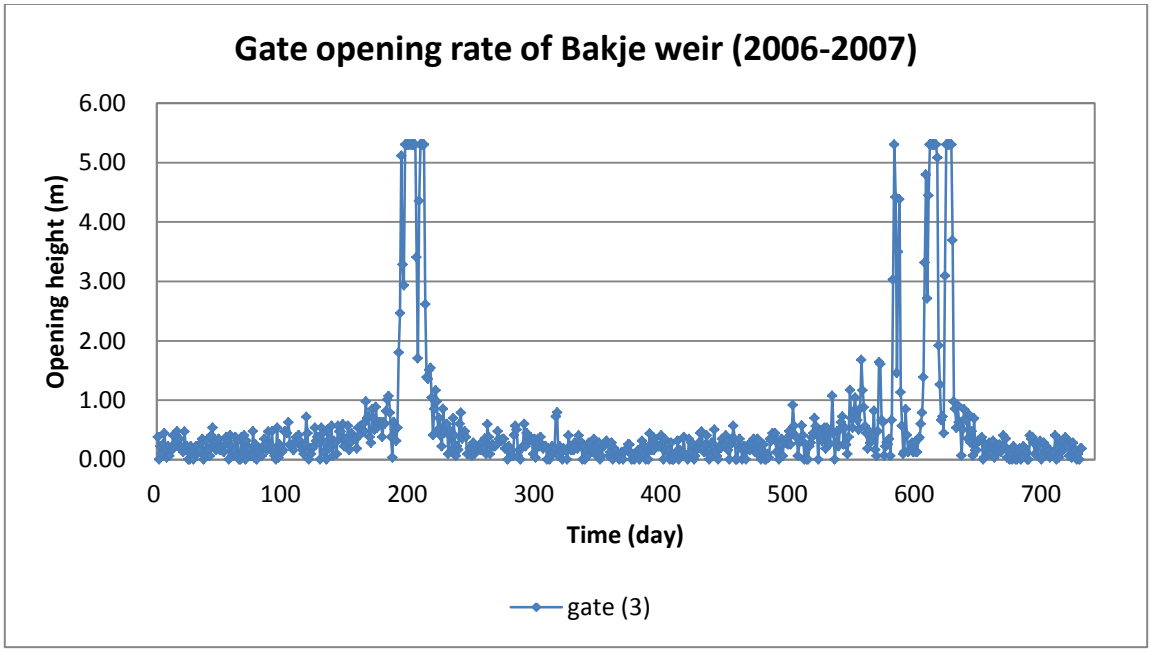

Figure 44. Gate Opening Rate of Bakje Weir

4.1.3 Sediment analysis (quasi-unsteady flow)

To simulate riverbed change, quasi-unsteady flow analysis was used. This case assumed an approximate continuous hydrograph with a series of discrete steady flow profiles, as shown in Figure 45, and was based on the sediment continuity equation, known as the Exner equation. The procedure to calculate sediment discharge in HEC-RAS is shown in Figure 46. The left side means the change in sediment volume, and right side means the difference between inflow sediment load and outflow sediment load. Inflow sediment load is entered as the upstream sediment and lateral sediment inflow with given discharge by the boundary condition. And transport capacities are then calculated for each cross section in the downstream direction, and the difference between the inflowing sediment load and the sediment transport capacity results in the net aggregation or degradation of the bed. If the inflow sediment load was larger than the outflow sediment load, deposition happened and fall velocity was used as the deposition limit. On the other hand, if the outflow sediment load was larger, the channel was subjected to erosion.

In this case, time dependent modifiers were applied to the surplus and deficit, respectively, using deposition rate which is a function of falling velocity and entrainment coefficient which is a function of characteristic length, because solution of the Exner equation will result in 100% of the computed surplus or deficit translating immediately into deposition or erosion, so this does not reflect on actual physical process.

The mass was converted into movable cross section or wetted section and the river bed change was calculated based on the amount of material added or removed before the hydrodynamics for the next flow was computed.

We can use sediment transport capacity with 6 equations for outflow sediment load with the initial condition in HEC-RAS: Ackers-White, Engelund-Hansen, Laursen, Meyer-Peter Muller, Toffaleti, and Yang. ASCE ranked these equations using 40 sets of field data and 165 sets of flume data, as shown in Table 8. Therefore, Yang, Laursen, and Ackers- White equation for bed-material load were chosen for sediment analysis. Especially, Laursen equation was chosen because it covered a vast range of sediments from 0.011 to 29 mm, so it was anticipated to represent well the characteristics of the Geum River.

Besides, the Toffaleti (1968) equation was formulated using regression on temperature and an empirical exponent that describes the relationship between sediment and hydraulic characteristics. This equation is considered as a 'large river' function, since many of the data sets used to develop it were for large suspended load systems (U.S. Army Corps of Engineers, 2010). Hence, it is appropriate for the Geum River. For the above reasons, four transport functions, which are Yang, Laursen, Ackers-White, and Toffaleti equations, were chosen for sediment transport capacity. The fall velocity method was computed using the Ruby equation and the maximum depth was input with 3.5 m (Daejeon Regional Construction Management Administration, 2009) except for the weir section (maximum depth = 0), as shown in Figures 47 to 49.

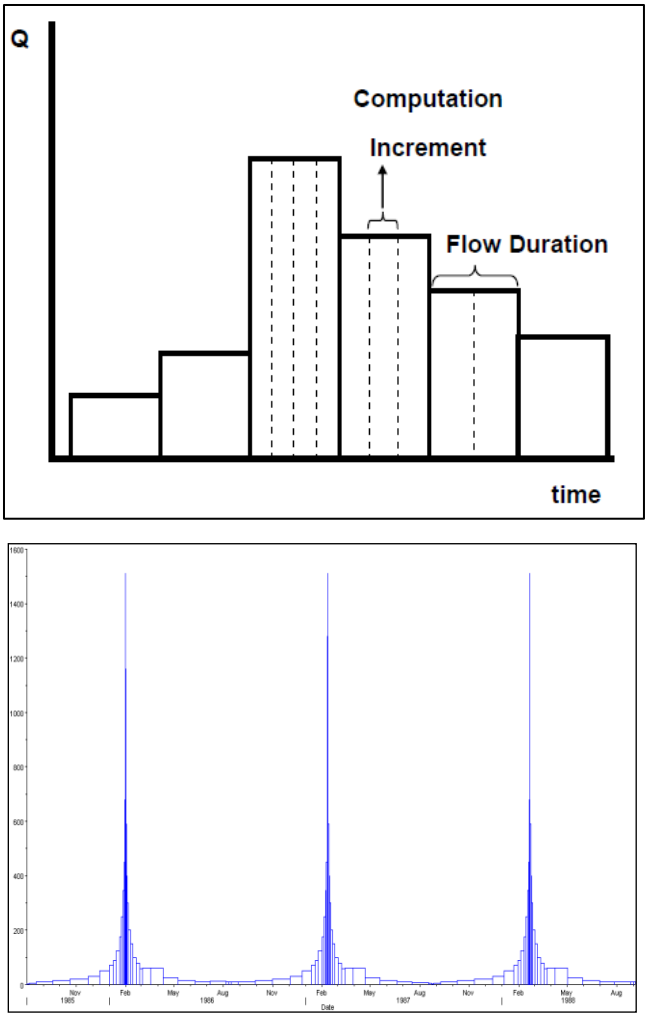

Figure 45. Concept of Quasi Unsteady Flows

Table 8. Summary of Sediment-Transport Equations Ranking by ASCE (1982)

Rank	Equation	Type
1	Yang (1973)	Bed-material load
2	Laursen (1958)	Bed-material load
3	Ackers and White (1973)	Bed-material load
4	Engelund and Hansen (1967)	Bed-material load
5	Bagnold (1956)	Bed load
6	Meyer-Peter and Muller (1948) and Einstein (1950)	Bed-material load
7	Meyer-Peter and Muller (1948)	Bed load
8	Yalin (1963)	Bed load

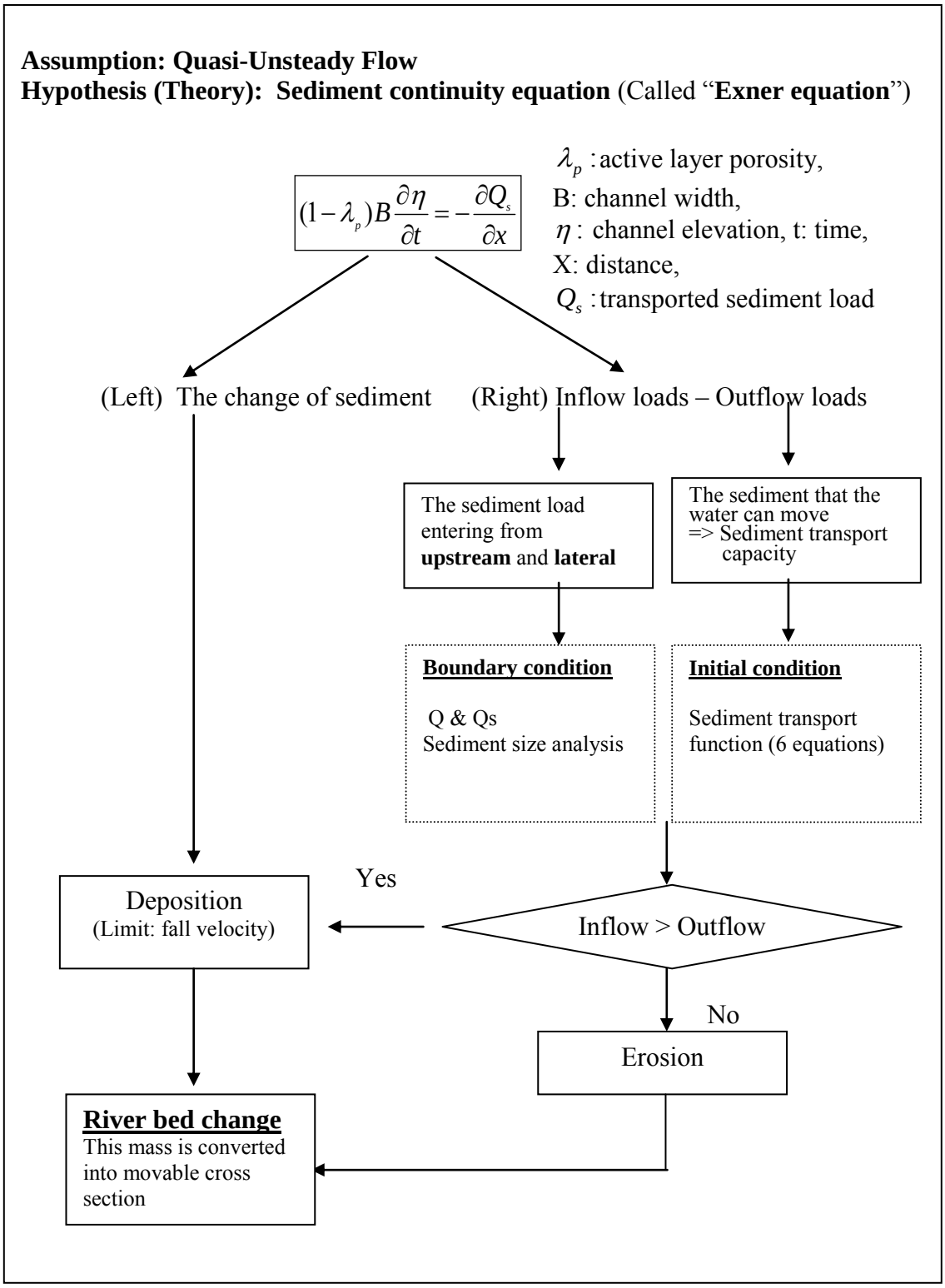

Figure 46. Procedure to Analyze Sediment in HEC-RAS

File Options View Help

Initial Conditions and Transport Parameters | Boundary Conditions

River: (All Rivers) | Transport Function: Yang | Define/Edit Bed Gradation ...

Reach: | Sorting Method: Exner 5

Fall Velocity Method: Ruby

	River	Reach	RS	Invert	Max Depth	Min Elev	Sta Left	Sta Right	Bed Grad
28	Kum Kang	Down-Stream	124.460	18.03	3.5		0	649.5	141
29	Kum Kang	Down-Stream	124.010	18.38	3.5		0	933.5	140
30	Kum Kang	Down-Stream	123.470	19.26	3.5		32.5	493	140
31	Kum Kang	Down-Stream	122.990	18.17	3.5		132.6	700	140
32	Kum Kang	Down-Stream	122.490	17.71	3.5		154	720	140
33	Kum Kang	Down-Stream	122.140	16.71	3.5		143.3	627.8	140
34	Kum Kang	Down-Stream	121.770	16.66	3.5		0	570.5	139
35	Kum Kang	Down-Stream	121.260	14.62	3.5		0	754.4	139
36	Kum Kang	Down-Stream	120.700	16.75	3.5		47.5	491	138
37	Kum Kang	Down-Stream	120.190	16.21	3.5		0	350.4	138
38	Kum Kang	Down-Stream	119.770	15.68	3.5		92.4	516.2	138
39	Kum Kang	Down-Stream	119.230	14.81	3.5		48	348.5	137
40	Kum Kang	Down-Stream	118.800	15.58	3.5		38.8	351.8	137
41	Kum Kang	Down-Stream	118.370	15.45	3.5		0	350.2	136
42	Kum Kang	Down-Stream	117.620	14.6	3.5		0	418.2	136
43	Kum Kang	Down-Stream	117.090	14.17	3.5		0	366.5	136

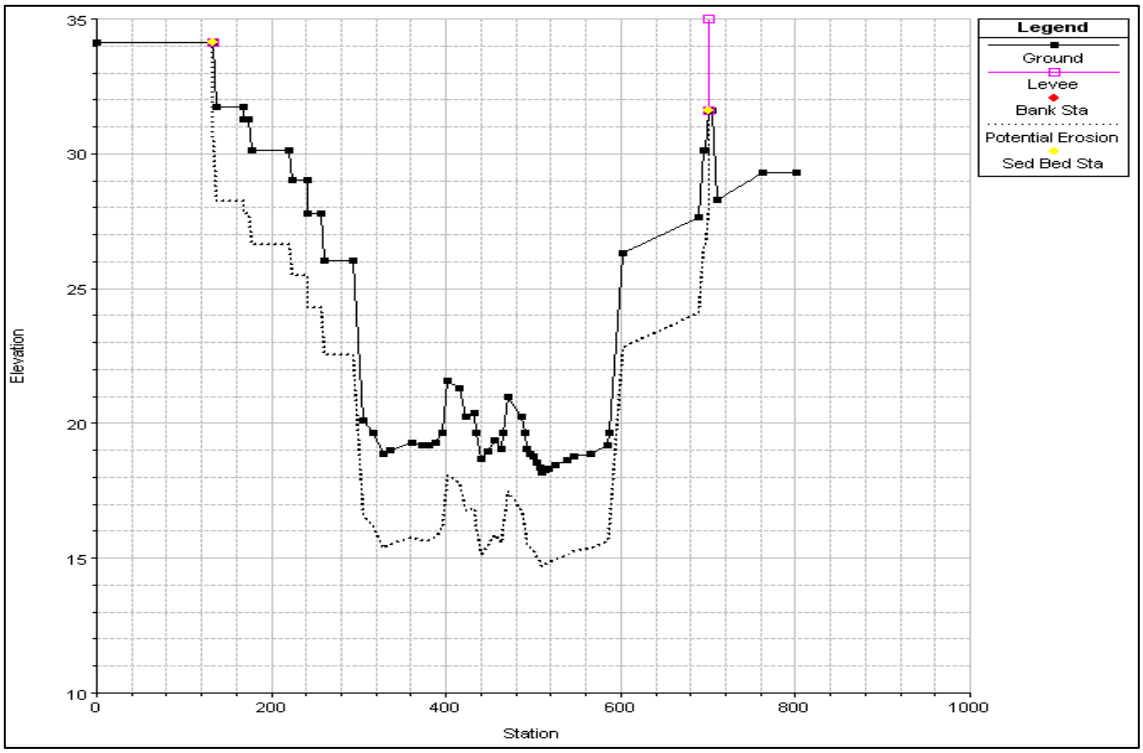

Figure 47. Sediment Data in HEC-RAS

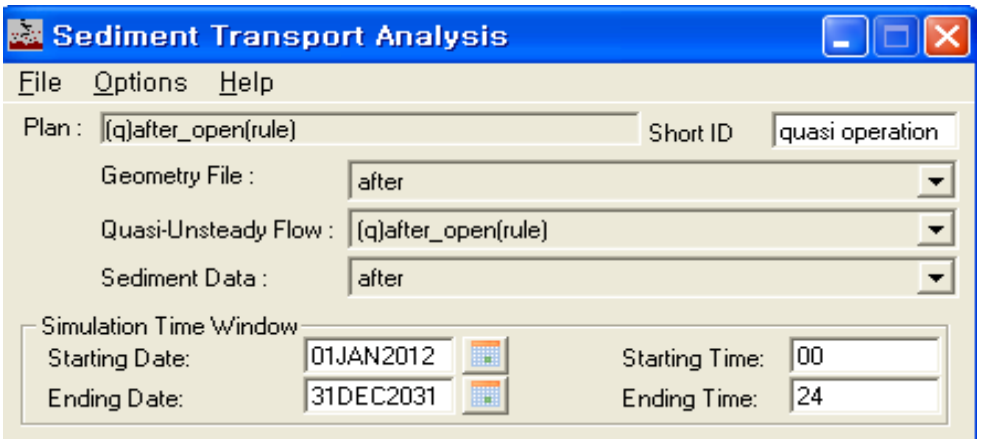

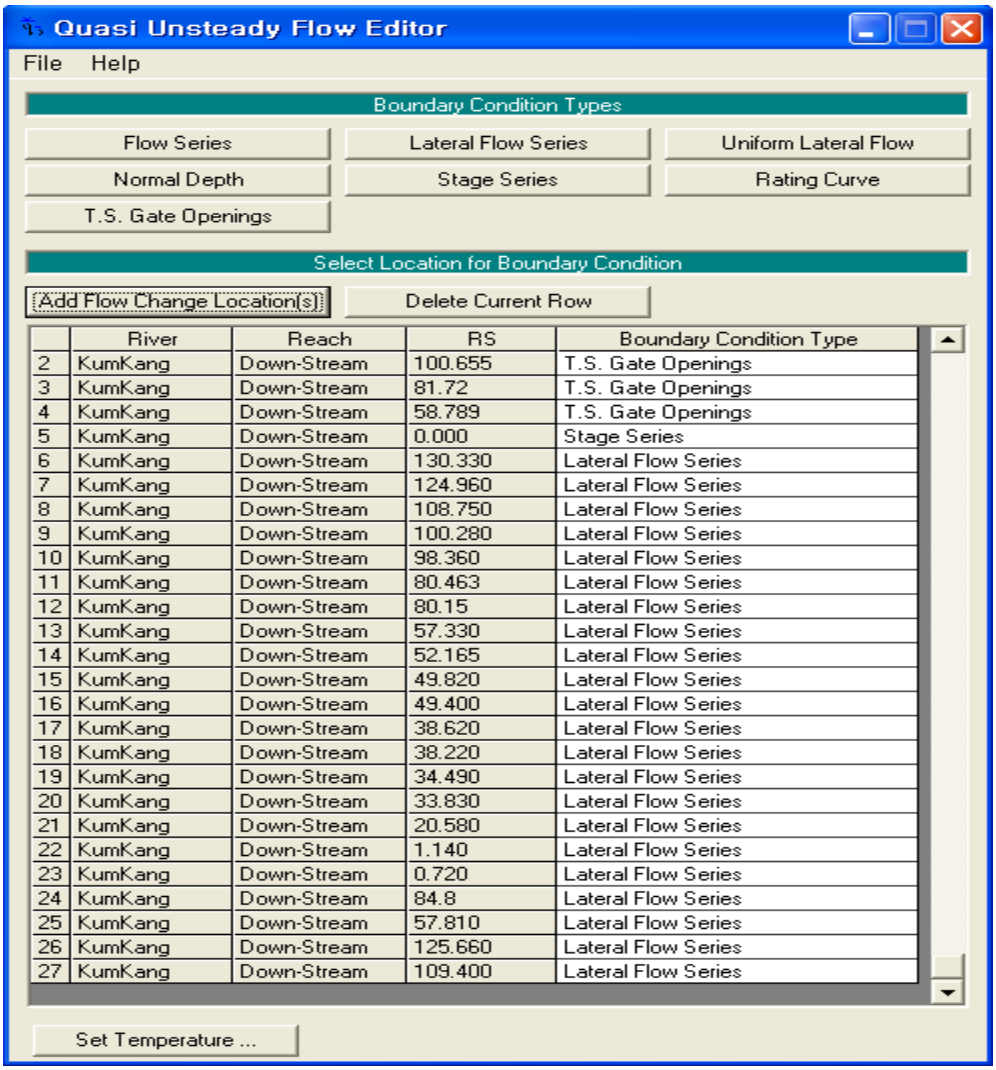

	River	Reach	RS	Boundary Condition Type
2	KumKang	Down-Stream	100.655	T.S. Gate Openings
3	KumKang	Down-Stream	81.72	T.S. Gate Openings
4	KumKang	Down-Stream	58.789	T.S. Gate Openings
5	KumKang	Down-Stream	0.000	Stage Series
6	KumKang	Down-Stream	130.330	Lateral Flow Series
7	KumKang	Down-Stream	124.960	Lateral Flow Series
8	KumKang	Down-Stream	108.750	Lateral Flow Series
9	KumKang	Down-Stream	100.280	Lateral Flow Series
10	KumKang	Down-Stream	98.360	Lateral Flow Series
11	KumKang	Down-Stream	80.463	Lateral Flow Series
12	KumKang	Down-Stream	80.15	Lateral Flow Series
13	KumKang	Down-Stream	57.330	Lateral Flow Series
14	KumKang	Down-Stream	52.165	Lateral Flow Series
15	KumKang	Down-Stream	49.820	Lateral Flow Series
16	KumKang	Down-Stream	49.400	Lateral Flow Series
17	KumKang	Down-Stream	38.620	Lateral Flow Series
18	KumKang	Down-Stream	38.220	Lateral Flow Series
19	KumKang	Down-Stream	34.490	Lateral Flow Series
20	KumKang	Down-Stream	33.830	Lateral Flow Series
21	KumKang	Down-Stream	20.580	Lateral Flow Series
22	KumKang	Down-Stream	1.140	Lateral Flow Series
23	KumKang	Down-Stream	0.720	Lateral Flow Series
24	KumKang	Down-Stream	84.8	Lateral Flow Series
25	KumKang	Down-Stream	57.810	Lateral Flow Series
26	KumKang	Down-Stream	125.660	Lateral Flow Series
27	KumKang	Down-Stream	109.400	Lateral Flow Series

Figure 48. Quasi-Unsteady Flow Data in HEC-RAS

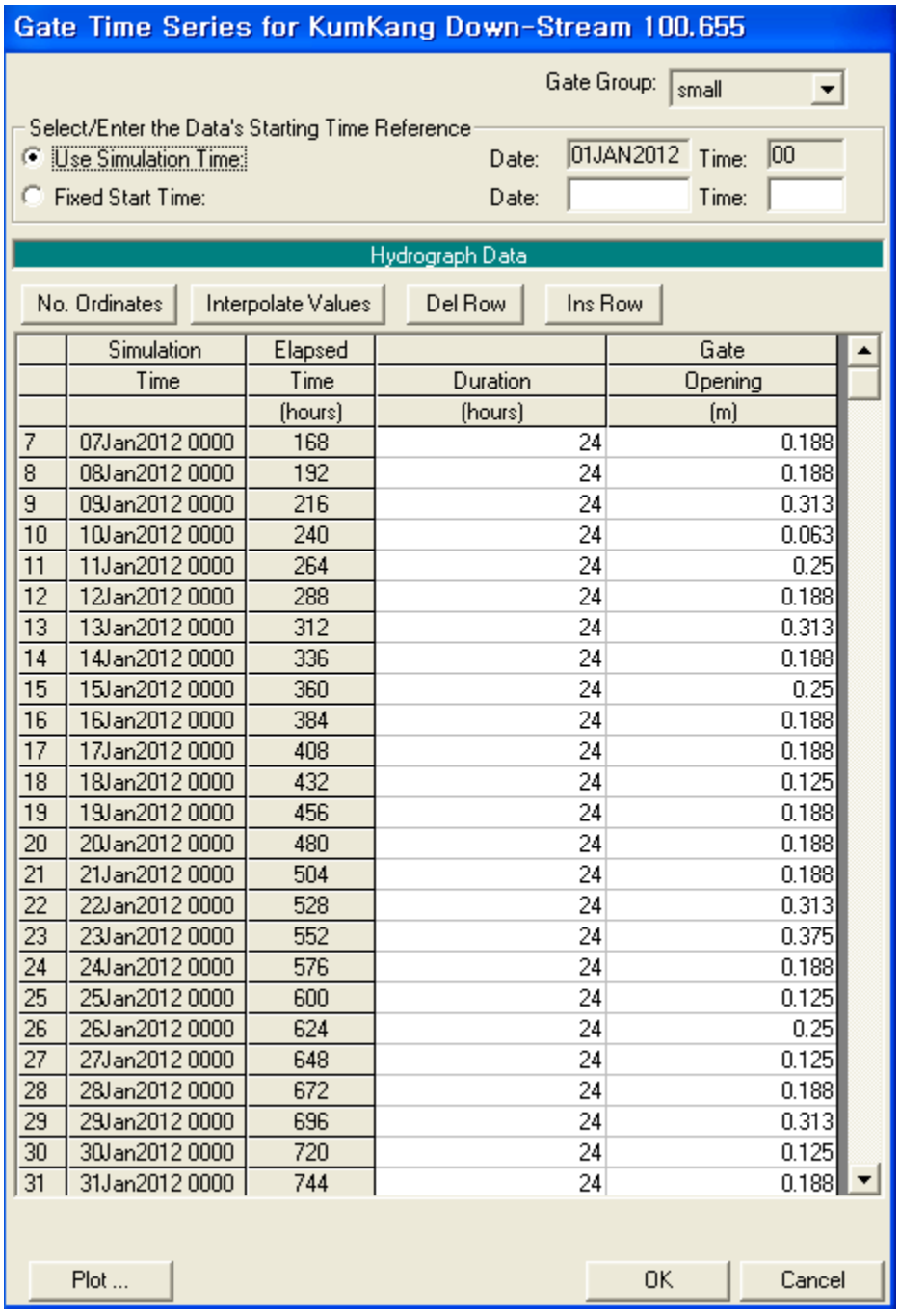

	Simulation Time	Elapsed Time (hours)	Duration (hours)	Gate Opening (m)
7	07Jan2012 0000	168	24	0.188
8	08Jan2012 0000	192	24	0.188
9	09Jan2012 0000	216	24	0.313
10	10Jan2012 0000	240	24	0.063
11	11Jan2012 0000	264	24	0.25
12	12Jan2012 0000	288	24	0.188
13	13Jan2012 0000	312	24	0.313
14	14Jan2012 0000	336	24	0.188
15	15Jan2012 0000	360	24	0.25
16	16Jan2012 0000	384	24	0.188
17	17Jan2012 0000	408	24	0.188
18	18Jan2012 0000	432	24	0.125
19	19Jan2012 0000	456	24	0.188
20	20Jan2012 0000	480	24	0.188
21	21Jan2012 0000	504	24	0.188
22	22Jan2012 0000	528	24	0.313
23	23Jan2012 0000	552	24	0.375
24	24Jan2012 0000	576	24	0.188
25	25Jan2012 0000	600	24	0.125
26	26Jan2012 0000	624	24	0.25
27	27Jan2012 0000	648	24	0.125
28	28Jan2012 0000	672	24	0.188
29	29Jan2012 0000	696	24	0.313
30	30Jan2012 0000	720	24	0.125
31	31Jan2012 0000	744	24	0.188

Figure 49. Gate Times Series Data in HEC-RAS (Sejong weir)

Due to the non-linear nature of alluvial sediment movement, transport is usually concentrated during large, peak flow events. These events are usually of relatively short duration and are characterized by rapidly changing flow. Because of this non-linearity, an irregular time step is desirable. Low flows, corresponding to small or moderate transport, are often approximated with large time steps. More detail (shorter time step) is beneficial during large flow and high transport regions of the hydrograph. So, considering flow event at Gongju water level station (Sta. No 85.07), computation intervals were classified into several steps according to flow, as shown in Figure 50.

Hydrograph Data

No. Ordinates | Interpolate Values | Del Row | Ins Row

	Simulation Time	Elapsed Time (hours)	Flow Duration (hours)	Computation Increment (hours)	Lateral Flow (m3/s)
1	01Jan2012 0000	24	24	24	1.91
2	02Jan2012 0000	48	24	24	6.37
3	03Jan2012 0000	72	24	24	1.75
4	04Jan2012 0000	96	24	24	2.54
5	05Jan2012 0000	120	24	24	10.71
6	06Jan2012 0000	144	24	24	5.56
7	07Jan2012 0000	168	24	24	1.58
8	08Jan2012 0000	192	24	24	3.39
9	09Jan2012 0000	216	24	24	10.98
10	10Jan2012 0000	240	24	24	11.01
11	11Jan2012 0000	264	24	24	1.52
12	12Jan2012 0000	288	24	24	3.79
13	13Jan2012 0000	312	24	24	8.64
14	14Jan2012 0000	336	24	24	2.4
15	15Jan2012 0000	360	24	24	16.1
16	16Jan2012 0000	384	24	24	34.76

☑ Compute computation increments based on flow

	Qlow	Qhigh	CI
1	0	500	24
2	500	1000	6
3	1000	1500	2
4	1500	4000	1

Figure 50. Computation Increments for Sediment Analysis

4.2 Development of the CCHE2D model

The CCHE2D (National **C**enter for **C**omputational **H**ydroscience and **E**ngineering's **2**-**D**imensional Model) is a hydrodynamic model for unsteady turbulent open channel flow and sediment transport simulation developed at the National Center for Computational Hydrosciences and Engineering (NCCHE), School of Engineering, the University of Mississippi. The CCHE2D model is based on the depth integrated two-dimensional equations.

Continuity Equation:

$$\frac{\partial Z}{\partial t}+\frac{\partial (hu)}{\partial x}+\frac{\partial (hv)}{\partial y}=0 \tag{8}$$

Momentum Equations:

$$\frac{\partial u}{\partial t}+u\frac{\partial u}{\partial x}+v\frac{\partial u}{\partial y}=-g\frac{\partial Z}{\partial x}+\frac{1}{h}[\frac{\partial (h\tau_{xx})}{\partial x}+\frac{\partial (h\tau_{xy})}{\partial y}]-\frac{\tau_{bx}}{\rho h}+f_{Cor}v \tag{9}$$

$$\frac{\partial v}{\partial t}+u\frac{\partial v}{\partial x}+v\frac{\partial v}{\partial y}=-g\frac{\partial Z}{\partial y}+\frac{1}{h}[\frac{\partial (h\tau_{yx})}{\partial x}+\frac{\partial (h\tau_{yy})}{\partial y}]-\frac{\tau_{by}}{\rho h}+f_{Cor}u \tag{10}$$

where u = the depth integrated velocity component in the x direction; v = the depth integrated velocity component in the y direction; g = gravitational acceleration; Z = the water surface elevation; h = local water depth; f_{Cor} = the Coriolis parameter; τ_{xx}, τ_{xy}, τ_{yx}, τ_{yy} = the depth integrated Reynolds stresses; and τ_{bx}, τ_{by} = the shear stress on the bed surface.

The turbulence Reynolds stresses are approximated based on Boussinesq's assumption that they are related to the main flow rate to the strains of the depth-averaged flow field with a coefficient of eddy viscosity:

$$\tau_{xx} = 2\nu_t \frac{\partial u}{\partial x} \tag{11}$$

$$\tau_{xy} = \tau_{yx} = \nu_t (\frac{\partial u}{\partial y} + \frac{\partial \nu}{\partial x}) \tag{12}$$

$$\tau_{yy} = 2\nu_t \frac{\partial \nu}{\partial y} \tag{13}$$

where ν_t is the eddy viscosity and is calculated by the depth-integrated parabolic model, the depth-integrated mixing length model or the k-ε model.

The mixing length model is used to calculate the eddy viscosity as a function of the depth-averaged mixing length and the gradients of depth-averaged velocities in the horizontal and vertical directions. The eddy viscosity is calculated by the following formula:

$$\nu_t = \bar{l}\sqrt{2(\frac{\partial u}{\partial x})^2 + 2(\frac{\partial \nu}{\partial x})^2 + (\frac{\partial u}{\partial x} + \frac{\partial \nu}{\partial x})^2 + (\frac{\partial \overline{U}}{\partial z})^2} \tag{14}$$

where $\bar{l}$ is the depth-averaged mixing length, and $\frac{\partial \overline{U}}{\partial z}$ is the gradient of total velocity in the vertical direction.

The parabolic eddy viscosity turbulence model only considers shear velocity, which is related to the velocity gradient in the vertical direction.

$$\nu_t = \frac{A_{xy}}{6} \kappa U^* h \tag{15}$$

where A_{xy} is an adjustable coefficient of eddy viscosity, κ is the von Karman constant, and U^* is the shear velocity.

The models are often referred to by the number of transport equations associated with the method. For example, the mixing length model and the parabolic model are "Zero Equation" models, because no transport equations are solved, whereas the k- ε is a "Two Equation" model, because two transport equations (one for k and one for ε) are solved. From the local values of k and , the local eddy viscosity can be evaluated as

$$\nu_t = \frac{c_\mu k^2}{\varepsilon} \tag{16}$$

were k is the turbulent kinetic energy, and ε is the rate of dissipation of turbulent energy. In this study, considering flow fields around dikes where flow separation and reverse occurs, the mixing length model, including both horizontal and vertical velocity gradients, was chosen.

The depth-integrated convection-diffusion equation of suspended load transport and the continuity equation of bed load are solved to simulate with the non-equilibrium transport in the CCHE2D model (Wu, 2004).

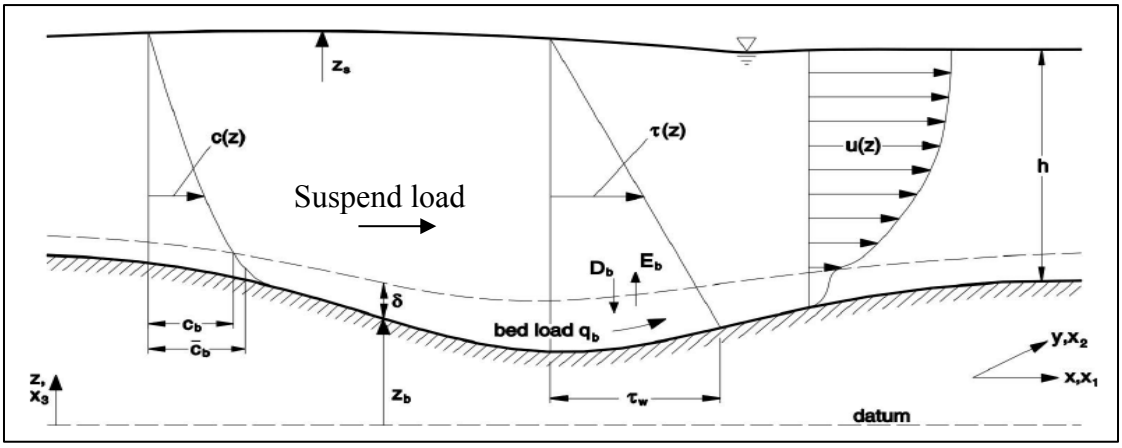

Figure 51. Configuration of Sediment Transport

As shown in Figure 51, the full water depth is divided into two zones: suspended-load zone and bed-load zone. In nonuniform sediment transport, the sediment mixture can be divided into several size classes. For each size class, the three-dimensional convection-diffusion equation of sediment transport is:

$$\frac{\partial(c_k)}{\partial t}+\frac{\partial(uc_k)}{\partial x}+\frac{\partial(vc_k)}{\partial y}+\frac{\partial(wc_k)}{\partial z}-\frac{\partial(\omega_{sk}c_k)}{\partial z}=\frac{\partial}{\partial x}(\varepsilon_s\frac{\partial c_k}{\partial x})+\frac{\partial}{\partial y}(\varepsilon_s\frac{\partial c_k}{\partial y})+\frac{\partial}{\partial z}(\varepsilon_s\frac{\partial c_k}{\partial z}) \quad (17)$$

where c_k = the concentration of the kth size class of sediment; u, v and w = the velocity components in the x, y and z directions, respectively; ω_{sk} = the settling velocity of the kth size class of sediment particles; and ε_s = the eddy diffusity of sediment. The integration of the three-dimensional equation over the suspended-load zone (h-δ) and the bed-load zone (δ: the thickness of bed-load zone) leads to:

$$\frac{\partial(hC_k)}{\partial t}+\frac{\partial(UhC_k)}{\partial x}+\frac{\partial(VhC_k)}{\partial y}=\frac{\partial}{\partial x}(\varepsilon_s h\frac{\partial C_k}{\partial x})+\frac{\partial}{\partial y}(\varepsilon_s h\frac{\partial C_k}{\partial y})+\alpha\omega_{sk}(C_{*k}-C_k) \quad (18)$$

$$\frac{\partial(\delta_b\bar{c}_{bk})}{\partial t}+\frac{\partial(\alpha_{bx}q_{bk})}{\partial x}+\frac{\partial(\alpha_{by}q_{bk})}{\partial y}+\alpha\omega_{sk}(C_{*k}-C_k)+(1-p'_m)(\frac{\partial z_b}{\partial t})_k=0 \quad (19)$$

where h = the flow depth; C_k = the depth-averaged concentration of the kth size class of suspended load; U and V = the depth-averaged flow velocities in the x and y directions, respectively; ε_s = the diffusity coefficient of sediment; α = the nonequilibrium adaptation coefficient of suspended load; ω_{sk} = the settling velocity of sediment particles; C_{*k} = the depth-averaged suspended load concentration under equilibrium conditions or the suspended load transport capacity; δ_b = the thickness of bed-load zone; $\bar{c}_{bk}$ = the average concentration of bed load at the bed-load zone; α_{bx} and α_{by} = the

direction cosines of bed-load movement, which are usually assumed to be along the direction of bed shear stress; q_{bk} = the actual transport rate of the kth size class of bed load; $p_m^{'}$ = the porosity of bed material; and $(\frac{\partial z_b}{\partial t})_k$ = the bed change rate corresponding to the kth size class of sediment. The bed deformation is calculated using the following equation:

$$(1-p_m^{'})(\frac{\partial z_b}{\partial t})_k = \frac{1}{L}(q_{tk}-q_{t^*k}) = \alpha\omega_{sk}(C_k - C_{*k}) + \frac{1}{L}(q_{bk}-q_{b^*k}) \quad (20)$$

where q_{tk} = the actual transport rate of the k-th size class of bed-material load, q_{t^*k} = the transport capacity of the k-th size class of bed-material load, L= the non-equilibrium adaptation length of sediment transport, and q_{b^*k} = the bed-load transport capacity or bed-load transport rate at the equilibrium state. Therefore, three unknown C_k, q_{bk}, and $(\frac{\partial z_b}{\partial t})_k$ can be solved using equations (18), (19), and (20).

If sediments move mainly as bed load, the diffusion of suspended load is negligible and the resulting governing equation for the bed-material load is similar to:

$$\frac{\partial(\delta_b \bar{c}_{bk})}{\partial t} + \frac{\partial(\alpha_{bx}q_{bk})}{\partial x} + \frac{\partial(\alpha_{by}q_{bk})}{\partial y} + \frac{1}{L}(q_{bk}-q_{b^*k}) = 0 \quad (21)$$

$$(1-p_m^{'})(\frac{\partial z_b}{\partial t})_k = \frac{1}{L}(q_{bk}-q_{b^*k}) \quad (22)$$

On the other hand, if the suspended load is the dominant transport mode, the resulting governing equation for the bed-material load is similar to:

$$\frac{\partial(hC_k)}{\partial t}+\frac{\partial(UhC_k)}{\partial x}+\frac{\partial(VhC_k)}{\partial y}=\frac{\partial}{\partial x}(\varepsilon_s h\frac{\partial C_k}{\partial x})+\frac{\partial}{\partial y}(\varepsilon_s h\frac{\partial C_k}{\partial y})+\alpha\omega_{sk}(C_{*k}-C_k) \quad (23)$$

$$(1-p'_m)(\frac{\partial z_b}{\partial t})_k=\alpha\omega_{sk}(C_k-C_{*k}) \quad (24)$$

The boundary of study area was chosen as Station No 92.85~96.46 (L=3.5 km) and it is located at 7.8 km downstream of Sejong weir. Much erosion was predicted to happen after 20 years depending on the result of HEC-RAS, as shown in Figure 52. Also, this boundary is not much influenced by gate operation, so it is meaningful to develop countermeasures preventing erosion. The detail location is seen in Figure 53.

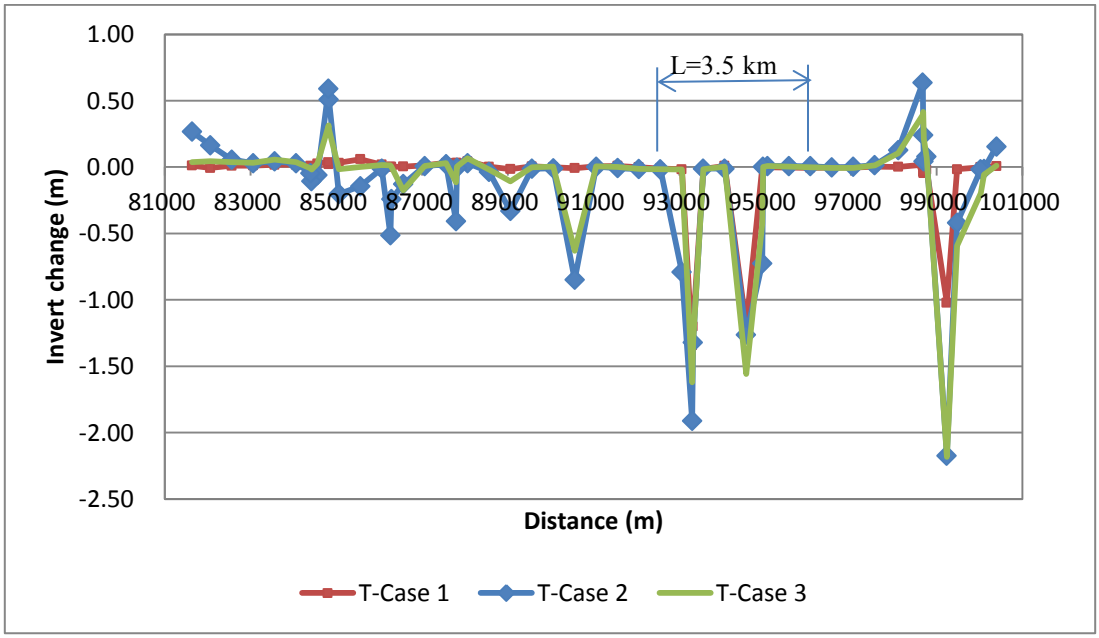

Figure 52. Study Area in 2D Analysis

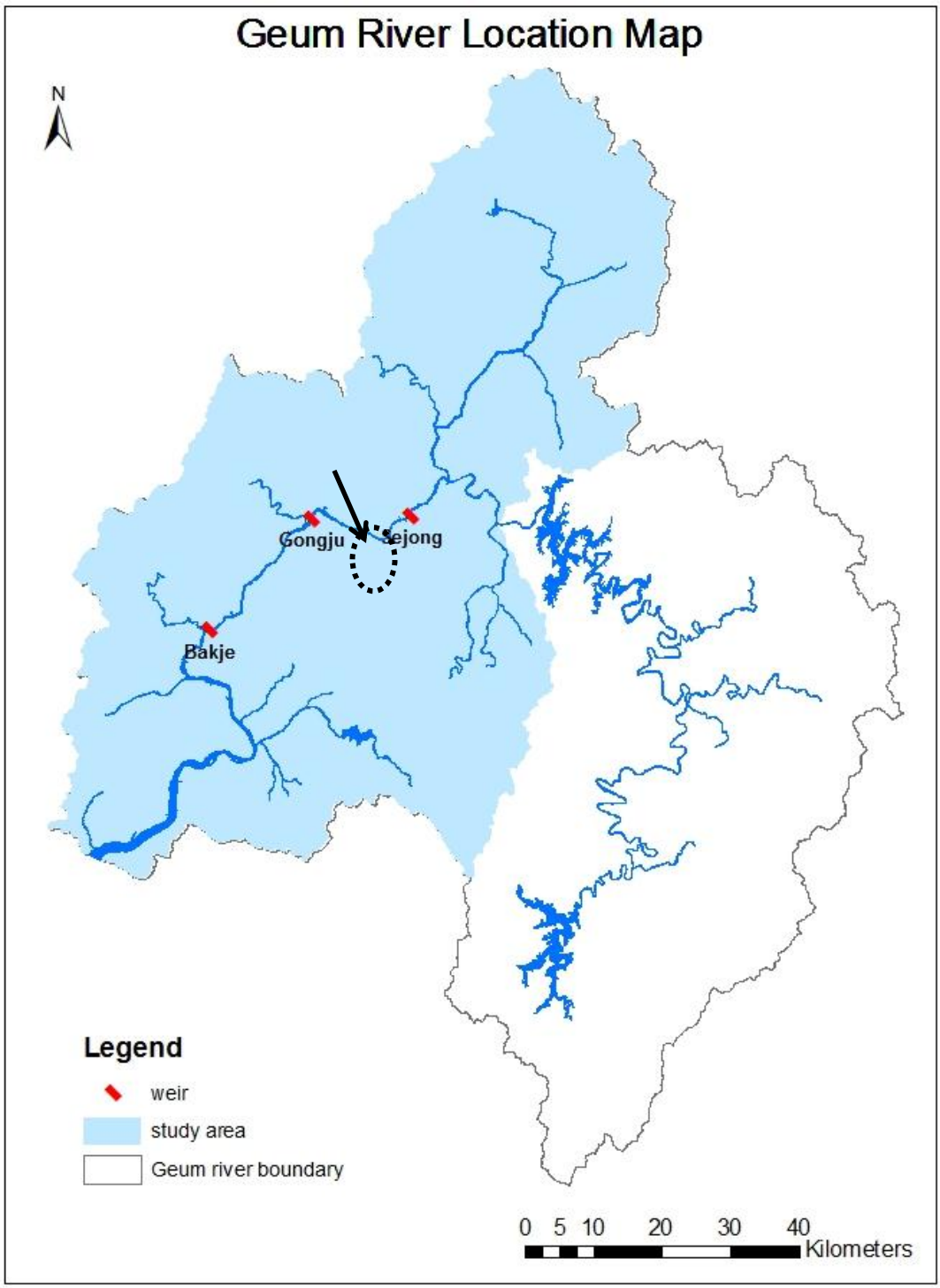

Figure 53. Location Map for 2D Analysis

The CCHE2D model is an integrated package for two-dimensional simulation and analysis of free surface flow, sediment transport and morphological processes. The package comprises numerical models, a mesh generator (CCHE2D Mesh Generator) and a graphical user interface (CCHE2D-GUI), as shown in Figure 54.

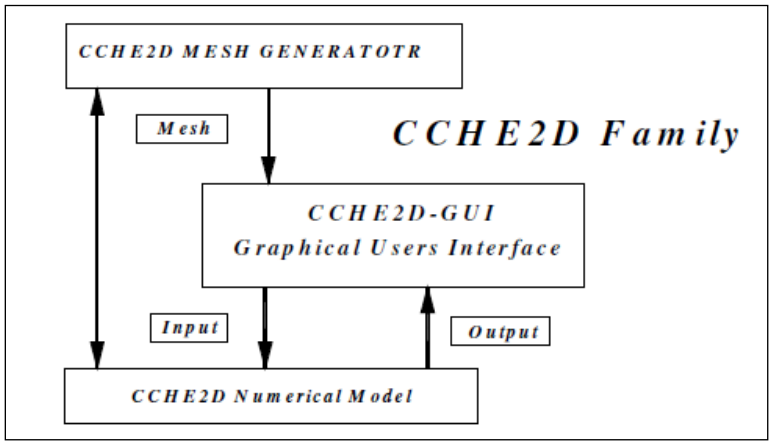

Figure 54. CCHE2D Package

The CCHE2D Mesh Generator helps with the creation of complex structured mesh system for the CCHE2D model. It is a comprehensive and user-friendly mesh generator for producing structured quadrilateral mesh for bed topography and bed elevation data. The procedure involves the following steps:

a) defining block boundaries;

b) generating algebraic mesh;

c) generating numerical mesh (improving and smoothing the mesh);

d) interpolating bed elevation; and

e) saving mesh into geo file, to be used for simulation by CCHE2D.

CCHE2D-GUI is a graphical user environment for the CCHE2D model with four main functions: preparation of initial conditions and boundary conditions, preparation of model parameters, running the numerical code, and visualization of modeling results. The procedure of simulation by the CCHE2D model is shown in Table 9 and Figure 55.

Table 9. General Procedure in CCHE2D

Type		**Flow analysis**	**Sediment analysis**
Step1	Make mesh		
Step2	Set initial condition	Initial bed elevation	Bed erodibility
		Initial water surface (up, down)	Maximum deposition thickness
		Bed roughness	Maximum erosion thickness
			Layer thickness (layer1, 2, 3)
			Layer sample (layer 1, 2, 3)
Step3	Set boundary condition	(Inlet) Total discharge Discharge hydrograph (*.dhg) (outlet) Water surface level Rating curve (*.rcv) Stage hydrograph (*.shg)	(Inlet) suspended load concentration (kg/㎥, SBC file) Bedload load transport rate (kg/m/s, BBC file)
Step4	Set model parameter	Time step (simulation time)	Sediment size classes (diameter)
		Time steps for output	Set bed material sample - porosity, size classes
		- Intermediate file	Sediment transport mode
		- History file	-Total load as bed + suspended
		Turbulence	- Total load as bed load
		- Parabolic Eddy Viscosity Model	- Total load as suspended load
		- Mixing Length Model	Sediment simulation mode
		- K-Epsilon Model	-Slow bed change with steady
		Unsteady Flow Computation	-Fast bed change with unsteady
		Bed roughness (n, Ks)	Sediment specific gravity
		Coriolis force coefficient	Bank erodibiltiy
		Gravity	
		von Karman constant	
		Fluid kinematic viscosity	
Step5	Run simulation	Start flow simulation from rest	Start sediment transport from flow field at time
		Continue flow simulation from flow field at time	Continue sediment transport from sediment result at time

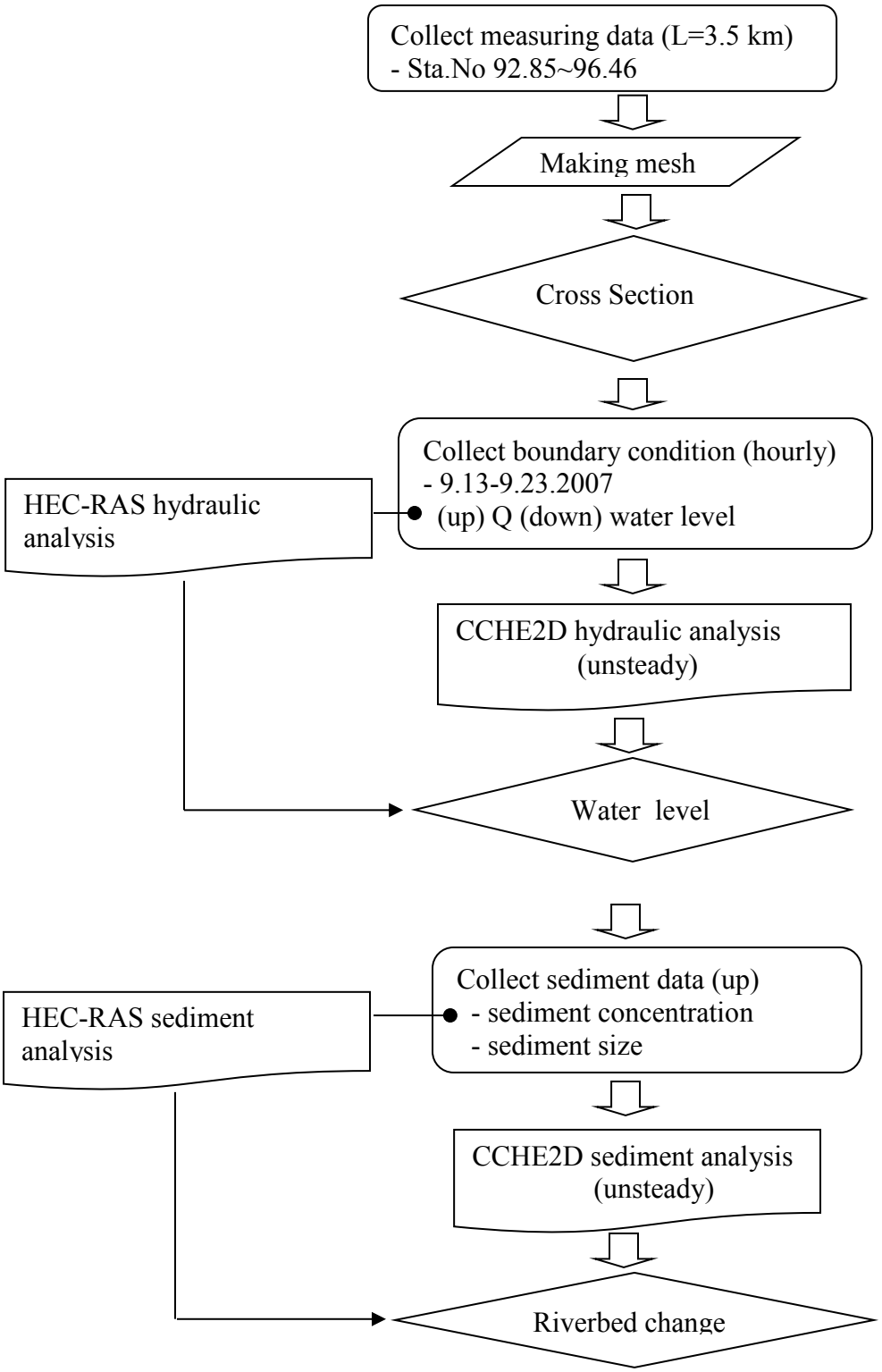

(a) Without Dike

Figure 55. 2-D Procedure in This Study (a) Without Dike and (b) With Dike

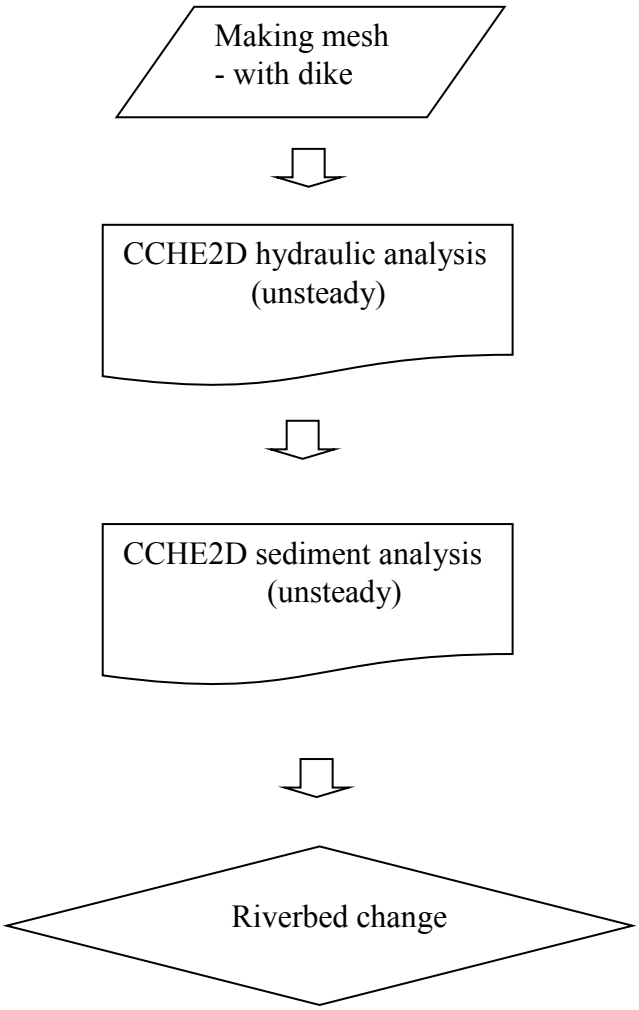

(b) With Dike

Figure 55. Continued

4.2.1 Making a mesh

Echo sounding data which were measured after dredging were used to make the mesh, as shown in Figure 56. First, the boundary file using CCHE2D_Mesh version 3.23 was made and the mesh consisted of 5,100 nodes where the minimum cell length was 3.8 m and maximum cell length was 8.3 m in the I direction (width direction). Also the minimum cell length was 4.7 m and the maximum cell length was 50.6 m in the J direction (flow direction), as shown in Figures 57, 58. There are two bridges (width: 3 m) which were made to change from an internal node to a boundary node, as shown in Figure 59. At last, to make a mesh practically useful, the bed elevation was interpolated from a topography database (*.mesh_xyz) using random interpolation, as shown in Figure 60. The result and procedure of the mesh are shown in Figure 61 to 62.

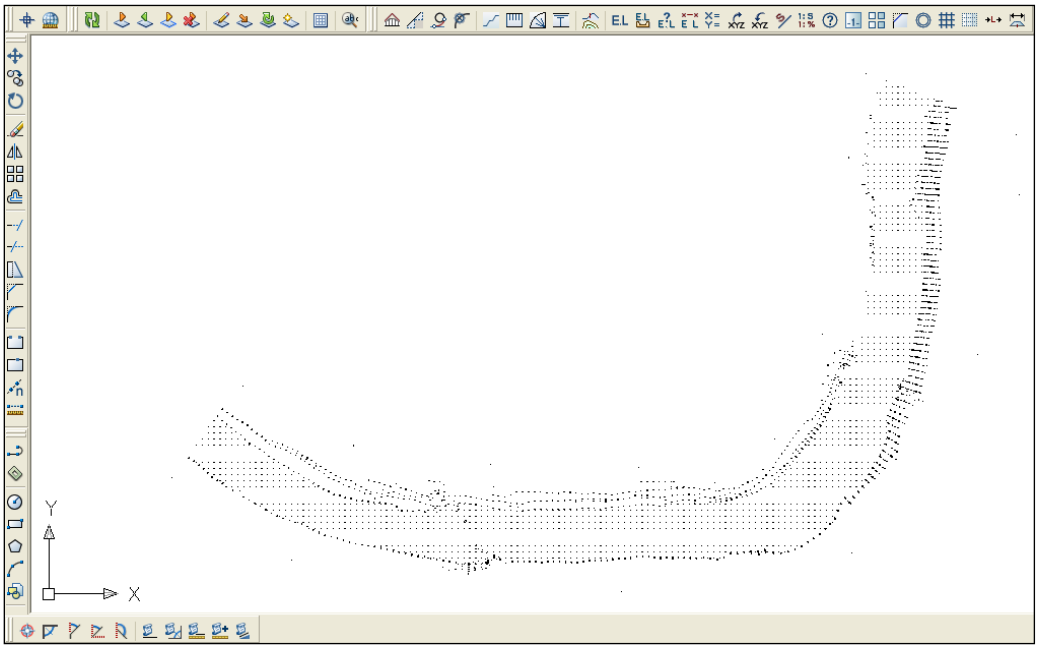

Figure 56. Echo Sounding Cross Section

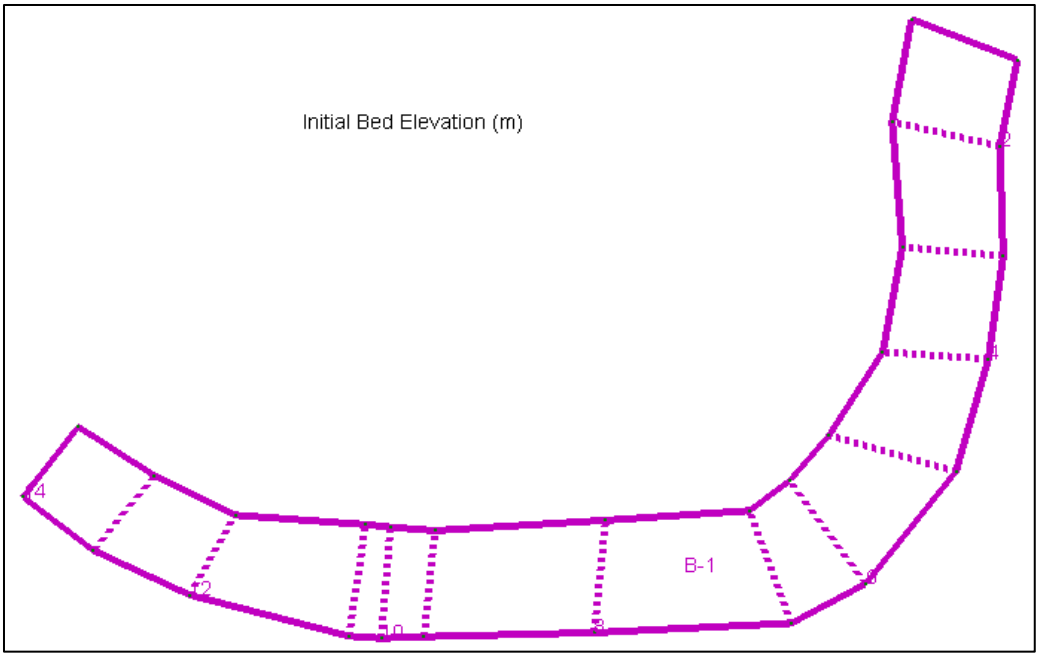

Figure 57. Boundary Block

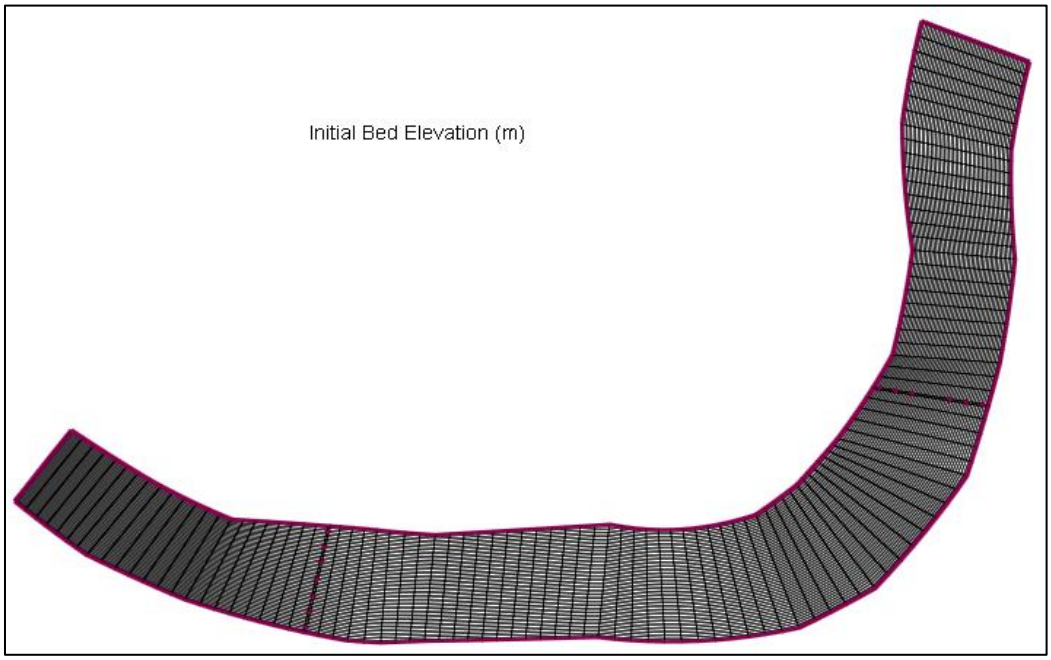

Figure 58. Generating Mesh

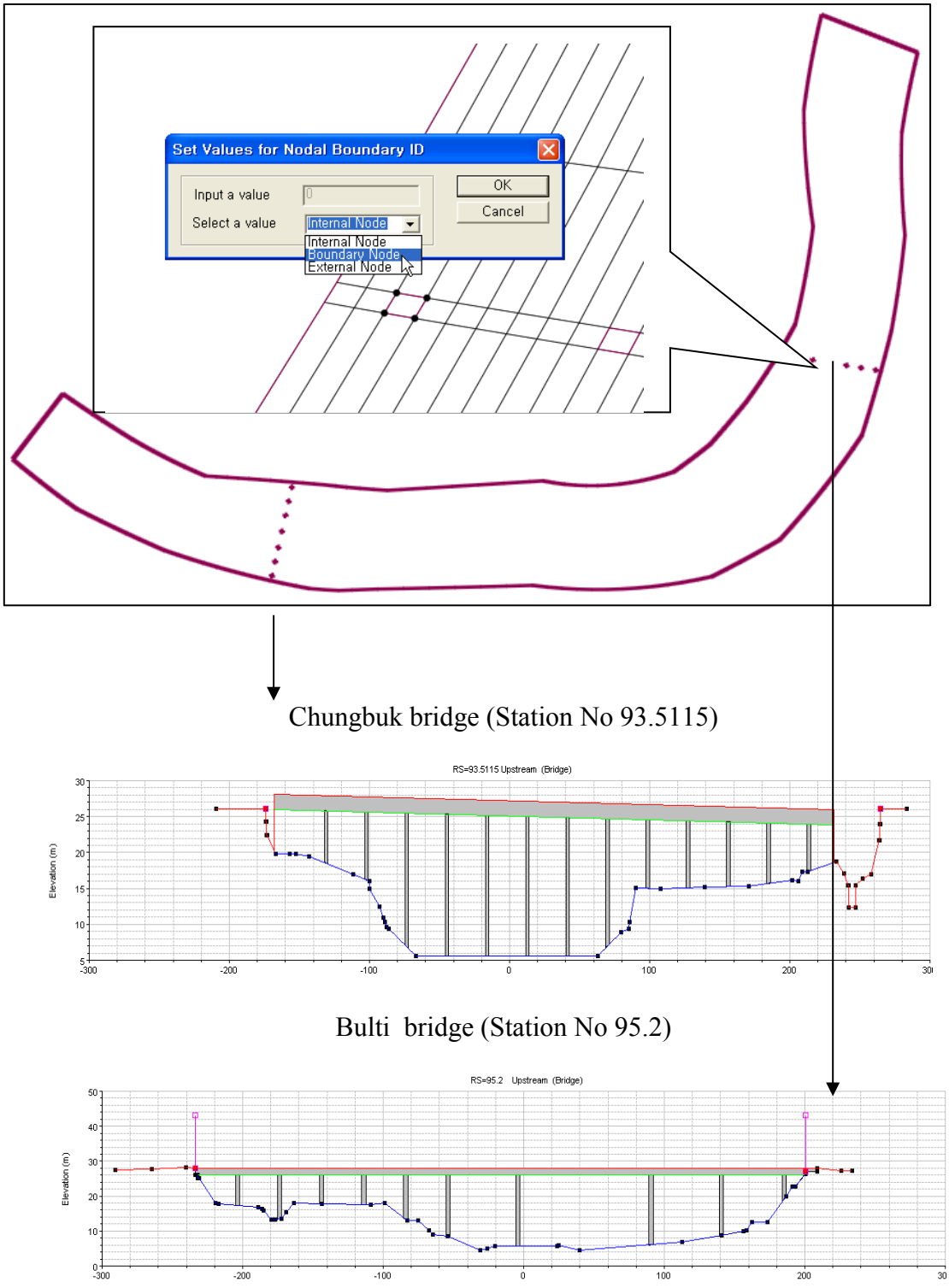

Figure 59. The Input of Bridges in CCHE2D

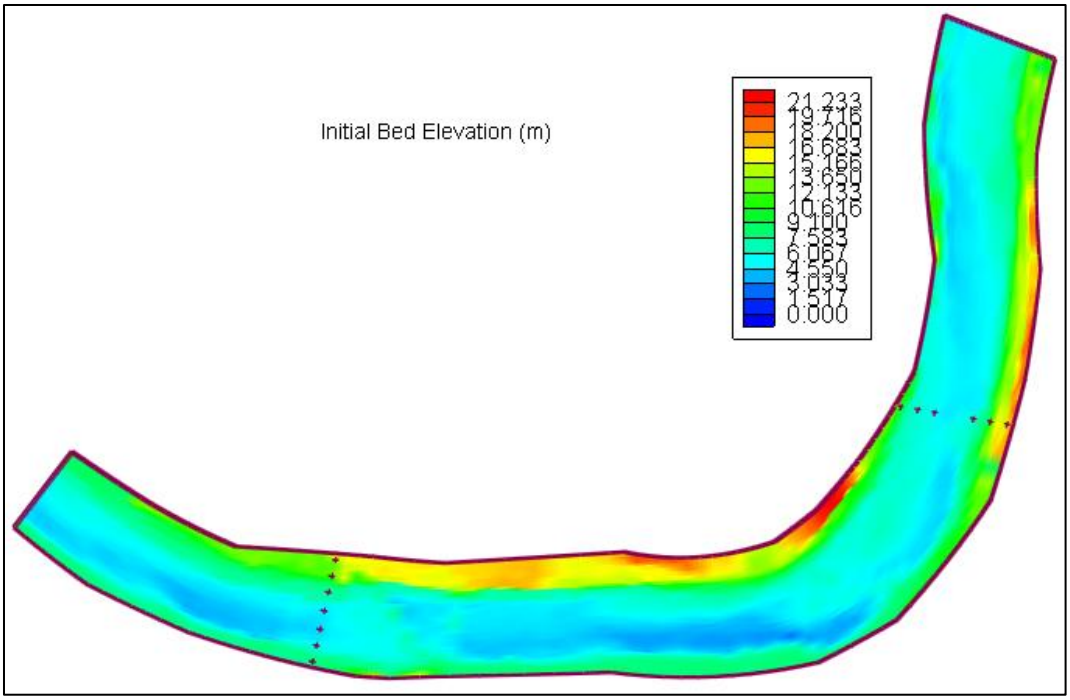

Figure 60. Interpolating Elevation

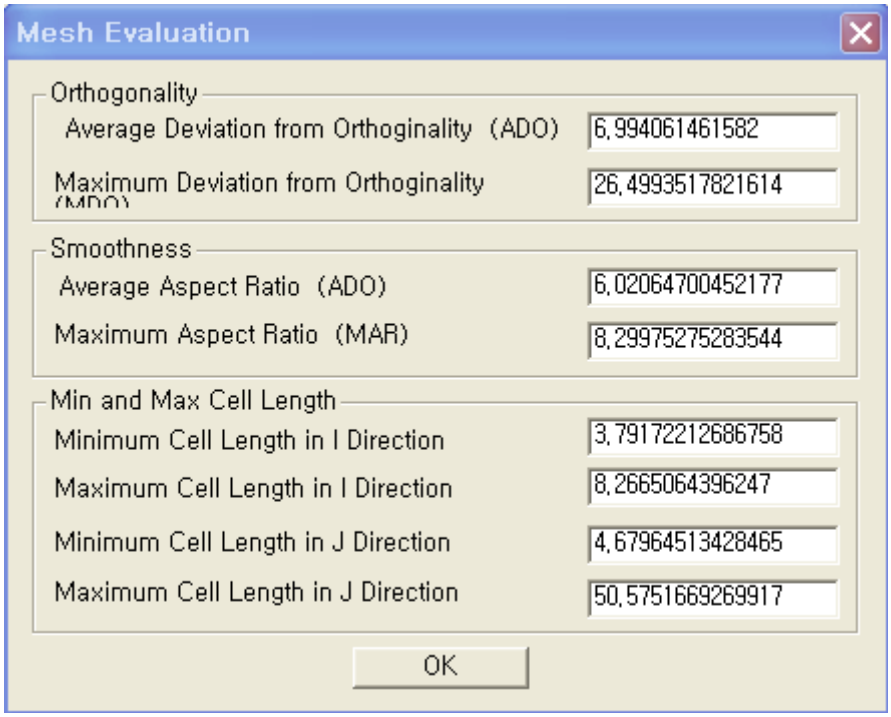

Figure 61. Mesh Evaluation

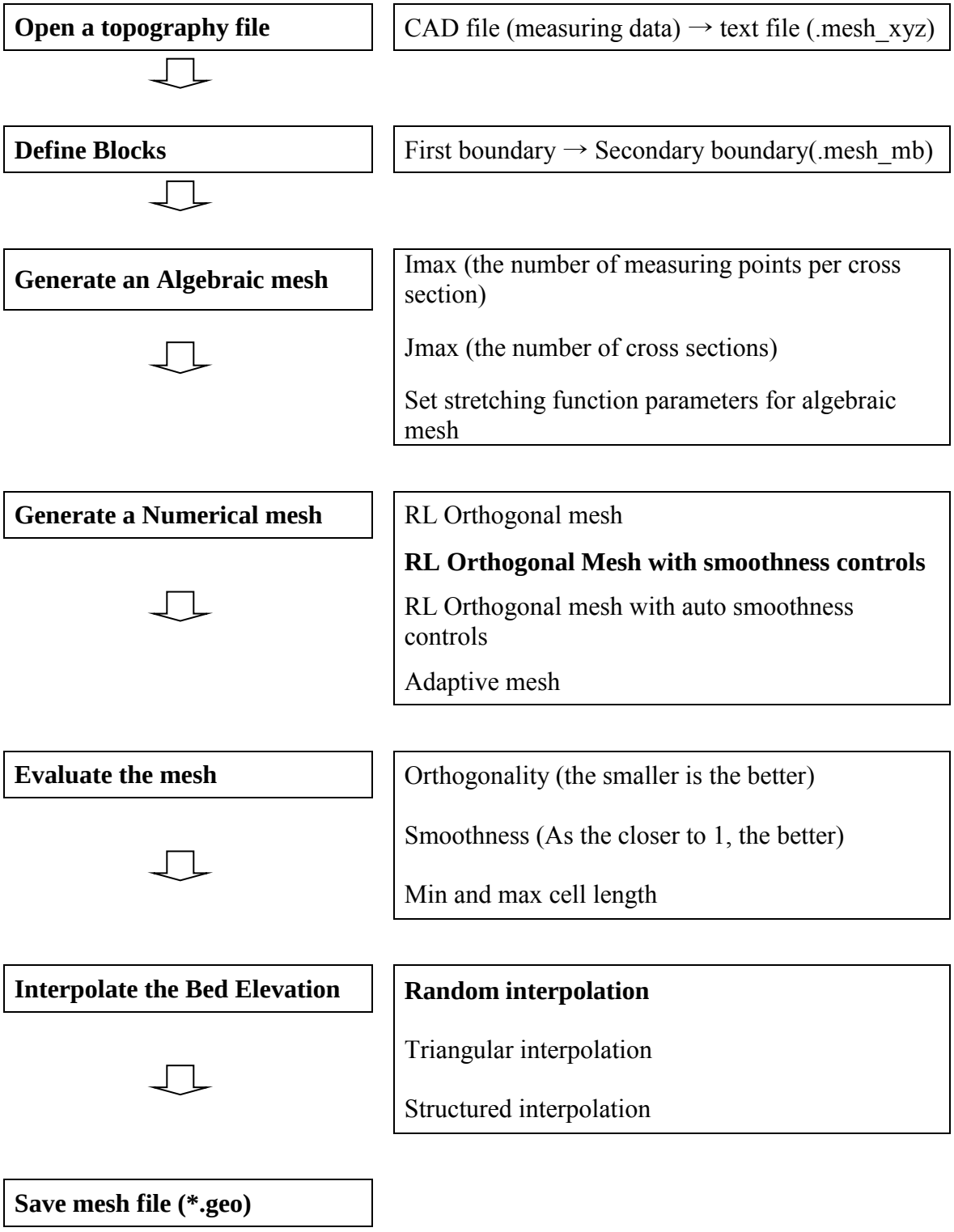

Figure 62. Procedure for Making the Mesh

When 5 cross sections of the 2-D case, as shown in Figure 63, are compared with that of the 1-D case, they have similar patterns, as shown in Figure 64. Of course, there are differences among them, because the cross section in 1-D is the planned section and the cross section in 2-D is actually the measured section. Therefore, when 1-D and 2-D models are simulated with the same measured data, the results can be anticipated to be more reliable.

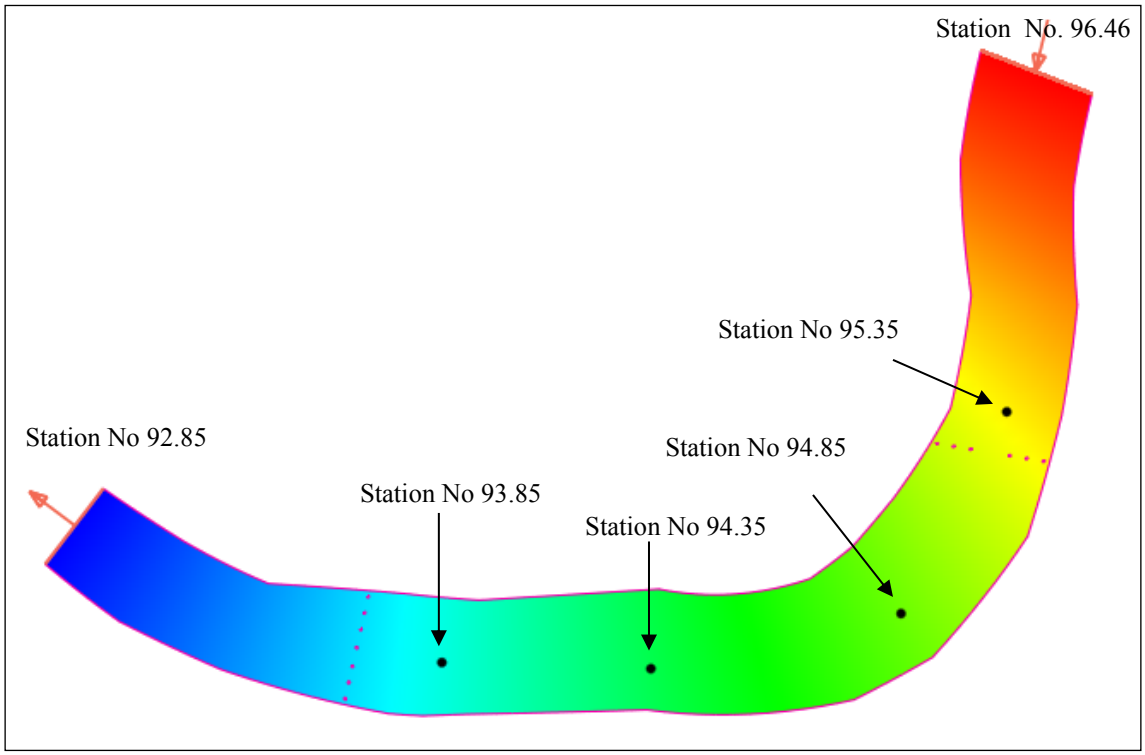

Figure 63. Study Area in the 2-D Model

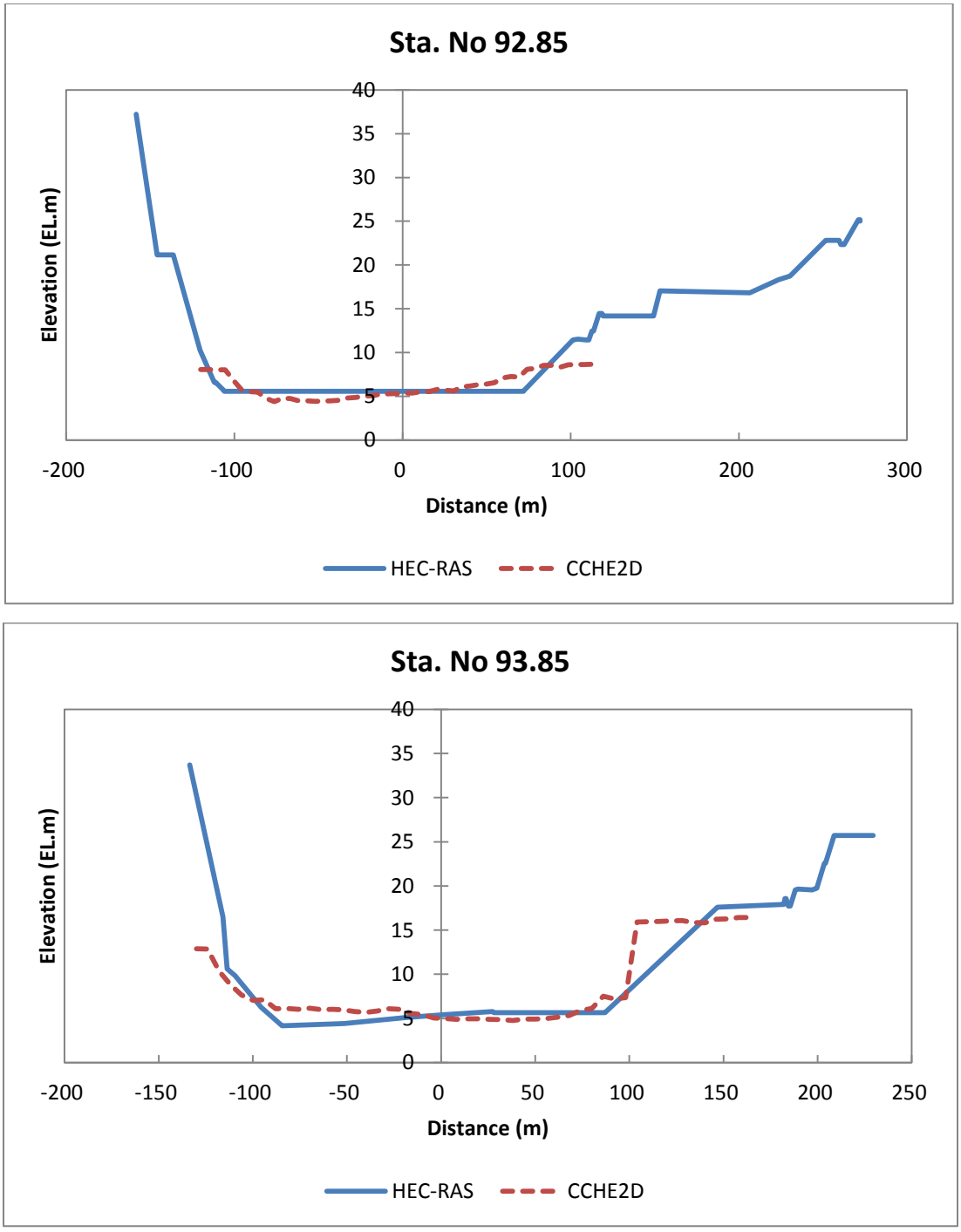

Figure 64. Comparison of Cross Sections between 1D and 2D models

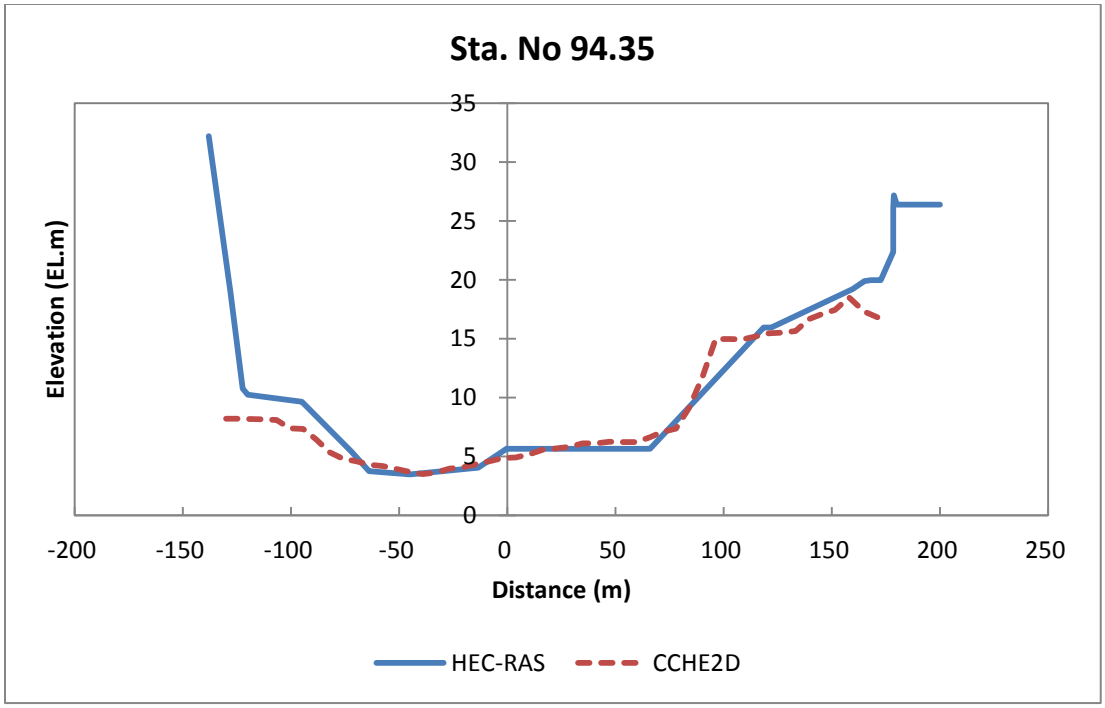

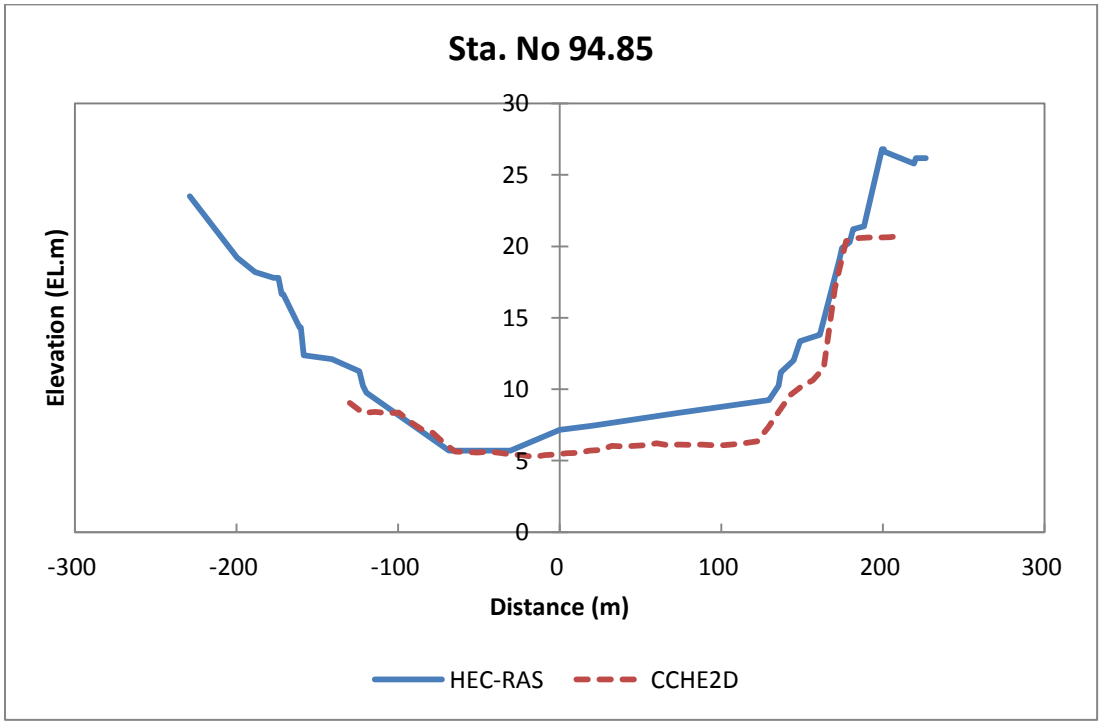

Figure 64. Continued

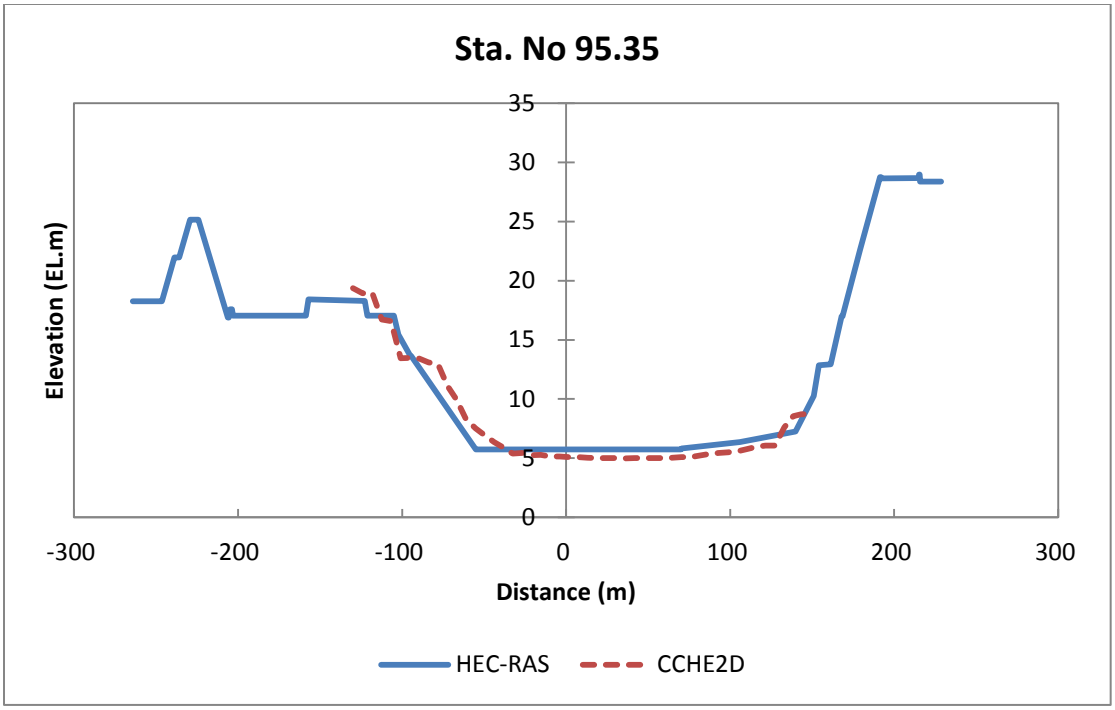

Figure 64. Continued

4.2.2 Unsteady analysis

To verify the 2-D model using CCHE2D_GUI version 3.28.8, it is necessary to compare the 1-D water level with the 2-D water level. Of course, the cross section of the 1-D model is the planned data, on the other side the cross section of 2-D model is the measured data. But it is assumed that the difference is so small that it has no impact on the water level. The 1-D unsteady analysis was made with the planned cross section for 9.13-9.23.2007 under case 3. There are two purposes: the first is to provide boundary conditions, which are hourly inflow, hourly water level, and initial water level, as shown in Figures 65 to 67, to overcome the weakness that the gate operation is impossible in the CCHE2D model. Second, results of the 1-D model were used to compare with the hydraulic output of the 2-D model. The Manning coefficient of 0.027 was applied, as in the 1-D case.

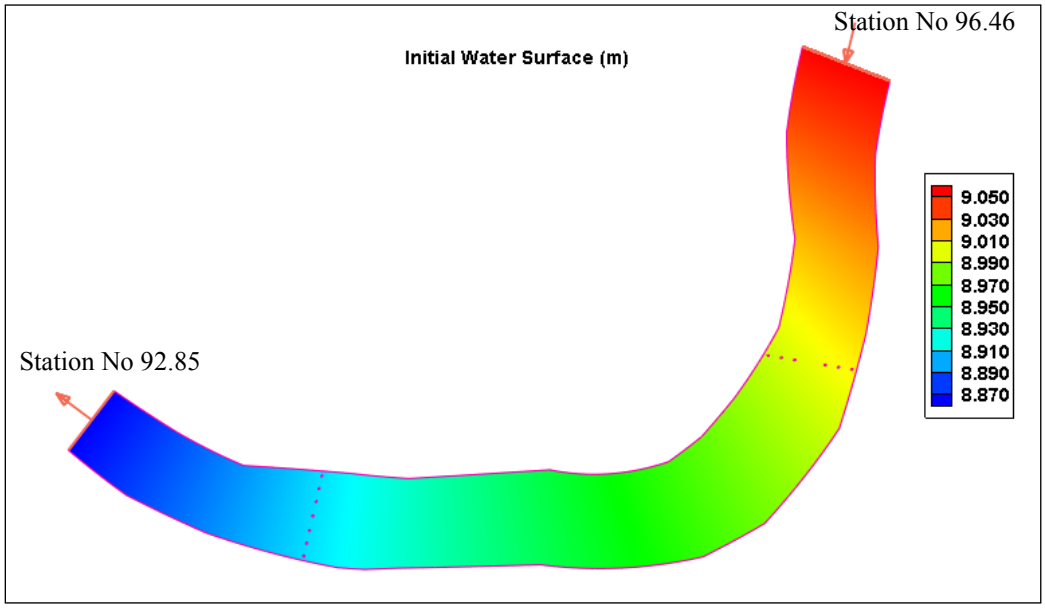

Figure 65. Initial Water Level

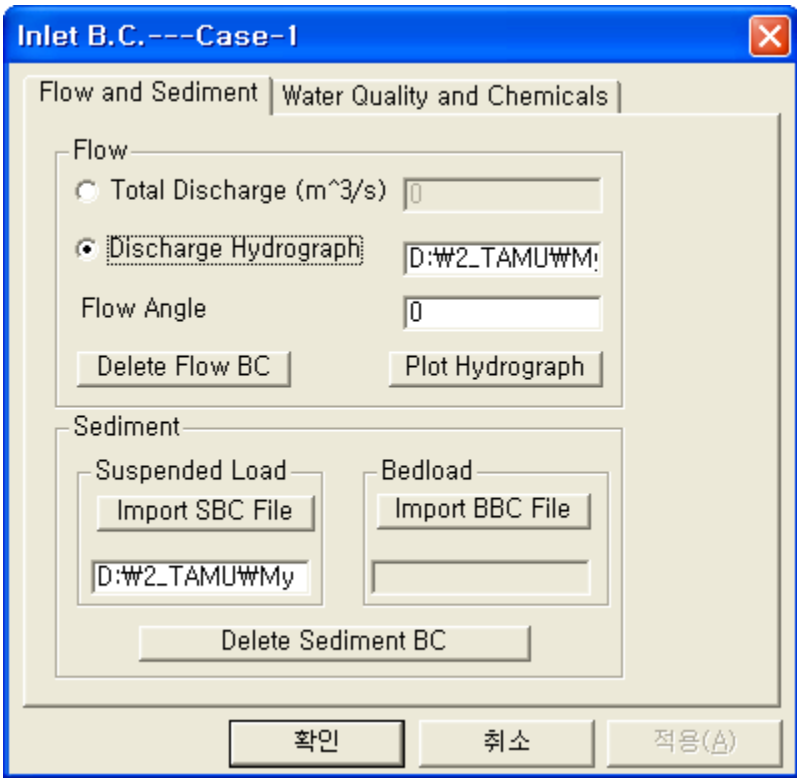

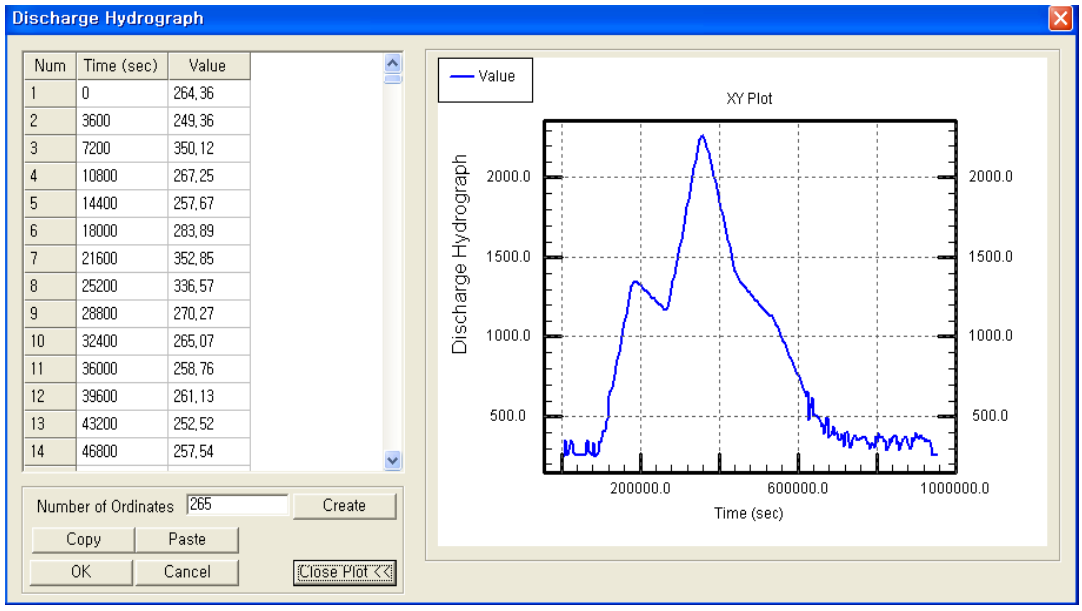

Figure 66. Inlet Boundary Condition

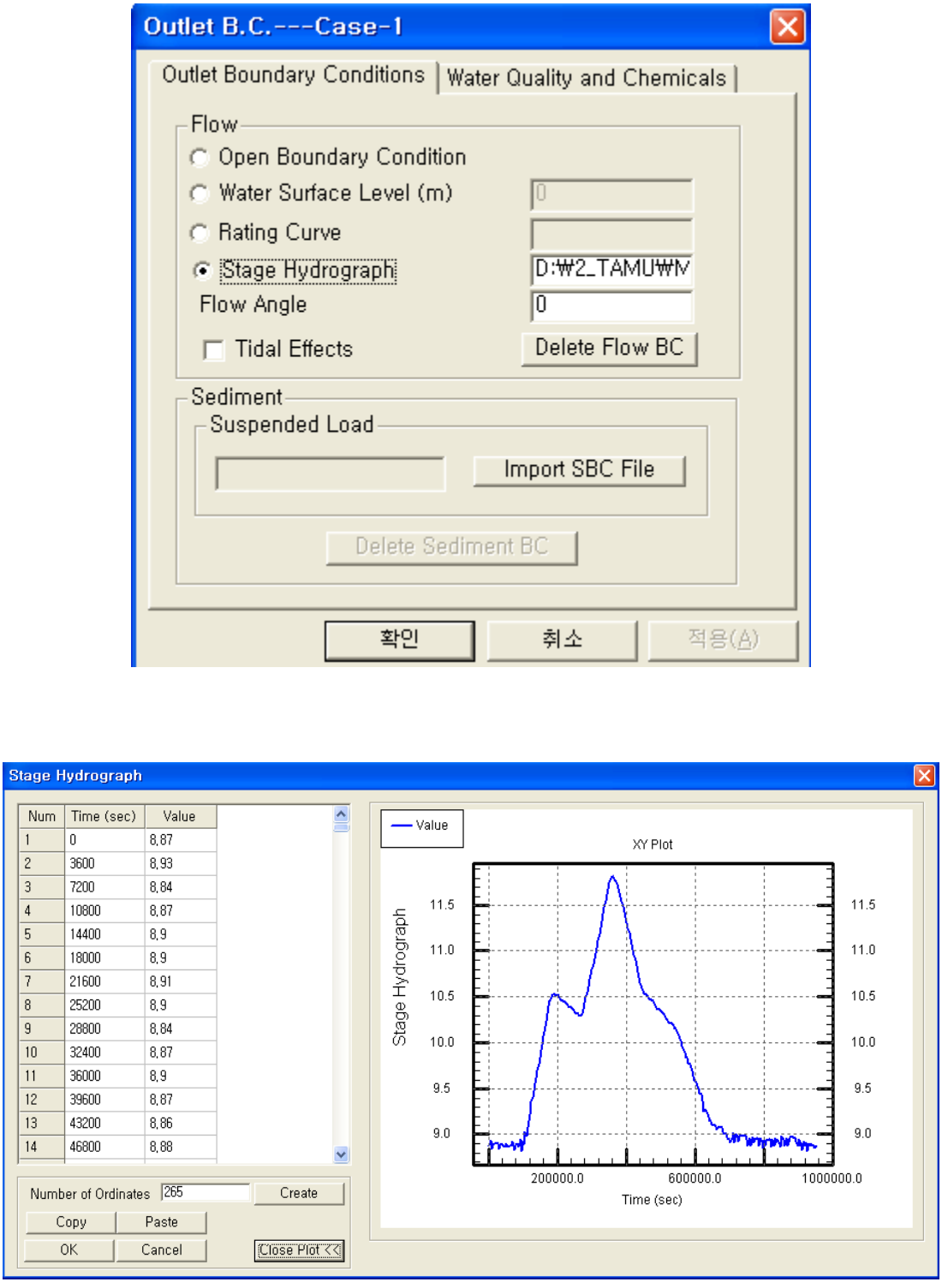

Figure 67. Outlet Boundary Condition

The simulation time was set as 950400 sec (from 9.13.00:00 to 9.23.24:00) and the time step was set 60 sec. History file is necessary to see results by a certain interval. So the time step was set 60 (time step * 60 = 60*60=3600s) to see results by 1 hr.

The mixing length model with turbulent viscosity coefficient equal to 1 was chosen as the turbulence model, as shown in Figure 68. The turbulent viscosity coefficient served as a multiplier, i.e., a value of 10 means that the turbulent viscosity was 10 times that computed from the selected turbulence model.

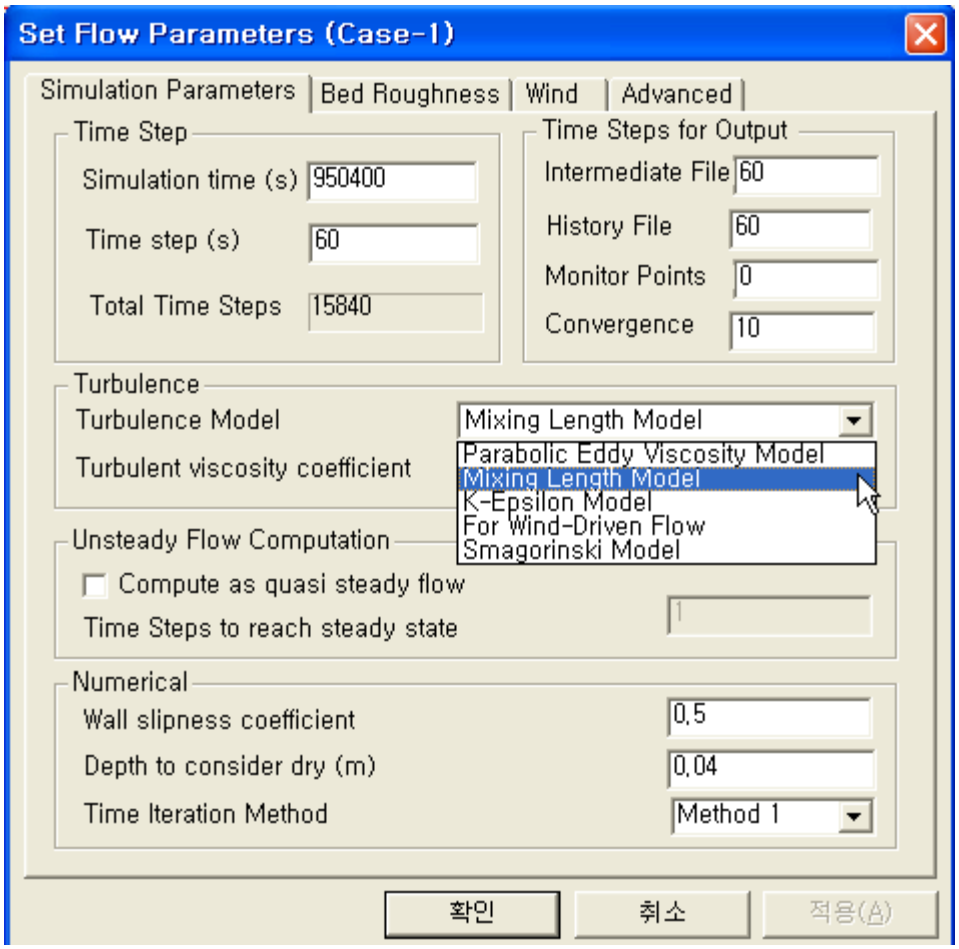

Figure 68. Set Flow Parameter

4.2.3 Sediment analysis

To simulate the riverbed change by unsteady flow analysis, at first it is necessary to include various sediment characteristics. The maximum number of sediment size classes is 5. So, 15 categories used in HEC-RAS were divided into 5 classes considering the particle size, as shown in Figure 69 and Tables 10 and 11. Also, the bed sample was classified into 4 samples considering the constitution of sediment, as shown in Figures 70 and 71.

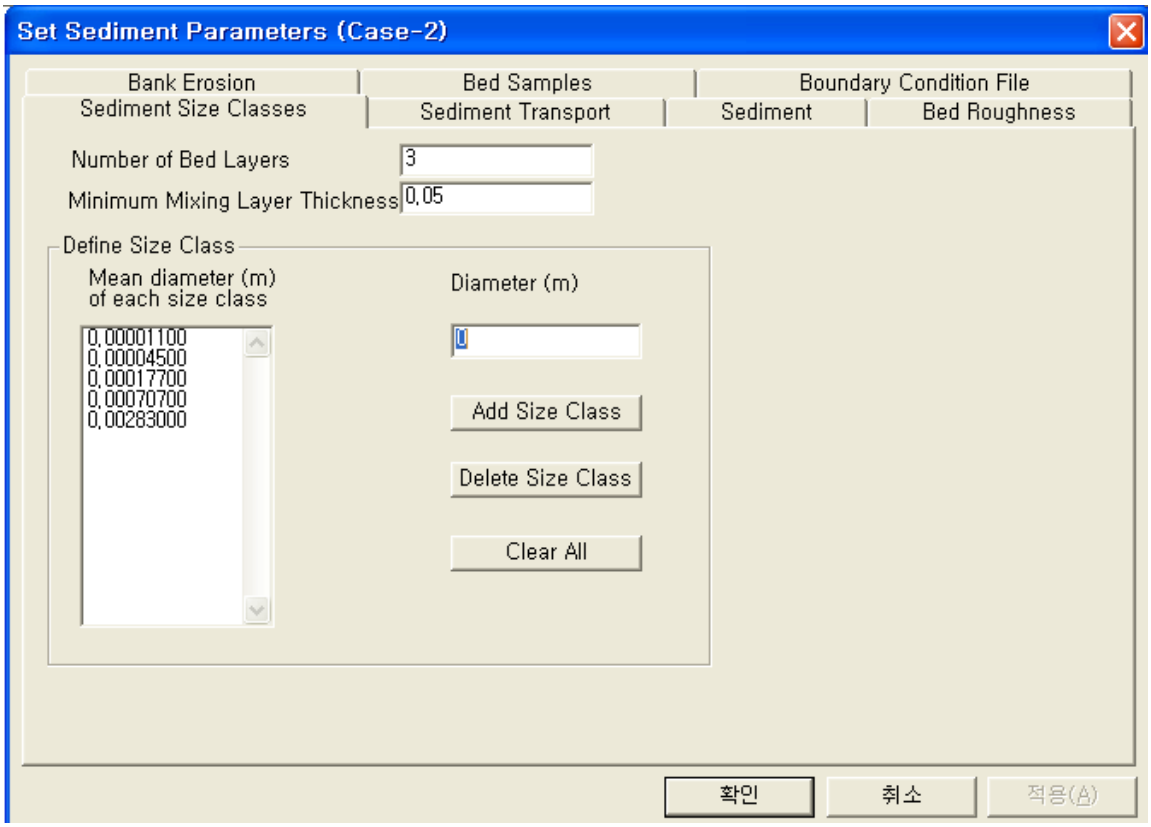

Figure 69. Sediment Size Class

Table 10. Sediment Size Class in the 1-D Model

Type	Class	Min (mm)	Max (mm)	Mean (mm)	Station. No				
					97.96	94.85	94.35	93.35	92.85
1	Clay	0.002	0.004	0.003					
2	VFM	0.004	0.008	0.006	32	22		9	9
3	FM	0.008	0.016	0.011	45	32		12	12
4	MM	0.016	0.032	0.023	61	43		17	17
5	CM	0.032	0.0625	0.045	72.5	58		22	22
6	VFS	0.0625	0.125	0.088	84	73		30	30
7	FS	0.125	0.25	0.177	92	85	3	54	54
8	MS	0.25	0.5	0.354	97	93	6	82	82
9	CS	0.5	1	0.707	99	99.5	20	100	100
10	VCS	1	2	1.41	100		57		
11	VFG	2	4	2.83			100		
12	FG	4	8	5.66					
13	MG	8	16	11.3					
14	CG	16	32	22.6					
15	VCG	32	64	45.3					

Table 11. Sediment Size Class in the 2-D Model

Type	Class	Min (mm)	Max (mm)	Mean (mm)	Type	Size (mm)	sample1		sample2		sample3	sample4		
							92.85	93.35	93.85	94.35	94.85	95.35	95.73	96.46
1	Clay	0.002	0.004	0.003										
2	VFM	0.004	0.008	0.006	Class 1	0.011	0.12		0.00		0.32	0.450		
3	FM	0.008	0.016	0.011										
4	MM	0.016	0.032	0.023	Class 2	0.045	0.10		0.00		0.26	0.275		
5	CM	0.032	0.0625	0.045										
6	VFS	0.0625	0.125	0.088	Class 3	0.177	0.32		0.03		0.27	0.195		
7	FS	0.125	0.25	0.177										
8	MS	0.25	0.5	0.354	Class 4	0.707	0.46		0.54		0.15	0.080		
9	CS	0.5	1	0.707										
10	VCS	1	2	1.41										
11	VFG	2	4	2.83	Class 5	2.830	0.00		0.43		0.00	0.000		
12	FG	4	8	5.66										
13	MG	8	16	11.3										
14	CG	16	32	22.6										
15	VCG	32	64	45.3										

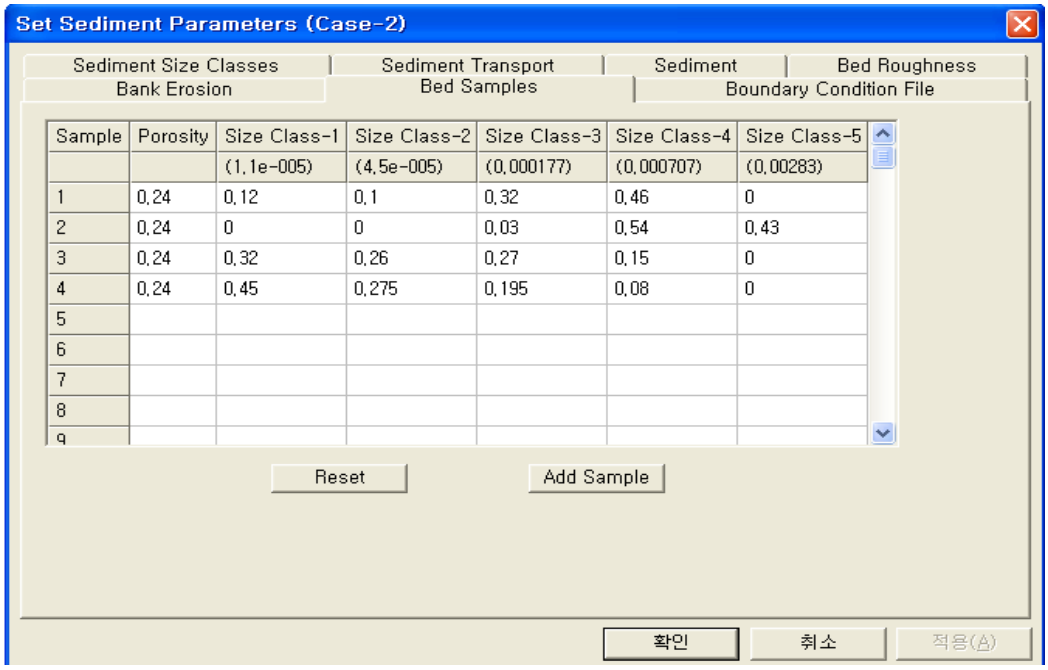

Figure 70. Bed Samples

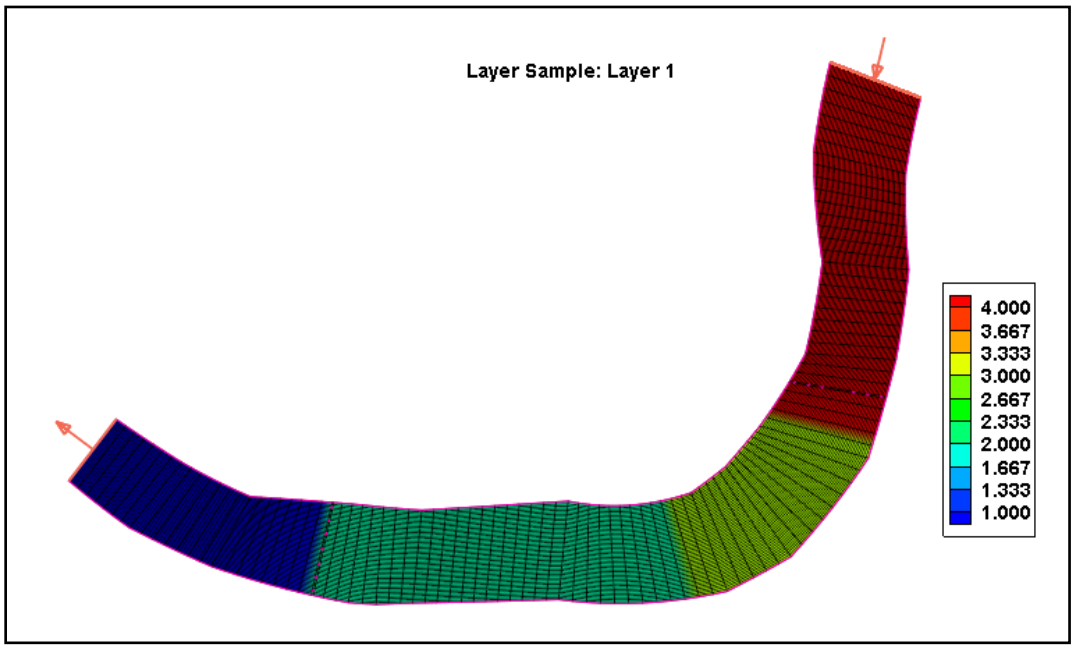

Figure 71. Layer Sample

Three approaches were adopted in CCHE2D nonuniform sediment transport modeling. One is a bed-load type model, which is to simulate bed load only or bed-material load without considering the diffusion of suspended load. The second approach is a suspended-load type that simulates suspended load only or treats bed-material load as suspended load. The third approach is to compute bed load and suspended load separately. In Geum River, suspended sediment is the dominant sediment, so transport mode was chosen as "Total Load as Suspended Load Model," as shown in Figure 72.

Four formulas were selected to determine the fractional non-cohesive sediment transport capacities C_{*k} and q_{b*k} in the CCHE2D model: Wu, Wang and Jia's formula, modified Ackers and White's formula, modified Engelund and Hansen's formula, and SEDTRA module which includes the Yang, Laursen, and Meyer-Peter and Muller equations. In this study, Wu, Wang and Jia's formula which has shown good results in the prediction of fractional transport rate of nonuniform sediment mixtures was used.

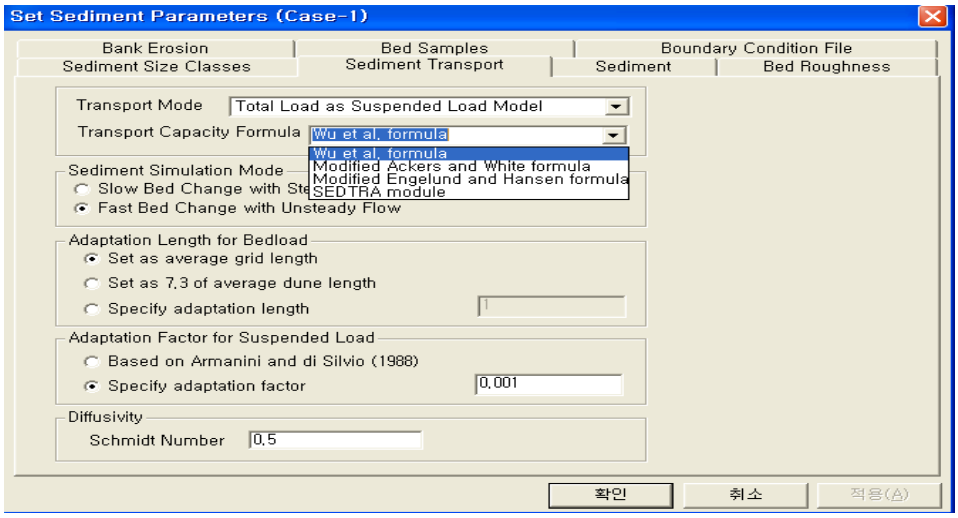

Figure 72. Sediment Parameters

For sediment transport under unsteady conditions, the time series of inflow sediment discharge is needed. Also, in the case of nonuniform sediment transport, the size distribution of the inflow sediment is needed. 1-D sediment analysis using quasi-steady flow was made with the planned cross-section for 9.13-9.23.2007 events under case 3 at an hourly time scale to match the time unit of the 2-D model. There are two purposes: First, results of the 1-D model are used to compare with the 2-D output. When invert change after 20 years was compared with that after 11 days about Station No 92.85-96.46 (L=3.5 km), the riverbed change showed similar tendencies, as shown in Figure 73. Second, is to provide boundary conditions, which are hourly inflow sediment discharge and the size distribution of the inflow sediment, as shown in Figure 74.

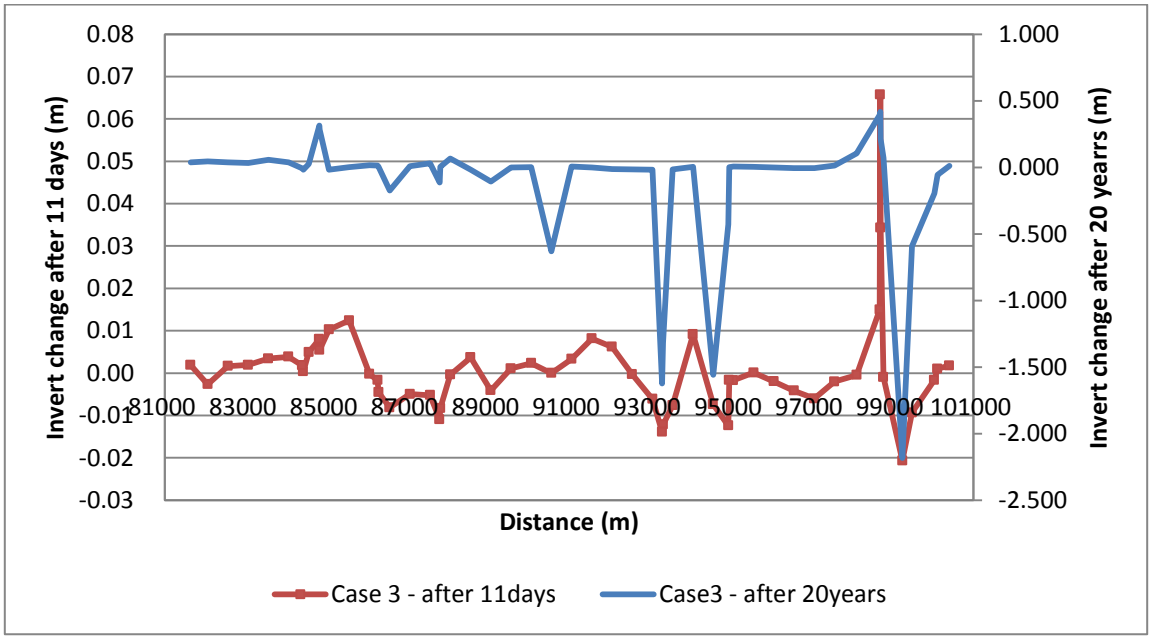

Figure 73. Riverbed Change in 1-D Model (L=3.5 km)

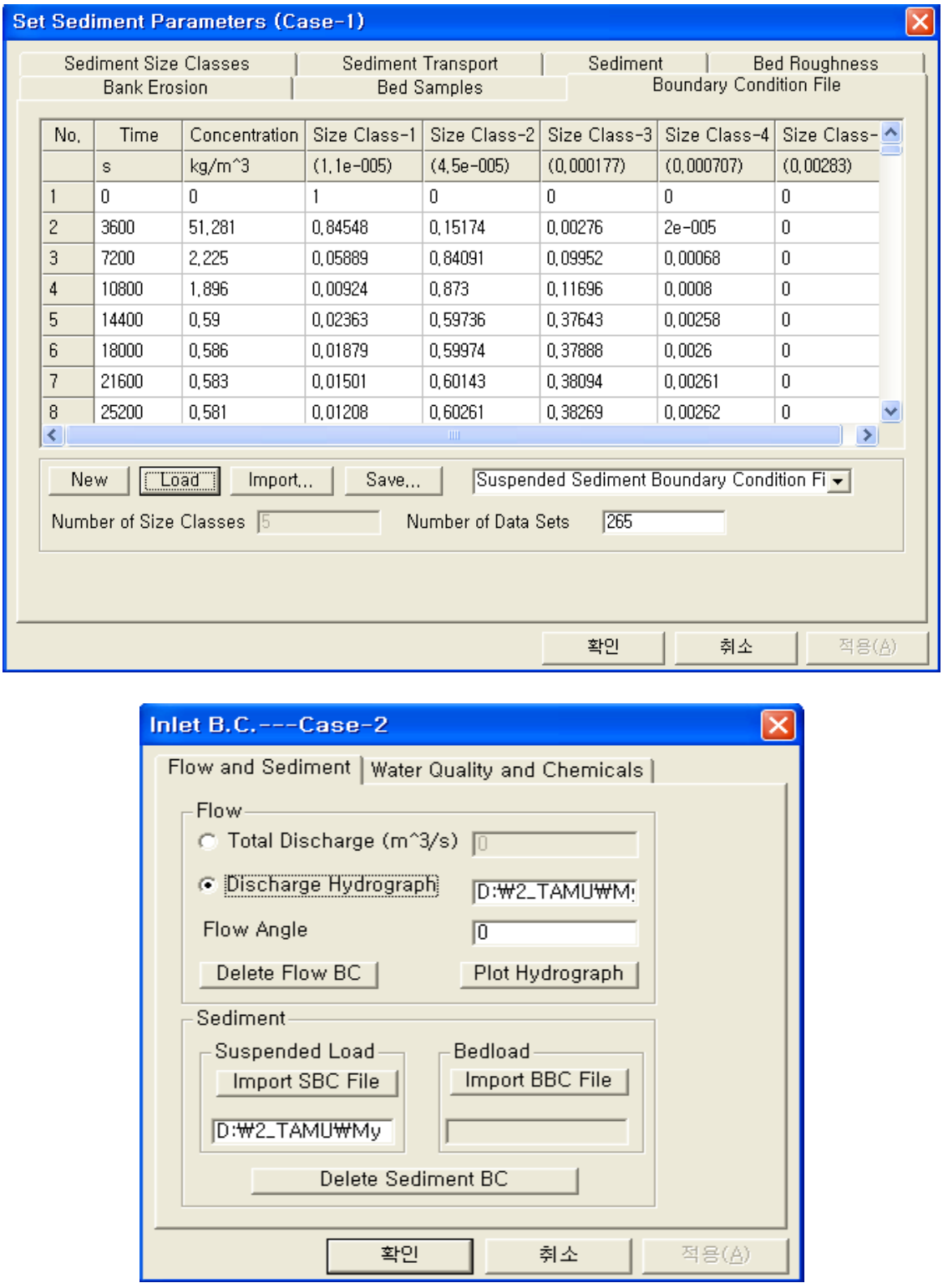

Figure 74. Inlet Boundary Condition of Sediment Discharge

The flow and sediment calculations were separately conducted in the CCHE2D. The sediment transport begins with the initial bed defined in the mesh file (geo) and the computed flow field at a selected time, as shown in Figure 75.

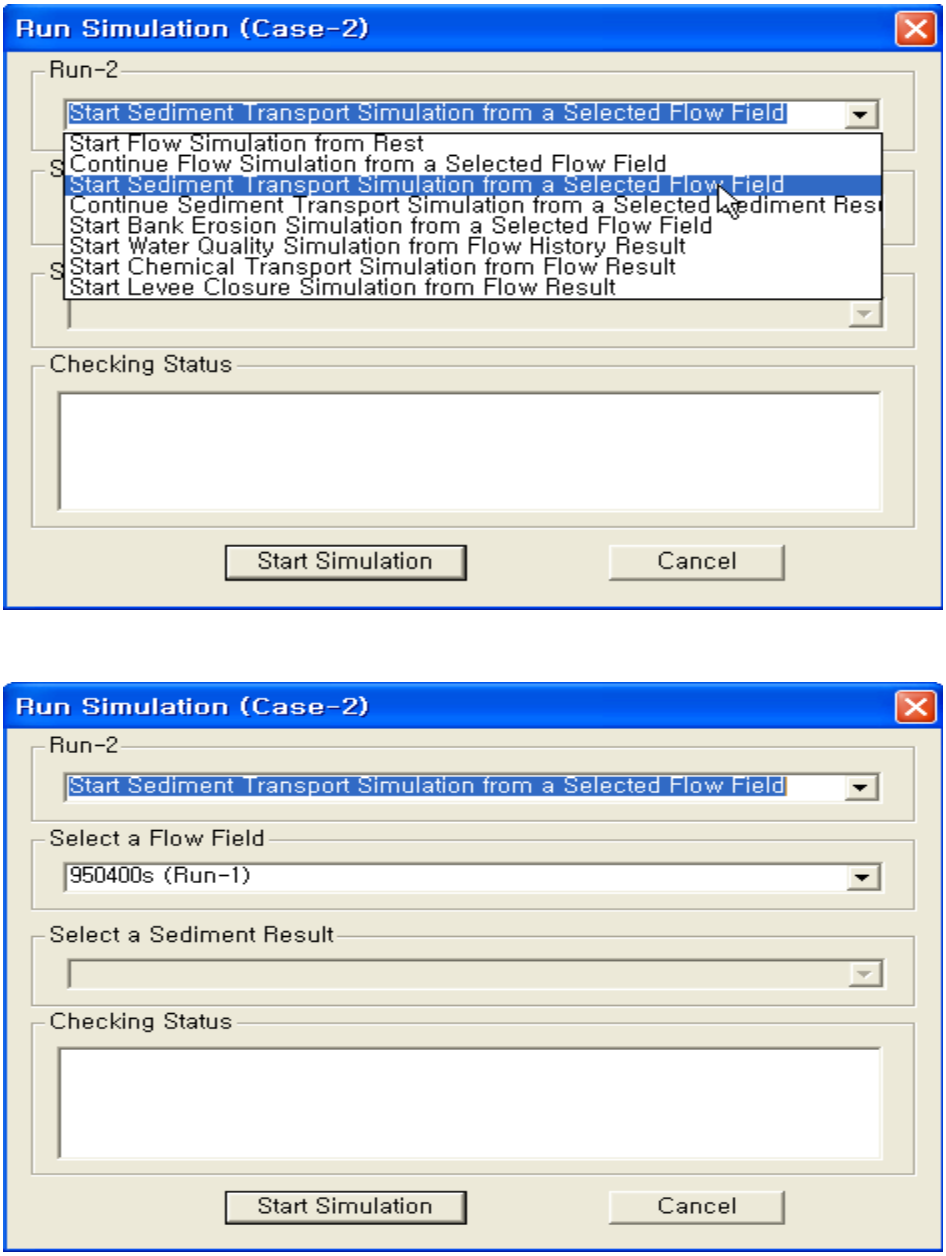

Figure 75. Run Simulation

5. RESULTS AND DISCUSSION

A 1-Dimensional analysis using the HEC-RAS model and 2-Dimensional analysis in the CCHE2D model were conducted to predict riverbed change focusing on the gate operation. The HEC-RAS model is based on quasi-unsteady flow to work sediment analysis and the CCHE2D model treat steady, quasi-unsteady and unsteady flow. Also, the HEC-RAS model assumes an equilibrium state, whereas the CCEHE2D model calculates actual sediment concentration or transport rate under non-equilibrium state. In this study, long-term riverbed change was conducted through the HEC-RAS model, and short-term riverbed change was worked through the CCHE2D model.

5.1 Assessment based on 1-dimensional analysis

The 1-D model was analyzed along the stream longitudinally, so we cannot evaluate the change in the transverse direction. Nevertheless, it is convenient for analyzing the long stream at once. Among the models, the HEC-RAS model is capable of simulating the gate operation, so we can evaluate the influence on both water level and sediment change by gate operation. Since the weir is not fixed but is movable, as gates operate, velocity and shear stress change. Therefore, gate operation will have an impact on the downstream surroundings, and as a result, habitat will change. In addition, if we suppose macro insights, the riverbed change can be predicted and we plan the budget of sediment in the same basin and in conclusion, we can design river restoration in concert with the ecosystem.

5.1.1 Steady flow analysis

The gate's purpose, which has much storage, depends on how much it rains. If it rains as drought flow and ordinary water flow, the purpose of the storage takes effect by closing the gate, as shown in Figure 76.

Drought flow

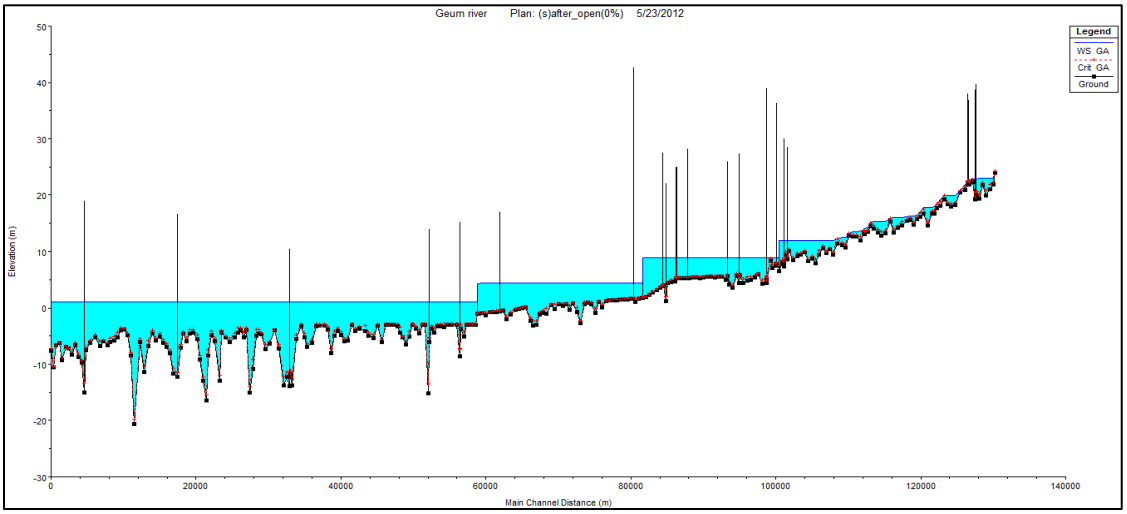

Ordinary water flow

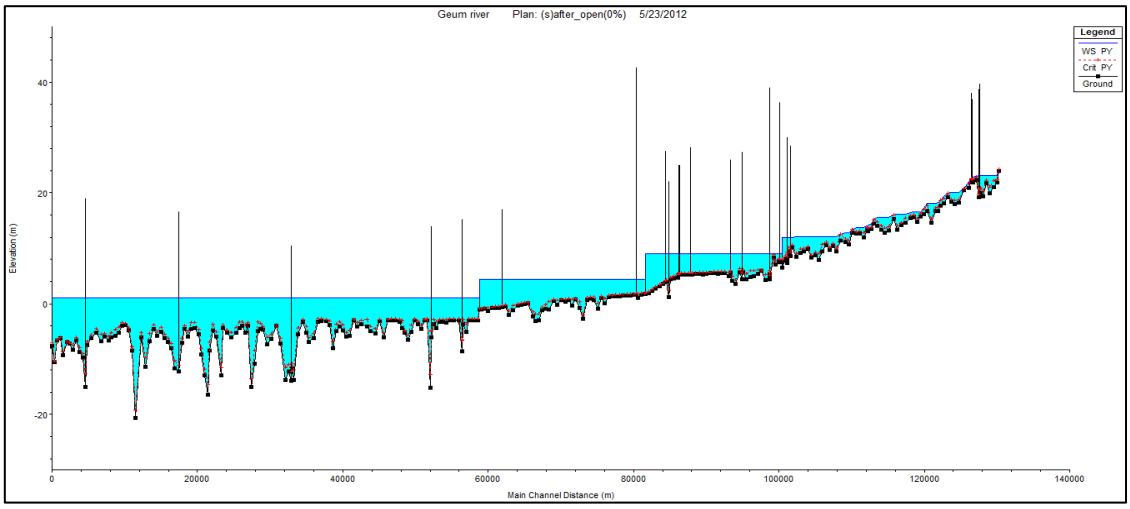

Figure 76. Steady Analysis in HEC-RAS (drought flow, ordinary water flow)

But if it rains by 1year frequency flow, the purpose of the storage is insignificant, because the water level when gates are open fully is similar to that when gates are closed fully, as shown in Figure 77. Also, in the case that gates are open fully, the difference in water level between upstream and downstream of Sejong weir, Gongju weir, and Bakje weir was, respectively, 0.04 m, 0.54 m, 0.17 m. This shows the water level rise upstream of weir, since the weir structure prevents flow.

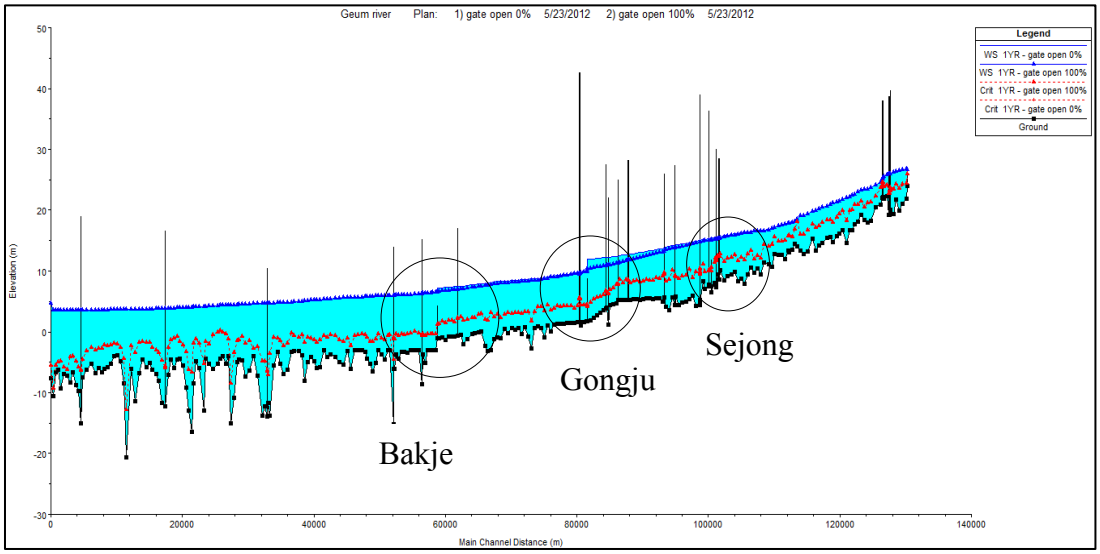

Figure 77. Steady Analysis in HEC-RAS (the 1year frequency flow)

5.1.2 Unsteady flow analysis

Unsteady analysis was done hourly and then averaged to make daily data and a flood event in 2006 was chosen to calibrate the model. The absolute mean difference (AMD) and root mean square errors (RMSE) between observed and simulated stages were used to determine the goodness of fit of hydrodynamic models. The absolute mean difference (AMD) is the mean of the absolute values of all differences between simulated and observed values:

$$AMD = \frac{1}{n}\sum_{1}^{n} ABS(Simulated - Observed)$$

The Root Mean Square Error (RMSE) between observed and modeled data was calculated by summing the square of the differences between the two, then taking the square root of the total and dividing it by the number of records:

$$RMSE = \sqrt{\frac{1}{n}\sum_{1}^{n} (Simulated - Observed)^2}$$

The AMD values varied from 0.26 to 0.33 and RMSE varied from 0.39 to 0.47 except for Gyumnam station, as shown in Table 12.

Table 12. RMSE and AMD in 2006

Type		Root Mean Square Difference (RMSE) in meter	Absolute Mean Difference (AMD) in meter
1	Gyumnam	0.80	0.50
2	Gongju	0.39	0.26
3	Jindu	0.43	0.28
4	Gyuam	0.47	0.31
5	Gangyeong	0.41	0.33

At Gyumnam station, daily water level in 7.29-7.31 had a difference between model results and observations. So, hourly water level was plotted and water level was constant for 7.29-7.31, as shown in Figure 78. An artificial activity, like installation of dike or sensor disorder, may be the cause, and except that, model values at Gongju station, Gindu station, Gyuam station, and Gangyung were similar to observed data, as shown in Figure 78.

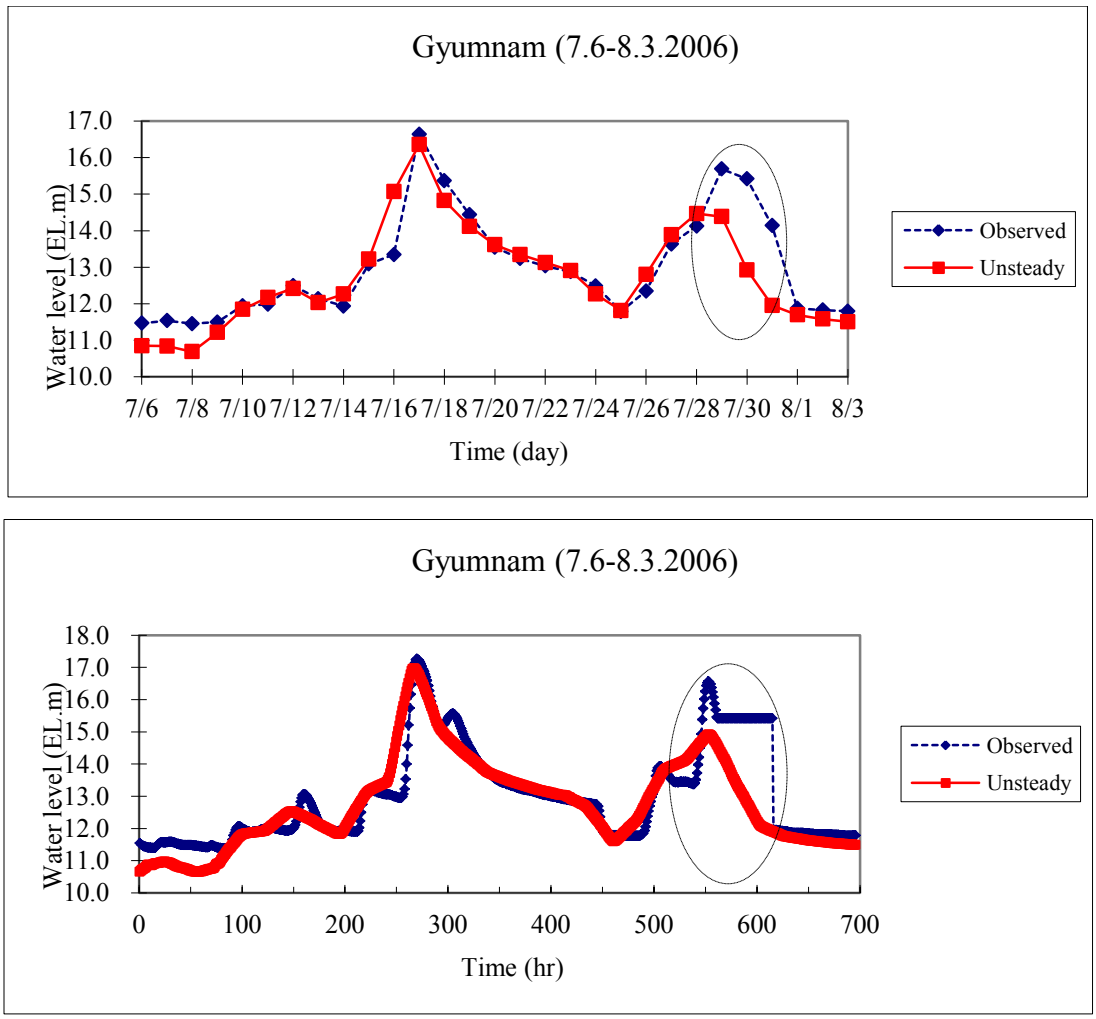

Figure 78. Comparison of Model and Observations in Unsteady Analysis (2006)

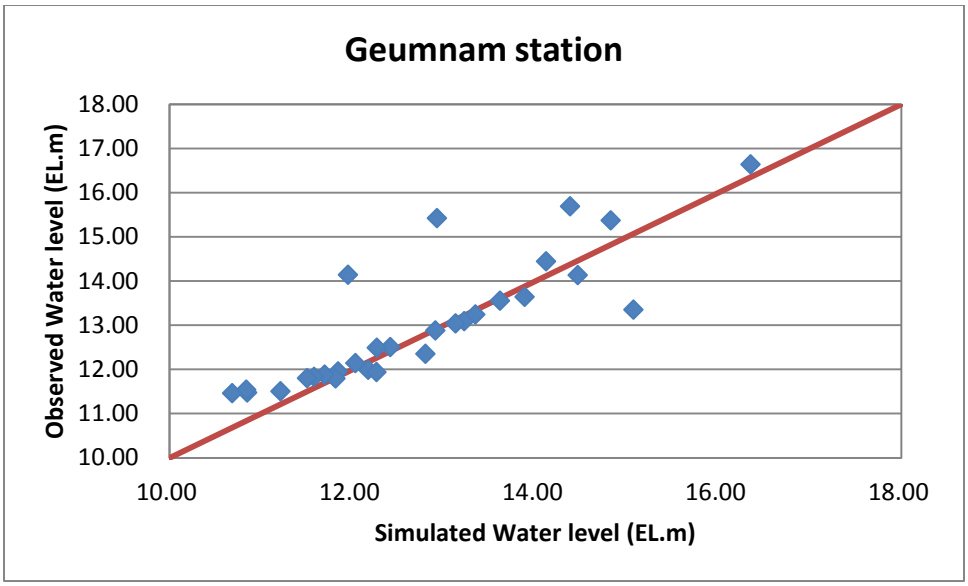

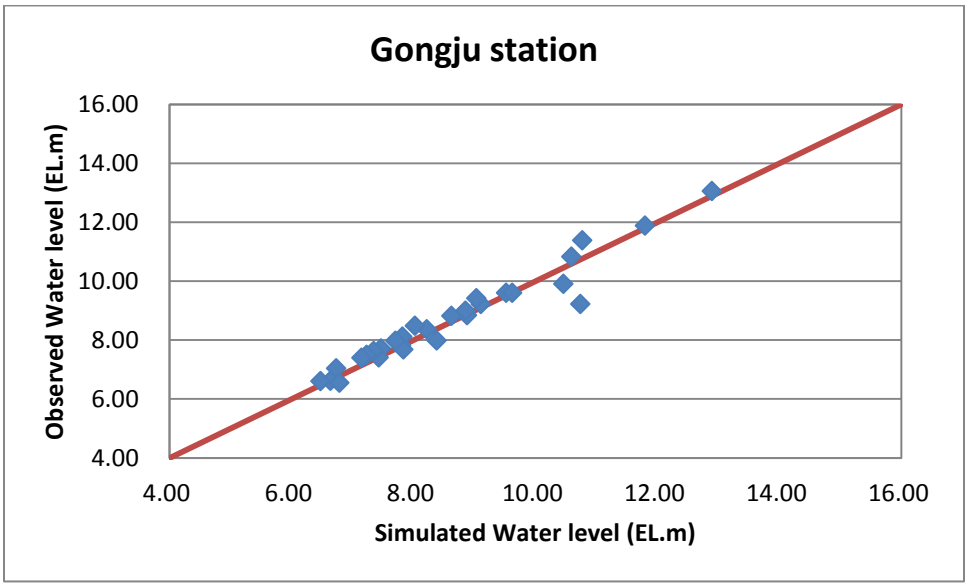

Figure 78. Continued

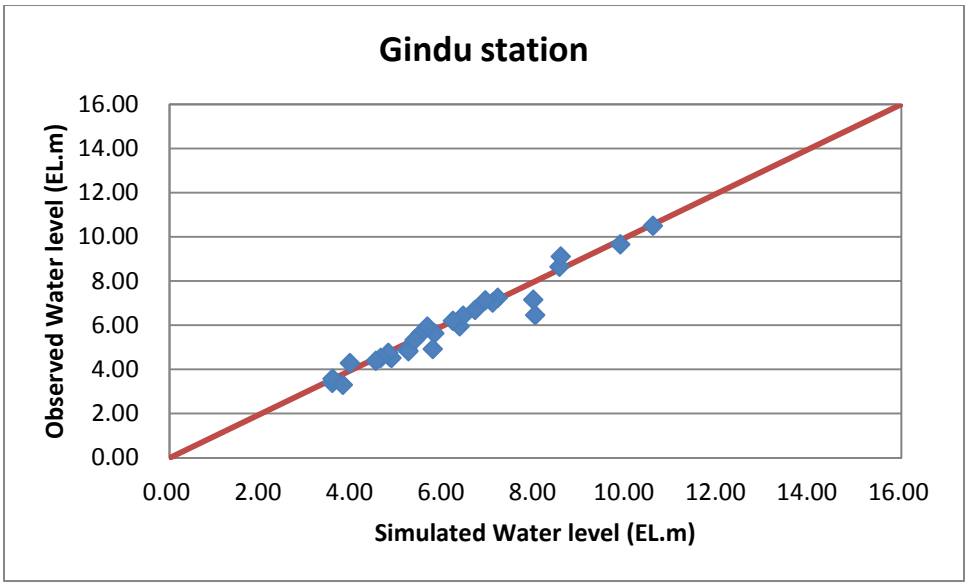

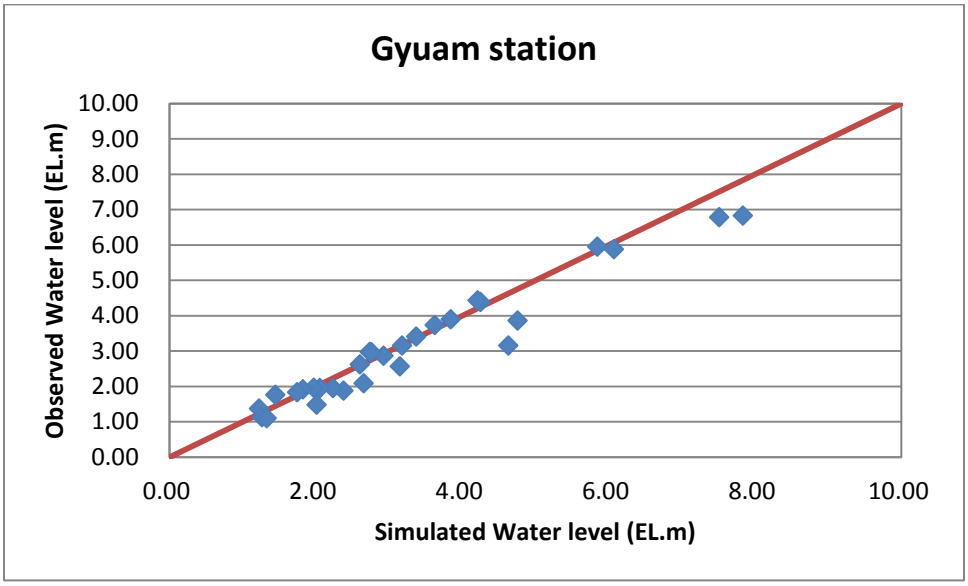

Figure 78. Continued

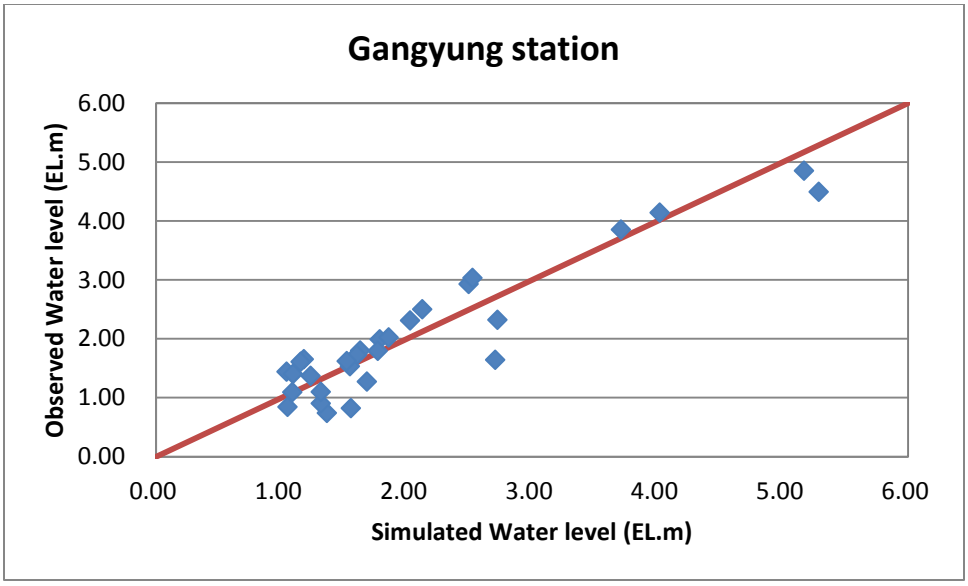

Figure 78. Continued

To verify the model, the flood event in 2007 was chosen. Similar to the results in 2006, the simulated result was similar to that of observations, as shown in Figure 79. In addition, quasi-unsteady analysis was compared with one another, since quasi-unsteady flow in HEC-RAS was used to analyze sediment load. As seen in Table 13 and Figure 79, the water level under quasi unsteady analysis was more similar to observed data than unsteady analysis. This result contributes to the use of daily data. In conclusion, quasi-unsteady flow analysis was enough to predict long-term riverbed change, since it approximately represent hydraulic characteristics.

Table 13. RMSE and AMD in 2007

Type		Root Mean Square Difference (RMSE) in meter		Absolute Mean Difference (AMD) in meter	
		Unsteady	Quasi	Unsteady	Quasi
1	Gyumnam	0.45	0.55	0.41	0.52
2	Gongju	0.42	0.36	0.38	0.32
3	Jindu	0.35	0.18	0.25	0.16
4	Gyuam	0.32	0.33	0.26	0.25
5	Gangyeong	0.41	0.39	0.33	0.32

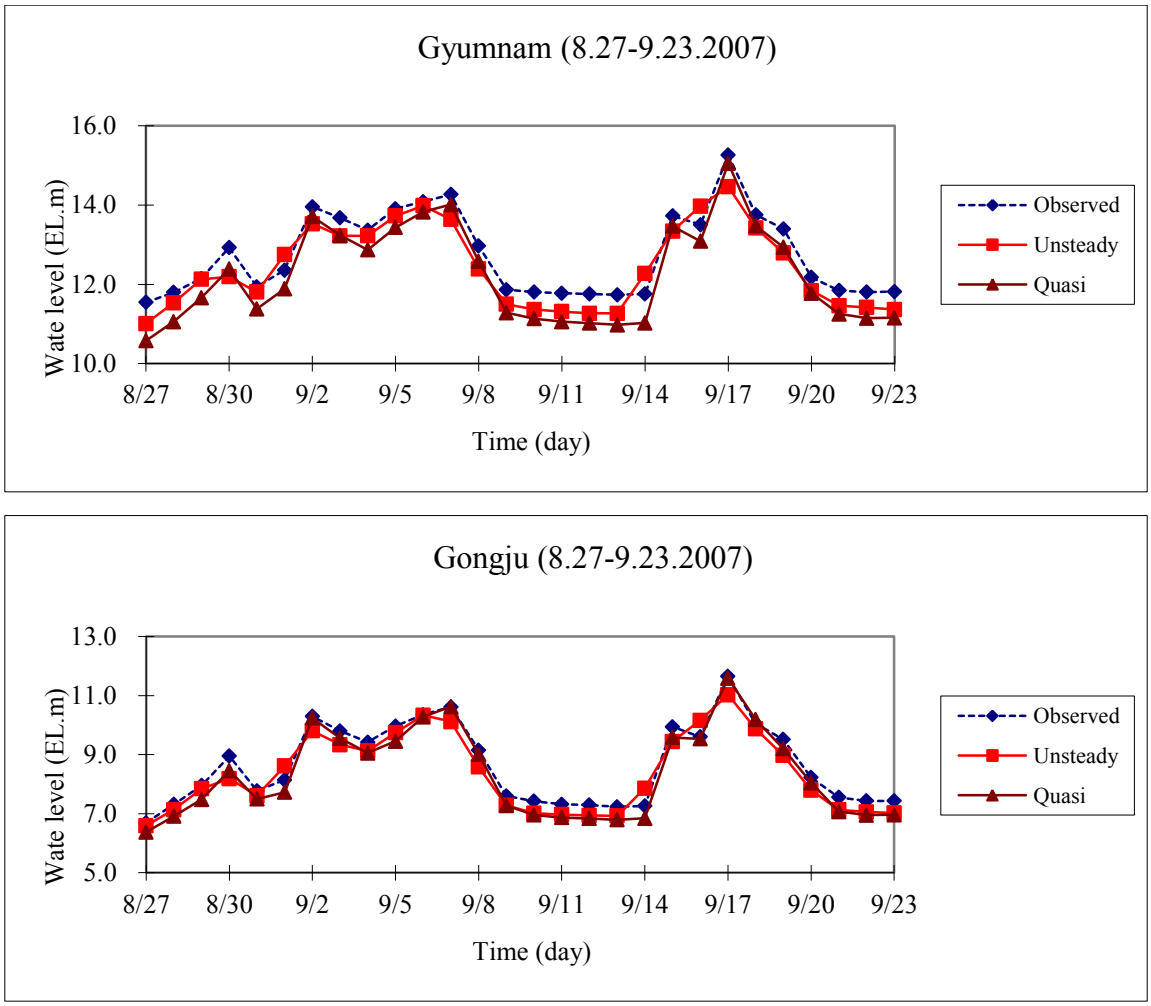

Figure 79. Comparison of Model Results and Observations in Unsteady Analysis (2007)

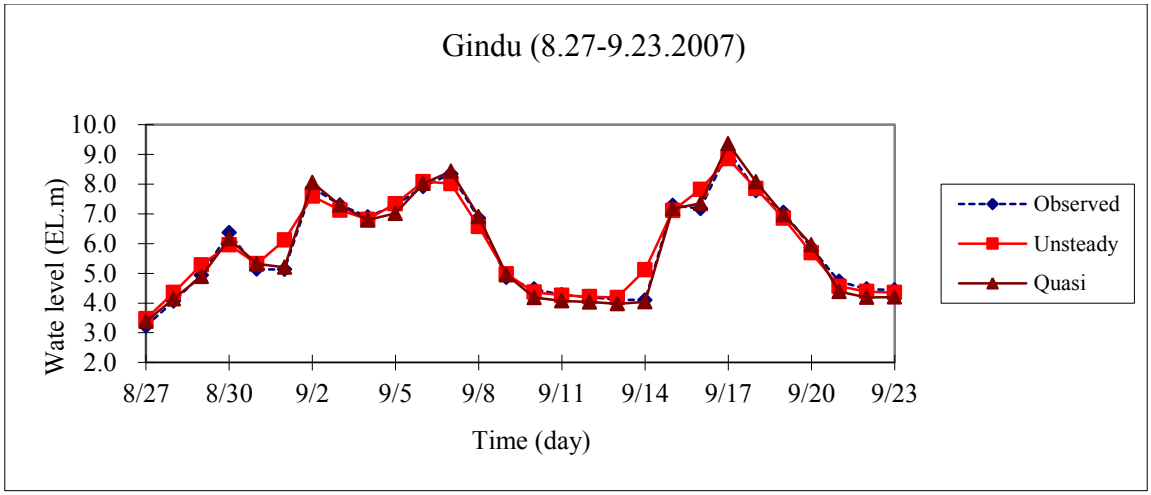

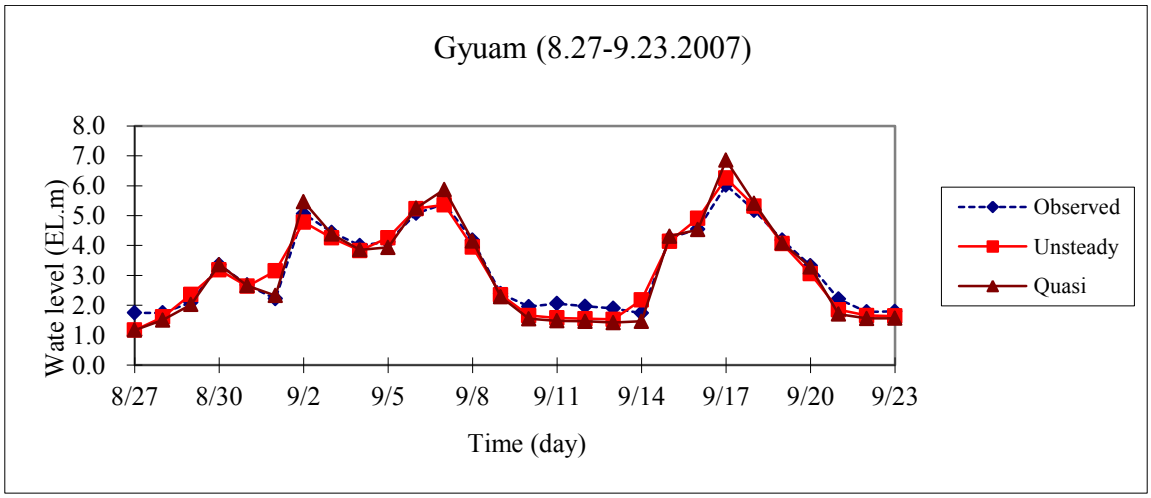

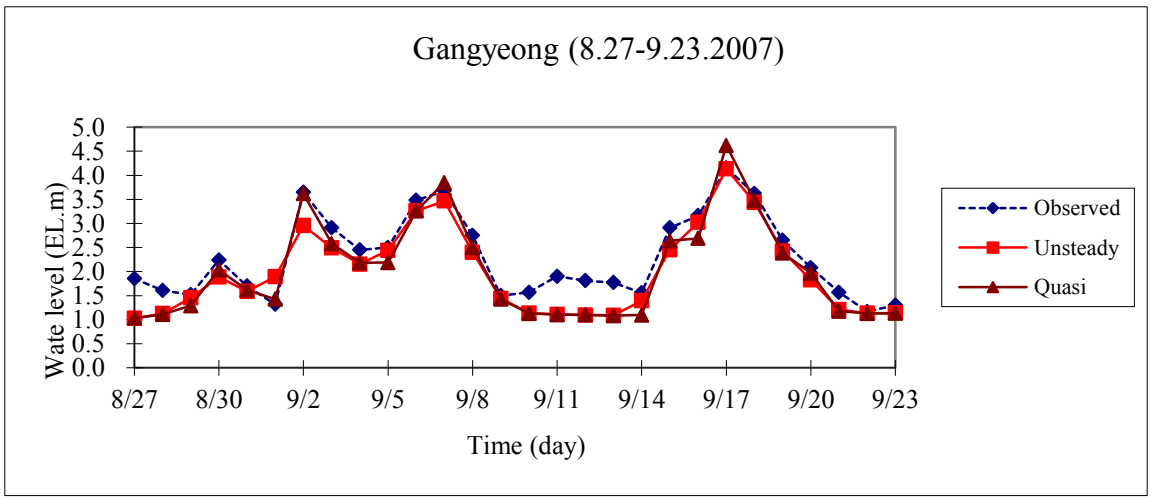

Figure 79. Continued

5.1.3 Sediment analysis

To predict the riverbed change, simulation was conducted during 2012-2031 (20 years) and it was assumed that inflow of 2006-2007 would repeat for 20 years. Three cases were considered to see the effect of gates which are installed in weir:

1) Case 1: the gate opening is 0 % (full close)

2) Case 2: the gate opening is 100 % (full open)

3) Case 3: the gate opening is operated by rule (to keep Management Water Level)

5.1.3.1 Hydraulic characteristics by a gate operation

As gates are more open, the larger velocity and shear force occur. To search for the gate effect in view of spatial aspect, we chose the 7.11.2012 event and the gate opening rate was like in Table 14 and Figure 80, which were calculated by unsteady analysis to keep the Management Water Level.

Table 14. Gate Opening Height (7.11.2012)

Type		Sejong Weir			Gongju Weir			Bakje Weir		
		Gate 1	Gate 2	Gate 3	Gate 1	Gate 2	Gate 3	Gate 1	Gate 2	Gate 3
Dimension (m)	B	81	81	61	41	41	20	40	40	40
	H	2.80	2.80	4.00	7.00	7.00	7.00	5.30	5.30	5.30
Opening height (m)		2.80	2.80	4.00	1.31	1.31	1.31	5.11	5.11	5.11

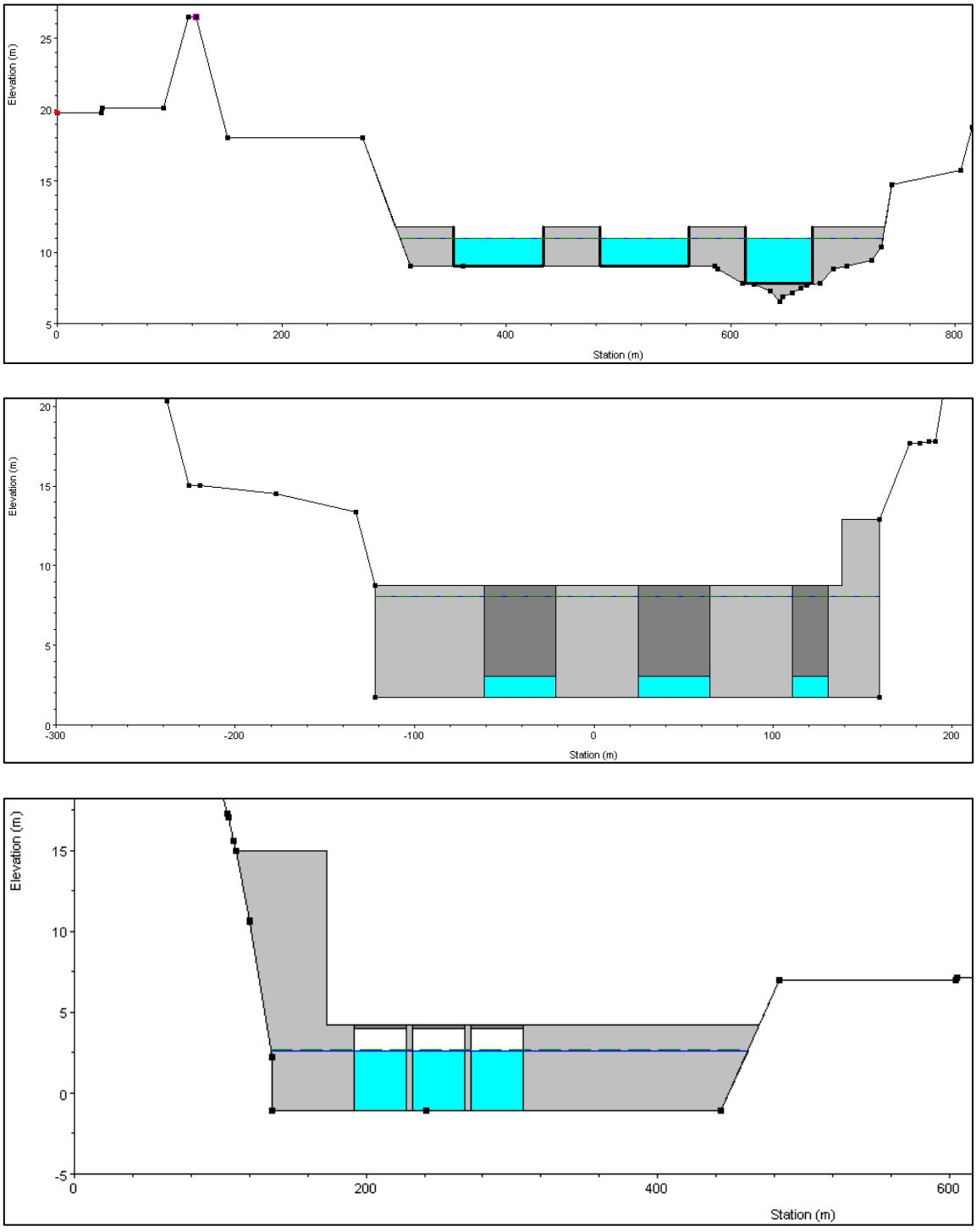

Figure 80. Gate Opening (up: Sejong, middle: Gongju, down: Bakje Weir, 7.11.2012)

The velocity in case 2 (full open) was large, because as the gate is more open, upstream water level is lower and therefore the velocity is larger. The velocity in case 1 (full close) was small, on the contrary, as shown in Table 15 and Figures 81-83. Results of hydraulics in section using the Yang equation are as follows.

Table 15. Hydraulic Characteristics Upstream of Gate (7.11.2012)

Type		Upstream of Sejong Weir (Sta. no 100.660)			Upstream of Gongju Weir (Sta. no 81.73)			Upstream of Bakje Weir (Sta. no 58.790)		
		Case 1	Case 2	Case 3	Case 1	Case 2	Case 3	Case 1	Case 2	Case 3
Yang	Water level (EL.m)	12.902	10.894	10.976	10.111	5.825	8.043	5.502	2.628	2.629
	Velocity (m/s)	0.447	0.859	0.842	0.420	0.910	0.572	0.408	0.835	0.834
Ackers & White	Water level (EL.m)	12.902	10.894	10.976	10.111	5.837	8.043	5.502	2.626	2.627
	Velocity (m/s)	0.447	0.875	0.846	0.420	0.917	0.572	0.408	0.836	0.834
Toffaleti	Water level (EL.m)	12.902	10.926	10.998	10.111	5.826	8.043	5.502	2.626	2.627
	Velocity (m/s)	0.447	0.860	0.833	0.420	0.908	0.572	0.408	0.835	0.834
Laursen	Water level (EL.m)	12.902	10.909	10.989	10.111	5.827	8.043	5.502	2.628	2.627
	Velocity (m/s)	0.447	0.871	0.837	0.420	0.915	0.572	0.408	0.834	0.834

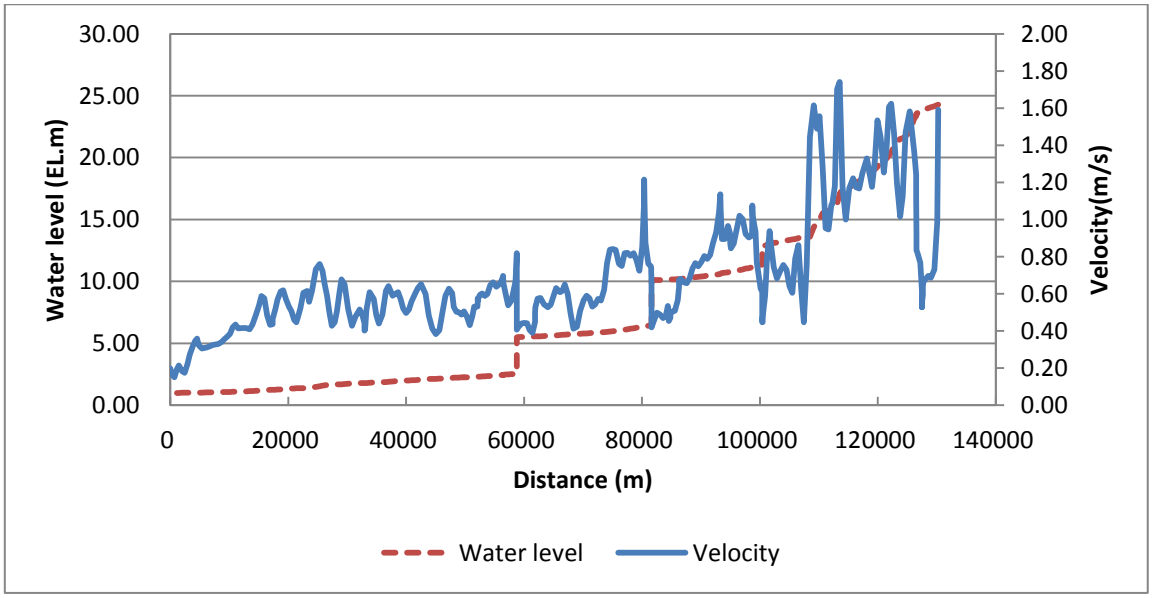

Figure 81. Water Level and Velocity (Yang equation, case 1, 7.11.2012)

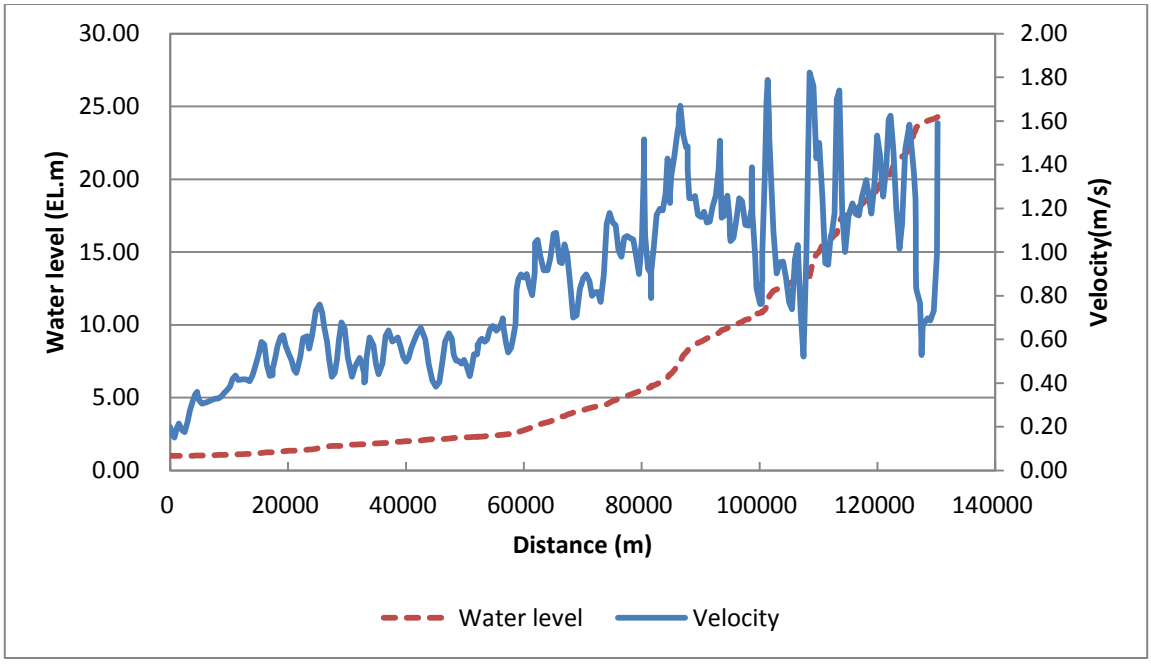

Figure 82. Water Level and Velocity (Yang equation, case 2, 7.11.2012)

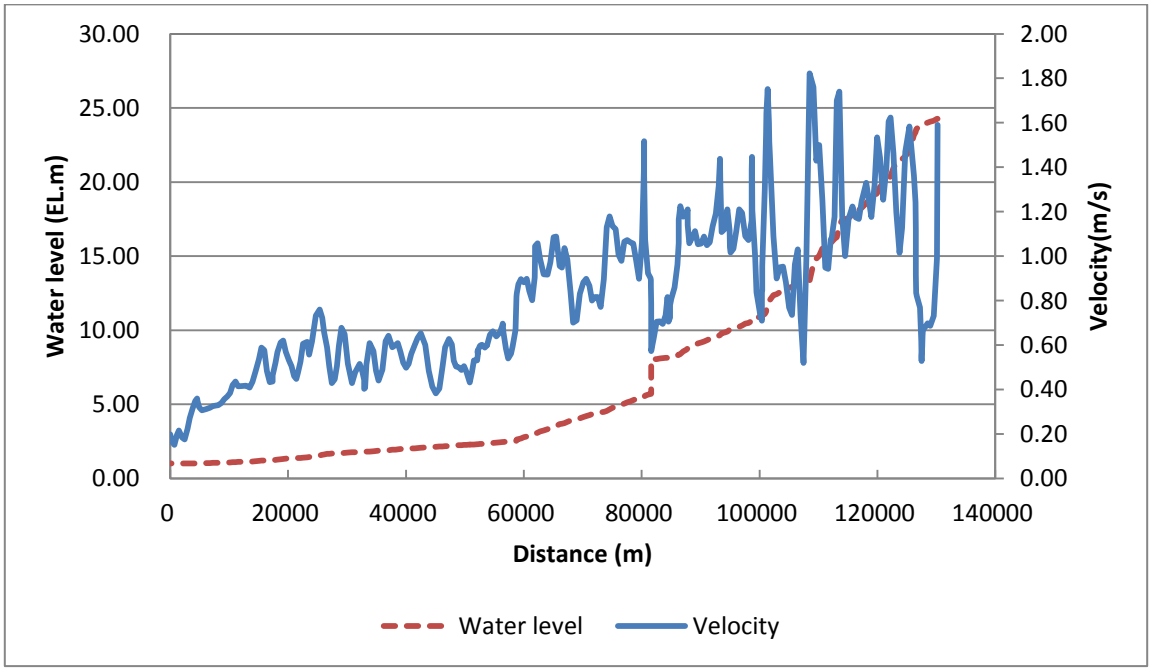

Figure 83. Water Level and Velocity (Yang equation, case 3, 7.11.2012)

5.1.3.1.1 Sejong weir-Daechung regulation dam

The water level of case 1 is lower than that of case 2 and case 3 8.1 km upstream of Sejong weir. The velocity and shear force of case 1 are lower than those of case 2 and case 3 8.7 km upstream of Sejong weir as shown in Figure 84. Gates are full open in 7.11.2012, therefore the hydraulic characteristics of case 2 and case 3 have the same results. As a result, the water level, velocity and shear force of both case 2 and case 3 do not have any discrepancy. But gates are close in case 1, so we can see what the difference in hydraulic characteristics contributes to the gates.

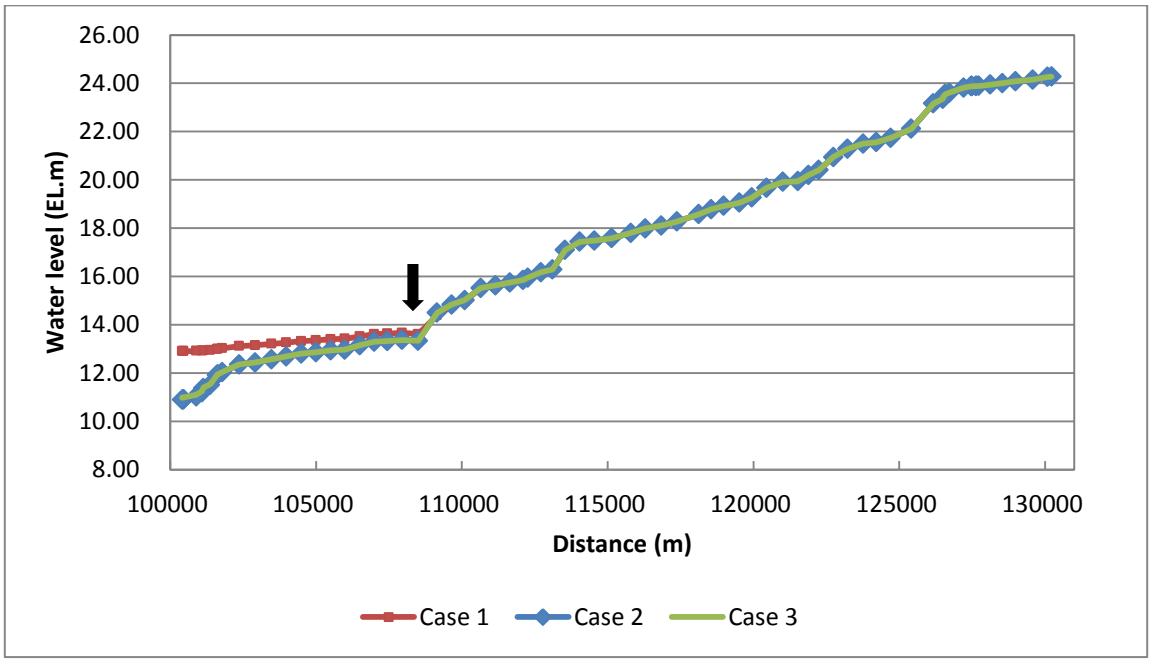

Figure 84. Hydraulic Characteristics from Sejong Weir to Daechung dam (7.11.2012)

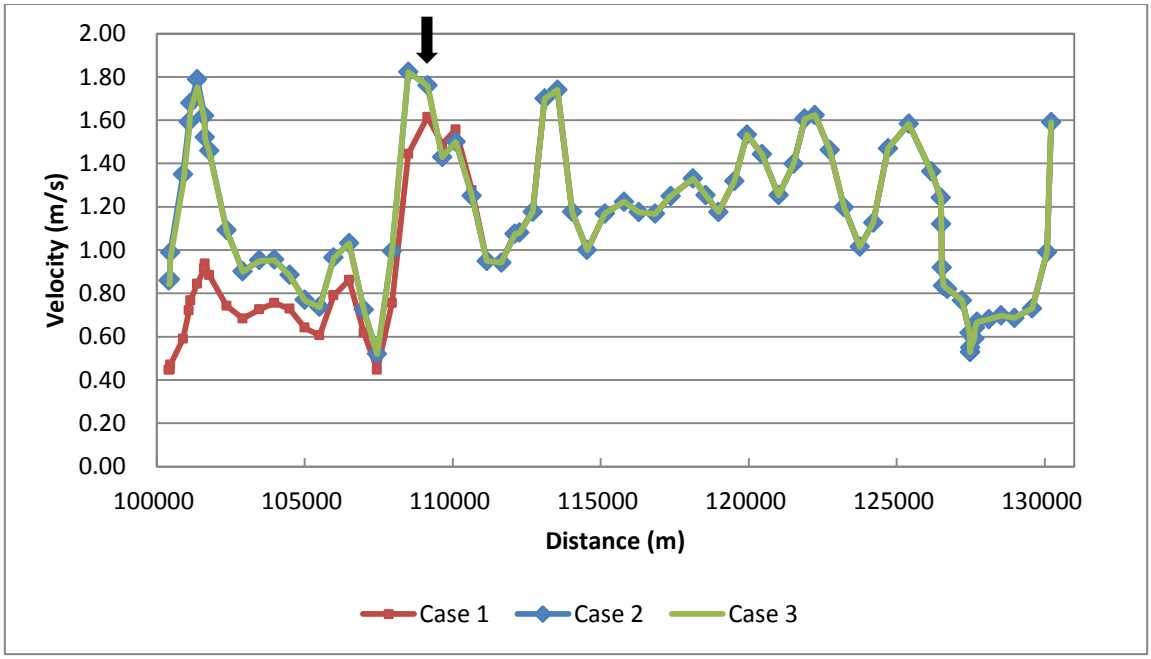

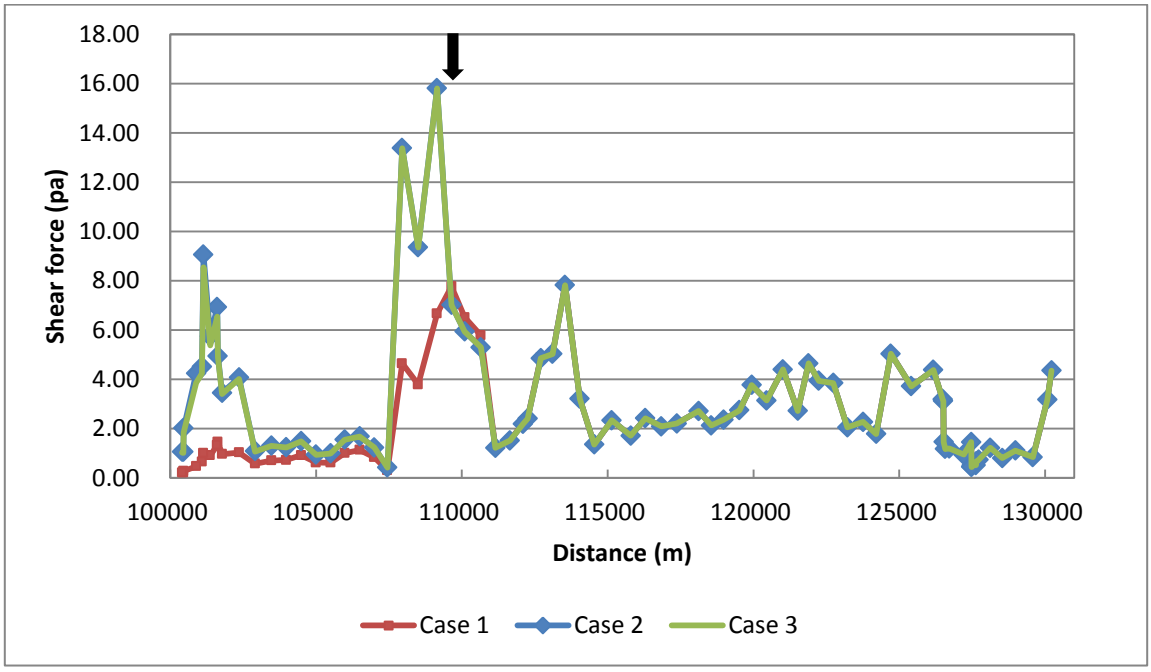

Figure 84. Continued

5.1.3.1.2 Gongju weir-Sejong weir

The water level upstream of Gongju weir in case 1 is maintaining the mild slope of water level, whereas water levels of case 2 and case 3 are different 15.9 km upstream of Sejong weir. Also velocity and shear stress of case 2 and case 3 are different at 17.1 km upstream of Sejong weir, as shown in Figure 85.

This boundary is simultaneously affected by both the opening of Sejong weir and the gate of Gongju weir. Especially, the gate of Sejong weir was fully open and the gate opening rate of Gongju weir was only 19 % (=1.31 m / 7.00 m) on 7.11.2012. Therefore, the impact of gates reached near the Sejong weir.

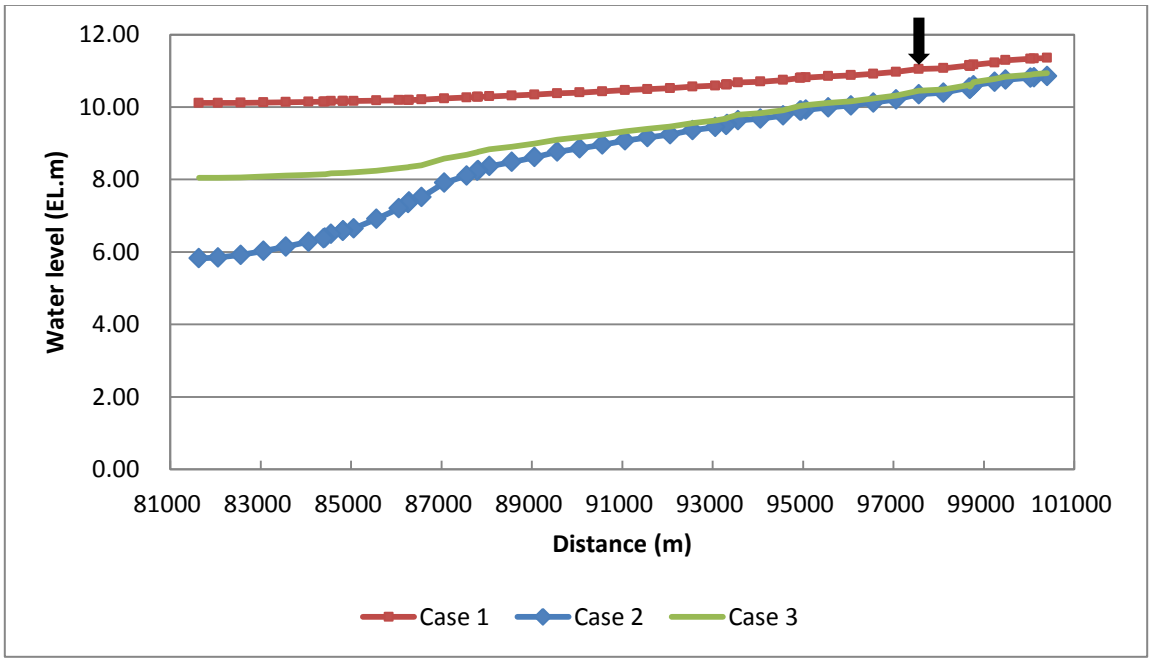

Figure 85. Hydraulic Characteristics from Gongju Weir to Sejong Weir (7.11.2012)

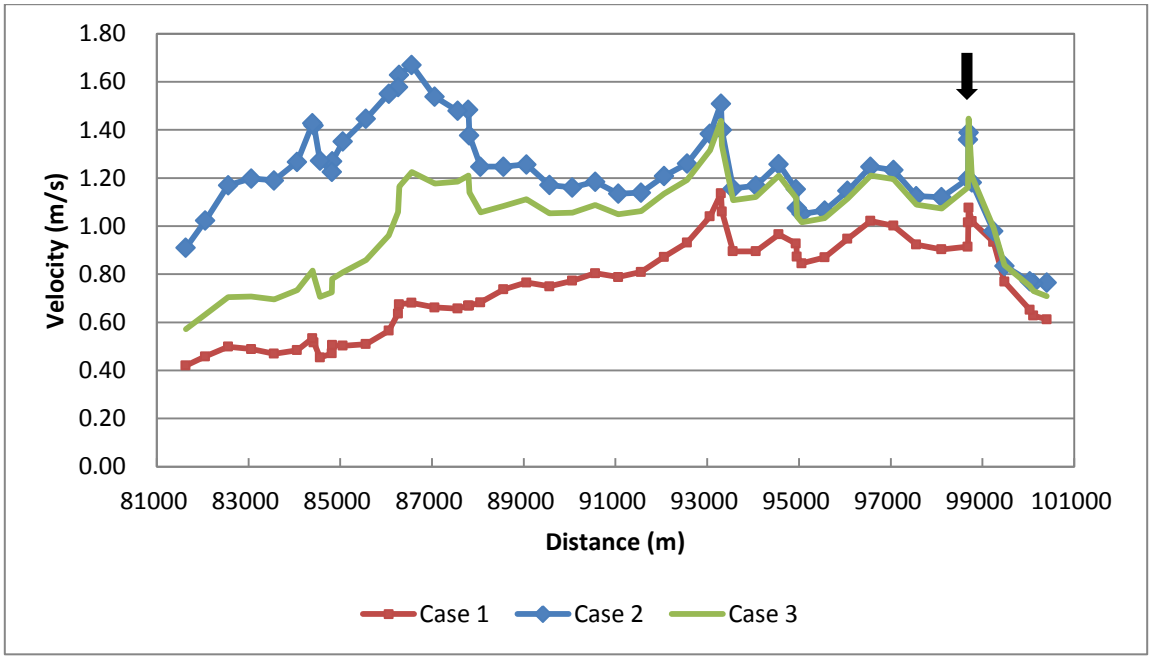

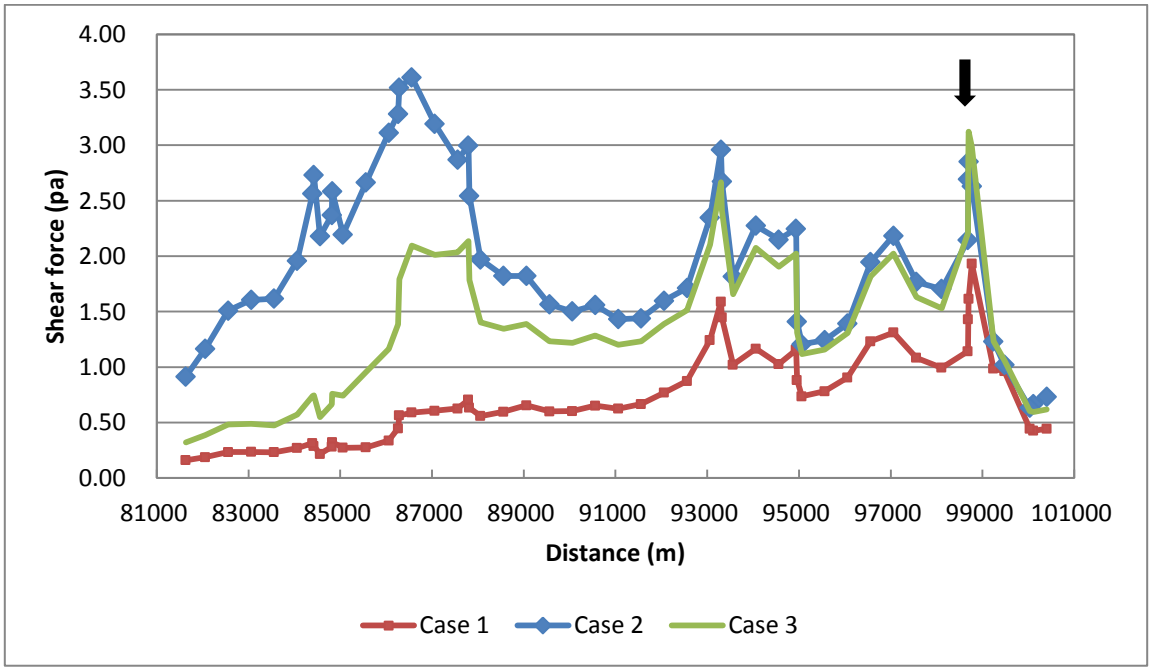

Figure 85. Continued

5.1.3.1.3 Bakje weir-Gongju weir

Velocity and shear force between case 2 and case 3 are similar as shown in Figure 86. This result is similar to that of Sejong weir –Daechung regulation dam where gates are fully open. In other words, gate operation does not affect the riverbed change on this boundary except case 1 when gates are completely close.

5.1.3.1.4 Estuary-Bakje weir

This boundary has similar hydraulic characteristics regardless of any case, because sediment analysis in HEC-RAS is based on quasi-unsteady analysis, as shown in Figure 87.

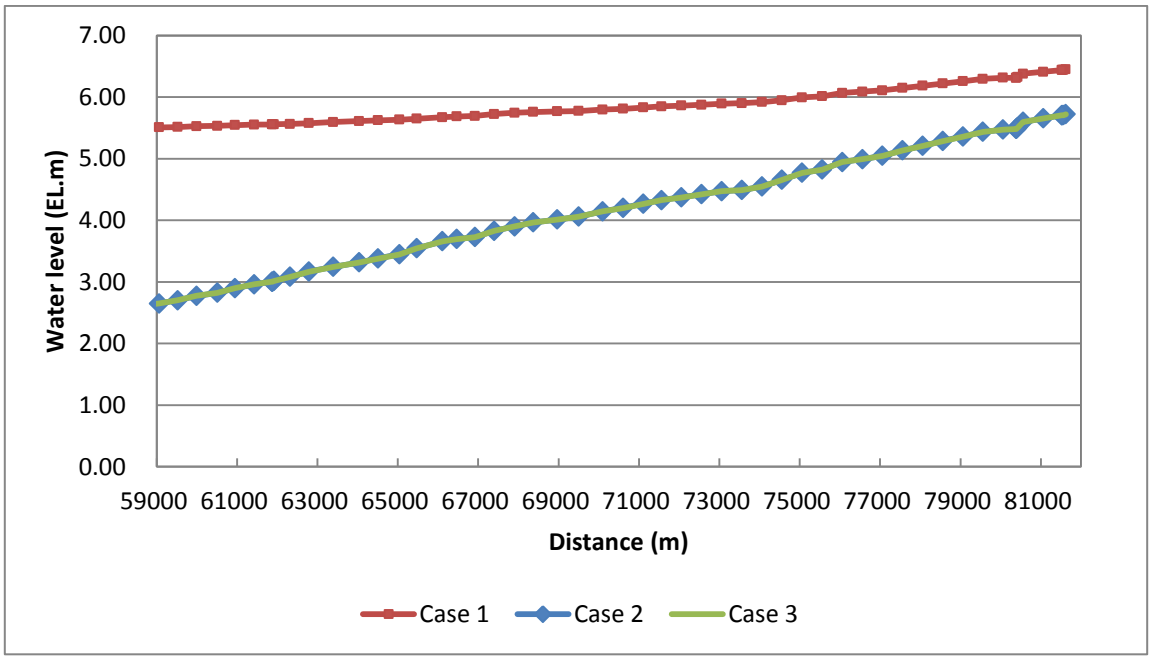

Figure 86. Hydraulic Characteristics from Bakje Weir to Gongju Weir (7.11.2012)

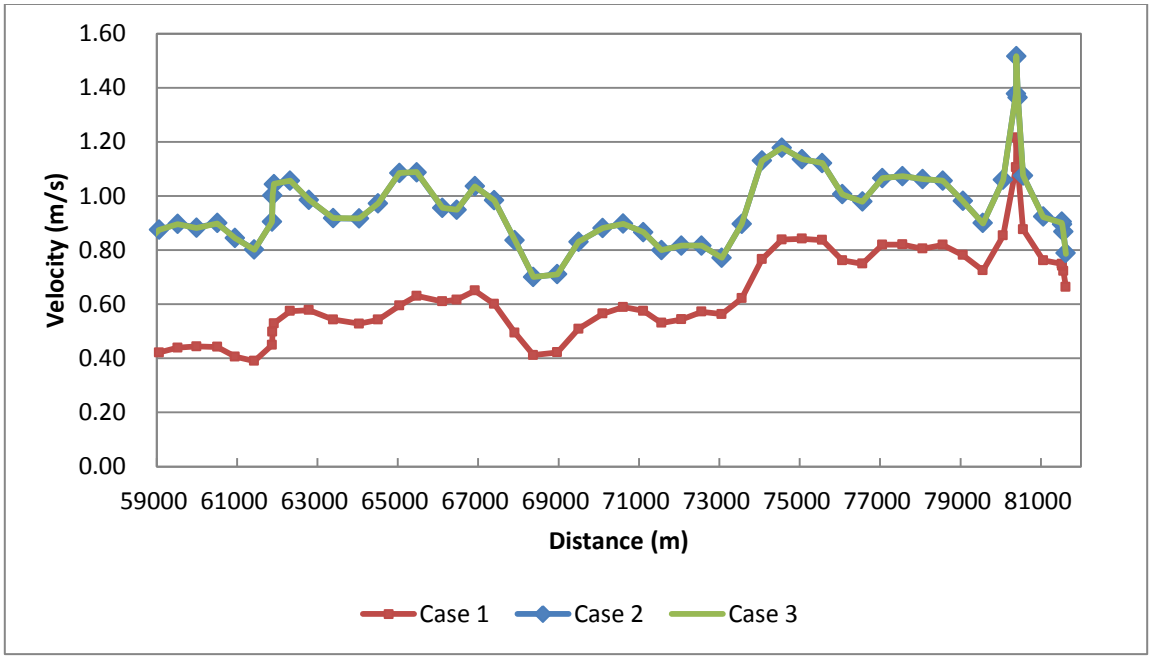

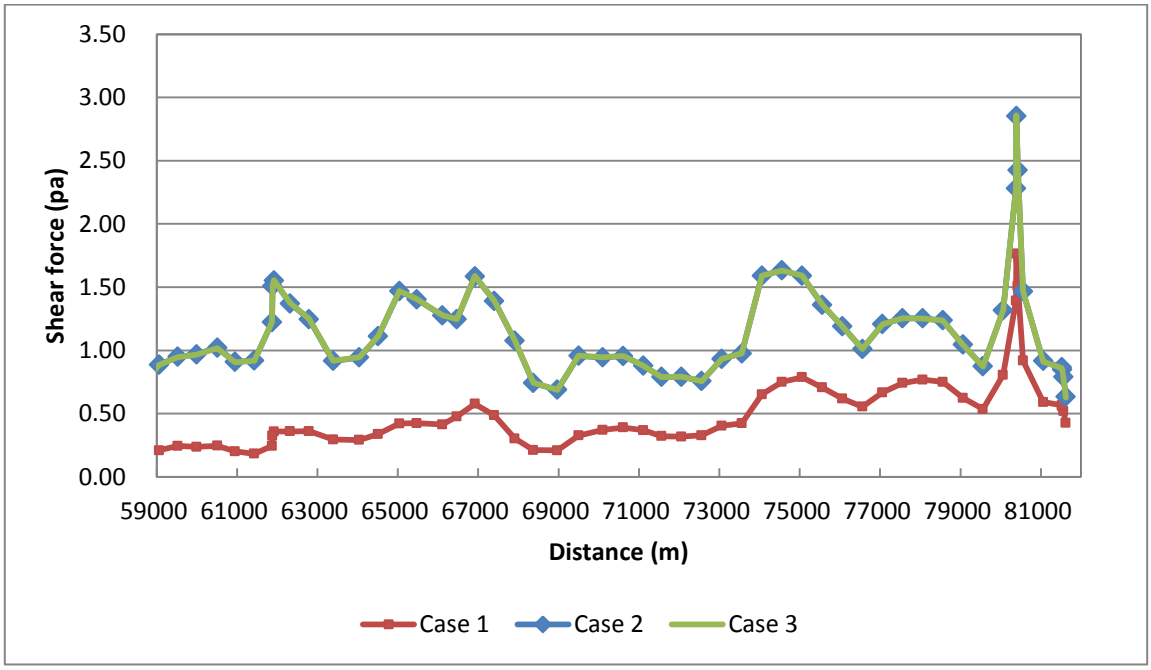

Figure 86. Continued

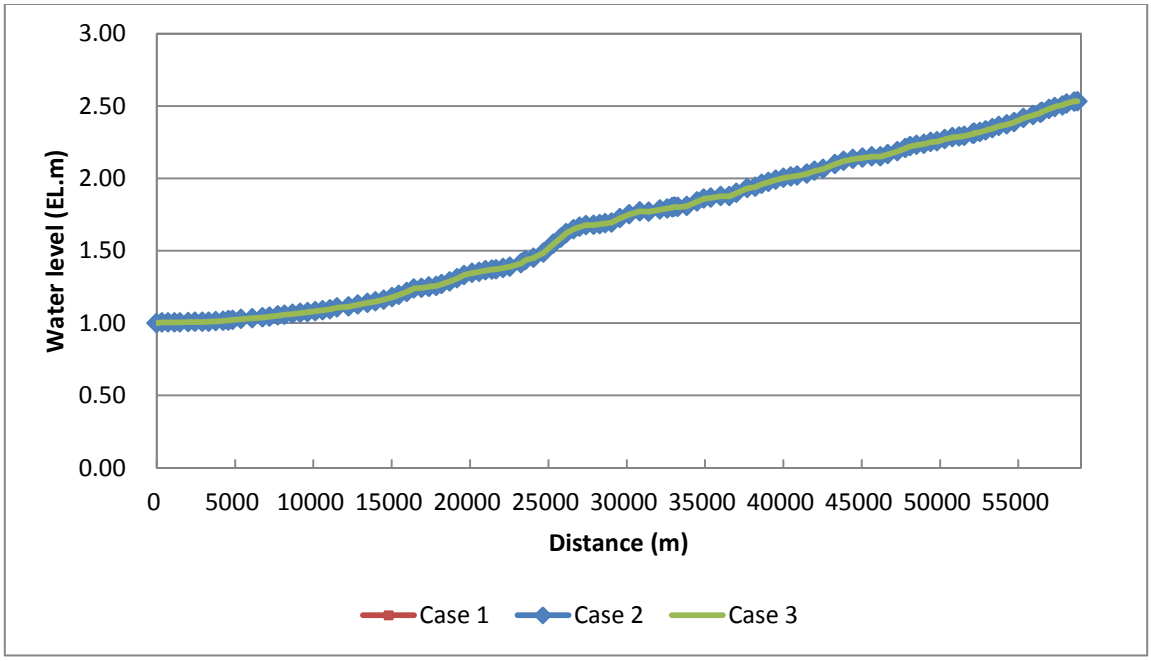

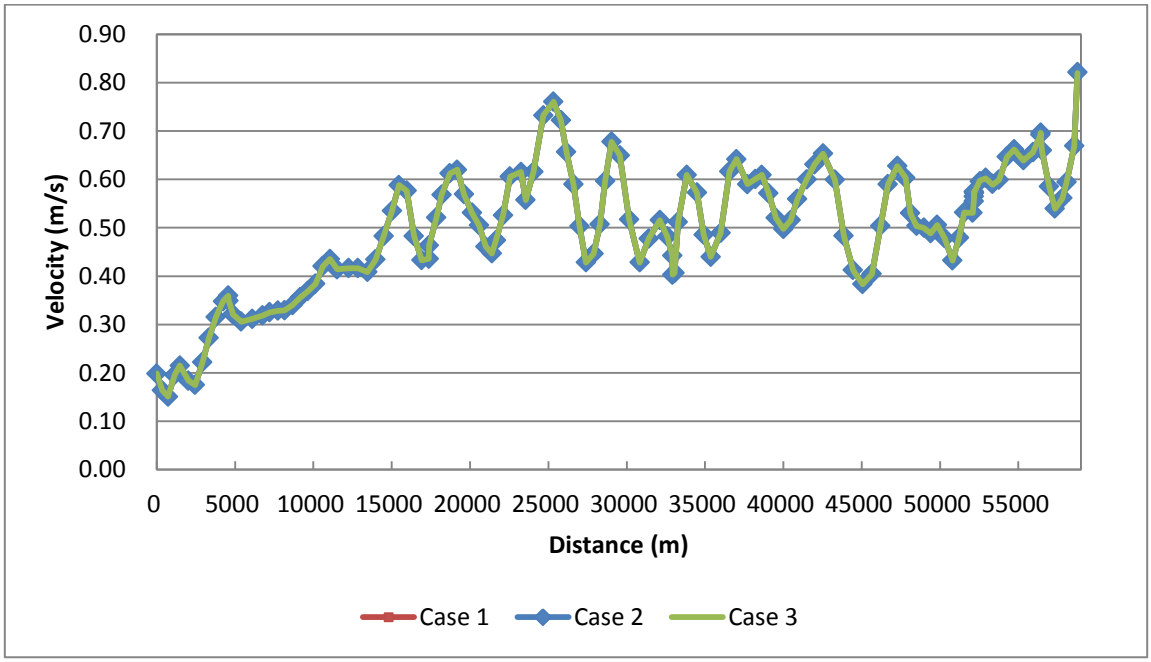

Figure 87. Hydraulic Characteristics from Estuary to Bakje Weir (7.11.2012)

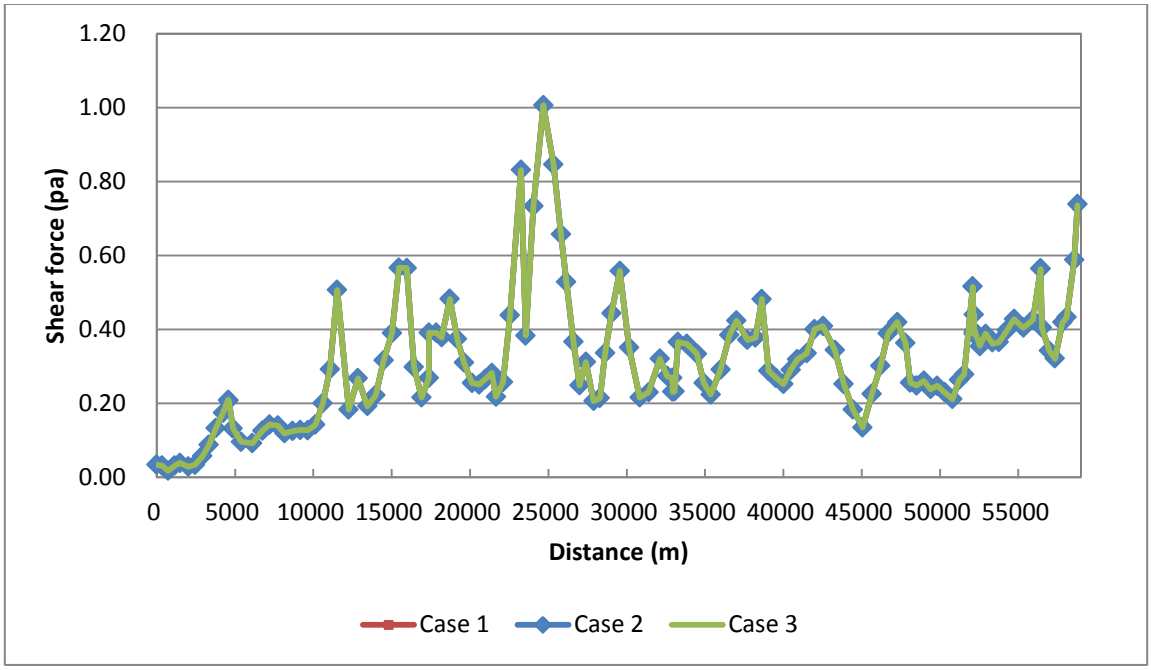

Figure 87. Continued

To see hydraulic characteristics according to gate opening in view of the temporal aspect using the Yang equation, we examined for 1 year (2012) at Station No 81.73 which is located 5 m upstream of Gongju weir. The discrepancy ratio [(case 2 – case 3) / case 2 * 100 %] was maximum at 91.2 % in velocity and was maximum at 99.6 % in shear stress, but there was no difference in flood season, because the gates are full open in flood season, as shown in Figure 88. This also showed the effect of gate operation.

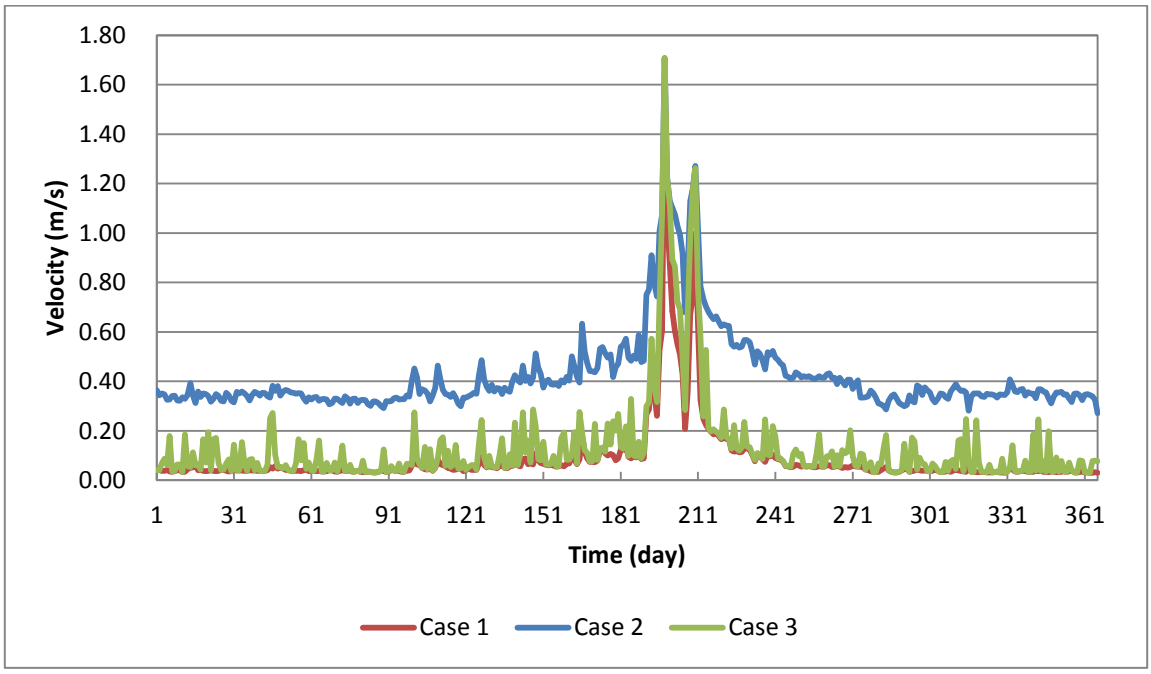

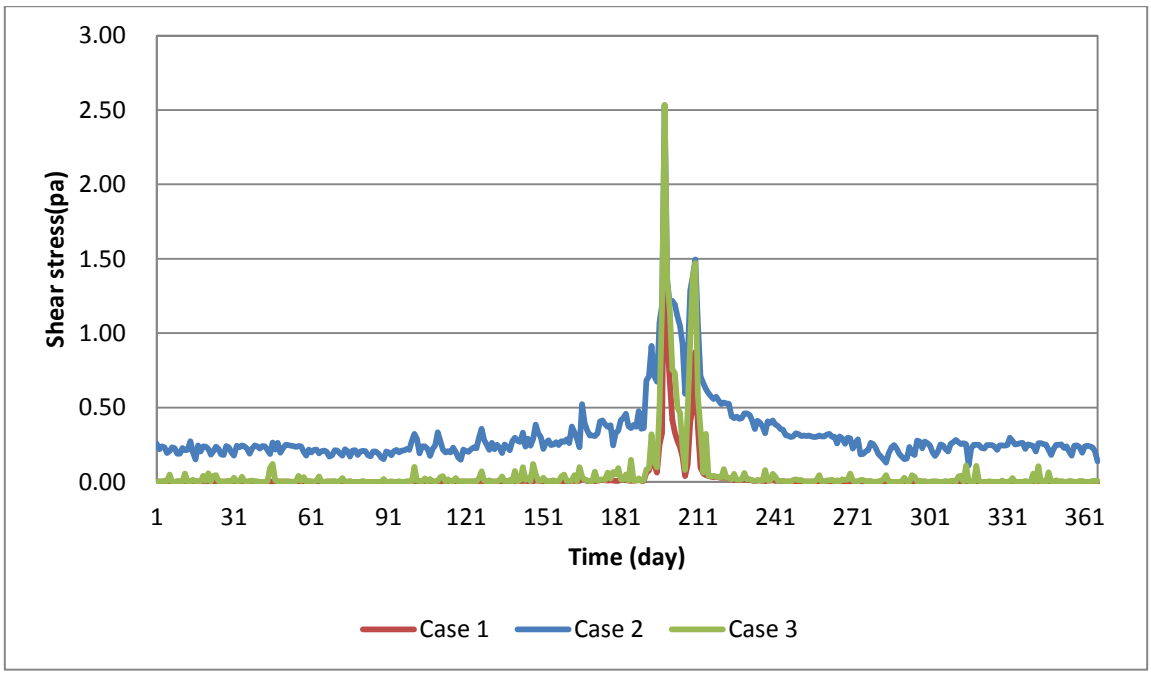

Figure 88. Temporal Comparison of Hydraulic Characteristics (Station No. 81.73)

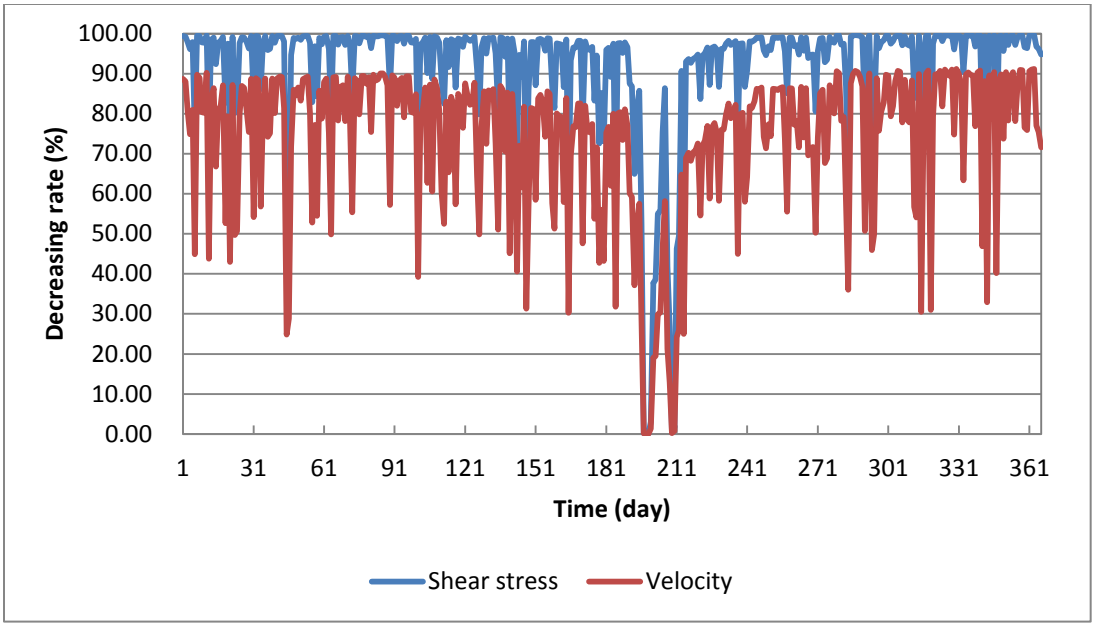

Figure 88. Continued

5.1.3.2 Long-term prediction of channel invert

Mass bed change and invert change were used to interpret the impact of gate operation on riverbed change in HEC-RAS. Mass bed change is a useful criterion to see trend, so longitudinal cumulative mass change was used. The longitudinal cumulative mass change means total change in bed mass, cumulative in space and time. The spatial accumulation is from the current cross section to the upstream end of the river in which this cross section resides. On the other hand, it is necessary to see how much the riverbed erodes or deposits by the amount of depth. In general, surplus becomes deposition and deficit translates into erosion, however, the difference between supply and capacity cannot be directly converted into a bed change in HEC-RAS, because there are physical constraints on the process of deposition and erosion. Comparing the vertical distance a particle has to travel to reach the bed surface and the vertical

distance a particle travels in a time step, HEC-RAS will determine the percentage of sediment surplus that can actually deposit in a given control volume in a given time step. Similar to deposition, erosion is also a temporally dependent process. The current theory implemented in HEC-RAS is based on the 'Characteristic Flow Length' principle. The governing assumption is that a flow field requires thirty times the water depth to fully entrain a continuity deficit (U.S. Army Corps of Engineers, 2010). The RMSE of simulated bed elevation with initial ground elevation was used, to see how much the riverbed changed.

$$RMSE = \sqrt{\frac{1}{N}\sum_{i=1}^{N}(x_i - \mu_i)^2} = \sqrt{\frac{1}{N}\sum_{i=1}^{N}(I_i)^2}$$

Where x_i =simulated bed elevation, μ_i=initial bed elevation, I_i =Invert change (x_i -μ_i), and N= the number of cross section. Results, as seen in Table 16, showed the gate operation made the riverbed less change considering case 2 and case 3.

Table 16. RMSE of Invert Change for 20 years

unit: m

Type	Equation	Case	Total	Sejong-Daechung	Gongju-Sejong	Bakje-Gongju	Estuary-Bakje
			(130km)	(29.8 km)	(18.8 km)	(22.8 km)	(58.8 km)
1	Yang	case 1	0.269	0.437	0.340	0.185	0.032
2		case 2	0.400	0.516	0.673	0.317	**0.027**
3		case 3	**0.332**	**0.460**	**0.512**	**0.278**	0.038
4	Ackers & White	case 1	0.414	0.557	0.408	0.598	0.128
5		case 2	0.475	0.686	0.639	**0.420**	0.170
6		case 3	**0.433**	**0.586**	**0.531**	0.528	**0.143**
7	Toffaleti	case 1	0.196	0.253	0.323	0.172	0.022
8		case 2	0.275	0.305	0.534	0.158	0.020
9		case 3	**0.250**	**0.275**	**0.489**	**0.139**	**0.018**
10	Laursen	case 1	0.372	0.667	0.359	0.206	0.066
11		case 2	0.592	0.896	0.864	0.394	0.077
12		case 3	**0.451**	**0.680**	**0.652**	**0.327**	**0.043**

5.1.3.2.1 Sejong weir - Daechung regulation dam (L=29.8 km)

Riverbed changes about longitudinal cumulative mass are plotted in Figure 89 and the invert changes are in Figure 90 for case 1, case 2, and case 3, using the Yang, Ackers & White, Toffaleti, and Laursen equations for sediment transport capacity. When we see the longitudinal cumulative mass change using Yang's equation in Figure 89 where the transverse axis represents the distance from estuary, the riverbed change of case 1 is the smallest among the three cases. In case 2 and case 3, the difference in a riverbed change exists 7.0 km upstream of Sejong weir (107450 m, sta. no 107.7). A boundary of impact by the gate operation using the Ackers & White equation is similar to the result of Yang's equation. In the Toffaleti equation, the riverbed change between case 2 and case 3 exists 2.0 km upstream of Sejong weir (102360 m, sta.no 102.61) and the riverbed change of Laursen equation happens 7.0 km upstream of Sejong weir (107450 m, sta.no 107.70), as shown in Figure 89.

When we see the invert change, the riverbed change shows the same results as the longitudinal cumulative mass change, as shown in Figure 90. As seen Table 17, a boundary of impact by the gate operation depends on which kind of sediment transport equation was applied. The maximum erosion depth of Laursen equation is the largest in a boundary of impact and that of Toffaleti equation is the smallest among the four results. In case of Laursen equation, the boundary of impact reaches at 6.1 km upstream of Sejong weir (106500 m, sta.no 106.75) which is shorter than 7.0 km in the longitudinal cumulative mass change. Results are shown in Table 18.

Table 17. Boundary of Impact by the Gate Operation (Sejong weir – Daechung dam)

Type		Yang	Ackers & White	Toffaleti	Laursen
A boundary of impact		7.0 km	7.0km	2.0 km	6.1 km
Maximum erosion depth	Case 2	1.242 m	1.540 m	0.639 m	3.102 m
	Case 3	0.232 m	0.559 m	0.018 m	1.091 m

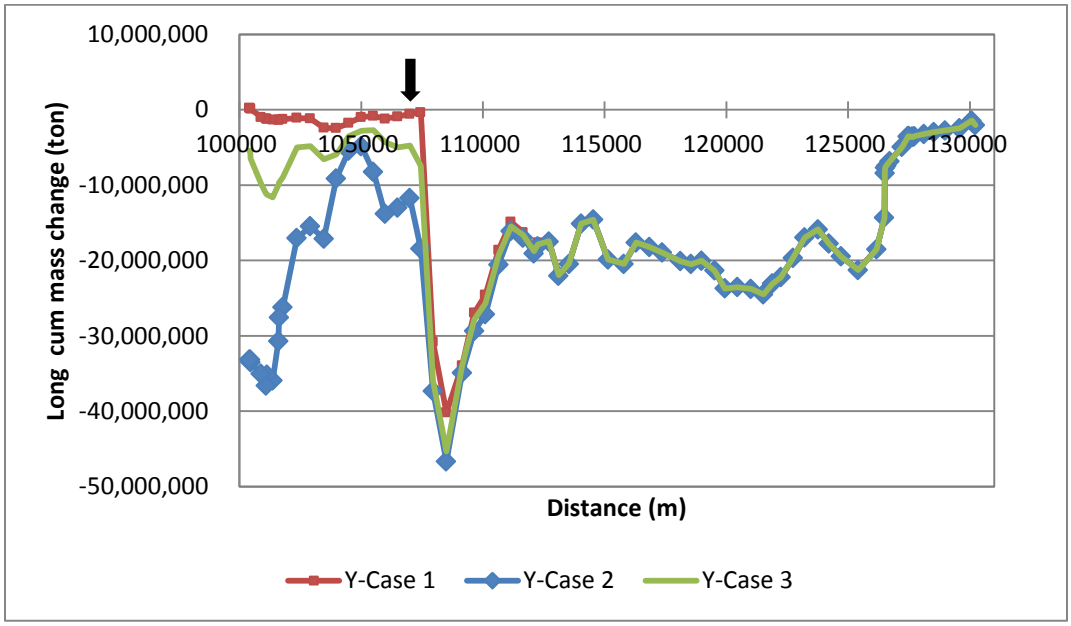

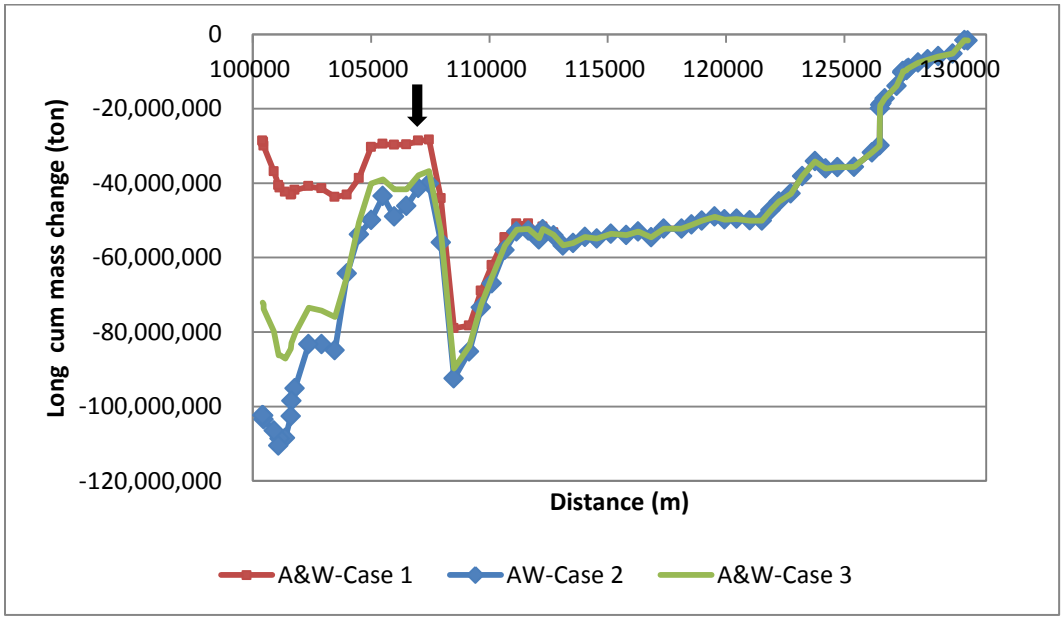

Figure 89. Mass Change from Sejong Weir to Daechung Dam by Gate Operation

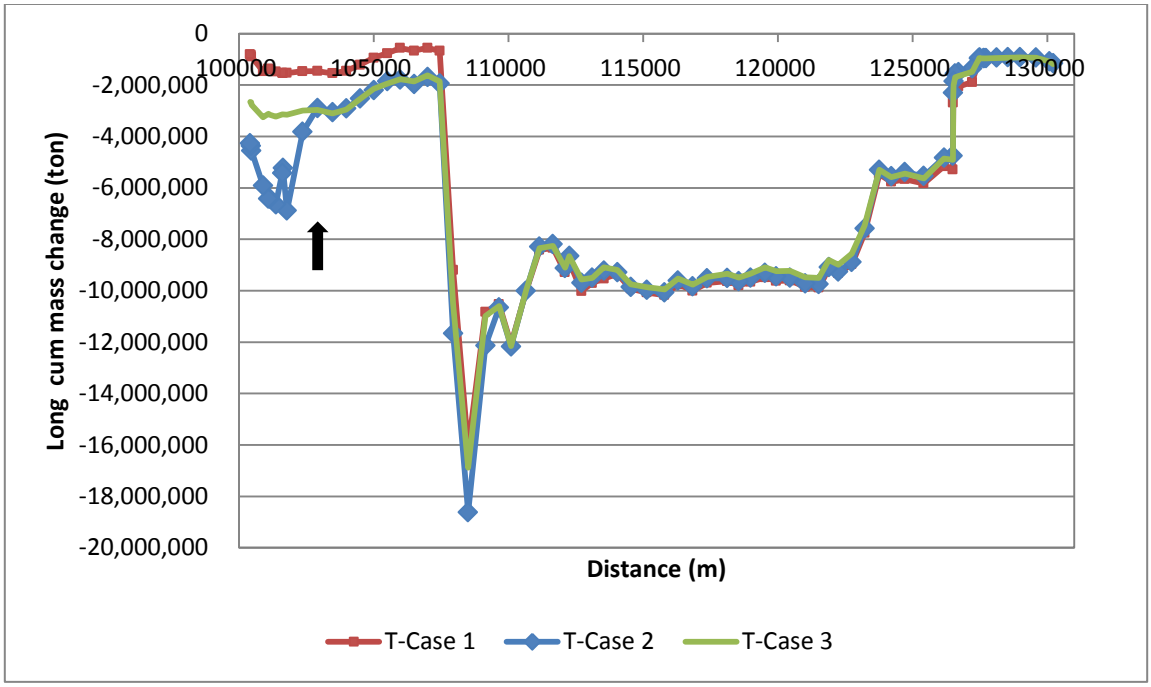

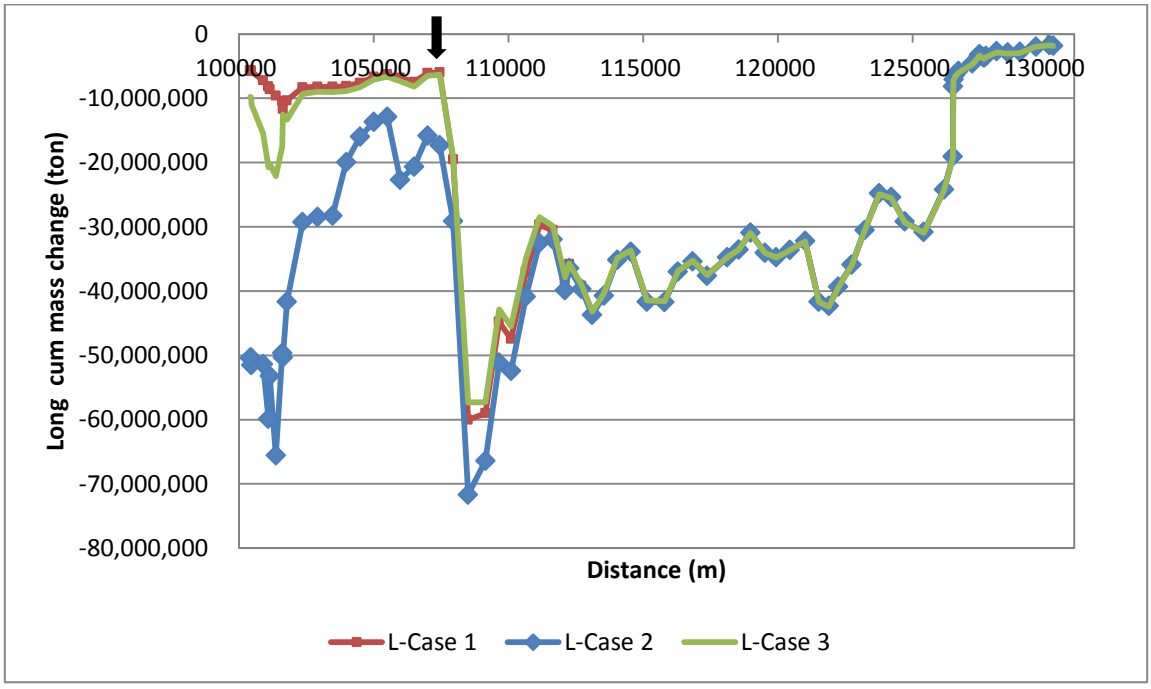

Figure 89. Continued

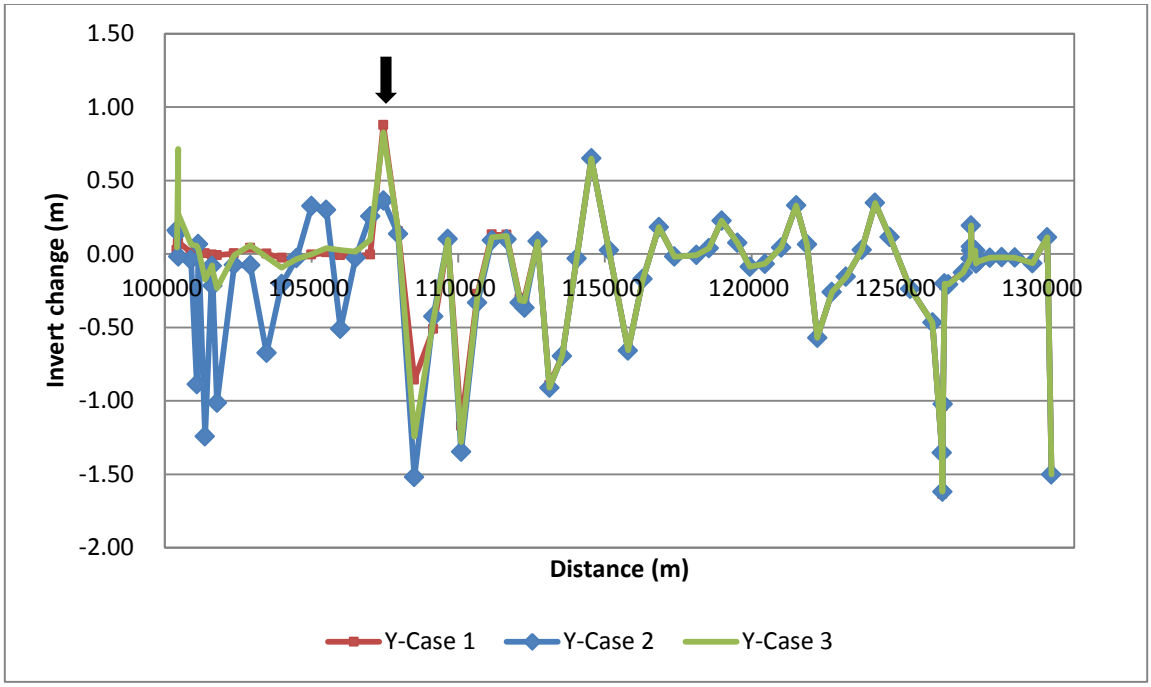

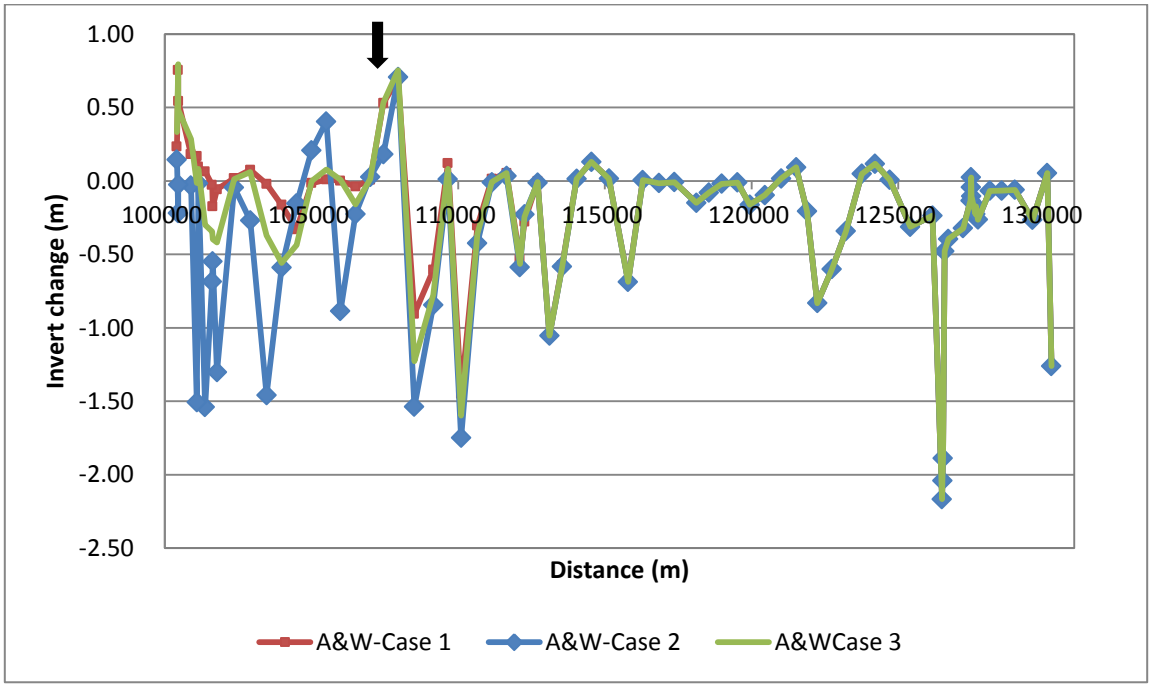

Figure 90. Invert Change from Sejong Weir to Daechung Dam by Gate Operation

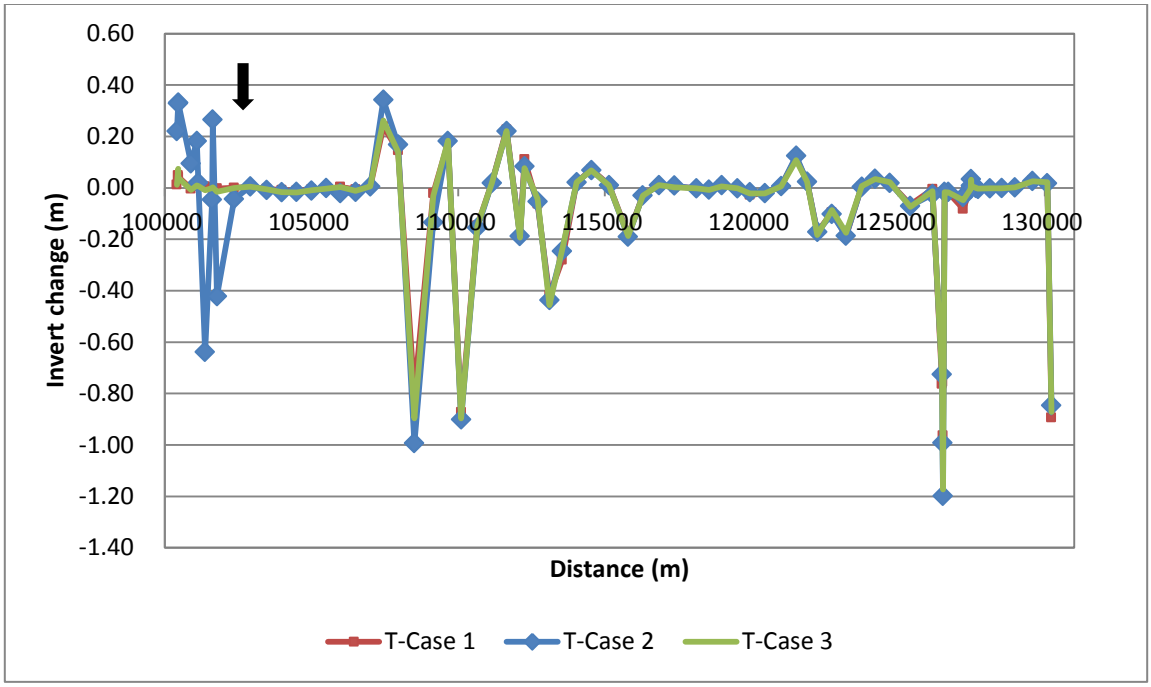

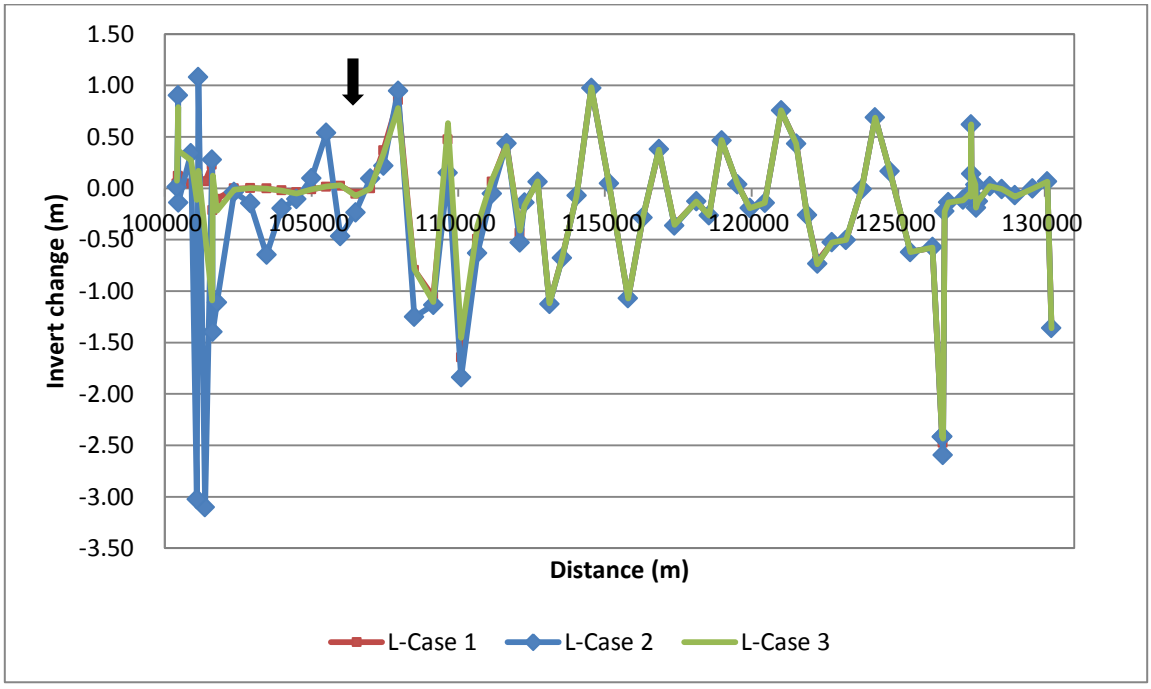

Figure 90. Continued

Table 18. Invert Change from Sejong Weir to Daechung Dam (after 20 years)

unit: m

Sta. no	Yang			Ackers&White			Toffaletti			Laursen		
	Case 1	Case 2	Case 3	Case 1	Case2	Case 3	Case 1	Case2	Case 3	Case 1	Case2	Case 3
130.47	-1.501	-1.501	-1.501	-1.261	-1.261	-1.261	-0.894	-0.846	-0.872	-1.357	-1.359	-1.360
130.33	0.113	0.113	0.113	0.053	0.053	0.053	0.019	0.018	0.022	0.066	0.065	0.064
129.83	-0.064	-0.064	-0.064	-0.266	-0.266	-0.266	0.028	0.026	0.026	-0.003	-0.002	-0.004
129.23	-0.025	-0.025	-0.025	-0.062	-0.062	-0.062	0.002	0.002	0.002	-0.068	-0.068	-0.081
128.78	-0.023	-0.023	-0.023	-0.067	-0.067	-0.067	-0.002	-0.002	-0.002	-0.008	-0.009	-0.009
128.37	-0.026	-0.026	-0.026	-0.068	-0.068	-0.068	-0.002	-0.002	-0.002	0.016	0.018	0.019
127.97	-0.052	-0.052	-0.052	-0.264	-0.264	-0.264	-0.001	-0.005	-0.003	-0.123	-0.126	-0.130
127.901	-0.067	-0.066	-0.066	-0.173	-0.173	-0.173	-0.001	-0.001	-0.001	-0.195	-0.189	-0.188
127.879	0.023	0.023	0.023	-0.226	-0.226	-0.226	0.001	0.001	0.001	0.034	0.035	0.035
127.745	0.024	0.024	0.024	-0.105	-0.105	-0.105	0.002	0.004	0.003	0.138	0.140	0.142
127.735	0.193	0.194	0.194	0.023	0.023	0.023	0.028	0.033	0.032	0.614	0.618	0.621
127.725	0.051	0.050	0.050	-0.044	-0.044	-0.044	0.006	0.009	0.009	-0.082	-0.083	-0.082
127.715	-0.033	-0.032	-0.032	-0.135	-0.135	-0.135	-0.005	-0.005	-0.005	-0.045	-0.045	-0.045
127.46	-0.127	-0.127	-0.127	-0.323	-0.323	-0.323	-0.082	-0.036	-0.048	-0.113	-0.113	-0.115
126.96	-0.195	-0.208	-0.208	-0.396	-0.396	-0.396	-0.019	-0.016	-0.018	-0.138	-0.137	-0.138
126.825	-0.214	-0.202	-0.202	-0.478	-0.478	-0.478	-0.016	-0.016	-0.016	-0.226	-0.225	-0.226
126.775	-1.037	-1.022	-1.022	-1.889	-1.889	-1.889	-0.963	-1.198	-1.173	-2.476	-2.595	-2.436
126.758	-1.635	-1.619	-1.619	-2.040	-2.040	-2.040	-0.756	-0.992	-0.932	-2.432	-2.415	-2.411
126.742	-1.355	-1.354	-1.354	-2.166	-2.166	-2.166	-0.763	-0.726	-0.735	-2.424	-2.419	-2.414
126.42	-0.468	-0.468	-0.468	-0.237	-0.237	-0.237	-0.005	-0.025	-0.013	-0.579	-0.574	-0.576
125.66	-0.238	-0.238	-0.238	-0.313	-0.313	-0.313	-0.066	-0.070	-0.075	-0.618	-0.621	-0.620
124.96	0.113	0.115	0.115	0.006	0.006	0.006	0.020	0.019	0.022	0.167	0.166	0.166
124.46	0.345	0.347	0.347	0.116	0.116	0.116	0.037	0.034	0.035	0.688	0.689	0.688
124.01	0.026	0.027	0.027	0.048	0.048	0.048	0.006	0.004	0.007	-0.009	-0.008	-0.008
123.47	-0.156	-0.156	-0.156	-0.340	-0.341	-0.341	-0.187	-0.187	-0.174	-0.507	-0.503	-0.502
122.99	-0.261	-0.260	-0.260	-0.600	-0.601	-0.601	-0.095	-0.102	-0.086	-0.527	-0.526	-0.526
122.49	-0.567	-0.571	-0.571	-0.833	-0.833	-0.833	-0.172	-0.171	-0.183	-0.710	-0.735	-0.739
122.14	0.063	0.064	0.064	-0.207	-0.208	-0.208	0.025	0.024	0.024	-0.271	-0.261	-0.264
121.77	0.331	0.330	0.330	0.092	0.092	0.092	0.118	0.124	0.108	0.449	0.433	0.435
121.26	0.044	0.043	0.043	0.016	0.016	0.016	0.007	0.007	0.006	0.748	0.757	0.758
120.7	-0.068	-0.068	-0.068	-0.097	-0.097	-0.097	-0.021	-0.021	-0.022	-0.138	-0.144	-0.141
120.19	-0.087	-0.087	-0.087	-0.163	-0.163	-0.163	-0.028	-0.018	-0.022	-0.189	-0.194	-0.195
119.77	0.077	0.075	0.075	-0.011	-0.011	-0.011	-0.002	-0.003	-0.002	0.037	0.038	0.038
119.23	0.229	0.226	0.226	-0.020	-0.020	-0.020	0.012	0.010	0.005	0.464	0.464	0.467
118.8	0.040	0.039	0.039	-0.079	-0.080	-0.080	-0.007	-0.007	-0.008	-0.267	-0.266	-0.265
118.37	-0.008	-0.008	-0.008	-0.146	-0.151	-0.148	-0.001	-0.003	-0.002	-0.130	-0.129	-0.129
117.62	-0.018	-0.019	-0.019	-0.009	-0.008	-0.009	0.004	0.008	0.002	-0.352	-0.365	-0.358
117.09	0.186	0.183	0.184	-0.015	-0.015	-0.015	0.012	0.010	0.010	0.369	0.378	0.374
116.54	-0.172	-0.171	-0.171	0.008	0.004	0.005	-0.030	-0.030	-0.031	-0.287	-0.286	-0.285
116.04	-0.653	-0.658	-0.656	-0.682	-0.687	-0.686	-0.183	-0.190	-0.187	-1.073	-1.071	-1.071
115.39	0.027	0.026	0.026	0.014	0.015	0.015	0.011	0.010	0.009	0.048	0.048	0.049
114.79	0.650	0.650	0.650	0.130	0.128	0.129	0.071	0.069	0.068	0.980	0.974	0.980
114.29	-0.032	-0.032	-0.032	0.015	0.014	0.014	0.022	0.022	0.022	-0.069	-0.071	-0.068
113.79	-0.691	-0.696	-0.693	-0.574	-0.584	-0.582	-0.280	-0.246	-0.239	-0.672	-0.678	-0.672
113.36	-0.893	-0.912	-0.910	-1.053	-1.054	-1.052	-0.417	-0.437	-0.456	-1.120	-1.125	-1.119
112.96	0.083	0.085	0.083	-0.003	-0.014	-0.007	-0.063	-0.054	-0.043	0.065	0.062	0.067
112.51	-0.300	-0.367	-0.323	-0.278	-0.228	-0.246	0.110	0.083	0.076	-0.155	-0.141	-0.171
112.35	-0.305	-0.332	-0.315	-0.534	-0.588	-0.565	-0.188	-0.188	-0.194	-0.436	-0.529	-0.413
111.9	0.129	0.100	0.123	0.053	0.032	0.054	0.227	0.220	0.222	0.434	0.437	0.409
111.4	0.132	0.093	0.114	0.012	-0.011	-0.007	0.020	0.018	0.018	0.062	-0.052	0.081
110.9	-0.273	-0.332	-0.286	-0.306	-0.424	-0.358	-0.147	-0.156	-0.147	-0.495	-0.633	-0.365
110.35	-1.170	-1.348	-1.280	-1.450	-1.749	-1.598	-0.873	-0.901	-0.896	-1.646	-1.840	-1.456

Table 18. Continued

unit: m

Sta. no	Yang			Ackers&White			Toffaletti			Laursen		
	Case 1	Case 2	Case 3	Case 1	Case2	Case 3	Case 1	Case2	Case 3	Case 1	Case2	Case 3
109.9	0.090	0.102	0.096	0.120	0.012	0.081	0.175	0.182	0.184	0.474	0.150	0.634
109.4	-0.511	-0.425	-0.456	-0.606	-0.846	-0.776	-0.021	-0.134	-0.032	-1.057	-1.135	-1.106
108.75	-0.857	-1.520	-1.243	-0.905	-1.538	-1.228	-0.802	-0.993	-0.897	-0.795	-1.251	-0.790
108.2	0.155	0.136	0.164	0.694	0.705	0.753	0.146	0.168	0.140	0.856	0.947	0.780
107.7	0.876	0.364	0.827	0.530	0.181	0.534	0.239	0.342	0.263	0.368	0.218	0.333
107.25	-0.005	0.256	0.095	0.008	0.027	0.011	0.003	0.005	0.005	-0.003	0.092	-0.004
06.75	-0.016	-0.027	0.016	-0.039	-0.226	-0.160	-0.006	-0.017	-0.012	-0.057	-0.236	-0.074
106.23	-0.009	-0.511	0.026	0.000	-0.887	0.008	0.003	-0.021	0.004	0.022	-0.467	0.030
105.75	0.009	0.301	0.040	0.009	0.403	0.077	-0.004	-0.001	-0.004	0.014	0.538	0.018
105.25	-0.005	0.327	-0.002	-0.015	0.208	0.000	-0.006	-0.011	-0.009	-0.012	0.098	-0.011
104.74	-0.034	-0.030	-0.034	-0.331	-0.155	-0.436	-0.011	-0.017	**-0.018**	-0.040	-0.104	-0.050
104.23	-0.027	-0.206	-0.094	-0.164	-0.591	**-0.559**	-0.009	-0.017	-0.016	-0.021	-0.196	-0.024
103.72	0.001	-0.675	-0.022	-0.021	-1.459	-0.371	-0.003	-0.008	-0.005	-0.004	-0.648	-0.006
103.16	0.040	-0.078	0.059	0.075	-0.270	0.061	0.003	0.005	0.004	0.001	-0.147	0.002
102.61	0.002	-0.076	-0.008	0.019	-0.045	0.012	0.001	-0.044	-0.001	-0.003	-0.037	-0.015
102.03	-0.009	-1.014	**-0.232**	-0.059	-1.301	-0.418	-0.003	-0.421	-0.015	-0.104	-1.111	-0.218
101.882	-0.012	-0.216	-0.118	-0.174	-0.548	-0.397	-0.001	0.265	0.002	-0.216	-1.397	0.124
101.858	-0.006	-0.081	-0.078	-0.027	-0.686	-0.345	0.003	-0.046	-0.001	0.228	0.276	**-1.091**
101.62	0.003	**-1.242**	-0.174	0.064	**-1.540**	-0.299	0.004	**-0.639**	-0.009	0.067	**-3.102**	-0.443
101.39	0.009	0.066	0.030	0.096	-0.016	0.082	0.007	0.020	0.007	0.089	1.081	0.169
101.34	0.017	-0.886	0.056	0.169	-1.507	-0.014	0.007	0.182	0.009	0.096	-3.024	-0.113
101.14	0.008	-0.040	0.065	0.181	-0.031	0.285	-0.004	0.095	-0.009	0.043	0.340	0.272
100.71	0.084	-0.019	0.273	0.544	-0.026	0.482	0.042	0.332	0.040	0.111	-0.139	0.367
100.7	0.066	0.148	0.715	0.754	-0.220	0.794	0.048	0.329	0.074	0.119	0.902	0.788
100.66	0.025	0.161	0.044	0.234	0.145	0.331	0.013	0.221	0.012	0.043	0.012	0.075

5.1.3.2.2 Gongju weir-Sejong weir (L=18.8 km)

When we see the longitudinal cumulative mass change using Yang's equation in Figure 91, the difference of a riverbed change between case 2 and case 3 exists 7.4 km upstream of Gongju weir (89060 m, sta. no 89.31) and this means gate operation affects riverbed change. A boundary of impact by the gate operation using the Ackers & White equation is 8.9 km from upstream of Gongju weir to sta. no 90.81 (90560 m). In the Toffaleti equation, the riverbed change between case 2 and case 3 exists 7.4 km upstream of Gongju weir, similar to Yang's equation. Also, the riverbed change of Laursen equation happens 9.5 km upstream of Gongju weir (91560 m, sta. no 91.85), as shown in Figure 91.

When we see the invert change, the riverbed change shows the same results as the longitudinal cumulative mass change, as shown in Figure 92. As seen Table 19, a boundary of impact by the gate operation depends on which kind of sediment transport equation was applied. The maximum erosion depth of Laursen equation was the largest in a boundary of impact and that of Toffaleti equation was the smallest among the four results. This results show similar trend from Sejong weir to Daechung regulation dam. Results are shown in Table 20.

Table 19. Boundary of Impact by the Gate Operation (Gongju weir – Sejong weir)

Type		Yang	Ackers & White	Toffaleti	Laursen
A boundary of impact		7.4 km	8.9 km	7.4 km	9.5 km
Maximum erosion depth	Case 2	1.505 m	1.360 m	0.849 m	1.455 m
	Case 3	0.431 m	0.450 m	0.107 m	1.153 m

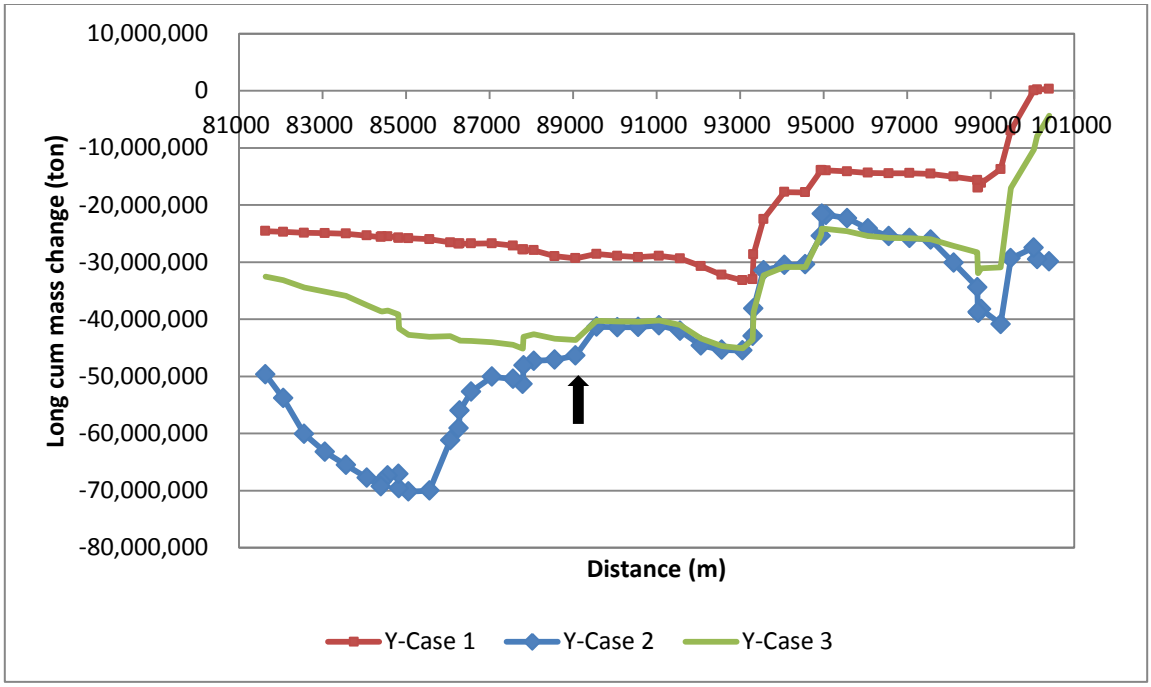

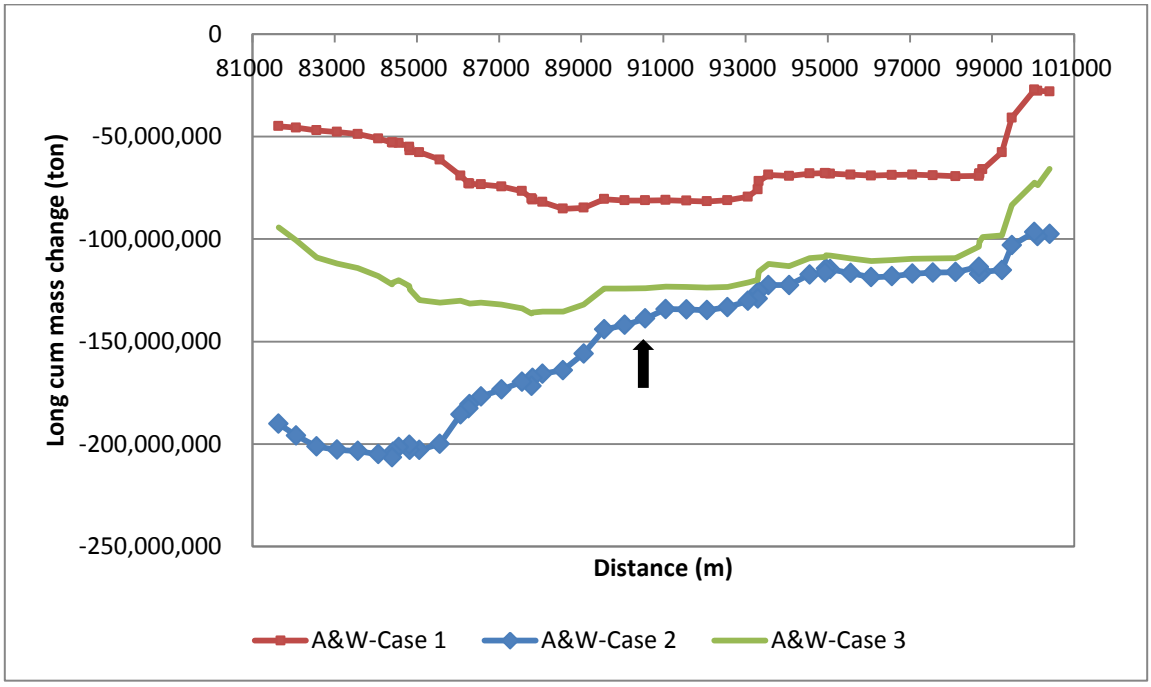

Figure 91. Mass Change from Gongju Weir to Sejong Weir by Gate Operation

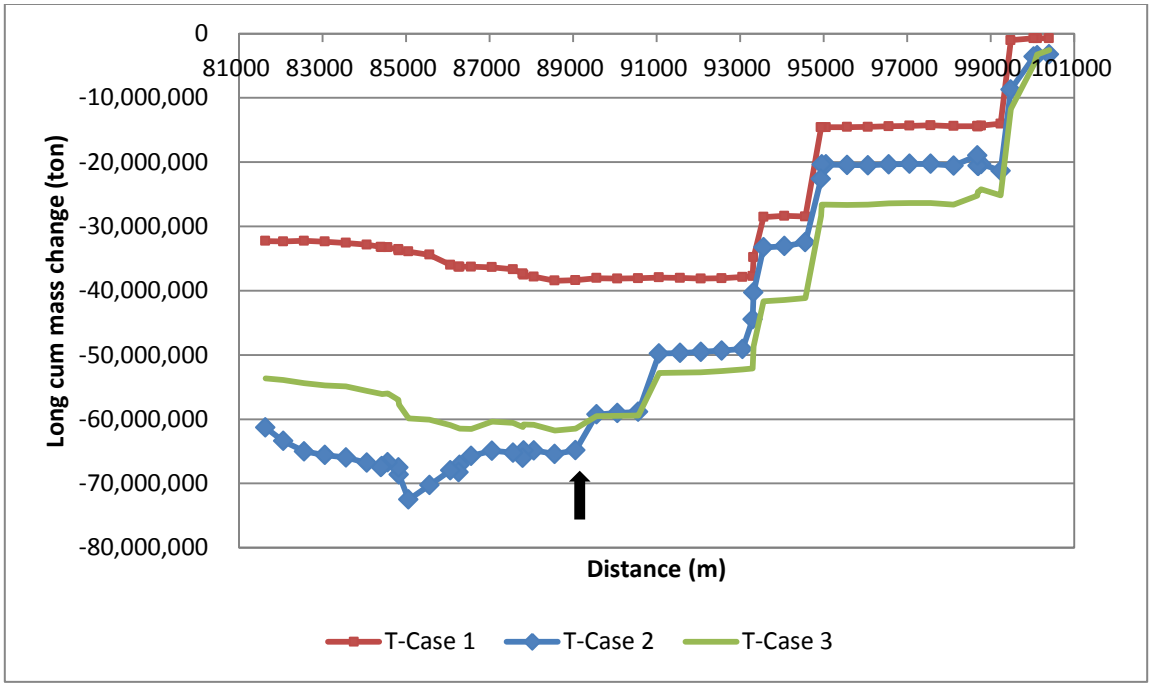

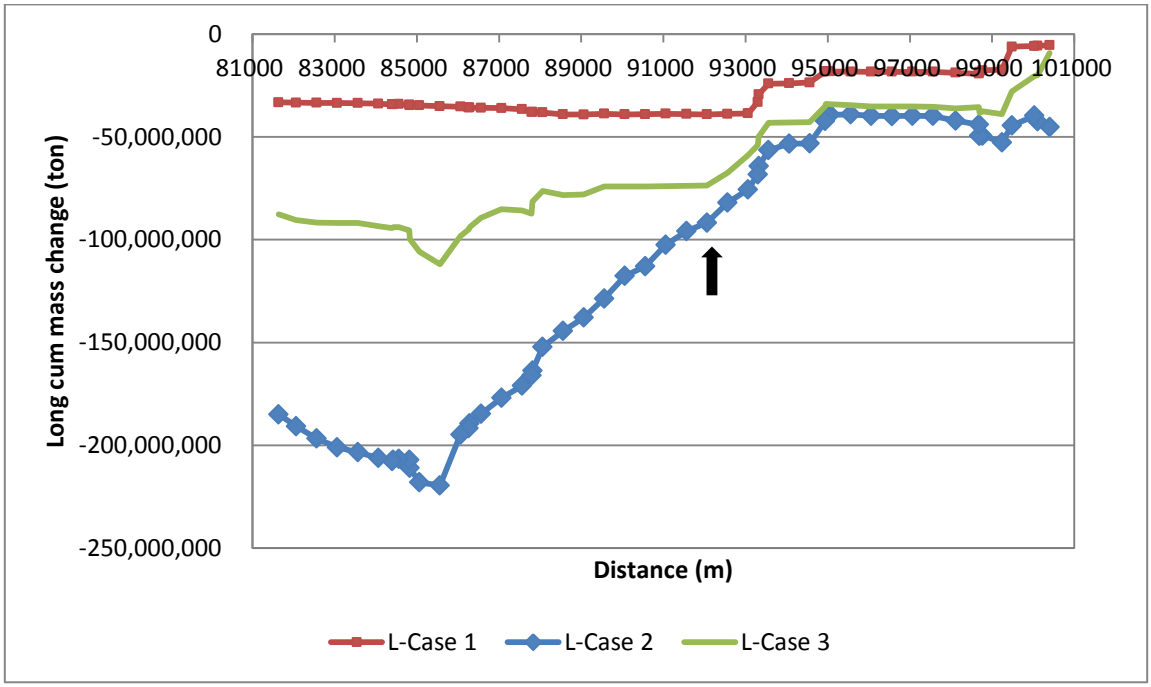

Figure 91. Continued

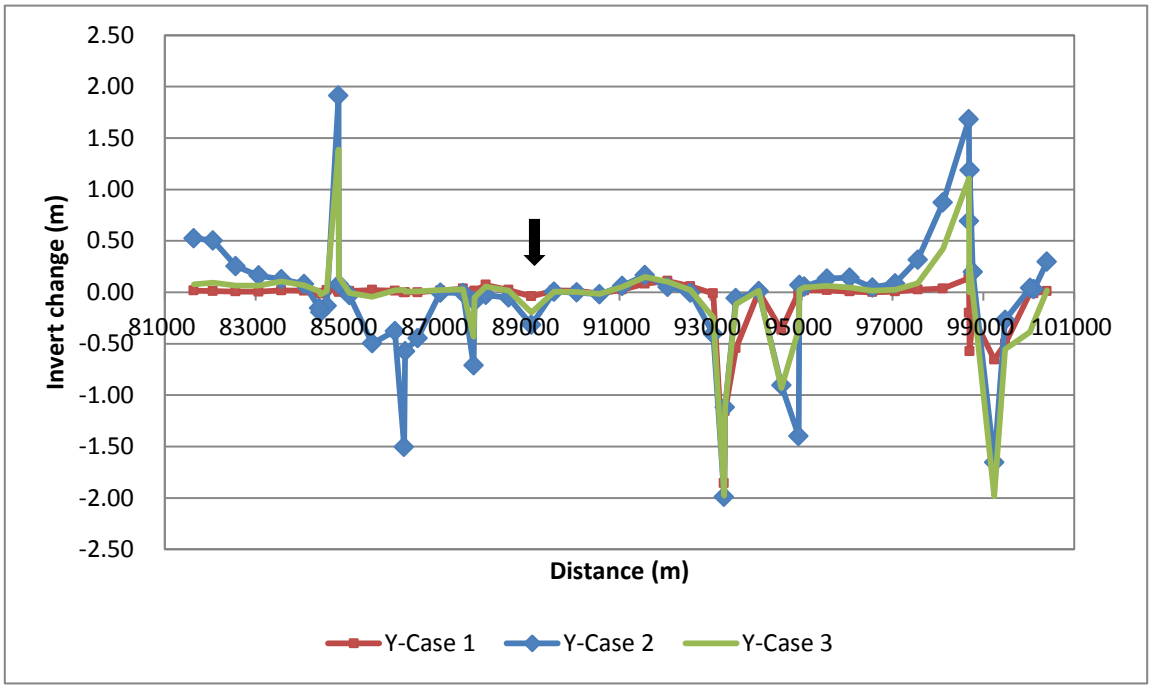

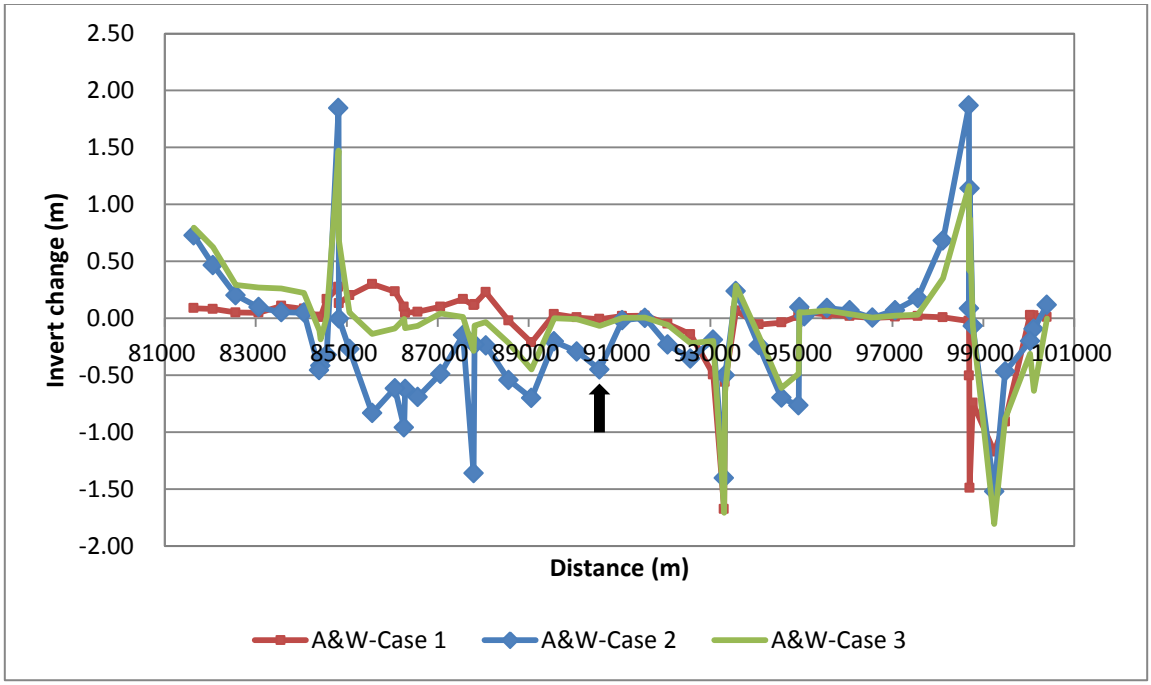

Figure 92. Invert Change from Gongju Weir to Sejong Weir by Gate Operation

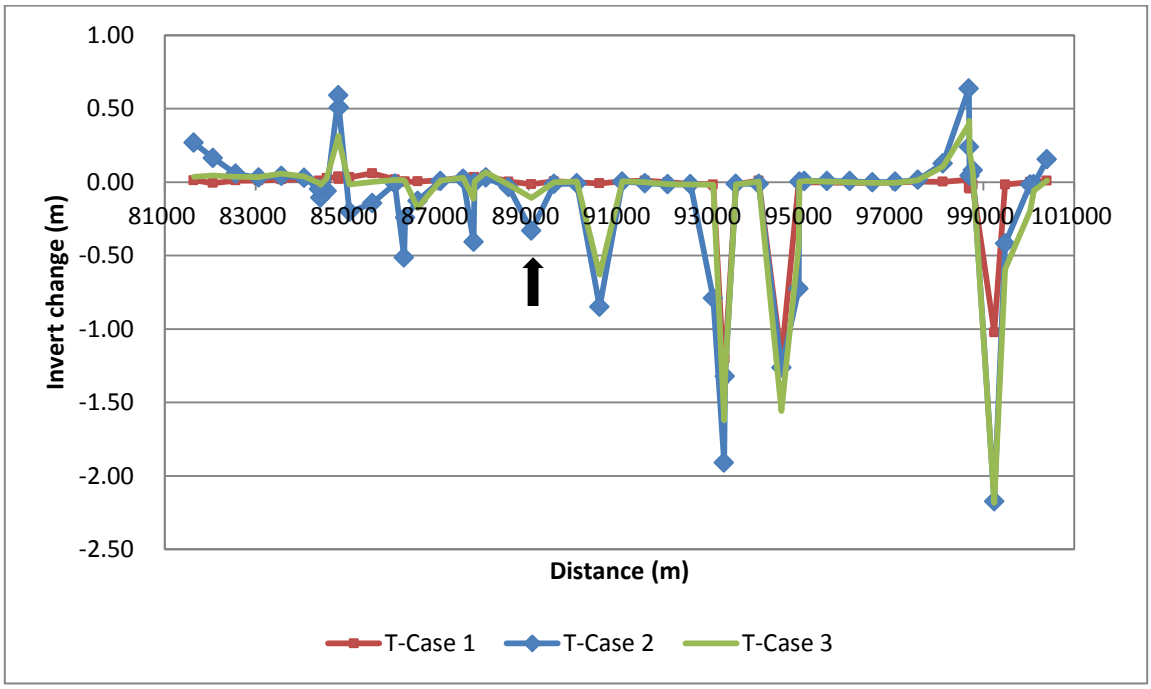

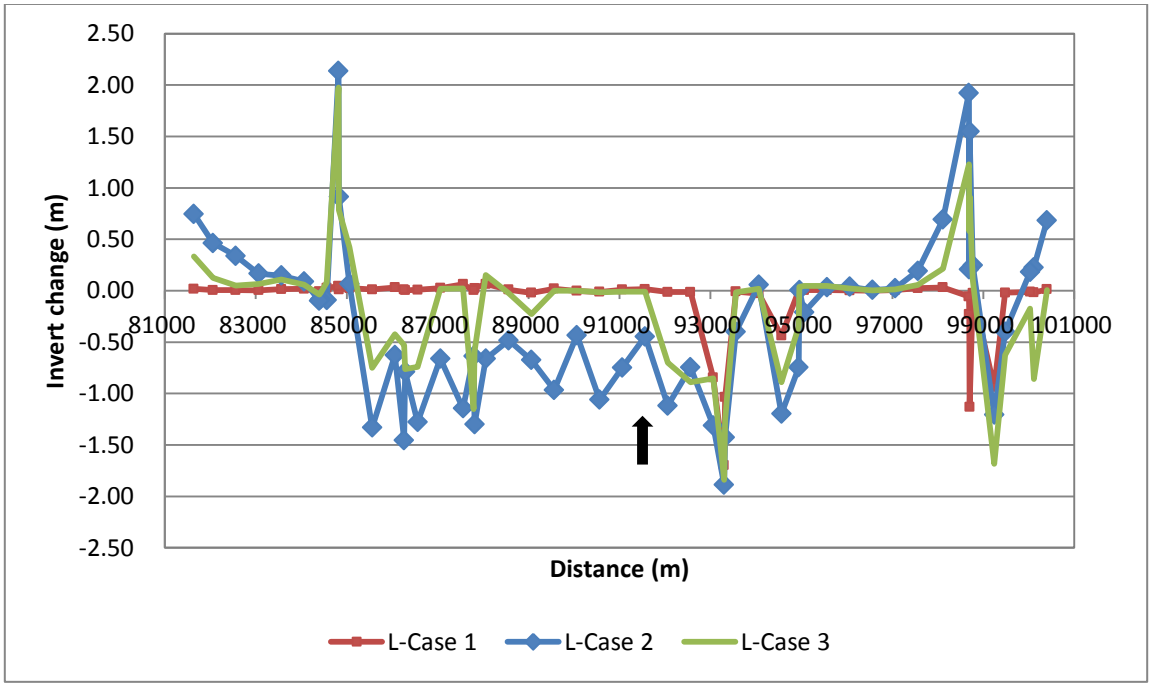

Figure 92. Continued

Table 20. Invert Change from Gongju Weir to Sejong Weir (after 20 years)

unit: m

Sta. no	Yang			Ackers&White			Toffaletti			Laursen		
	Case 1	Case 2	Case 3	Case1	Case 2	Case 3	Case1	Case 2	Case 3	Case1	Case 2	Case 3
100.65	0.010	0.297	0.018	0.012	0.118	-0.003	0.008	0.154	0.011	0.012	0.684	0.007
100.36	-0.010	0.029	-0.288	0.025	-0.094	-0.635	0.002	-0.014	-0.057	-0.019	0.227	-0.859
100.28	-0.007	0.040	-0.386	0.028	-0.200	-0.312	0.000	-0.017	-0.196	-0.012	0.182	-0.175
99.73	-0.501	-0.269	-0.553	-0.907	-0.468	-0.881	-0.017	-0.419	-0.592	-0.020	-0.400	-0.625
99.49	-0.655	-1.654	-1.984	-1.171	-1.519	-1.804	-1.023	-2.174	-2.183	-0.939	-1.208	-1.683
99.02	-0.235	0.197	-0.012	-0.742	-0.069	-0.065	-0.020	0.080	0.071	-0.024	0.247	0.104
98.95	-0.575	1.187	0.264	-1.489	1.139	0.882	-0.046	0.043	0.214	-1.130	1.547	0.918
98.94	-0.200	0.693	0.001	-0.503	0.087	0.420	-0.036	0.240	0.416	-0.228	0.206	0.579
98.93	0.135	1.683	1.108	-0.024	1.867	1.162	0.017	0.637	0.393	-0.057	1.923	1.229
98.36	0.037	0.872	0.424	0.009	0.683	0.353	0.001	0.128	0.105	0.031	0.692	0.216
97.96	0.025	0.316	0.088	0.019	0.177	0.033	0.004	0.015	0.013	0.023	0.192	0.057
97.46	0.006	0.086	0.025	0.013	0.070	0.025	-0.003	0.002	-0.006	0.005	0.023	0.014
96.96	0.000	0.046	0.014	0.003	0.005	0.007	-0.005	-0.002	-0.006	-0.001	0.007	0.002
96.46	0.007	0.142	0.048	0.019	0.070	0.039	-0.005	0.006	-0.001	0.002	0.038	0.023
95.73	0.019	0.133	0.062	0.034	0.090	0.069	-0.003	0.007	0.003	0.006	0.032	0.046
95.35	0.018	0.053	0.047	0.050	0.016	0.051	-0.002	0.008	0.007	0.005	-0.210	0.047
95.21	0.005	0.070	0.021	0.031	0.099	0.054	-0.003	0.003	0.002	0.001	0.005	0.035
95.19	0.002	-1.398	-0.360	0.020	-0.765	-0.485	-0.003	-0.725	-0.428	0.000	-0.746	-0.350
94.85	-0.367	-0.906	-0.930	-0.037	-0.697	-0.612	-1.197	-1.264	-1.559	-0.439	-1.197	-0.890
94.35	0.006	0.010	0.015	-0.054	-0.238	-0.152	0.009	-0.012	0.003	-0.027	0.056	0.020
93.85	-0.544	-0.059	-0.117	0.066	0.238	0.286	-0.014	-0.012	-0.017	-0.009	-0.400	-0.016
93.522	-1.156	-1.120	-1.109	-0.560	-0.500	-0.645	-1.200	-1.321	-1.317	-1.036	-1.427	-1.258
93.501	-1.855	-1.989	-1.977	-1.676	-1.404	-1.708	-1.343	-1.911	-1.622	-1.698	-1.889	-1.840
93.35	-0.012	-0.406	-0.247	-0.494	-0.188	-0.199	-0.017	-0.791	-0.019	-0.846	-1.314	-0.852
92.85	0.059	-0.005	0.022	-0.140	-0.353	-0.217	-0.011	-0.016	-0.015	-0.014	-0.746	-0.891
92.35	0.109	0.051	0.102	-0.049	-0.232	-0.057	-0.001	-0.015	-0.013	-0.014	-1.118	-0.701
91.85	0.083	0.167	0.150	0.023	0.003	0.007	0.009	-0.007	0.000	0.015	-0.447	-0.011
91.31	0.025	0.061	0.052	0.020	-0.017	0.004	0.005	0.003	0.006	0.009	-0.747	-0.010
90.81	-0.011	-0.019	-0.015	-0.006	-0.449	-0.066	-0.009	**-0.849**	-0.630	-0.013	-1.060	-0.015
90.31	0.014	-0.003	0.003	0.008	-0.292	-0.008	-0.001	-0.009	0.003	-0.002	-0.434	-0.001
89.81	0.020	0.005	0.006	0.037	-0.204	0.002	0.006	-0.013	-0.002	0.018	-0.966	0.000
89.31	-0.040	-0.317	-0.196	-0.212	-0.701	**-0.450**	-0.015	-0.332	**-0.107**	-0.022	-0.675	-0.228
88.8	0.022	-0.052	0.016	-0.020	-0.542	-0.219	0.002	-0.035	-0.017	0.009	-0.484	-0.025
88.3	0.072	-0.028	0.054	0.229	-0.238	-0.033	0.044	0.030	0.066	0.064	-0.663	0.153
88.0405	0.014	-0.088	-0.051	0.124	-0.230	-0.062	0.032	-0.004	0.004	0.024	-1.300	-0.590
88.0195	0.001	-0.712	**-0.431**	0.114	**-1.360**	-0.286	0.032	-0.407	-0.114	0.004	-0.636	**-1.153**
87.8	0.034	-0.007	0.029	0.169	-0.147	0.014	0.032	0.021	0.029	0.062	-1.144	0.023
87.3	0.018	-0.004	0.020	0.101	-0.488	0.044	0.013	0.007	0.009	0.025	-0.661	0.018
86.8	0.000	-0.448	0.009	0.056	-0.692	-0.067	0.004	-0.128	-0.174	0.008	-1.279	-0.740
86.512	-0.002	-0.574	0.007	0.048	-0.621	-0.086	0.001	-0.242	0.004	0.004	-0.789	-0.762
86.488	-0.001	**-1.505**	0.026	0.100	-0.959	-0.005	0.003	-0.514	0.013	0.010	**-1.455**	-0.529
86.3	0.014	-0.377	0.019	0.235	-0.615	-0.090	0.019	-0.012	0.015	0.031	-0.628	-0.423
85.8	0.022	-0.498	-0.045	0.301	-0.833	-0.136	0.059	-0.145	0.001	0.011	-1.331	-0.751
85.3	0.011	-0.030	-0.006	0.201	-0.270	0.052	0.032	-0.203	-0.017	0.025	0.065	0.423
85.075	0.001	0.077	0.149	0.131	-0.002	0.687	0.021	0.508	0.282	0.012	0.914	0.783
85.065	0.017	1.911	1.388	0.274	1.846	1.474	0.036	0.590	0.315	0.044	2.135	1.975
84.8	0.021	-0.134	0.013	0.168	-0.320	0.013	0.027	-0.060	0.025	0.027	-0.092	0.080
84.713	-0.009	-0.194	-0.022	0.011	-0.417	-0.184	0.005	-0.106	-0.017	-0.015	-0.082	-0.021
84.687	-0.014	-0.154	0.008	0.011	-0.454	-0.105	0.008	-0.047	-0.008	-0.009	-0.098	-0.038
84.32	0.014	0.081	0.068	0.083	0.049	0.224	0.017	0.029	0.037	0.017	0.089	0.059
83.74	0.018	0.127	0.104	0.109	0.054	0.263	0.018	0.042	0.058	0.015	0.146	0.110
83.15	0.006	0.163	0.065	0.050	0.097	0.270	0.011	0.030	0.033	0.004	0.166	0.064
82.65	0.006	0.254	0.064	0.051	0.203	0.294	0.011	0.056	0.037	0.005	0.339	0.050
82.15	0.011	0.503	0.094	0.081	0.467	0.626	-0.007	0.164	0.044	0.006	0.463	0.124
81.73	0.016	0.524	0.079	0.089	0.727	0.797	0.011	0.267	0.037	0.017	0.745	0.334

5.1.3.2.3 Bakje weir - Gongju weir (L=22.8 km)

Riverbed changes in the longitudinal cumulative mass are plotted in Figure 93 and invert changes are in Figure 94 for case 1, case 2, and case 3 using the Yang, Ackers & White, Toffaleti and Laursen equations. When we see the longitudinal cumulative mass change using Yang's equation, erosion happens downstream of Gongju weir and deposition occurs upstream of Bakje weir mainly. Especially, the trends between case 2 and case 3 are similar to each other and this shows this boundary is not affected by the gate operation. This tendency is similar to those with the other equations.

When we see the invert change, the riverbed change shows the same results in the longitudinal cumulative mass change, such as downstream of Gongju weir much erosion was predicted to happen, as shown in Figure 94. Results are shown in Table 21.

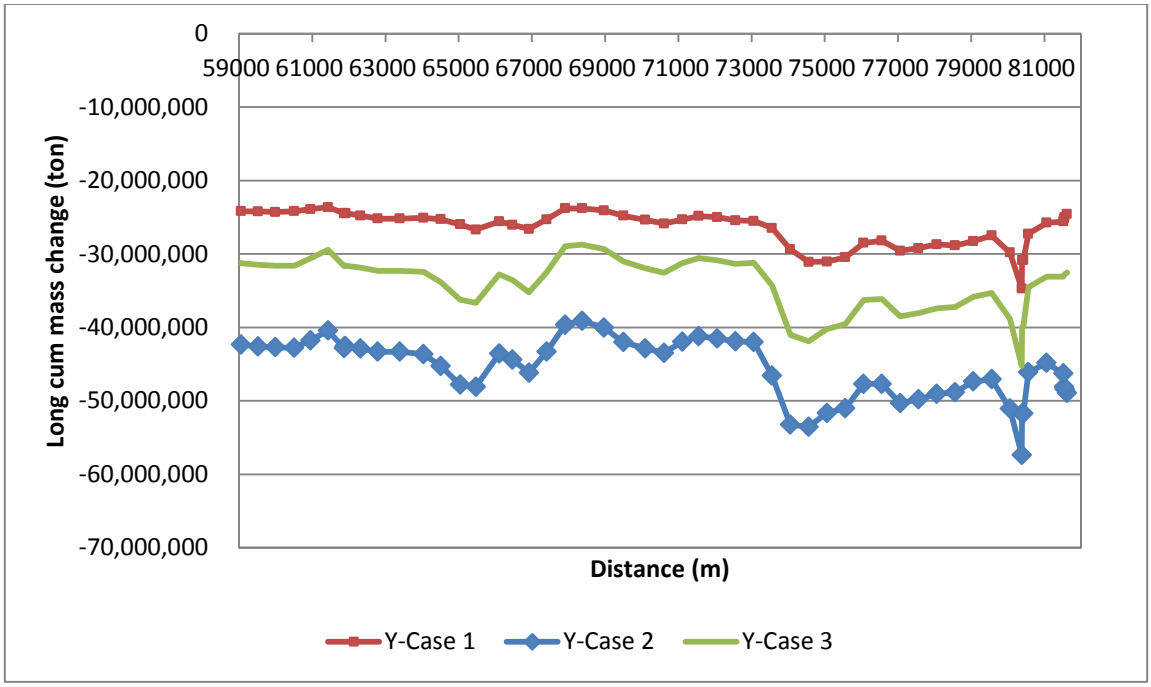

Figure 93. Mass Change from Bakje Weir to Gongju Weir by Gate Operation

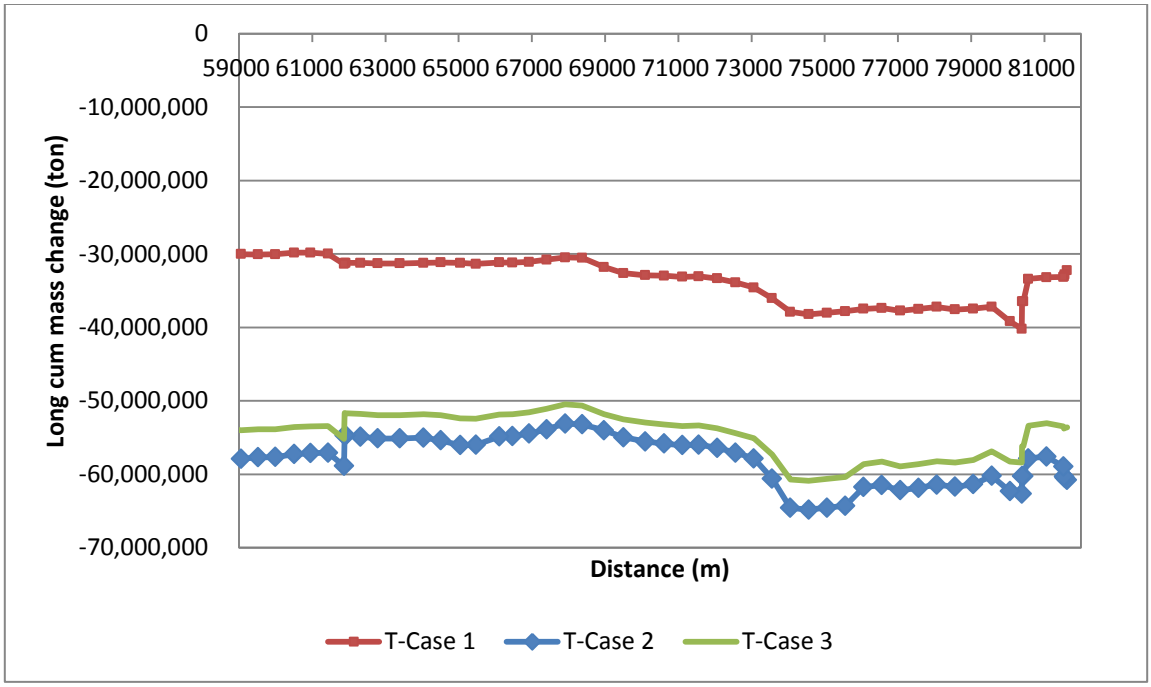

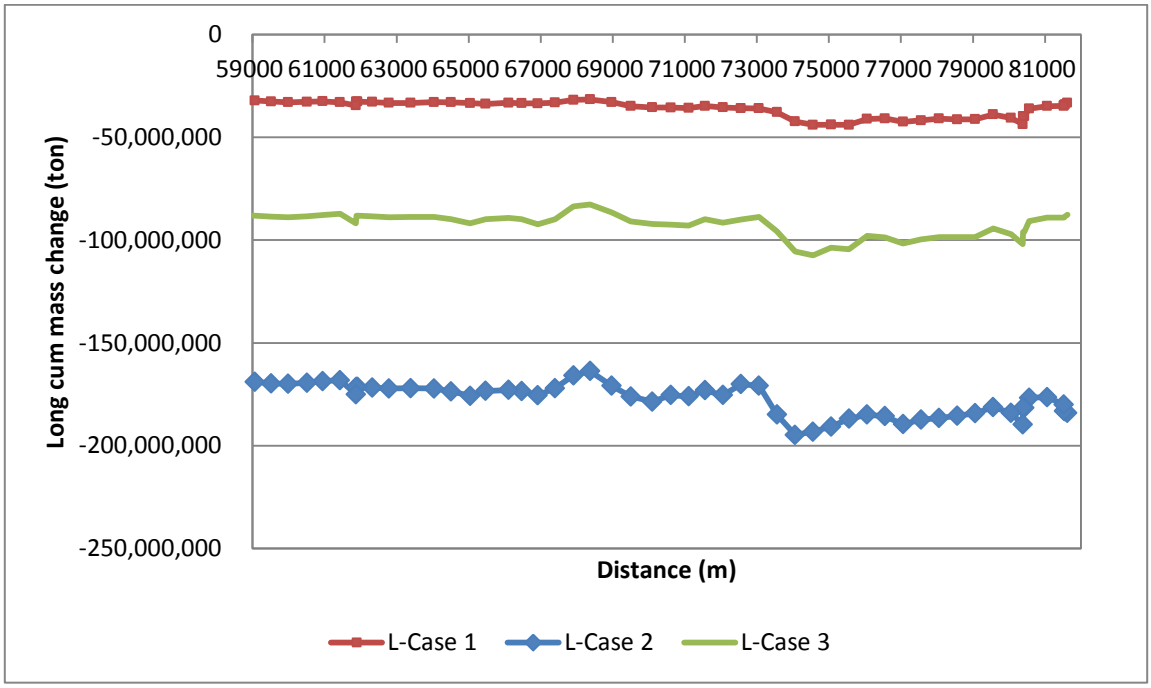

Figure 93. Continued

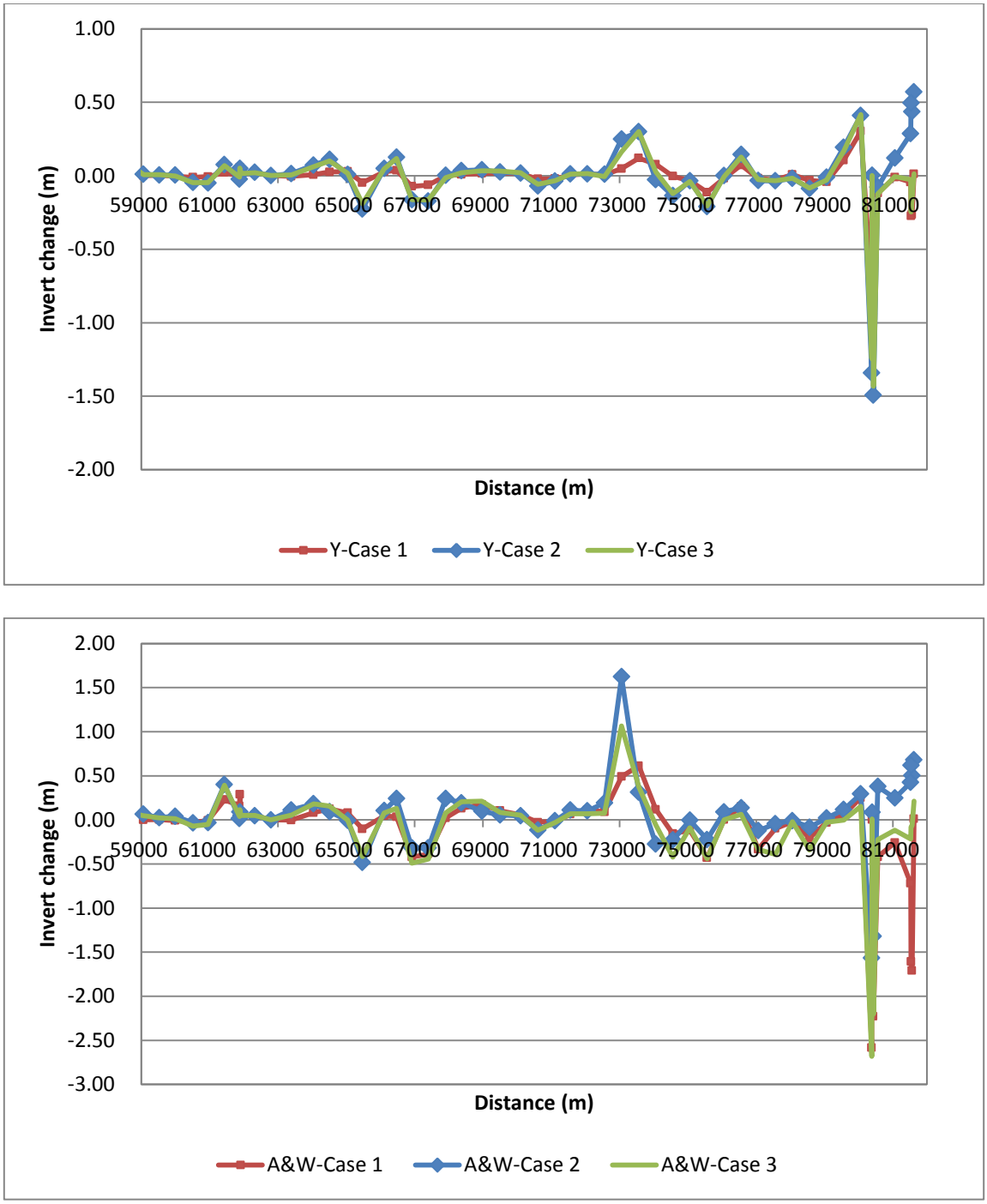

Figure 94. Invert Change from Bakje Weir to Gongju Weir by Gate Operation

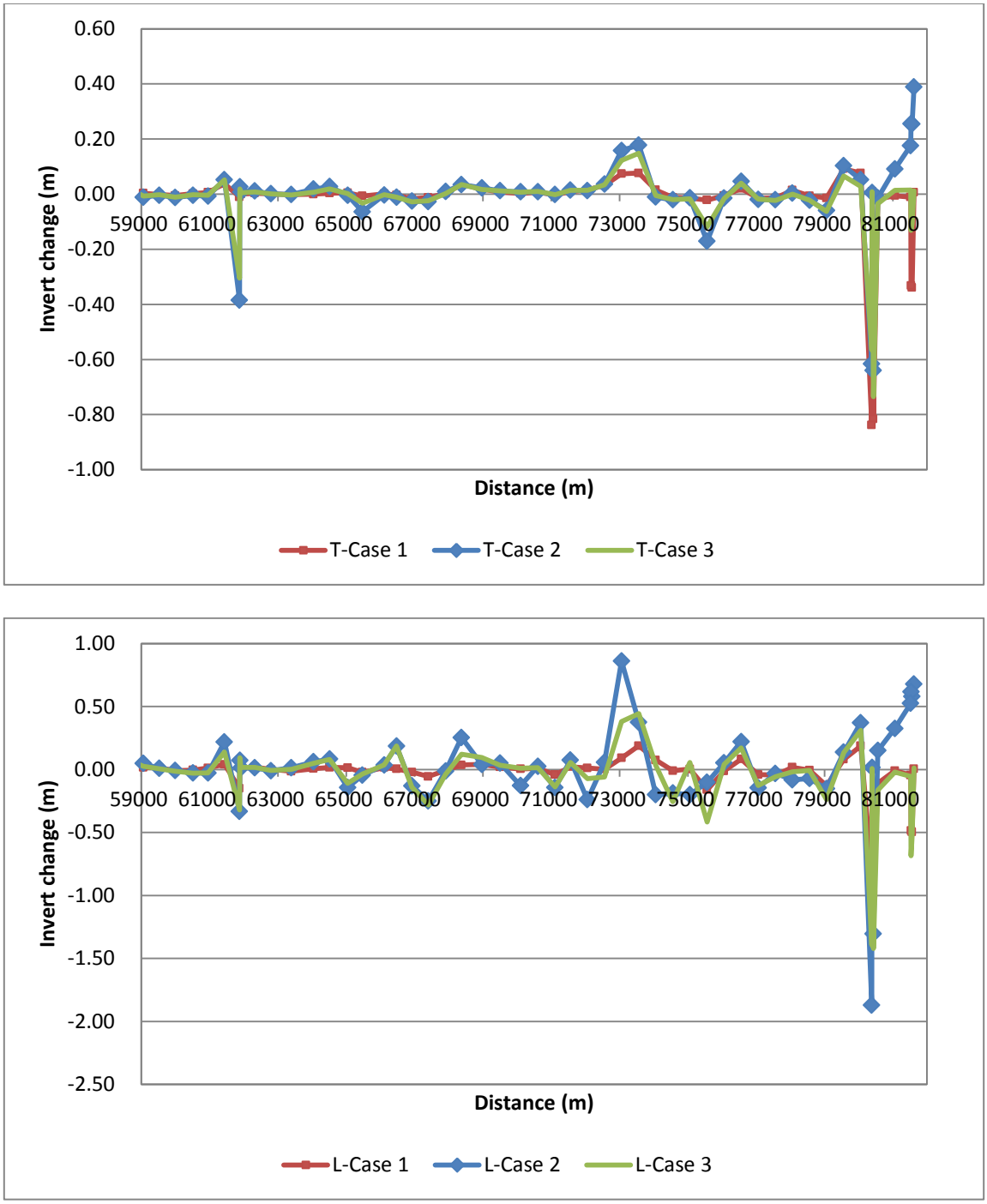

Figure 94. Continued

Table 21. Invert Change from Bakje Weir to Gongju Weir (after 20 years) (unit: m)

Sta. no	Yang			Ackers&White			Toffaletti			Laursen		
	Case 1	Case 2	Case 3	Case 1	Case2	Case 3	Case 1	Case 2	Case 3	Case 1	Case 2	Case 3
81.715	0.012	0.570	0.013	0.011	0.681	0.212	0.006	0.389	0.012	0.005	0.677	0.012
81.65	-0.264	0.436	-0.157	-1.708	0.504	-0.064	-0.339	0.254	-0.107	-0.497	0.580	-0.531
81.625	-0.274	0.497	-0.247	-1.608	0.619	-0.080	-0.332	0.256	-0.131	-0.485	0.617	-0.685
81.61	-0.043	0.287	-0.026	-0.721	0.425	-0.216	-0.011	0.176	0.015	-0.045	0.525	-0.054
81.15	-0.010	0.121	-0.005	-0.258	0.248	-0.119	-0.006	0.091	0.014	-0.010	0.325	-0.021
80.65	-0.119	-0.076	-0.124	-0.420	0.378	-0.224	-0.018	-0.014	-0.034	-0.109	0.150	-0.164
80.498	-0.958	-1.493	-1.432	-2.228	-1.321	-2.204	-0.816	-0.639	-0.735	-0.989	-1.304	-1.420
80.463	0.009	0.003	0.002	0.002	0.085	0.012	0.009	0.006	0.009	0.006	0.015	0.008
80.453	-0.796	-1.342	-1.243	-2.585	-1.566	-2.682	-0.838	-0.615	-0.566	-0.817	-1.871	-1.392
80.15	0.303	0.410	0.417	0.252	0.293	0.154	0.077	0.052	0.028	0.187	0.371	0.311
79.65	0.106	0.194	0.168	0.058	0.117	-0.002	0.092	0.103	0.066	0.080	0.137	0.135
79.15	-0.042	-0.011	-0.029	-0.032	0.020	-0.027	-0.014	-0.060	-0.062	-0.129	-0.153	-0.239
78.65	-0.031	-0.086	-0.084	-0.205	-0.085	-0.343	-0.006	-0.022	-0.022	-0.006	-0.072	-0.007
78.15	0.008	-0.018	-0.016	-0.020	-0.009	-0.022	0.014	0.004	0.000	0.017	-0.082	-0.018
77.65	-0.028	-0.035	-0.033	-0.098	-0.044	-0.391	-0.014	-0.021	-0.023	-0.044	-0.032	-0.058
77.15	-0.018	-0.032	-0.026	-0.332	-0.122	-0.336	-0.014	-0.019	-0.018	-0.041	-0.146	-0.128
76.55	0.072	0.146	0.128	0.151	0.137	0.063	0.020	0.047	0.040	0.083	0.220	0.171
76.05	-0.017	0.002	-0.006	0.004	0.090	0.000	-0.005	-0.015	-0.016	-0.012	0.053	0.040
75.55	-0.112	-0.209	-0.205	-0.431	-0.224	-0.442	-0.022	-0.171	-0.118	-0.162	-0.103	-0.417
75.05	-0.033	-0.035	-0.039	-0.118	-0.005	-0.088	-0.014	-0.014	-0.017	0.003	-0.200	0.055
74.55	-0.003	-0.136	-0.121	-0.158	-0.228	-0.422	-0.012	-0.021	-0.020	-0.010	-0.188	-0.257
74.05	0.078	-0.027	0.027	0.117	-0.274	-0.060	0.015	-0.011	-0.005	0.075	-0.201	0.032
73.55	0.120	0.299	0.300	0.613	0.313	0.373	0.076	0.178	0.149	0.188	0.376	0.443
73.05	0.048	0.250	0.163	0.490	1.622	1.065	0.074	0.158	0.122	0.092	0.862	0.380
72.55	0.006	0.010	-0.006	0.090	0.193	0.076	0.032	0.036	0.033	0.002	0.058	-0.060
72.06	0.013	0.012	0.015	0.112	0.101	0.071	0.016	0.012	0.014	0.012	-0.240	-0.074
71.56	0.006	0.012	0.012	0.064	0.110	0.070	0.009	0.014	0.014	0.022	0.074	0.057
71.11	-0.020	-0.035	-0.033	-0.014	-0.010	-0.029	-0.003	-0.002	-0.002	-0.041	-0.144	-0.138
70.61	-0.022	-0.069	-0.058	-0.028	-0.118	-0.118	0.007	0.008	0.010	0.009	0.025	0.013
70.1	0.015	0.018	0.021	0.058	0.045	0.052	0.002	0.008	0.007	0.004	-0.129	0.010
69.5	0.018	0.025	0.032	0.104	0.056	0.085	0.008	0.012	0.012	0.019	0.051	0.034
68.97	0.016	0.041	0.035	0.175	0.098	0.214	0.018	0.023	0.017	0.040	0.039	0.095
68.37	0.010	0.035	0.022	0.131	0.193	0.207	0.036	0.034	0.035	0.035	0.253	0.121
67.91	0.001	0.002	-0.012	0.022	0.241	0.080	0.002	0.009	0.002	-0.007	-0.013	-0.037
67.4	-0.063	-0.172	-0.165	-0.387	-0.318	-0.446	-0.012	-0.028	-0.024	-0.056	-0.250	-0.281
66.92	-0.072	-0.164	-0.162	-0.421	-0.317	-0.491	-0.017	-0.025	-0.027	-0.021	-0.130	-0.140
66.47	0.037	0.127	0.118	0.034	0.242	0.132	-0.003	-0.012	-0.011	0.005	0.185	0.186
66.11	0.027	0.049	0.046	0.045	0.105	0.078	0.001	-0.003	-0.002	0.015	0.036	0.036
65.47	-0.047	-0.226	-0.190	-0.102	-0.483	-0.418	-0.007	-0.064	-0.033	-0.023	-0.046	-0.035
65.04	0.029	0.009	0.016	0.079	-0.006	-0.002	0.005	-0.004	0.002	0.014	-0.143	-0.109
64.51	0.026	0.112	0.101	0.124	0.092	0.155	0.003	0.027	0.019	0.016	0.082	0.081
64.04	0.008	0.073	0.061	0.080	0.181	0.180	0.000	0.018	0.007	0.006	0.061	0.049
63.39	-0.004	0.015	0.005	-0.003	0.112	0.054	-0.002	-0.001	-0.003	-0.015	0.014	0.002
62.79	0.001	0.001	0.001	0.001	0.000	0.001	0.001	0.001	0.001	0.001	-0.011	-0.007
62.32	0.020	0.023	0.021	0.049	0.047	0.050	0.003	0.011	0.008	0.020	0.013	0.015
61.916	0.016	0.015	0.015	0.056	0.050	0.050	0.000	0.008	0.005	0.011	0.014	0.016
61.884	0.056	0.050	0.053	0.288	0.090	0.116	0.001	0.026	0.019	0.049	0.071	0.092
61.87	0.000	-0.023	-0.008	0.158	0.015	0.038	-0.010	-0.385	-0.305	-0.149	-0.332	-0.321
61.43	0.022	0.076	0.069	0.229	0.399	0.393	0.037	0.053	0.052	0.040	0.218	0.139
60.95	-0.006	-0.049	-0.046	-0.008	-0.031	-0.053	0.006	-0.007	-0.004	0.011	-0.029	-0.026
60.51	-0.010	-0.045	-0.047	-0.028	-0.035	-0.070	0.002	-0.005	-0.002	-0.005	-0.028	-0.030
59.99	-0.003	0.004	-0.001	-0.007	0.040	0.012	-0.005	-0.012	-0.011	-0.009	-0.009	-0.015
59.52	0.004	0.005	0.008	0.003	0.025	0.022	-0.001	-0.004	-0.002	0.014	0.008	0.007
59.06	0.001	0.010	0.009	0.000	0.064	0.047	0.003	-0.011	-0.007	0.016	0.048	0.025
58.79	0.033	0.050	0.056	0.011	0.175	0.070	0.010	0.011	0.011	0.011	0.084	0.055

5.1.3.2.4 Estuary - Bakje weir (L= 58.8 km)

Riverbed changes in terms of longitudinal cumulative mass are plotted in Figure 95 and invert changes are in Figure 96 for case 1, case 2, and case 3, using the Yang, Ackers & White, Toffaleti, and Laursen equations. When we see the longitudinal cumulative mass change using Yang's equation, erosion happens in case 1 downstream of Bakje weir due to less inflowing sediment, whereas deposition happens in case 2 and case 3 due to more inflowing sediment. Overall, as estuary approaches, deposition happens. Also, this boundary was not affected by gates, because the slope had the same trend among them. Results were similar to those for the Ackers & White, Toffaleti, and Laursen equations.

When Yang's equation was used in case 3, severe erosion happened at station no 31.4. This was anticipated to cause from eroding of fine sediments which are class 1 (mean diameter 0.003 mm), class 2 (mean diameter 0.006 mm), and class 3 (mean diameter 0.011 mm) and these results are guessed to relation to the characteristics of Yang's equation.

When we saw the invert change, the riverbed change showed the same results of the longitudinal cumulative mass change, as shown in Figure 96. Results are shown in Table 22.

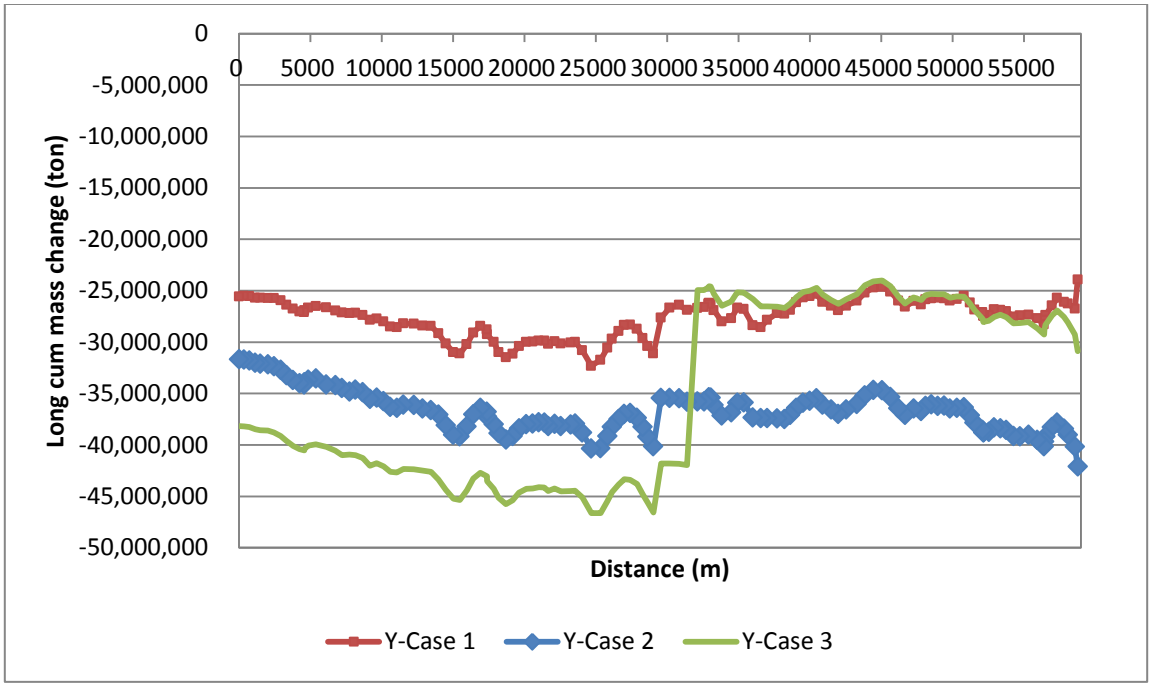

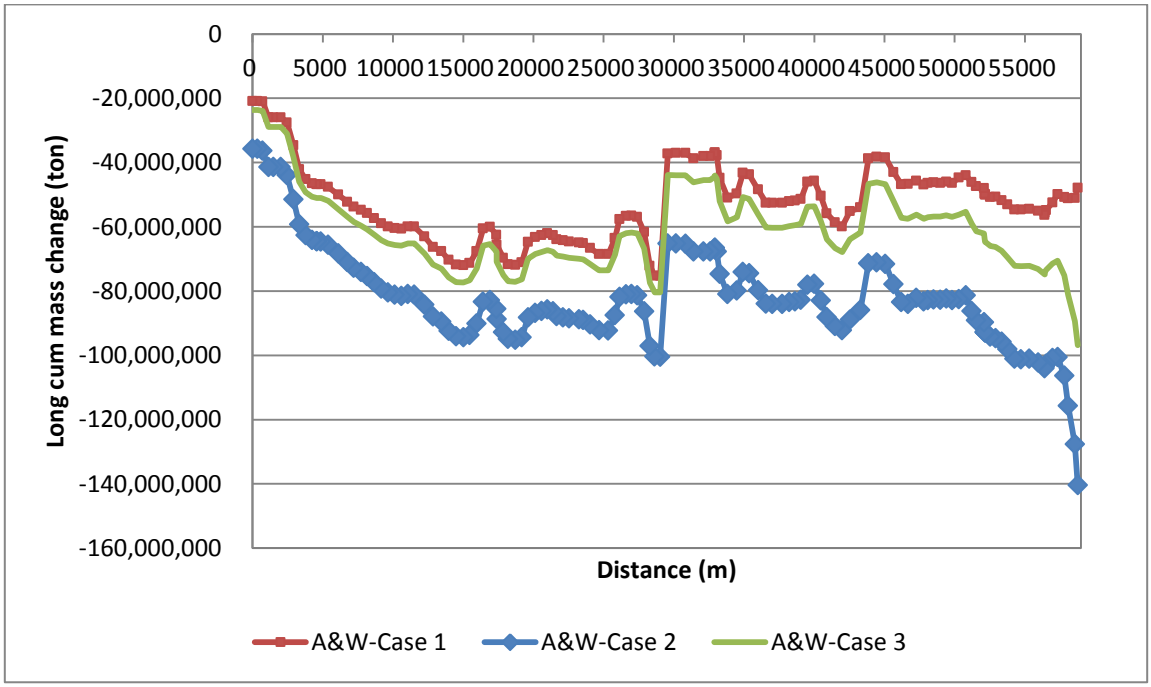

Figure 95. Mass Change from Estuary to Bakje Weir by Gate Operation

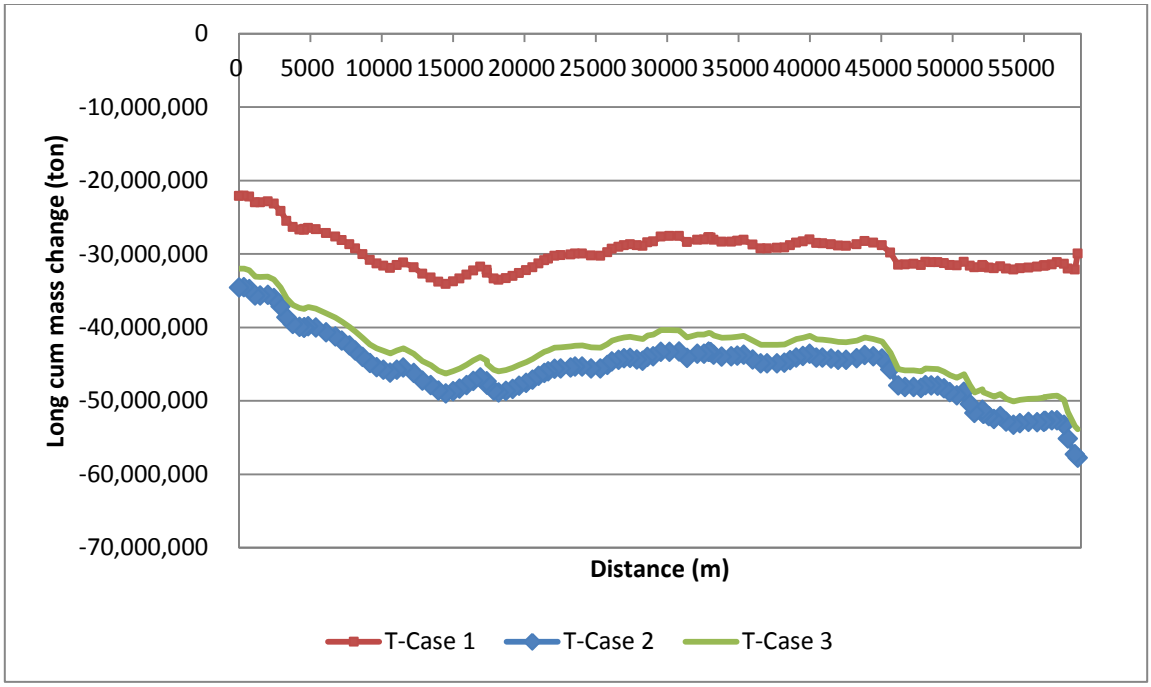

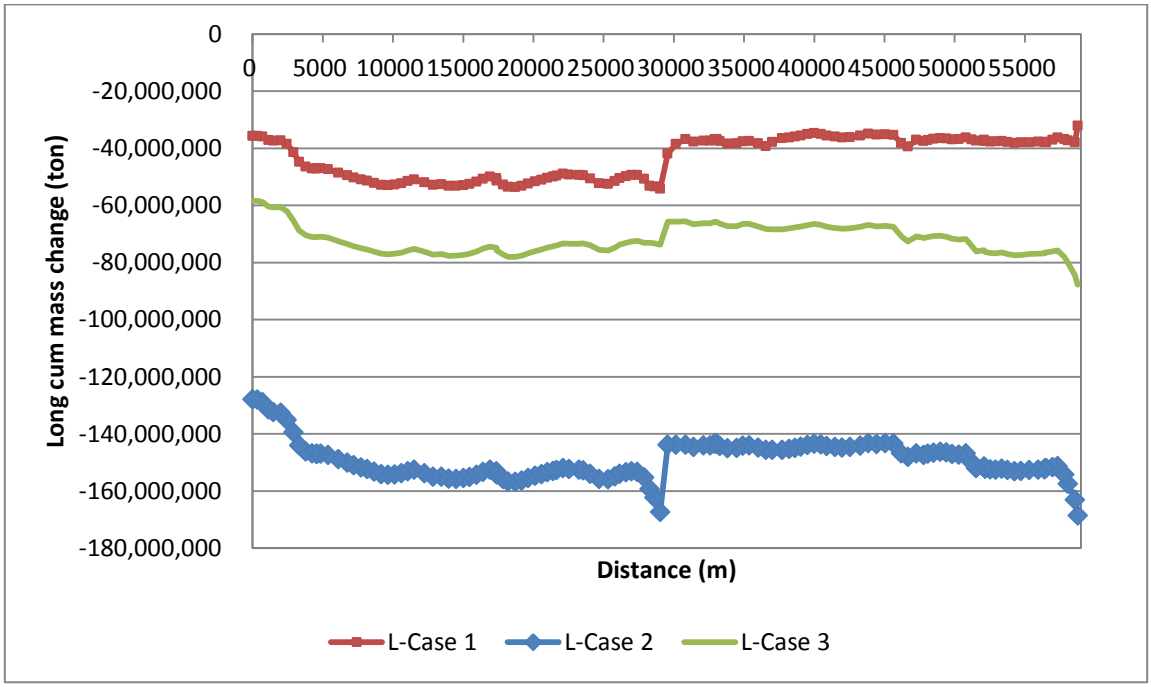

Figure 95. Continued

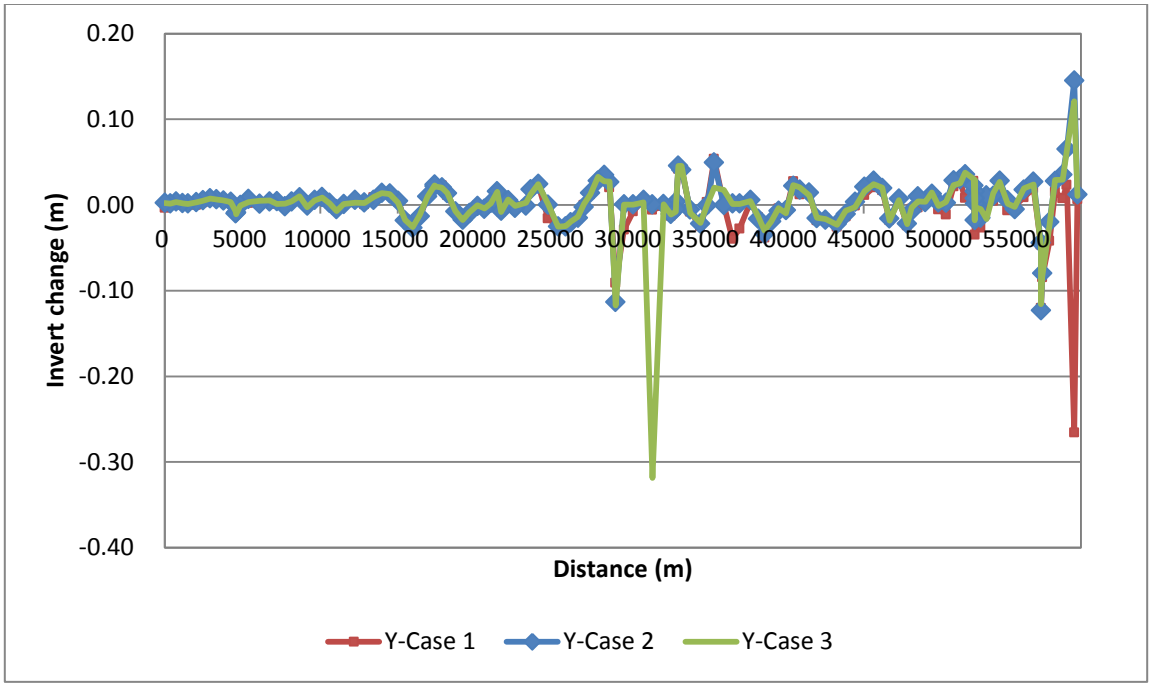

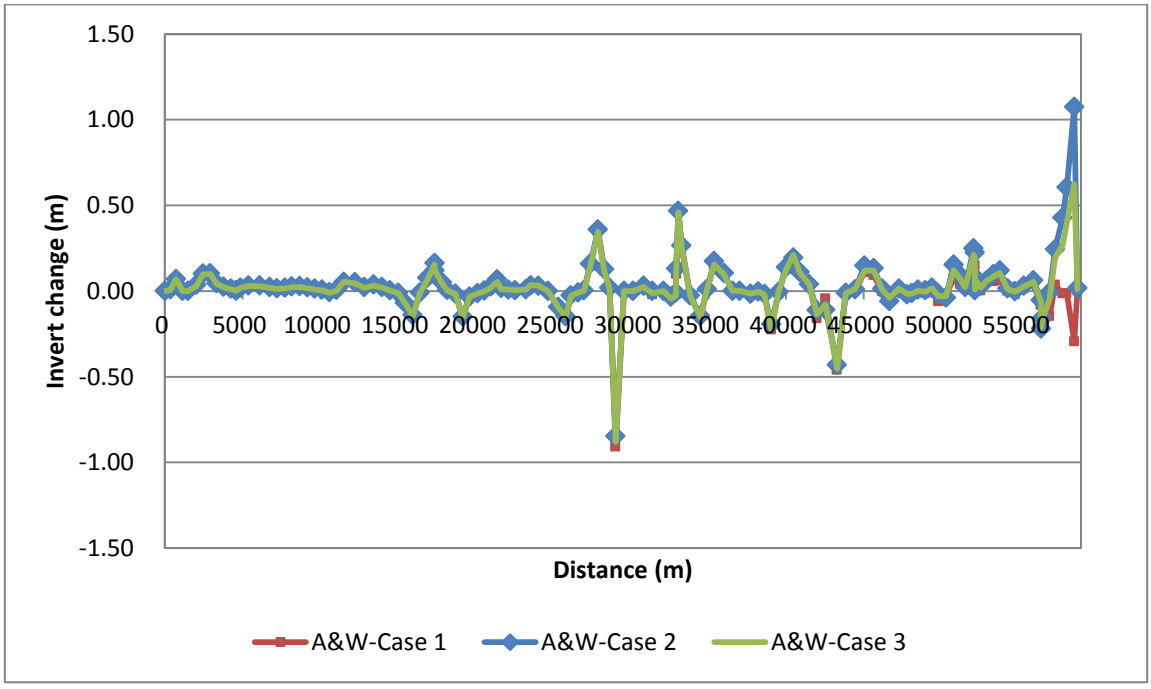

Figure 96. Invert Change from Estuary to Bakje Weir by Gate Operation

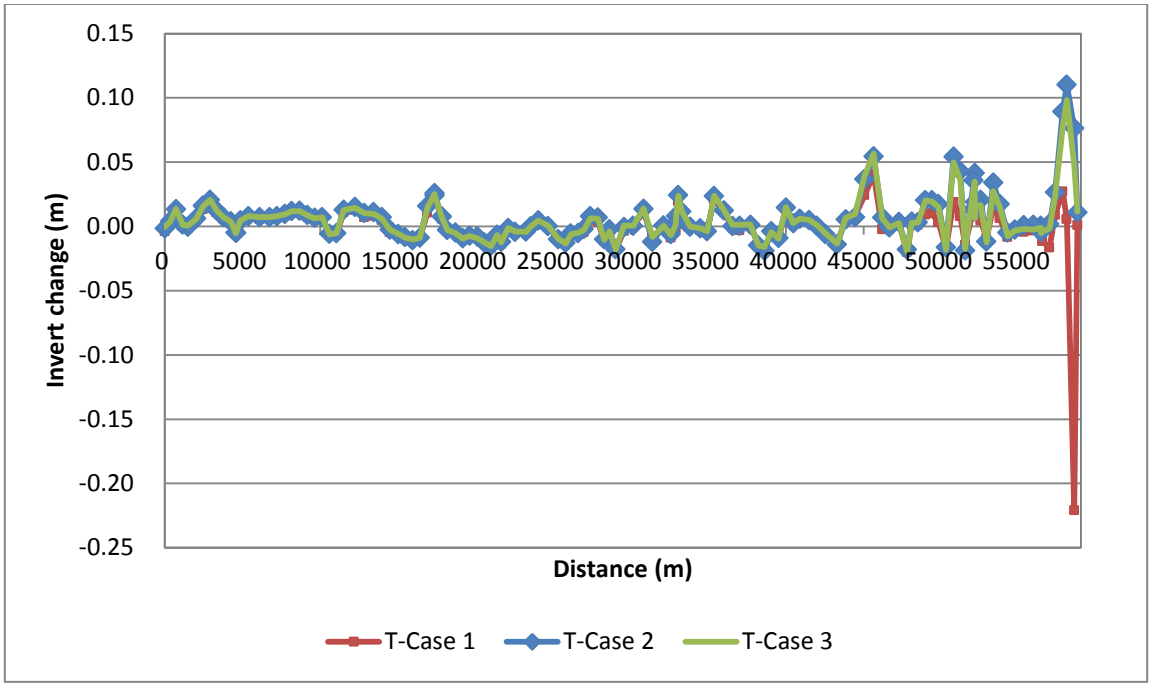

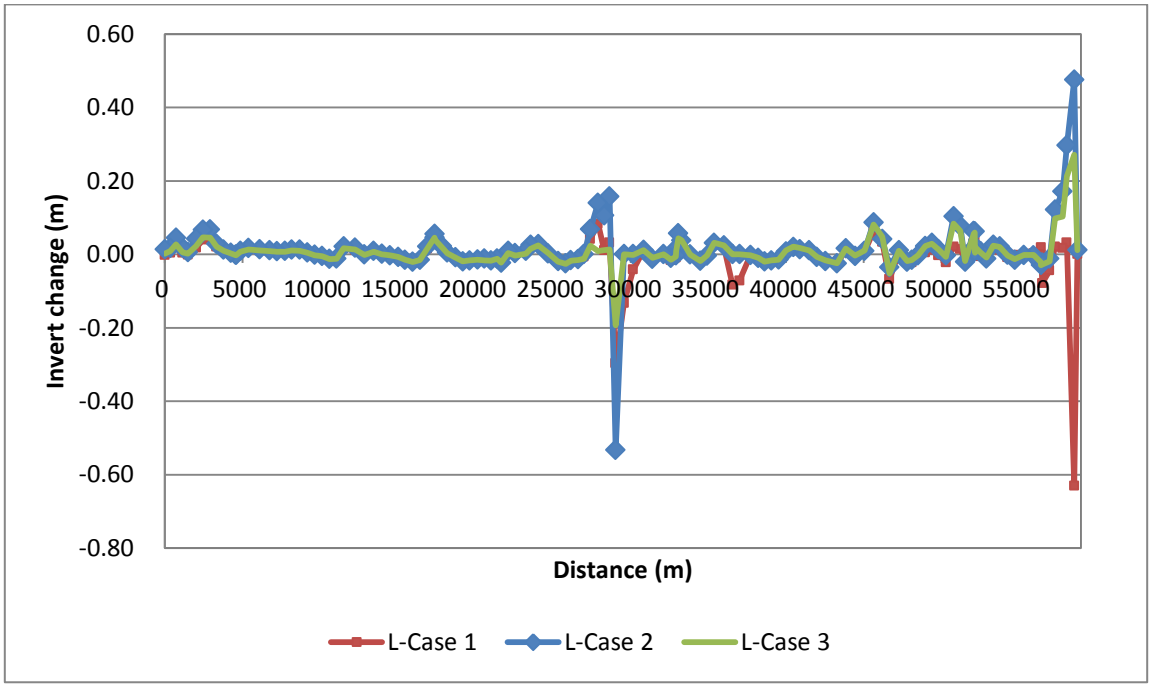

Figure 96. Continued

Table 22. Invert Change from Estuary to Bakje Weir (after 20 years)

unit: m

Sta. no	Yang			Ackers&White			Toffaletti			Laursen		
	Case 1	Case 2	Case 3	Case 1	Case 2	Case 3	Case 1	Case2	Case 3	Case 1	Case2	Case 3
58.775	0.006	0.012	0.011	0.001	0.018	0.011	0.001	0.011	0.011	0.000	0.012	0.011
58.57	-0.266	0.145	0.121	-0.294	1.075	0.623	-0.221	0.076	0.048	-0.630	0.475	0.271
58.08	0.023	0.065	0.063	-0.014	0.607	0.402	0.006	0.110	0.098	0.032	0.297	0.213
57.81	0.008	0.035	0.029	-0.015	0.429	0.269	0.027	0.089	0.077	0.017	0.171	0.103
57.33	0.015	0.028	0.029	0.037	0.244	0.194	0.009	0.026	0.023	0.021	0.122	0.097
56.97	-0.042	-0.020	-0.023	-0.147	-0.008	-0.047	-0.017	0.002	-0.001	-0.044	-0.012	-0.019
56.51	-0.085	-0.080	-0.084	-0.216	-0.156	-0.174	-0.012	-0.002	-0.004	-0.078	-0.023	-0.028
56.427	-0.120	-0.123	-0.116	-0.219	-0.220	-0.214	-0.006	-0.004	-0.005	0.018	-0.029	-0.030
56.413	-0.046	-0.044	-0.048	-0.081	-0.053	-0.060	-0.003	0.000	-0.001	-0.001	-0.023	-0.022
55.94	0.019	0.027	0.024	0.043	0.063	0.054	-0.003	0.001	-0.002	0.002	-0.003	-0.001
55.32	0.009	0.018	0.020	0.014	0.031	0.026	-0.004	0.001	-0.002	-0.005	-0.002	-0.002
54.73	-0.001	-0.005	-0.002	-0.006	-0.002	-0.004	-0.002	-0.003	-0.003	-0.002	-0.015	-0.013
54.27	-0.006	0.005	0.001	0.001	0.016	0.010	-0.008	-0.005	-0.008	-0.008	-0.001	-0.003
53.76	0.021	0.028	0.027	0.063	0.120	0.107	0.006	0.017	0.015	0.012	0.022	0.020
53.35	0.005	0.011	0.014	0.056	0.097	0.085	0.015	0.034	0.028	0.015	0.025	0.024
52.91	0.005	0.011	-0.017	0.054	0.061	0.060	-0.010	-0.012	-0.013	-0.004	-0.012	-0.009
52.54	-0.027	-0.015	-0.005	0.002	0.030	0.020	0.004	0.021	0.016	-0.005	0.009	0.004
52.192	0.000	0.002	-0.003	0.045	0.072	0.065	0.009	0.019	0.016	0.011	0.021	0.019
52.17	0.011	0.016	0.029	0.034	0.082	0.067	0.010	0.015	0.013	0.009	0.009	0.012
52.165	0.001	0.008	0.005	0.008	0.004	0.009	0.012	0.012	0.007	0.011	0.009	0.005
52.156	-0.035	-0.018	-0.018	0.151	0.225	0.200	0.020	0.042	0.035	0.045	0.063	0.059
52.09	0.028	0.022	0.030	0.149	0.249	0.212	0.014	0.036	0.030	0.030	0.063	0.055
51.54	0.008	0.036	0.038	0.024	0.024	0.023	-0.014	-0.019	-0.018	-0.014	-0.020	-0.018
51.22	0.027	0.030	0.025	0.040	0.093	0.071	0.008	0.043	0.036	0.014	0.078	0.064
50.8	0.022	0.029	0.023	0.070	0.154	0.121	0.019	0.054	0.050	0.021	0.103	0.084
50.3	-0.011	0.002	0.004	-0.023	-0.038	-0.029	-0.017	-0.016	-0.018	-0.022	-0.003	-0.007
49.82	-0.005	0.003	-0.001	-0.061	-0.017	-0.030	0.003	0.017	0.015	-0.003	0.014	0.013
49.4	0.009	0.013	0.014	0.016	0.020	0.017	0.010	0.020	0.019	0.012	0.031	0.029
48.97	0.005	0.003	0.004	-0.013	0.004	-0.004	0.009	0.020	0.020	0.005	0.022	0.023
48.5	-0.003	0.010	0.004	0.010	0.007	0.002	0.001	0.003	0.003	-0.004	-0.003	-0.002
48.1	-0.005	-0.007	-0.003	-0.015	-0.011	-0.014	0.002	0.004	0.003	-0.022	-0.015	-0.016
47.8	-0.024	-0.022	-0.022	-0.016	-0.019	-0.017	-0.020	-0.018	-0.020	-0.020	-0.020	-0.018
47.27	0.007	0.007	0.006	0.012	0.013	0.015	0.002	0.003	0.003	0.006	0.011	0.010
46.67	-0.018	-0.016	-0.018	-0.031	-0.059	-0.040	-0.002	-0.001	-0.001	-0.068	-0.035	-0.052
46.2	0.017	0.020	0.020	-0.004	0.014	0.007	-0.002	0.007	0.006	0.034	0.041	0.048
45.65	0.020	0.028	0.024	0.093	0.134	0.122	0.041	0.054	0.056	0.063	0.087	0.081
45.06	0.011	0.021	0.016	0.109	0.148	0.119	0.024	0.037	0.040	0.008	0.010	0.011
44.45	-0.001	0.004	-0.003	0.003	0.010	0.010	0.008	0.007	0.009	-0.005	-0.005	-0.004
43.85	-0.013	-0.011	-0.007	-0.013	-0.010	-0.013	0.006	0.005	0.007	0.011	0.016	0.016
43.29	-0.026	-0.022	-0.023	-0.461	-0.430	-0.453	-0.014	-0.014	-0.013	-0.023	-0.024	-0.024
42.54	-0.016	-0.017	-0.016	-0.045	-0.109	-0.079	-0.006	-0.006	-0.005	-0.018	-0.018	-0.017
41.99	-0.018	-0.015	-0.015	-0.160	-0.111	-0.137	0.001	0.000	0.001	-0.008	-0.007	-0.007
41.49	0.013	0.014	0.011	0.041	0.041	0.039	0.004	0.005	0.005	0.009	0.011	0.010
40.89	0.012	0.018	0.021	0.107	0.111	0.108	0.005	0.006	0.006	0.015	0.014	0.017
40.47	0.028	0.022	0.023	0.202	0.194	0.210	0.003	0.002	0.002	0.020	0.020	0.021
40	-0.008	-0.006	-0.010	0.126	0.140	0.121	0.013	0.015	0.015	0.009	0.007	0.011
39.52	-0.004	-0.007	-0.004	-0.006	-0.006	-0.002	-0.010	-0.009	-0.009	-0.013	-0.014	-0.014
39.05	-0.019	-0.019	-0.020	-0.225	-0.194	-0.221	-0.006	-0.004	-0.004	-0.020	-0.017	-0.017
38.62	-0.038	-0.034	-0.030	-0.022	-0.017	-0.021	-0.017	-0.019	-0.016	-0.022	-0.020	-0.020
38.22	-0.014	-0.016	-0.014	-0.005	-0.002	-0.004	-0.015	-0.015	-0.015	-0.011	-0.010	-0.010
37.71	0.003	0.006	0.005	-0.011	-0.015	-0.014	0.001	0.001	0.002	-0.002	-0.002	-0.003
37.01	-0.028	0.002	0.001	-0.001	0.001	0.001	-0.003	0.000	0.001	-0.072	0.001	0.000
36.56	-0.040	0.002	0.001	-0.001	0.001	0.001	-0.001	0.000	0.001	-0.083	0.001	0.001

Table 22. Continued

unit: m

Sta. no	Yang			Ackers&White			Toffaletti			Laursen		
	Case 1	Case 2	Case 3	Case 1	Case 2	Case 3	Case 1	Case2	Case 3	Case 1	Case2	Case 3
36	0.000	0.000	0.017	0.103	0.105	0.100	0.011	0.012	0.013	0.022	0.024	0.024
35.37	0.054	0.050	0.020	0.154	0.174	0.154	0.021	0.024	0.024	0.026	0.031	0.031
34.92	0.003	-0.001	0.000	0.014	0.011	0.016	-0.003	-0.004	-0.004	-0.003	-0.004	-0.002
34.49	-0.025	-0.022	-0.021	-0.154	-0.144	-0.153	-0.003	-0.002	-0.001	-0.020	-0.017	-0.018
33.83	-0.008	-0.005	-0.009	-0.029	-0.024	-0.028	0.000	0.000	0.000	-0.001	0.000	-0.001
33.27	0.043	0.041	0.045	0.255	0.266	0.259	0.012	0.012	0.012	0.038	0.038	0.038
33.06	0.042	0.046	0.045	0.467	0.468	0.459	0.020	0.024	0.024	0.040	0.057	0.044
32.927	0.003	0.004	0.004	0.100	0.131	0.110	0.005	0.008	0.008	0.006	0.016	0.009
32.913	-0.006	-0.005	-0.008	-0.019	-0.009	-0.028	-0.002	0.003	0.002	-0.009	-0.003	-0.006
32.59	-0.013	-0.010	-0.011	-0.035	-0.033	-0.045	-0.009	-0.006	-0.007	-0.016	-0.010	-0.014
32.12	-0.001	0.001	0.001	-0.001	0.000	0.000	-0.001	0.001	0.001	0.000	0.001	0.000
31.4	-0.006	0.000	-0.319	-0.019	0.001	-0.013	-0.008	-0.012	-0.008	-0.009	-0.012	-0.009
30.83	0.006	0.006	0.003	0.021	0.031	0.025	0.011	0.013	0.014	0.011	0.012	0.012
30.16	-0.008	0.001	0.000	0.000	0.000	0.001	0.000	0.000	0.000	-0.042	0.001	-0.001
29.57	-0.029	0.000	0.000	-0.004	0.000	0.001	-0.004	-0.001	0.001	-0.133	0.000	0.000
29.03	-0.091	-0.113	-0.117	-0.909	-0.848	-0.879	-0.018	-0.018	-0.018	-0.296	-0.533	-0.193
28.63	0.020	0.027	0.027	0.017	0.019	0.015	-0.005	-0.002	-0.004	0.032	0.157	0.013
28.29	0.027	0.035	0.028	0.118	0.128	0.117	-0.011	-0.010	-0.010	0.011	0.106	0.011
27.89	0.028	0.028	0.033	0.347	0.359	0.345	0.003	0.007	0.006	0.084	0.140	0.009
27.4	0.012	0.014	0.012	0.146	0.160	0.145	0.005	0.008	0.006	0.042	0.068	0.024
26.99	0.000	-0.003	0.001	0.004	0.004	0.001	-0.005	-0.002	-0.003	-0.006	0.000	-0.012
26.6	-0.016	-0.015	-0.014	-0.011	-0.009	-0.010	-0.006	-0.005	-0.005	-0.016	-0.014	-0.015
26.14	-0.020	-0.020	-0.019	-0.028	-0.025	-0.028	-0.007	-0.006	-0.006	-0.019	-0.016	-0.018
25.81	-0.025	-0.025	-0.025	-0.154	-0.147	-0.149	-0.013	-0.013	-0.013	-0.025	-0.025	-0.026
25.33	-0.026	-0.025	-0.025	-0.095	-0.092	-0.094	-0.009	-0.010	-0.010	-0.020	-0.018	-0.020
24.68	-0.016	0.000	0.001	-0.001	0.000	0.000	0.001	0.000	0.000	0.003	0.002	0.003
24.05	0.024	0.025	0.024	0.032	0.030	0.032	0.005	0.005	0.005	0.027	0.028	0.024
23.55	0.017	0.018	0.013	0.036	0.033	0.035	0.000	0.000	0.000	0.023	0.026	0.015
23.25	0.000	-0.001	0.003	0.009	0.010	0.010	-0.004	-0.004	-0.004	0.007	0.009	0.002
22.55	-0.002	-0.003	-0.001	0.005	0.005	0.005	-0.003	-0.004	-0.004	0.000	0.003	-0.003
22.11	0.005	0.006	0.006	0.010	0.009	0.010	-0.001	-0.001	-0.001	0.007	0.009	0.004
21.66	-0.008	-0.007	-0.008	0.015	0.018	0.011	-0.014	-0.012	-0.012	-0.023	-0.023	-0.023
21.4	0.014	0.016	0.016	0.056	0.068	0.053	-0.009	-0.006	-0.007	-0.014	-0.011	-0.012
21	0.001	0.002	0.002	0.023	0.027	0.020	-0.017	-0.015	-0.015	-0.017	-0.017	-0.017
20.58	-0.003	-0.005	-0.004	0.001	0.003	-0.001	-0.012	-0.012	-0.012	-0.016	-0.012	-0.016
20.13	-0.001	-0.001	-0.001	-0.014	-0.012	-0.015	-0.009	-0.008	-0.009	-0.014	-0.014	-0.015
19.62	-0.009	-0.009	-0.008	-0.035	-0.032	-0.034	-0.008	-0.007	-0.007	-0.016	-0.017	-0.016
19.18	-0.017	-0.017	-0.018	-0.155	-0.148	-0.154	-0.009	-0.009	-0.009	-0.018	-0.020	-0.019
18.71	-0.006	-0.007	-0.007	-0.015	-0.016	-0.017	-0.005	-0.005	-0.005	-0.010	-0.009	-0.009
18.19	0.011	0.014	0.014	0.005	0.006	0.004	-0.003	-0.003	-0.003	0.003	0.005	0.003
17.85	0.023	0.020	0.020	0.048	0.051	0.046	0.006	0.008	0.007	0.019	0.023	0.019
17.386	0.021	0.022	0.022	0.118	0.120	0.119	0.022	0.024	0.024	0.040	0.046	0.040
17.373	0.023	0.024	0.023	0.153	0.162	0.155	0.023	0.026	0.025	0.044	0.056	0.045
16.91	0.010	0.010	0.010	0.067	0.078	0.068	0.011	0.016	0.015	0.016	0.021	0.016
16.42	-0.014	-0.013	-0.012	-0.010	-0.009	-0.011	-0.009	-0.009	-0.009	-0.017	-0.015	-0.016
15.96	-0.025	-0.027	-0.026	-0.145	-0.139	-0.145	-0.011	-0.011	-0.010	-0.020	-0.020	-0.021
15.46	-0.017	-0.018	-0.018	-0.072	-0.069	-0.072	-0.009	-0.008	-0.009	-0.014	-0.015	-0.015
15.02	0.004	0.005	0.002	-0.012	-0.011	-0.011	-0.007	-0.006	-0.006	-0.007	-0.008	-0.007
14.49	0.012	0.013	0.013	0.004	0.005	0.003	-0.005	-0.003	-0.002	-0.004	-0.003	-0.003
13.97	0.014	0.014	0.014	0.021	0.024	0.020	0.005	0.007	0.006	0.000	0.001	0.000
13.45	0.009	0.006	0.009	0.032	0.037	0.032	0.008	0.011	0.010	0.007	0.010	0.007
12.85	0.001	0.003	0.002	0.019	0.023	0.019	0.007	0.010	0.010	-0.002	0.000	-0.001
12.25	0.003	0.006	0.003	0.044	0.051	0.045	0.013	0.015	0.014	0.012	0.018	0.013

Table 22. Continued

unit: m

Sta. no	Yang			Ackers&White			Toffaletti			Laursen		
	Case 1	Case 2	Case 3	Case 1	Case 2	Case 3	Case 1	Case2	Case 3	Case 1	Case2	Case 3
11.52	0.000	0.001	0.001	0.052	0.053	0.054	0.011	0.013	0.013	0.016	0.022	0.017
11.06	-0.006	-0.005	-0.007	0.001	0.006	0.002	-0.007	-0.005	-0.005	-0.013	-0.011	-0.012
10.6	0.001	0.002	0.002	-0.010	-0.007	-0.010	-0.006	-0.006	-0.006	-0.012	-0.012	-0.013
10.13	0.008	0.009	0.009	0.003	0.008	0.004	0.006	0.007	0.007	-0.006	-0.005	-0.005
9.64	0.005	0.006	0.005	0.008	0.013	0.009	0.005	0.007	0.006	-0.003	-0.001	-0.002
9.17	-0.001	-0.001	-0.003	0.015	0.021	0.016	0.007	0.009	0.009	0.004	0.005	0.004
8.67	0.006	0.009	0.010	0.022	0.028	0.023	0.011	0.012	0.012	0.010	0.013	0.009
8.16	0.003	0.004	0.004	0.021	0.026	0.022	0.010	0.012	0.012	0.010	0.013	0.011
7.74	0.000	-0.002	0.002	0.014	0.019	0.016	0.008	0.010	0.010	0.007	0.009	0.007
7.21	0.001	0.004	0.001	0.011	0.016	0.013	0.006	0.008	0.008	0.006	0.009	0.007
6.75	0.003	0.004	0.005	0.017	0.022	0.019	0.006	0.007	0.007	0.008	0.011	0.009
6.11	0.003	0.001	0.005	0.025	0.032	0.028	0.006	0.007	0.007	0.010	0.014	0.011
5.39	0.002	0.007	0.003	0.026	0.033	0.029	0.006	0.008	0.008	0.013	0.017	0.013
4.86	-0.002	0.000	-0.001	0.015	0.020	0.018	0.003	0.005	0.004	0.007	0.009	0.007
4.593	-0.010	-0.009	-0.011	0.000	0.002	0.001	-0.005	-0.005	-0.005	-0.003	-0.001	-0.002
4.567	-0.009	-0.010	-0.008	0.000	0.004	0.001	-0.006	-0.005	-0.005	-0.003	-0.001	-0.003
4.24	0.002	0.004	0.003	0.008	0.013	0.011	0.002	0.004	0.004	0.002	0.004	0.003
3.78	0.004	0.005	0.005	0.021	0.025	0.023	0.006	0.007	0.007	0.009	0.013	0.009
3.33	0.005	0.006	0.006	0.041	0.046	0.043	0.011	0.013	0.013	0.021	0.028	0.021
2.92	0.006	0.008	0.007	0.097	0.103	0.100	0.018	0.021	0.021	0.046	0.068	0.046
2.45	0.003	0.005	0.005	0.092	0.102	0.097	0.013	0.016	0.016	0.040	0.067	0.046
2.02	0.000	0.003	0.003	0.022	0.037	0.029	0.005	0.006	0.006	0.018	0.042	0.023
1.48	0.001	0.002	0.001	0.000	0.000	0.000	-0.002	0.000	0.001	-0.001	0.006	0.001
1.14	0.000	0.002	0.002	0.000	0.001	0.000	0.000	0.001	0.001	0.004	0.018	0.006
0.72	0.002	0.004	0.004	0.067	0.070	0.069	0.011	0.013	0.014	0.018	0.045	0.027
0.35	0.001	0.002	0.002	0.001	0.010	0.005	0.003	0.004	0.004	0.004	0.017	0.009
0	-0.004	0.002	0.002	-0.001	0.000	0.000	-0.004	-0.002	-0.001	-0.002	0.013	0.002

5.2 Assessment based on 2-dimensional analysis

In spite of the gate operation, results of the 1-D model showed that there were some areas where erosion and deposition occur severely. So station no. 92.85-96.46 (L=3.5 km) downstream of the Sejong weir was analyzed using the 2-D model. Most of all, simulation was conducted for 11 days under a certain rainfall event (9.13-9.23.2007) to predict the riverbed change and was compared with the 1-D results. Also, by installing a dike, it was examined how important a role the structure played in the riverbed change.

5.2.1 Unsteady flow analysis

After setting 4 monitoring points, water levels of 2-D was extracted, as shown in Figures 97-98 and were compared with the 1-D unsteady analysis results. The RMSE values varied from 0.028 to 0.068 and AMD varied from 0.021 to 0.057, as shown in Table 23. These results show that the 2-D simulation with the roughness coefficient calibrated by 1-D model is important, as seen in Figure 99.

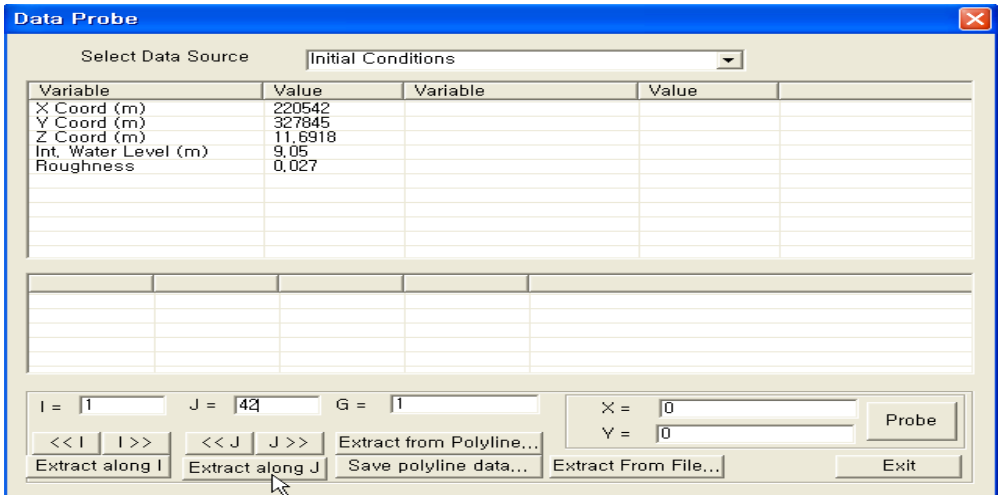

Figure 97. Data Probe

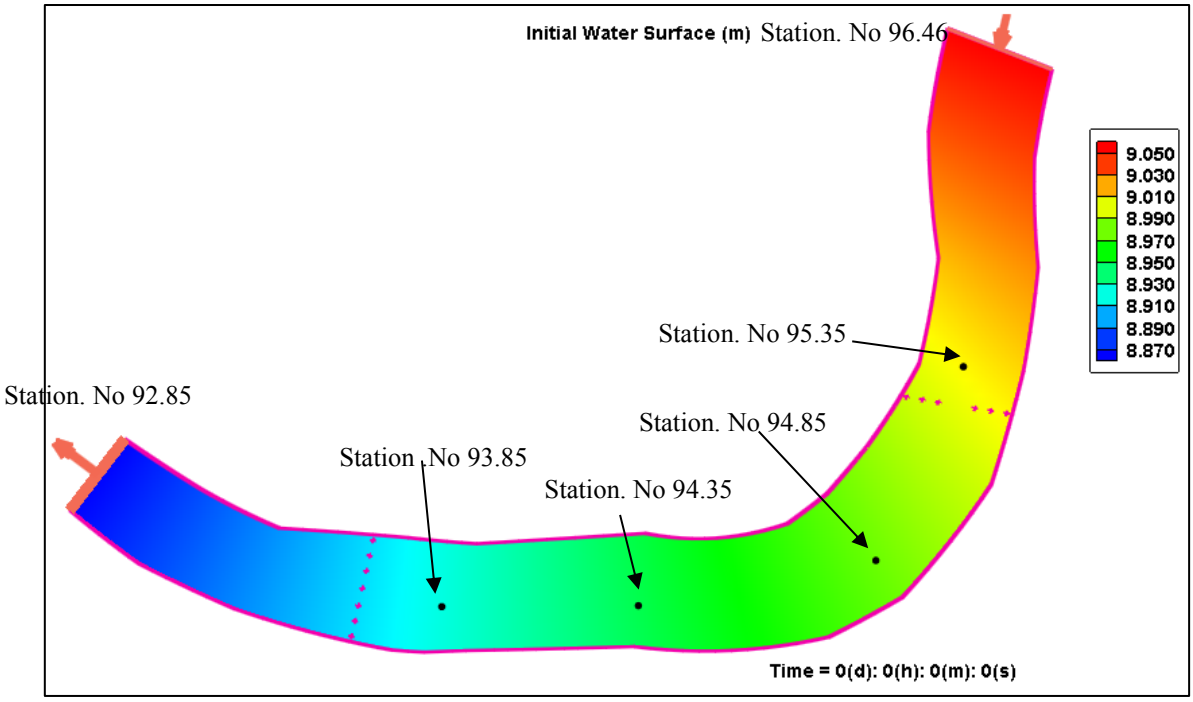

Figure 98. Monitoring Points in 2-D Model

Table 23. RMSE and AMD in 2007 for a 2-D Model

Type	Root Mean Square Difference (RMSE) in meter	Absolute Mean Difference (AMD) in meter
Sta.no 93.85	0.028	0.021
Sta.no 94.35	0.043	0.037
Sta.no 94.85	0.064	0.050
Sta.no 95.35	0.068	0.057

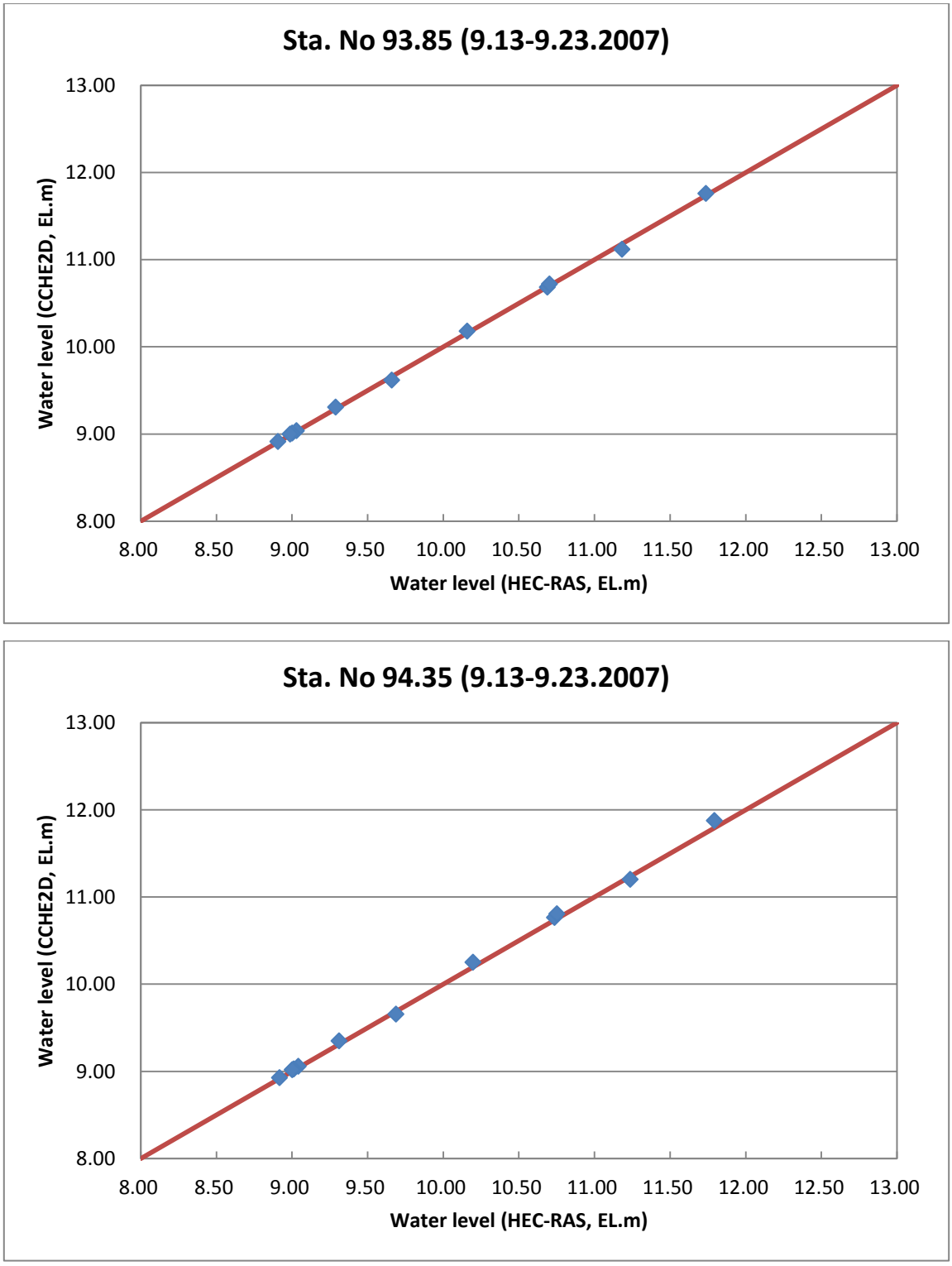

Figure 99. Comparison of Water Levels in 2-D Unsteady Analysis

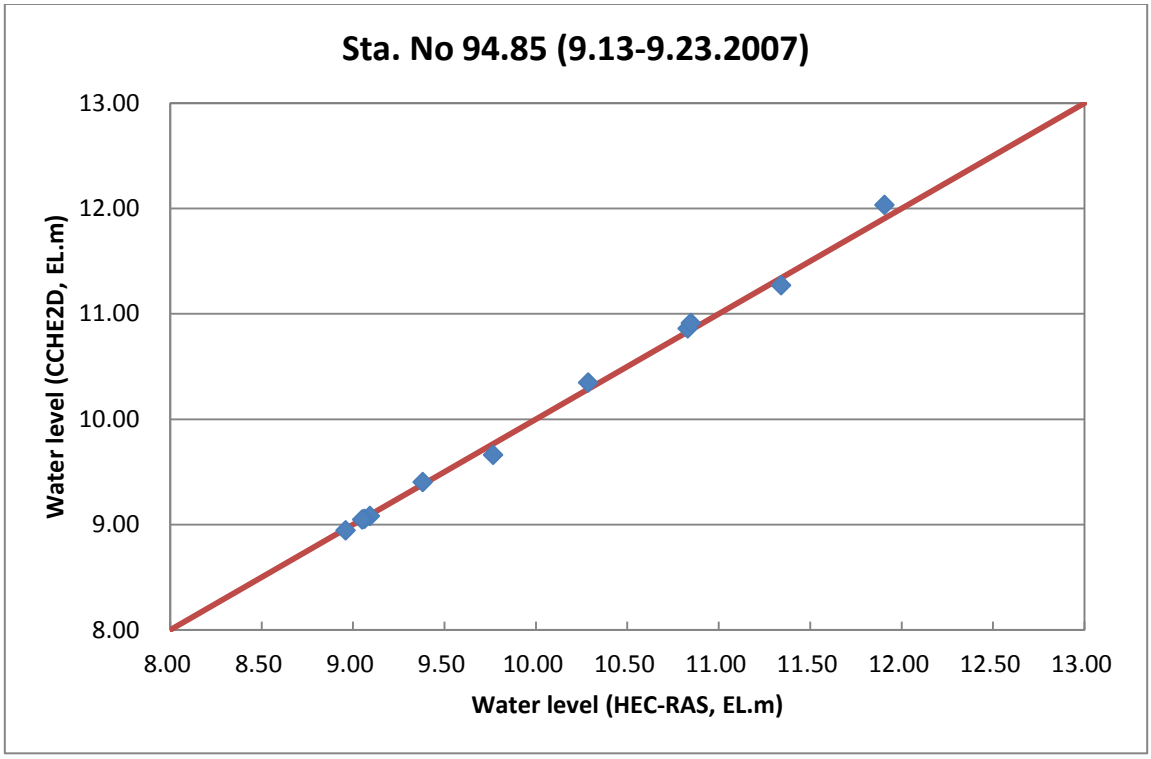

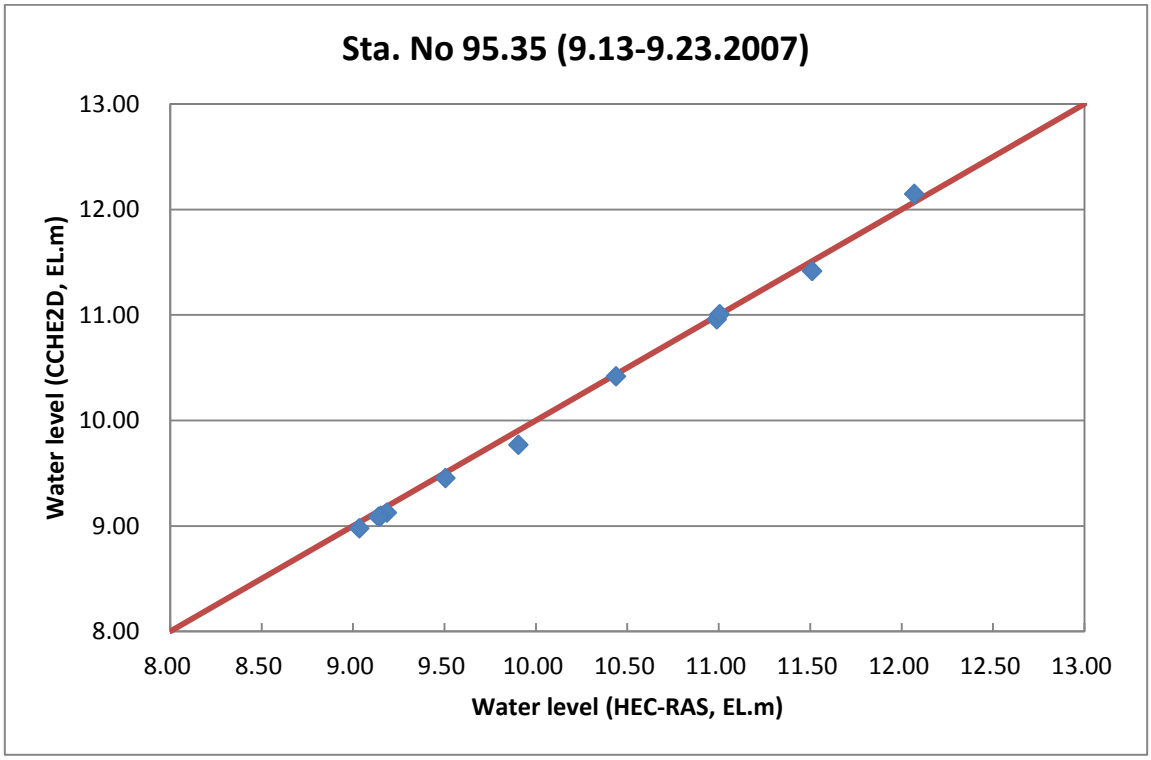

Figure 99. Continued

5.2.2 Sediment analysis

In the CCHE2D model, the non-equilibrium adaptation length L characterizes the distance for sediment to adjust from a non-equilibrium state to an equilibrium state. It is a length scale for the riverbed to respond to the disturbances of environment, such as hydraulic structure construction, channel geometry changes and incoming sediment variation. L is a very important parameter for numerical stability, but it has been given significantly different values by different researchers. In the CCHE2D model, let the non-equilibrium adaptation length be input as a coefficient in the case of suspended load transport mode and its physical meaning is the ratio between the near-bed concentration and the depth-averaged concentration. The riverbed changes through various adaptation length factors were compared with the results by the 1-D riverbed change using the Toffaleti equation, which is for large and suspended system, to determine the desirable coefficient value. To lessen errors among models, sediment was calculated by 1 hour in HEC-RAS and upstream boundary condition Qs of CCHE2D used results of HEC-RAS. But, there are differences between HEC-RAS and CCHE2D. The sediment analysis in HED-RAS is performed under quasi-unsteady and equilibrium state, whereas sediment in CCHE2D is calculated under unsteady state and non-equilibrium state. Therefore, comparison with observation data must be needed in future to find proper adaptation length factor.

5.2.2.1 Adaptation length factor

The non-equilibrium adaptation coefficient of suspended load, α, was calculated using the Armanini and de Silvio's (1988) method:

$$\frac{1}{\alpha} = \frac{a}{h} + (1 - \frac{a}{h}) \exp[-1.5(\frac{a}{h})^{-1/6} \frac{\omega_{sk}}{u_*}]$$

where a is the thickness of bottom layer, h is the flow depth; ω_{sk} = the settling velocity of sediment particles; and u_* is the bed shear velocity. Values of α calculated by the above equation were usually larger than 1. In practice, α has been given significantly different values, mostly less than 1, by many researchers. Han et al. (1980) and Wu and Li (1992) suggested α =1 for strong scour, α=0.25 for strong deposition, and α=0.5 for weak scour and deposition. However, α was given very small values, such as 0.001 in the Yellow River (Wei, 1999) and the Rio Grande River (Yang et al., 1998), in which sediment concentration is higher, and rapid erosion and deposition often occur. In this study, six cases of α, which are 1.0, 0.5, 0.1, 0.05, 0.02 and 0.001, were reflected in the model. For example, input of α=0.001 was shown in Figure 100.

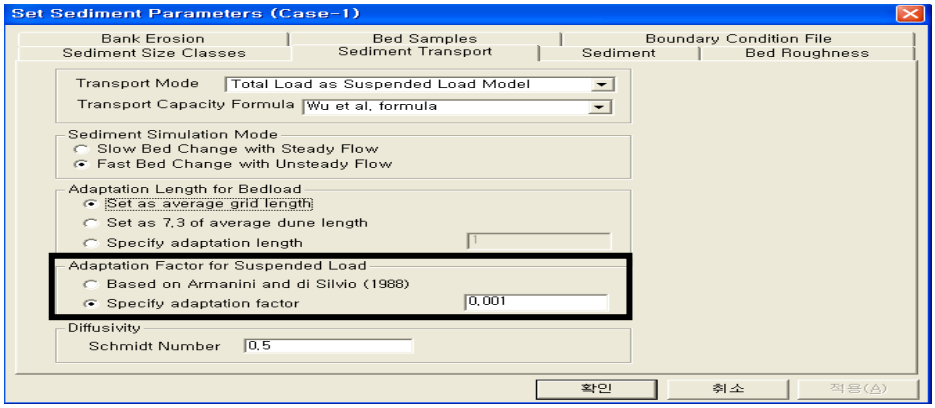

Figure 100. Sediment Parameter Input (Adaptation Factor = 0.001)

5.2.2.2 Sensitivity analysis of adaptation length factor

The invert change of the 1-D model is shown in Figure 101. When the riverbed change of the 2-D model was compared with the 1-D model about maximum invert change, minimum invert change, and mean invert change, 0.001 of α was similar to the that of the 1-D model, as shown in Table 24. Also, erosion happened downstream of Bulti bridge (station no. 95.19) and downstream of Chungbuk bridge (station no. 93.501) in HEC-RAS model, as shown in Figure 101. This result was shown in CCHE2D model and the result of 0.001 of α was similar to that of the 1-D model as shown in Table 25, Figures 102 and 103. We can see the riverbed according to α in Figure 104 to 109, and in future one needs to find an accurate adaptation factor by comparing with the measured cross section data, sediment discharge, and sediment concentration.

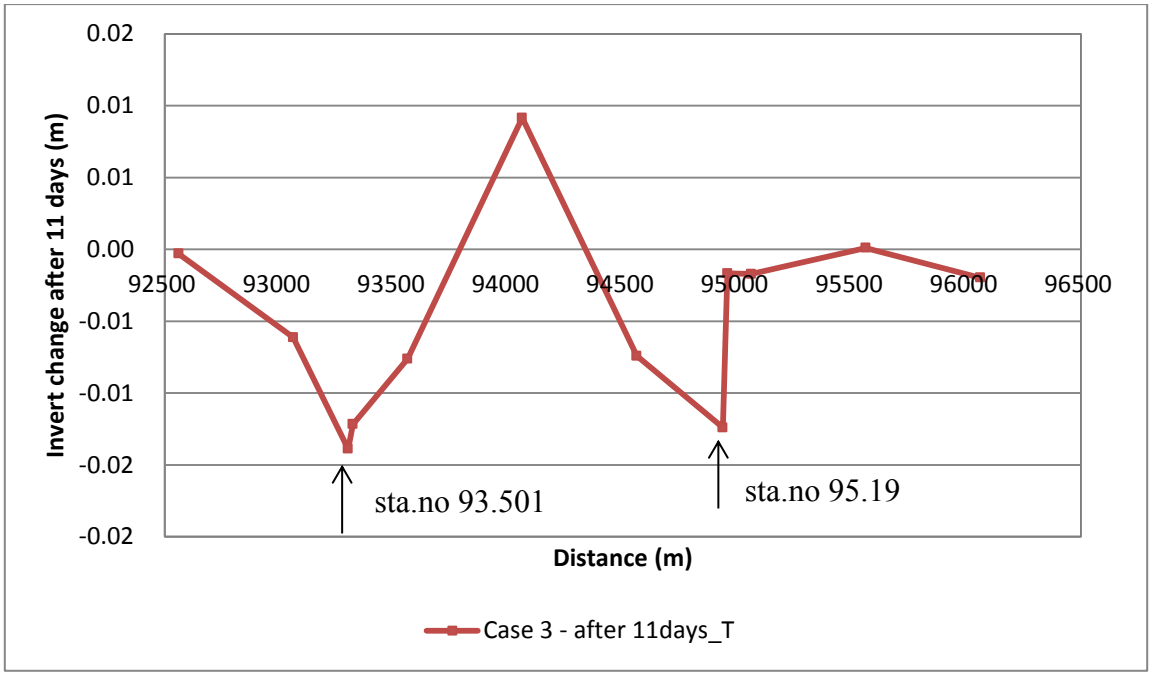

Figure 101. Riverbed Change after 11 days in HEC-RAS

Table 24. Riverbed Change between 1-D and 2-D Models

Sta. No	1-D	2-D					
		α=1.0	α=0.5	α=0.1	α=0.05	α=0.02	**α=0.001**
Max. invert change (cm)	0.9	142.4	100.7	26.1	13.5	5.7	0.3
Min. invert change (cm)	-1.4	-235	-203.5	-102.7	-70.3	-37	-3.2
Mean invert change (cm)	-0.5	-0.3	-1.5	-1.5	-1.2	-0.8	-0.3
Total change (㎥)	-	-3,418	-14,774	-15,312	-12053	-8,252	-3,153

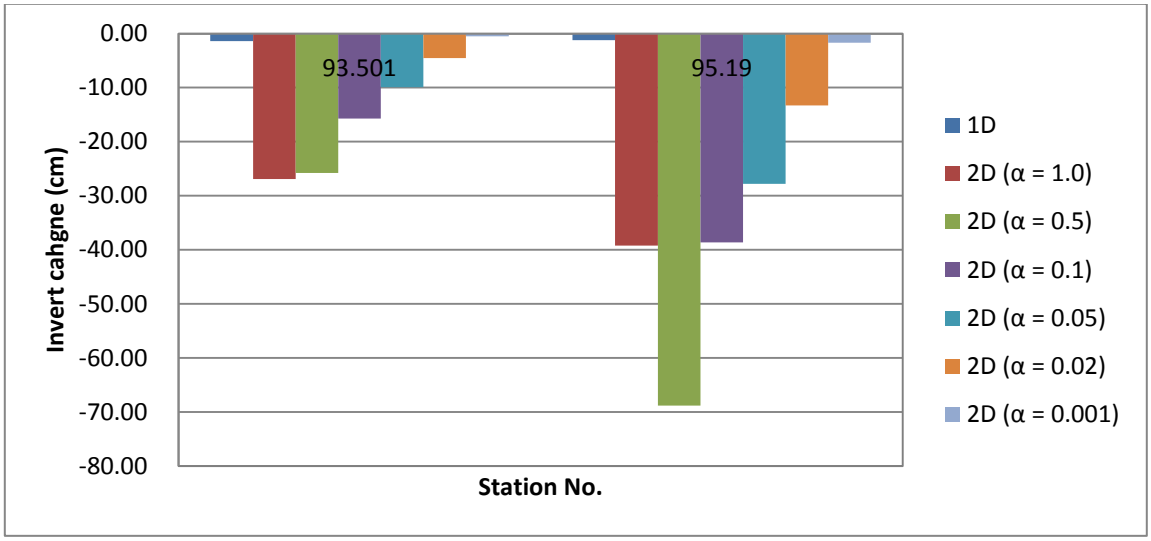

Figure 102. Sensitivity Analysis of Adaptation Length Factor

Table 25. Invert Change Downstream of Bridges

unit: cm

Sta. No	1-D	2-D					
		α=1.0	α=0.5	α=0.1	α=0.05	α=0.02	**α=0.001**
93.501	-1.4	-26.9	-25.8	-15.7	-9.9	-4.5	-0.5
95.19	-1.2	-39.2	-68.8	-38.6	-27.8	-13.3	-1.7

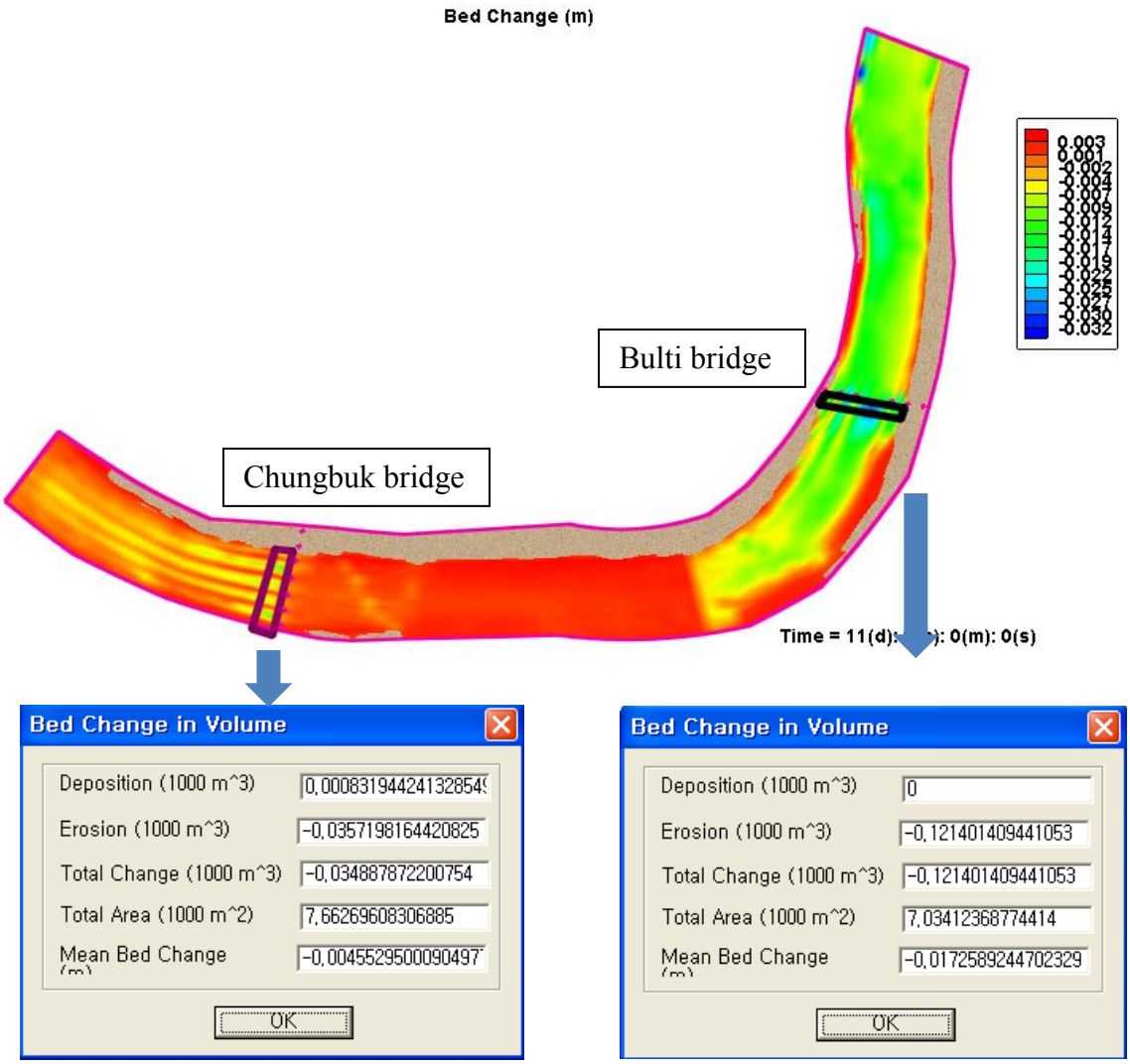

Figure 103. Riverbed Change of Bridges (Adaptation Length Factor = 0.001)

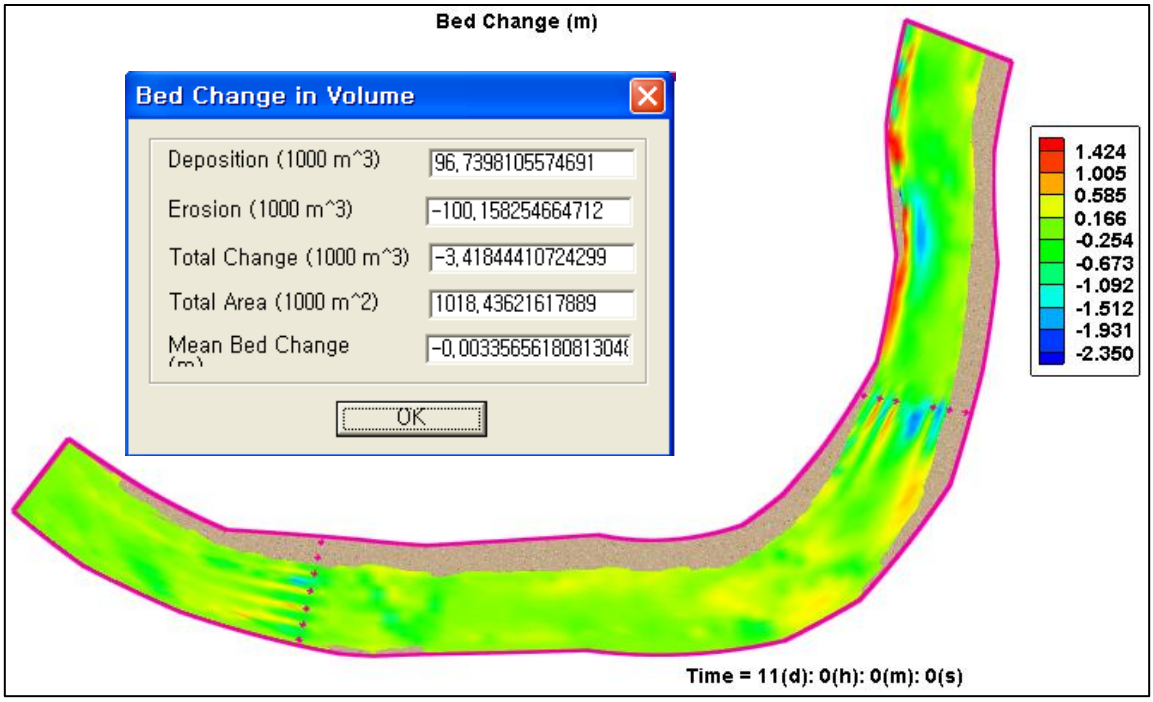

Figure 104. Riverbed Change (Adaptation Length Factor = 1.0)

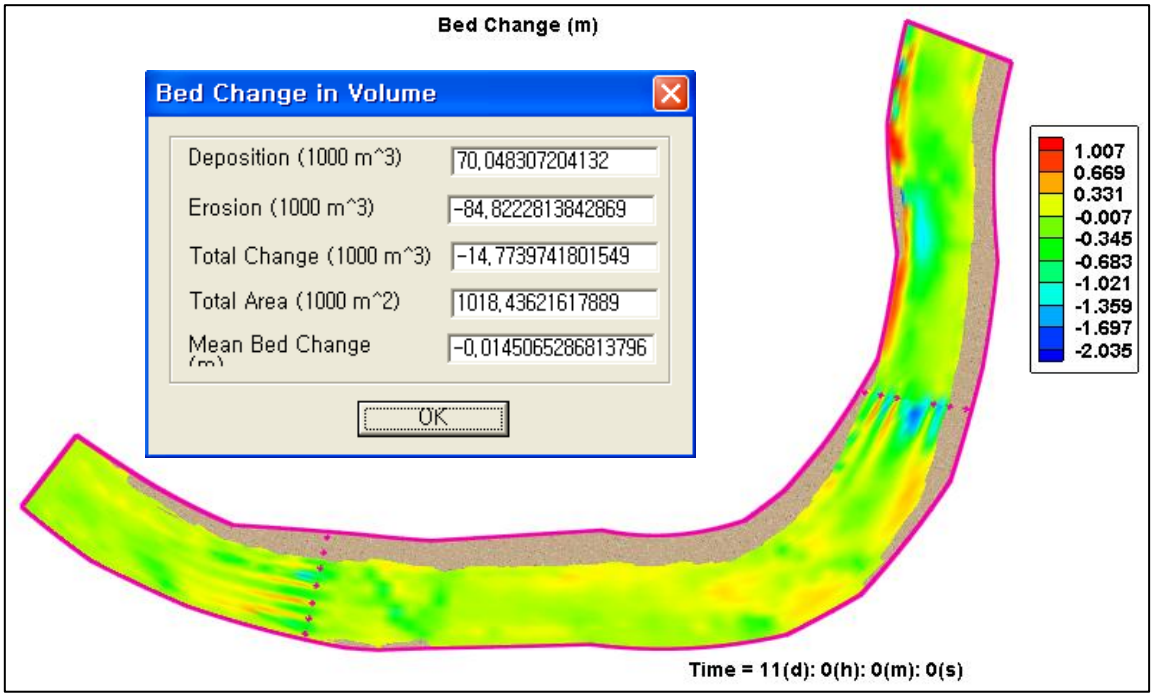

Figure 105. Riverbed Change (Adaptation Length Factor = 0.5)

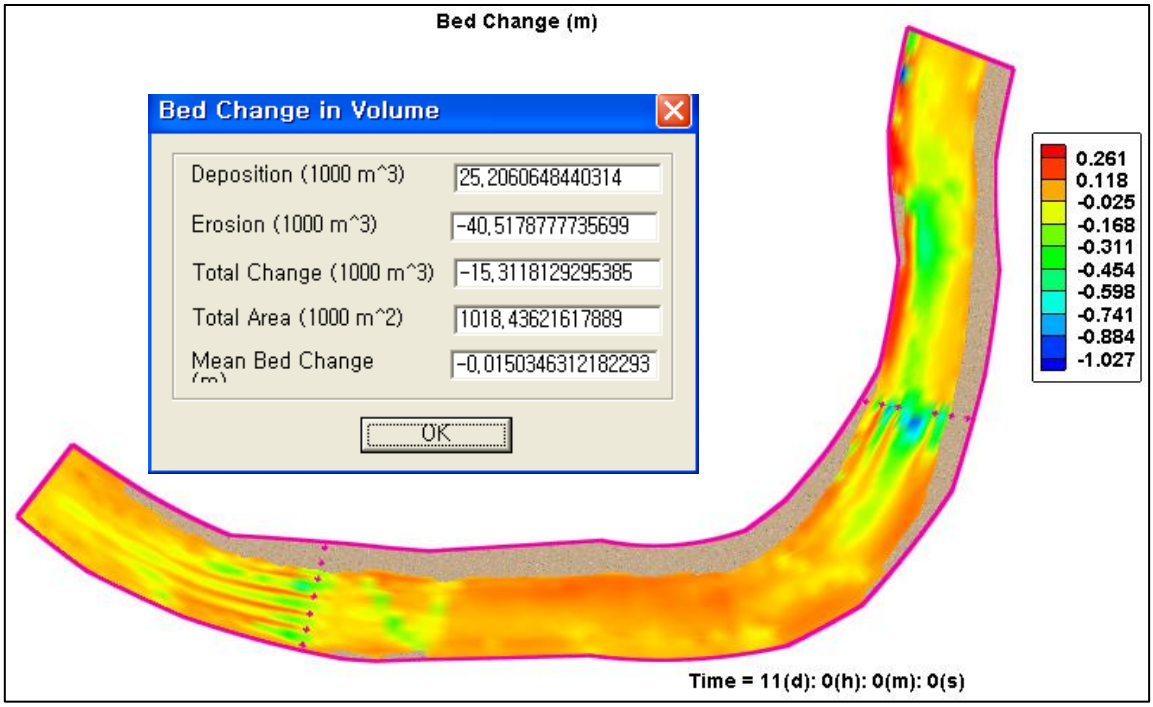

Figure 106. Riverbed Change (Adaptation Length Factor = 0.1)

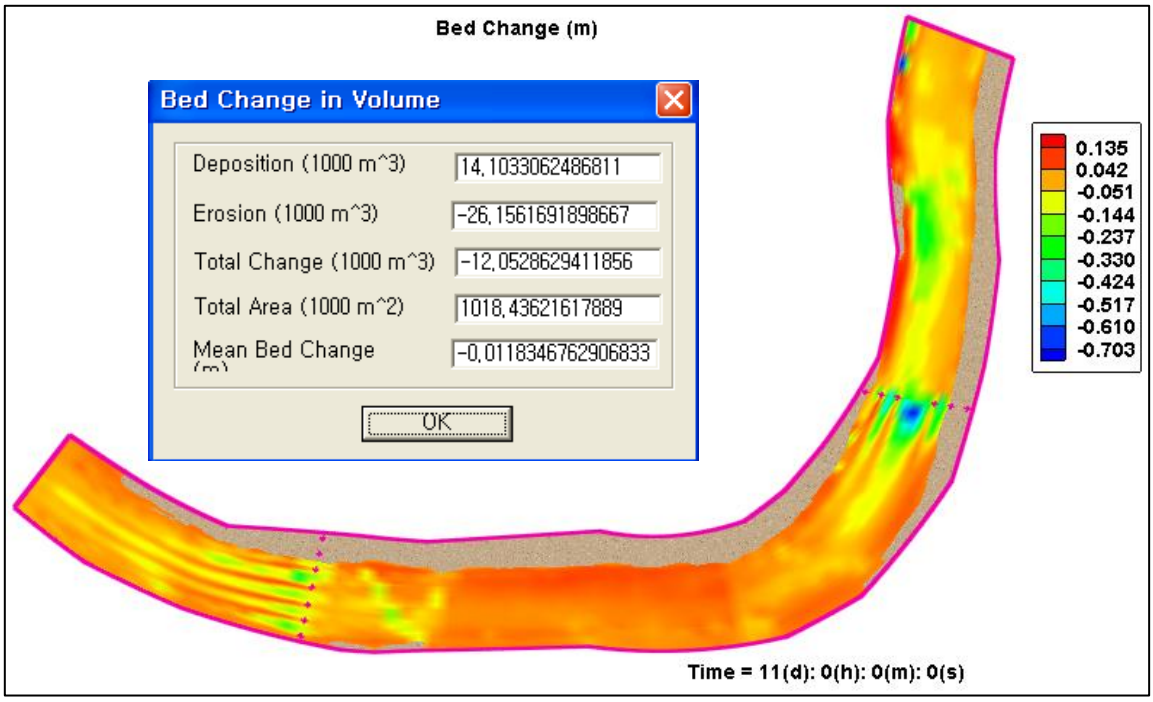

Figure 107. Riverbed Change (Adaptation Length Factor = 0.05)

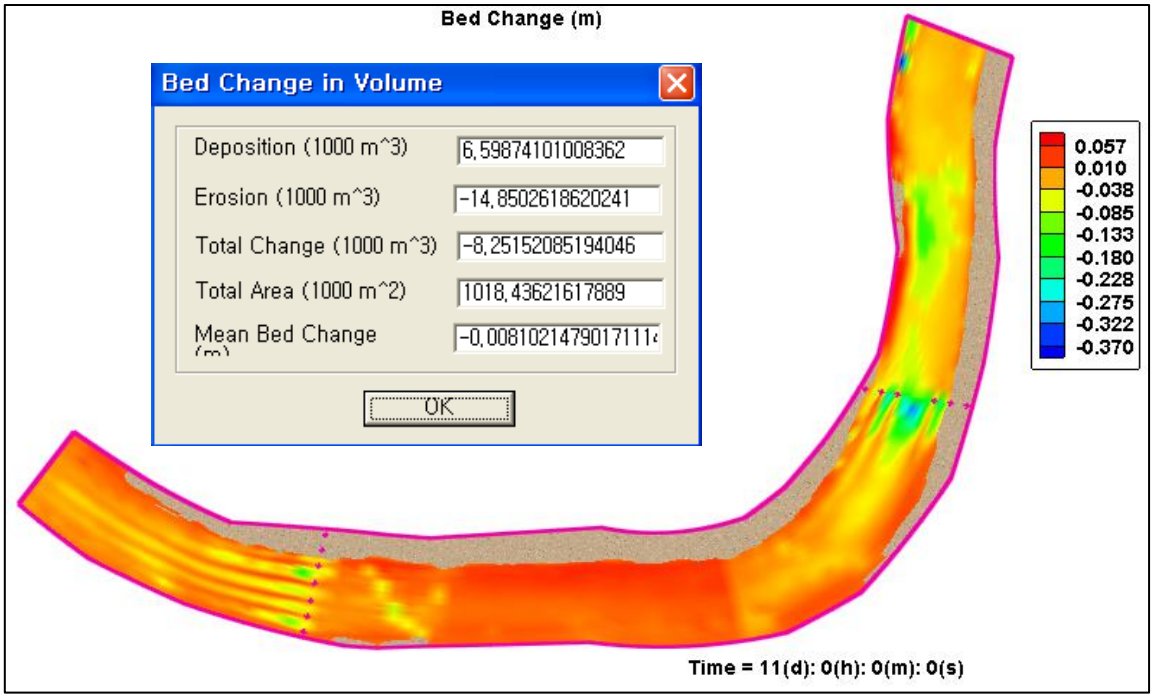

Figure 108. Riverbed Change (Adaptation Length Factor = 0.02)

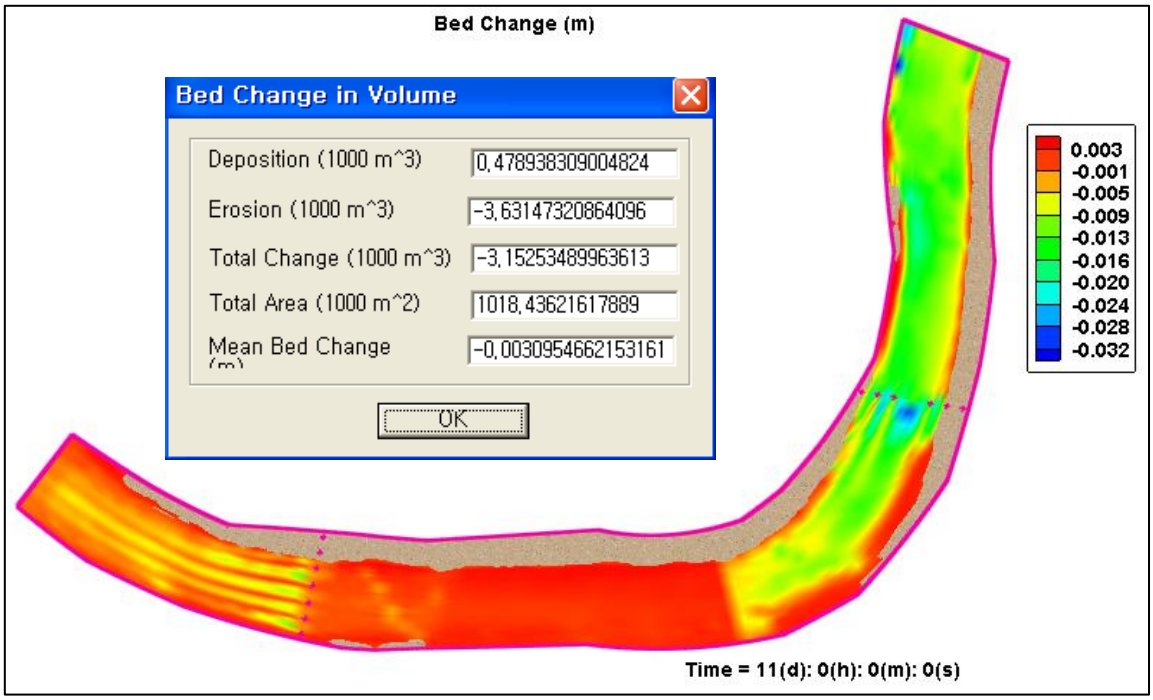

Figure 109. Riverbed Change (Adaptation Length Factor = 0.001)

The velocity was examined in case of 2,259 ㎥/s (4 day 3 hr) which is a peak flow during the simulation time. The velocity was high near bridges, as shown in Figure 110 and this result showed that erosion also happened at the same place. The downstream channels have high speeds but there was no erosion because that area consisted of coarse sediment.

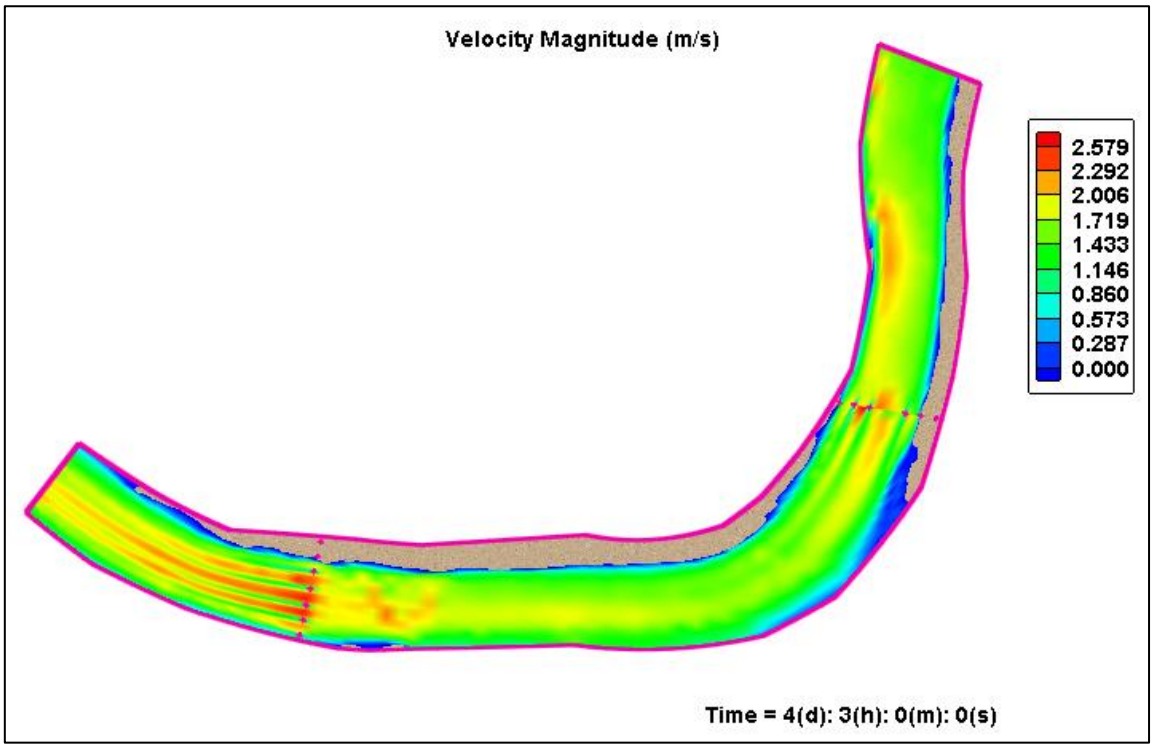

Figure 110. Velocity Distribution (Adaptation Length Factor = 0.001)

5.2.3 Structural measure (Installation of a dike)

Results of the 2-D Model showed the erosion of Bulti bridge was inclined to the right side of the river, seen from upstream, as shown in Figure 111. This section was also predicted to erode in HEC-RAS. A groin has been used as one of the most common methods of organizing and controlling erosion in the bend or straight direction. One of the reasons for building the groin is to mitigate the scouring effects around these structures which necessitate the study of important parameters which could protect the banks from destruction. Therefore, a dike installed in this area to change the flow direction to the left side of the river was analyzed to see the effect of dike on the riverbed change. In the CCHE2D Model, a 1-D dike was emplaced in the erosion area using a 1-D hydraulic structure, as shown in Figure 111 and the adaptation length factor (α) of 0.001 was applied.

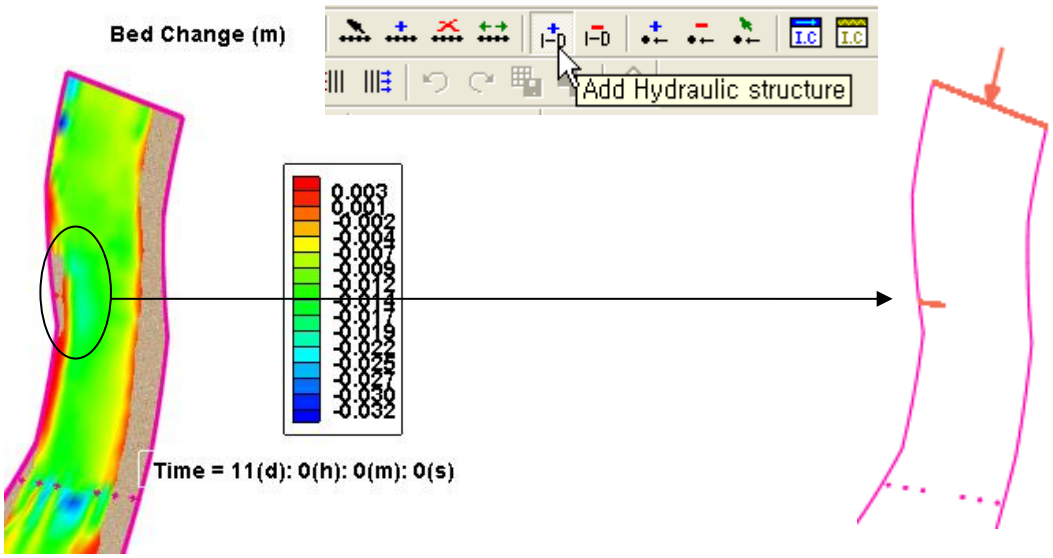

Figure 111. Dike Installation in 2-D Simulation

Erosion to the maximum of 3.4 cm with dike was predicted to happen whereas erosion to the maximum of 1.9 cm was without dike. Also, the most eroded section was shifted to the left side as well as downstream, as shown in Figure 112.

The velocity and riverbed near the dike increased and that of the downstream bridge also increased due to the dike, as shown in Figure 113. When examined the effect of the dike from the cross section from J=15 where dike was installed to J=17, the deepest bed elevation was shifted to the left side by 34 m, as shown in Figures 114 to 116.

That means that dikes have an advantage in that a certain area can be protected from erosion and a disadvantage in that a hydraulic problem can happen downstream.

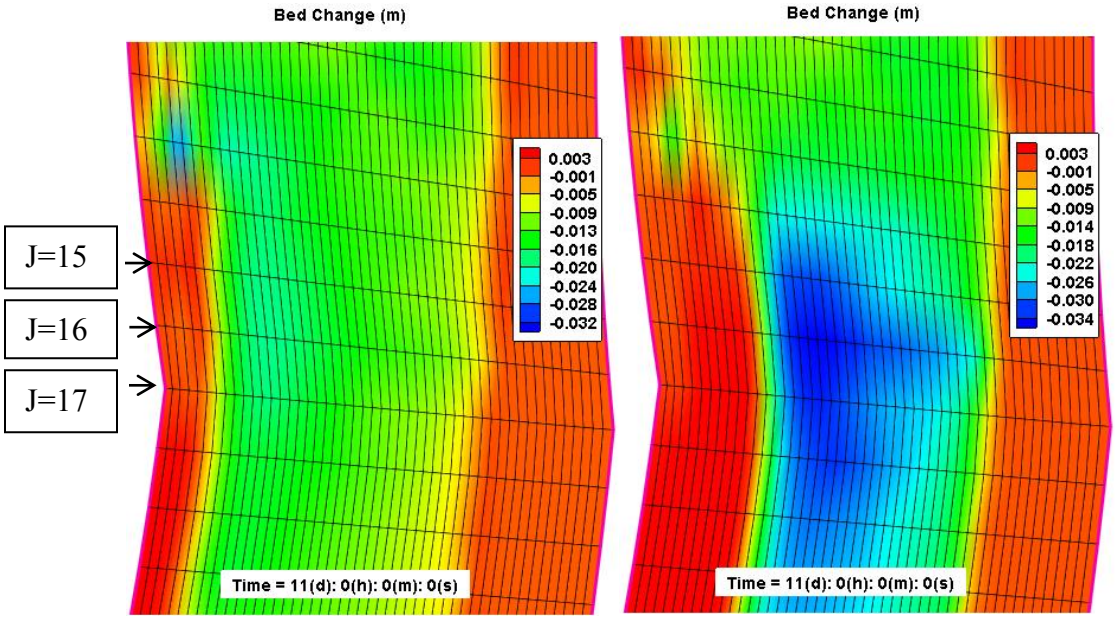

Figure 112. Deepest Riverbed Change without Dike (left) and with Dike (right)

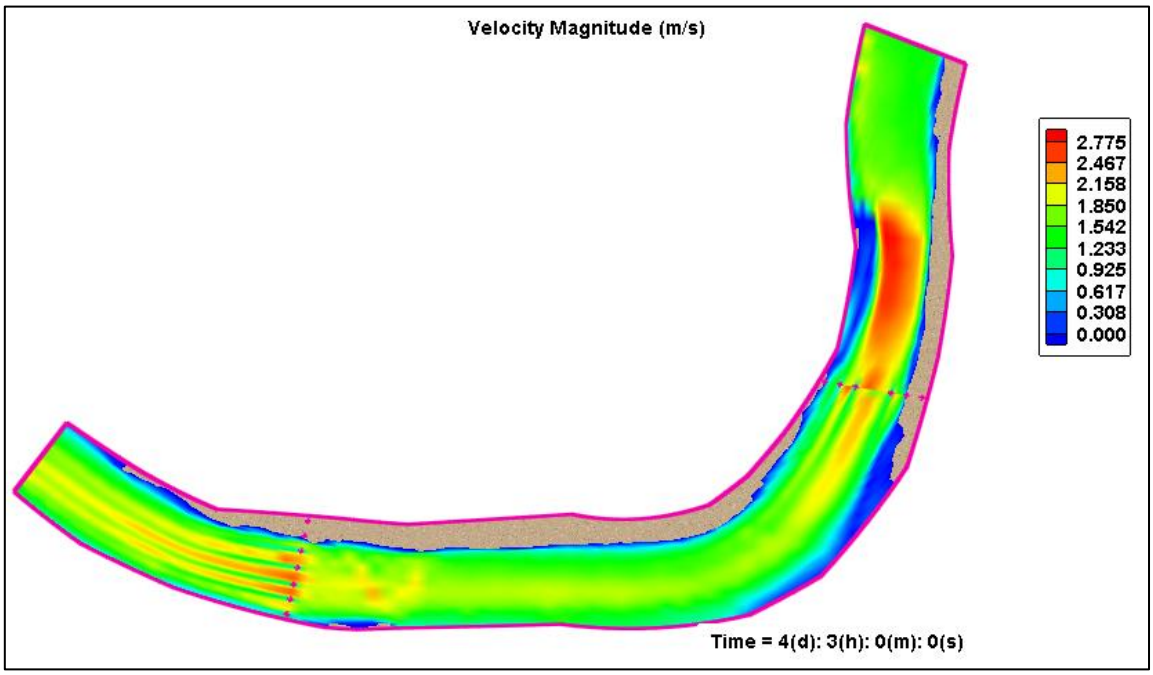

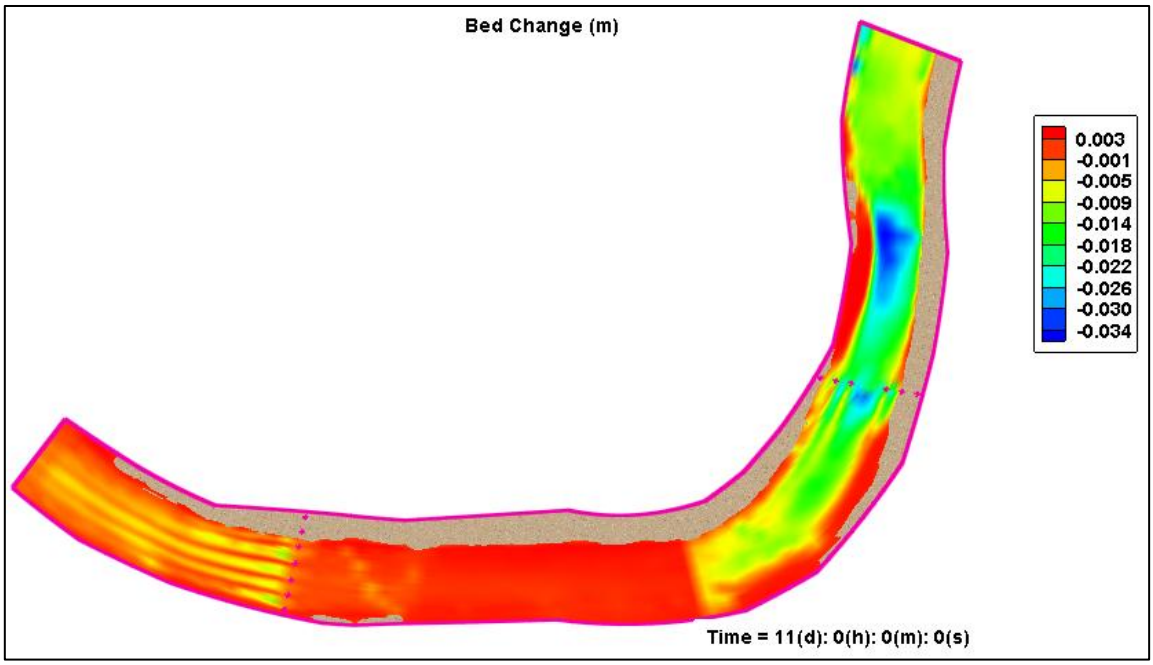

Figure 113. Velocity and Bed Change with Dike

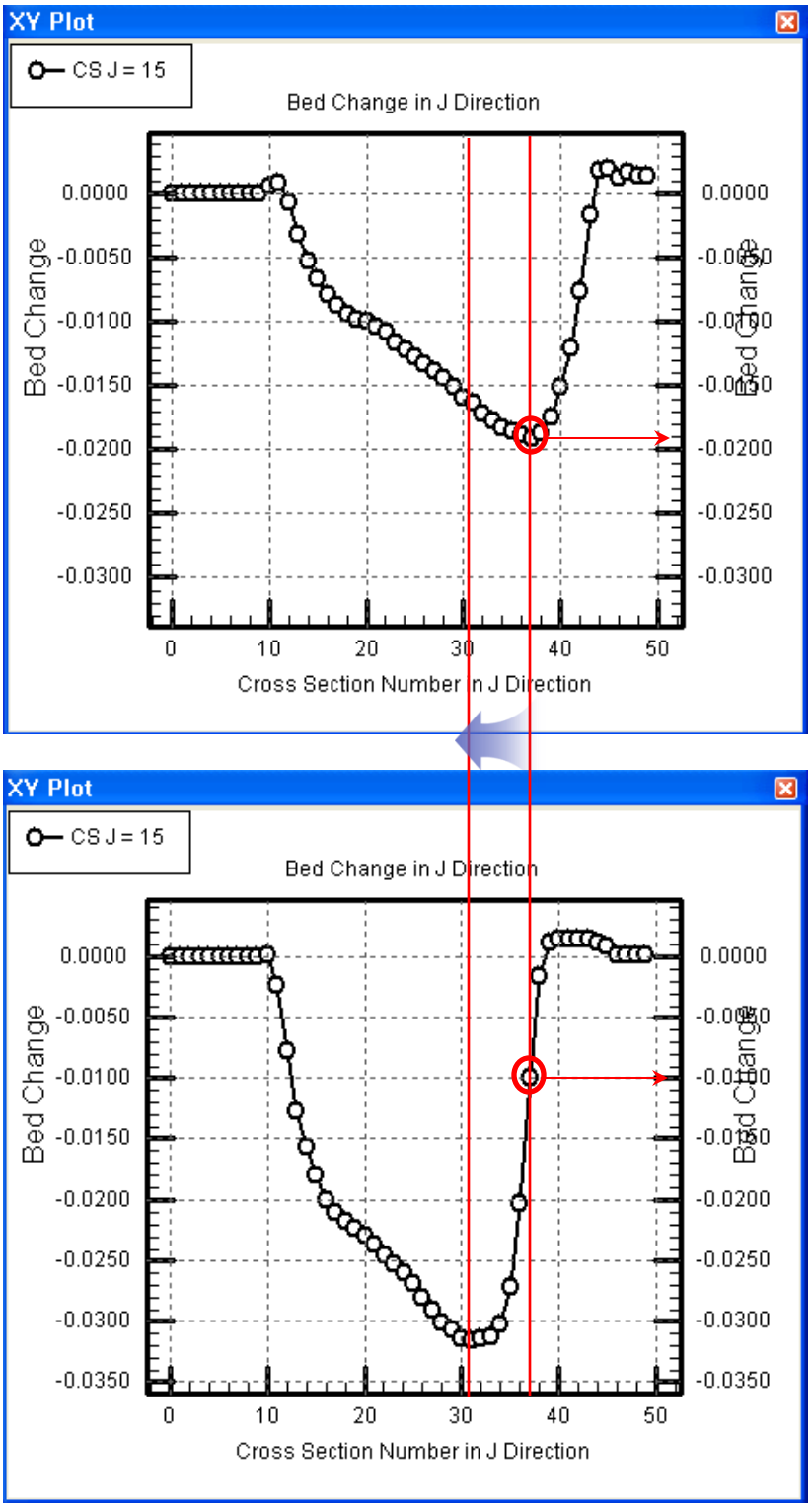

Figure 114. Bed Change (J=15) without Dike (up) and with Dike (down)

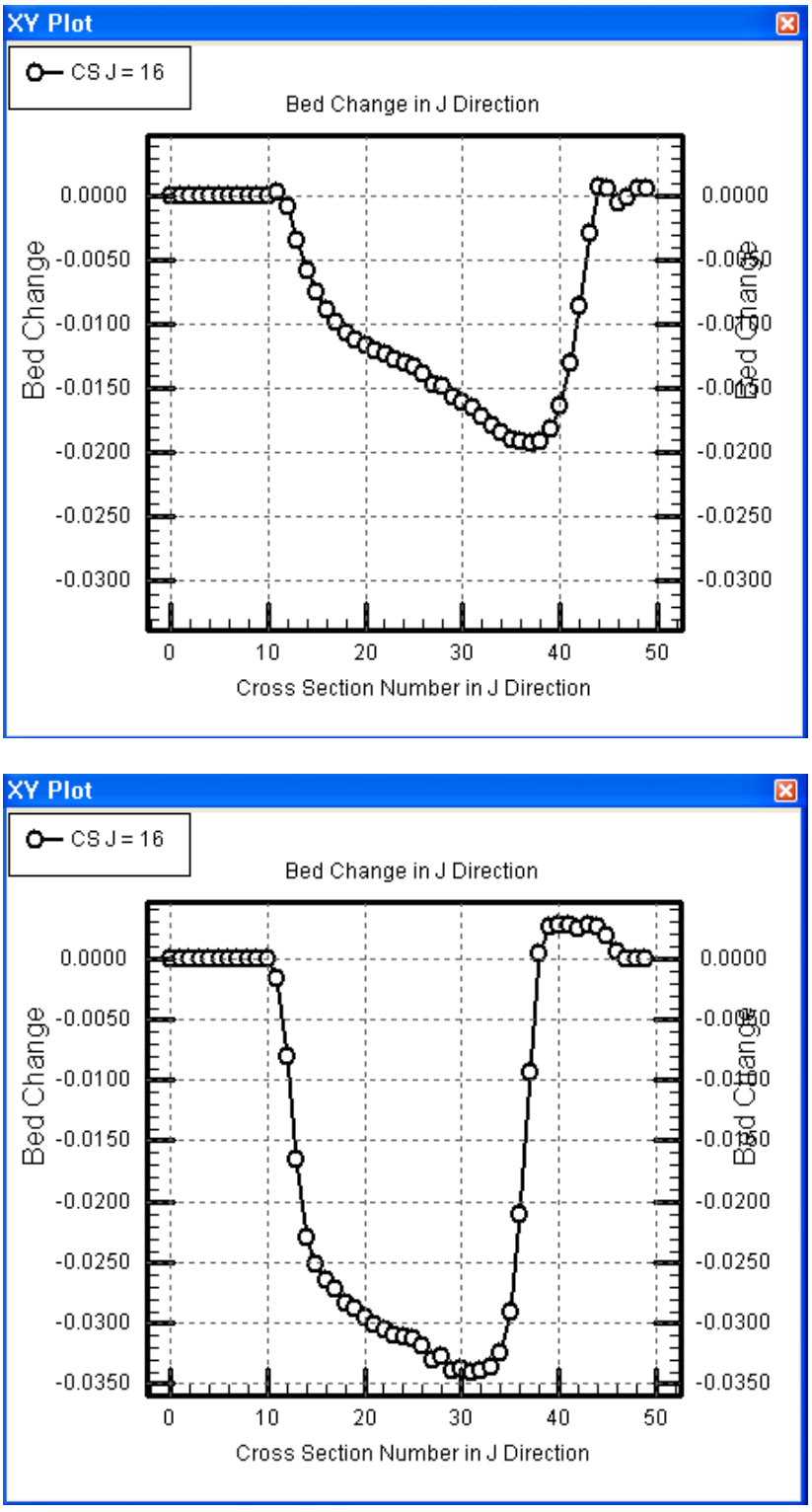

Figure 115. Bed Change (J=16) without Dike (up) and with Dike (down)

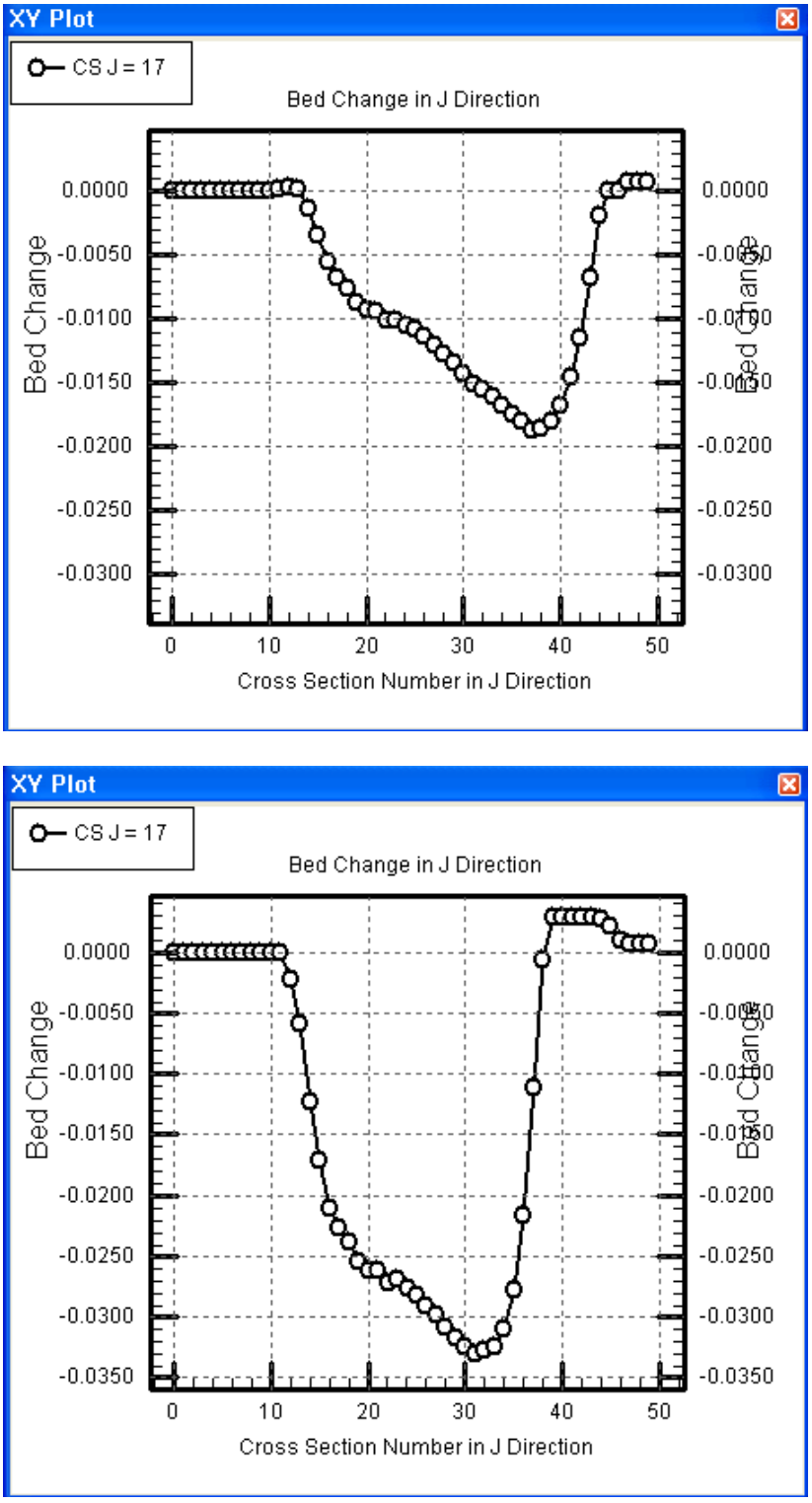

Figure 116. Bed Change (J=17) without Dike (up) and with Dike (down)

6. CONCLUSIONS AND RECOMMENDATIONS

6.1 Conclusions

After the Four Major Rivers Restoration Project, long-term riverbed change for 20 years was analyzed by the 1-D model (HEC-RAS) from Daechung regulation dam to Geum estuary (L=130km), assuming that flow events in 2006-2007 would repeat. To simulate realistic conditions, daily runoff data were calibrated with the PRMS value based on a hydraulic unit map. Then, unsteady analysis in HEC-RAS was done for the gate opening height in order to maintain the management water level, and then the riverbed change was calculated through quasi-unsteady analysis. Also, to investigate the effect of movable weirs, sediment analysis was done for three cases: case 1 means gate is closed fully, case 2 means gate is open fully, and case 3 means gate is regulated by an operating rule. First of all, the impact of gate operation on long-term (20 years) riverbed change was examined using HEC-RAS with 4 types of sediment transport equations.

When case 2 and case 3 were compared, the impact of gate occurred upstream of Sejong weir and Gongju weir and depended on sediment transport equations, as shown in Figure 117. For example, in case of Yang's equation, upstream of Sejong weir (L=7.0 km) and upstream of Gongju weir (L=7.4 km) were predicted to be affected by the gate operation, as shown in Table 26.

Table 26. Boundary of Impact by the Gate Operation (Gongju-Daechung)

Type	Yang	Ackers & White	Toffaleti	Laursen
Sejong-Daechung dam	7.0 km	7.0km	2.0 km	6.1 km
Gongju-Sejong	7.4 km	8.9 km	7.4 km	9.5 km

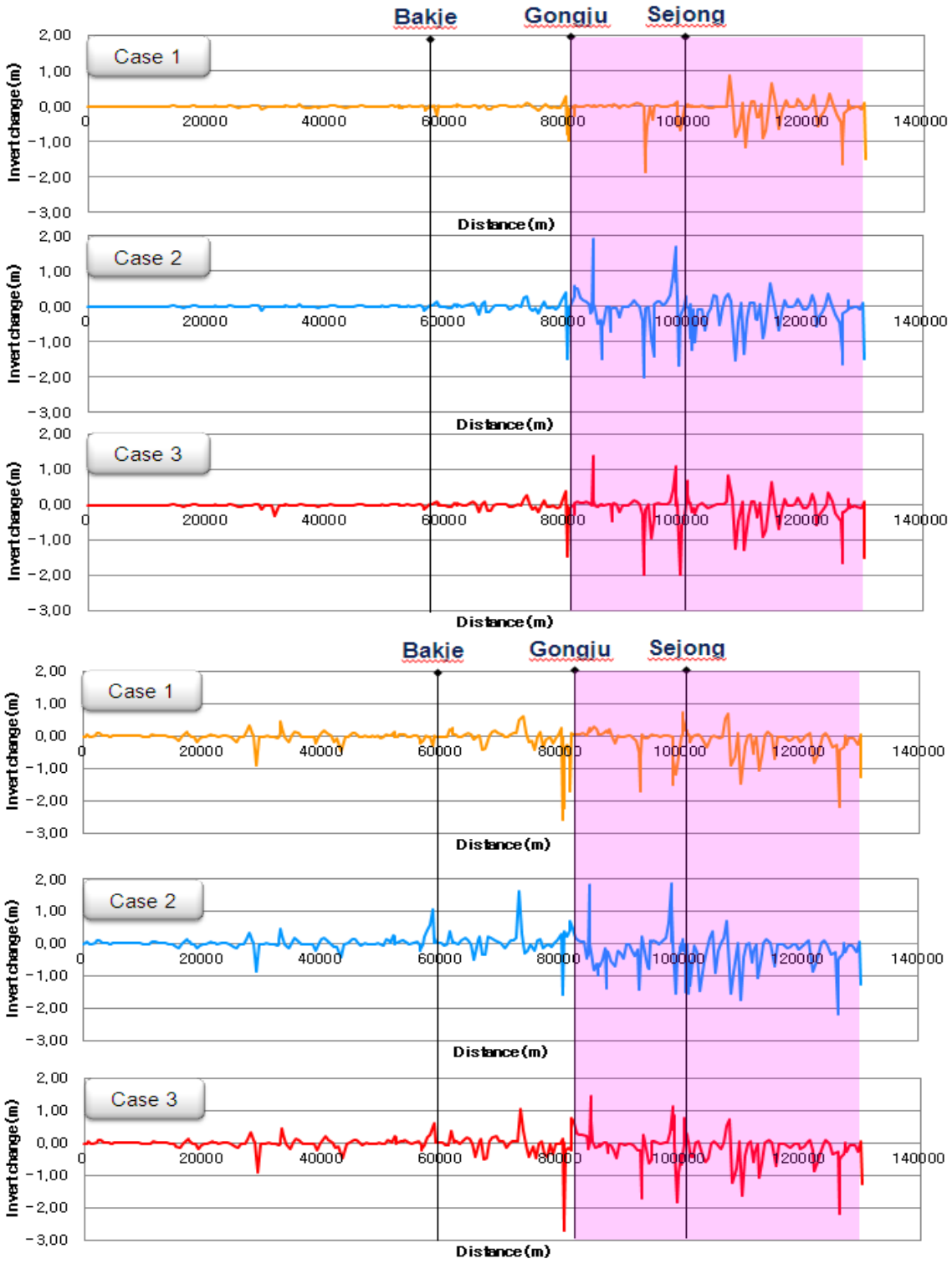

Figure 117. Riverbed change (up: Yang equation, down: Ackers & White equation)

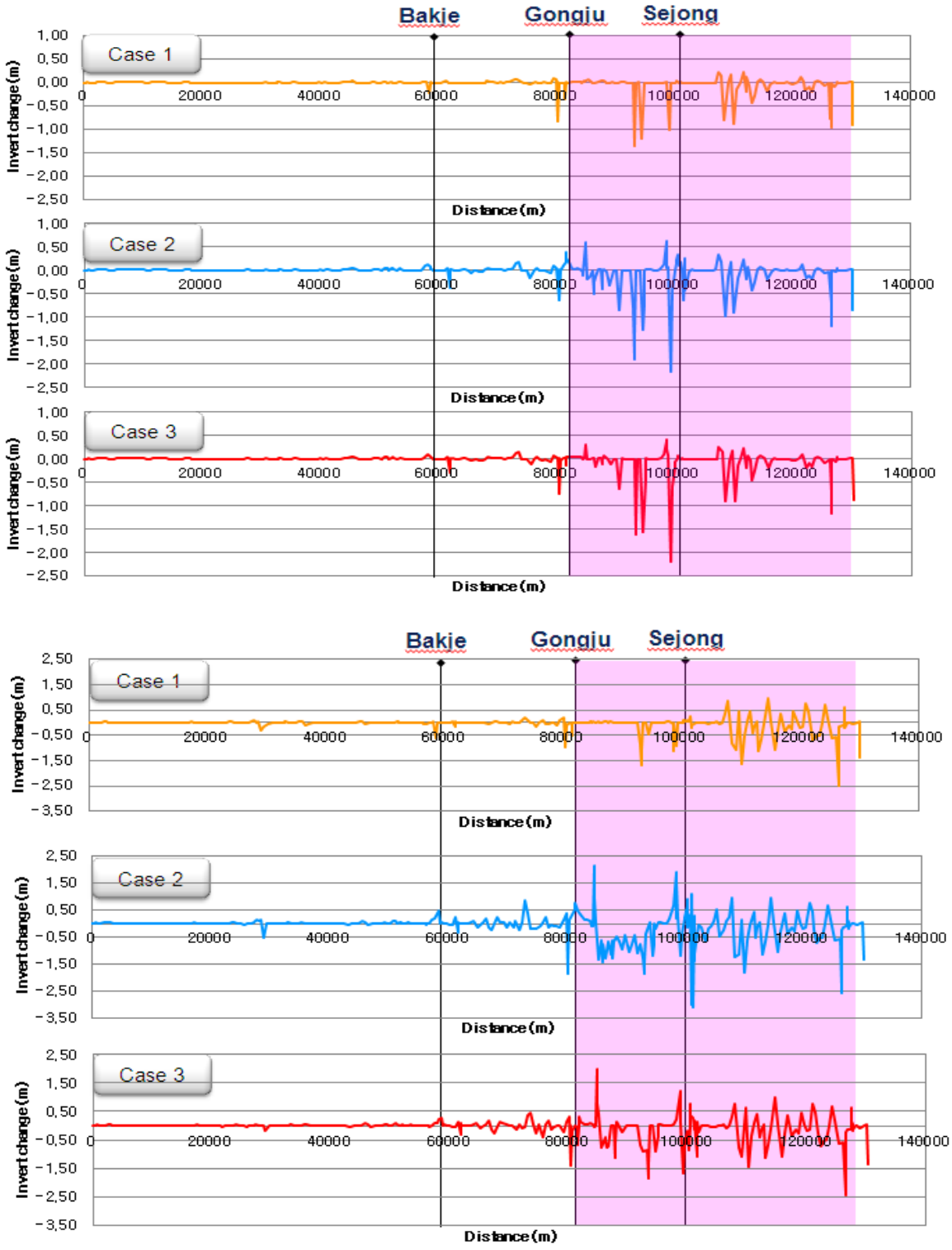

Figure 117. Continued

To examine the magnitude of riverbed change, RMSE was calculated with the original bed elevation and simulated bed elevation. In case of 130 km, the riverbed change of case 2 took place the most and that of case 3 was less than case 2. This result was clearly seen upstream of Sejong weir and Gongju weir, in Figure 118. This explains the gate effect on the riverbed. Also, when comparing with sediment transport equations, the invert change by the Laursen equation, which is based on shear stress, was the largest and that of the Toffaleti equation which has a probabilistic concept of particle movement, was the smallest. Also, the Yang equation, based on unit stream power, the velocity-slope product, and Ackers and White equation, which have a concept of the stream power, the shear stress-velocity product, had middle values, as shown in Figure 119. The calibration of fixed bed was only conducted in Geum River due to much dredging, therefore a proper sediment equation with the calibration of movable bed is needed for predicting riverbed change in the future.

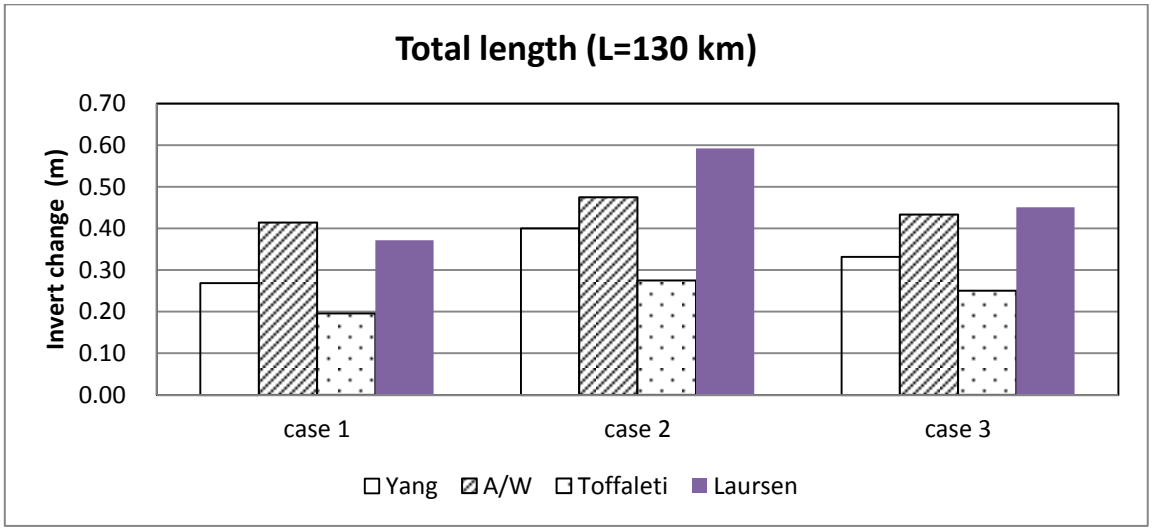

Figure 118. RMSE in Riverbed Change due to Gate Operation

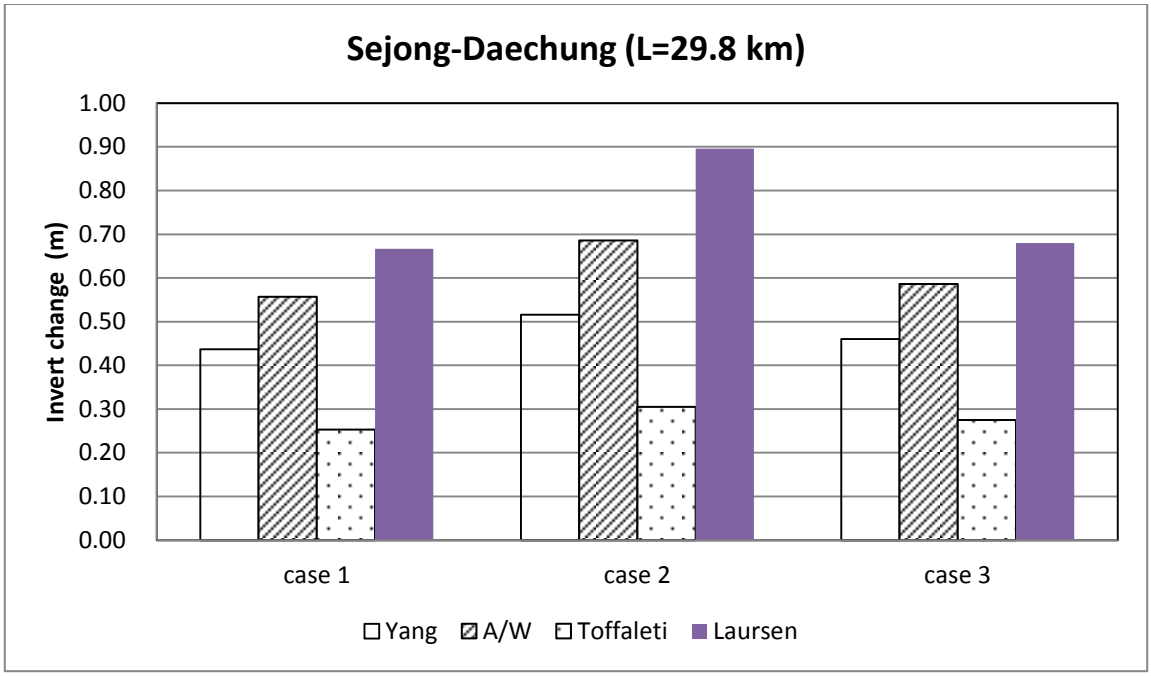

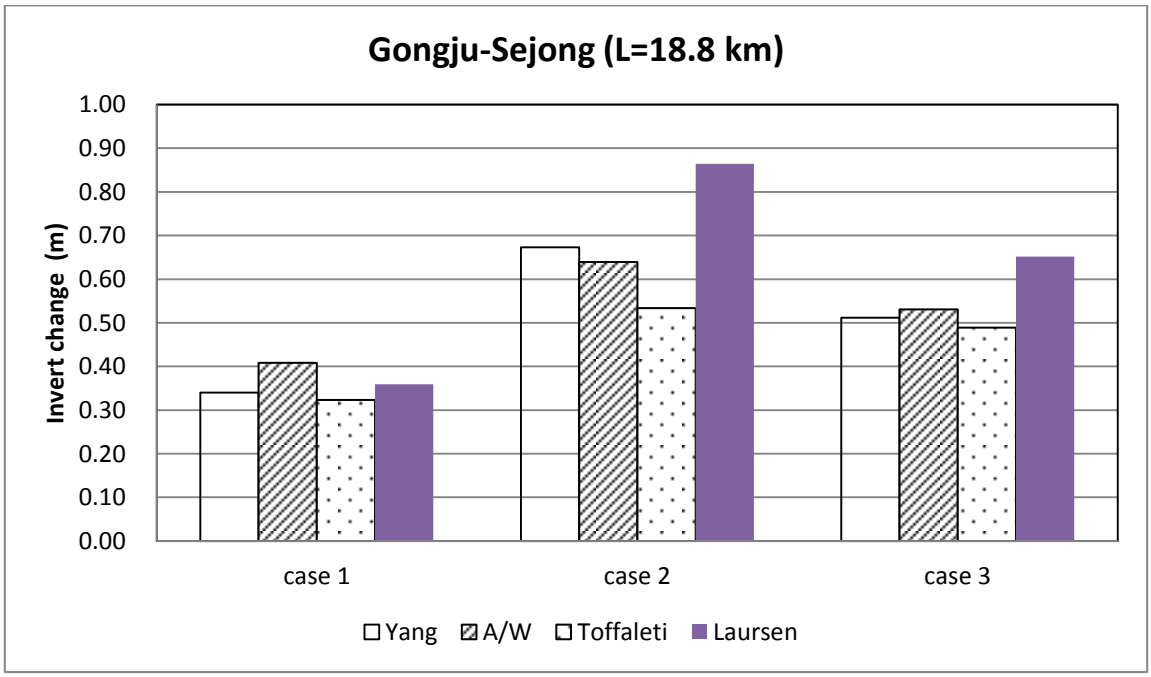

Figure 118. RMSE in Riverbed Change due to Gate Operation

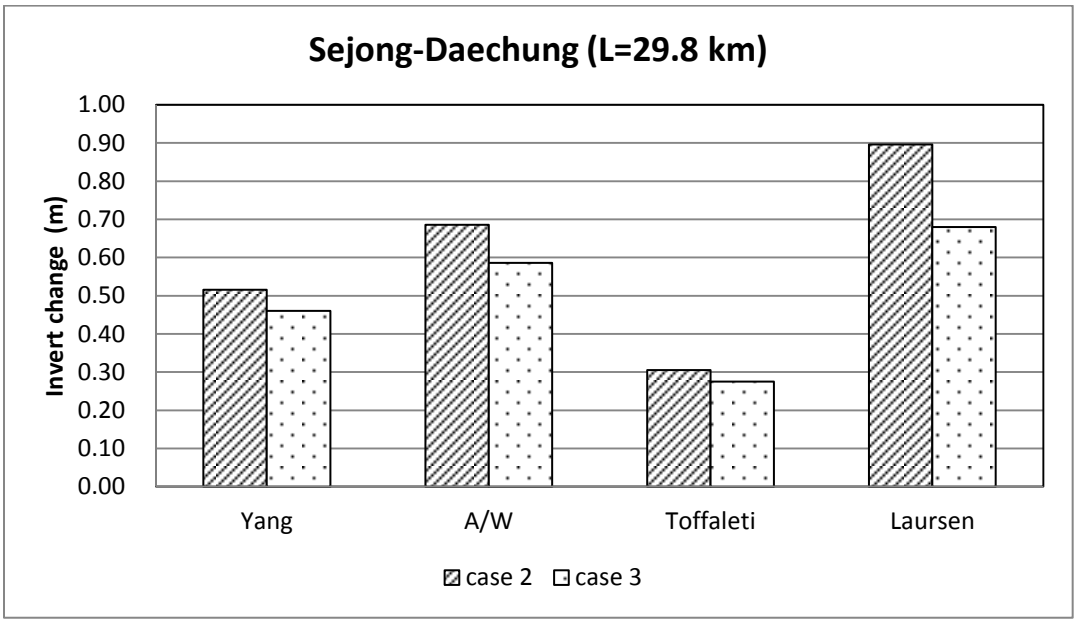

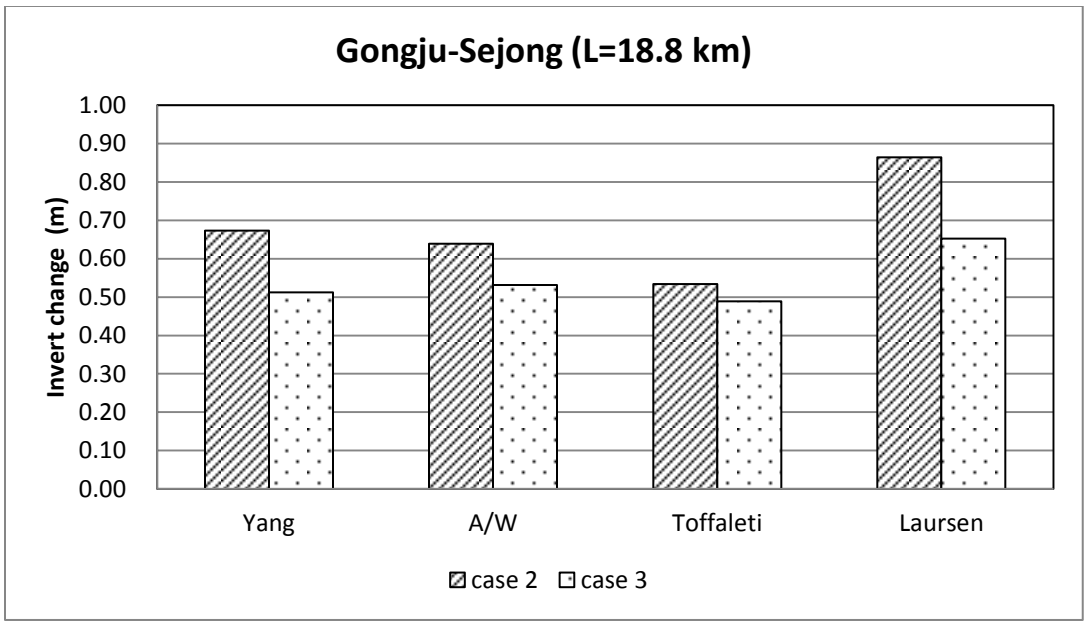

Figure 119. RMSE in Riverbed Change with Sediment Transport Equations

Then, as a result of 1-D results, sediment analysis at Station No 92.85-96.46 (L=3.5 km) downstream of Sejong weir was analyzed using the 2-D model (CCHE2D) for 11 days (9.13-9.23.2007 event). This area was not affected by gate operation and was predicted to be much eroded. First, the adaptation length factor (α) is important, because Geum River is dominated by suspended sediment load. Results of the 2-D model with the adaptation length factor (α) of 0.001 were similar to those of the 1-D model. Of course, they have uncertainty when compared with each other, because 2-D results were calculated from non-equilibrium state and convection-diffusion equation whereas 1-D results were obtained using equilibrium state and continuity sediment equation. Therefore, it is necessary to find proper α through monitoring and observation.

Second, locally bad erosion was predicted on the left side of upstream of the Bulti bridge, therefore the dike was installed to convert erosion to the centerline of river. As a result of dike effect, the velocity increased and the most eroded section was shifted to the left side by about 34 m, as shown in Figures 120. In other words, dike has an advantage in that a certain area can be protected from erosion and also a disadvantage in that hydraulic problem can happen downstream.

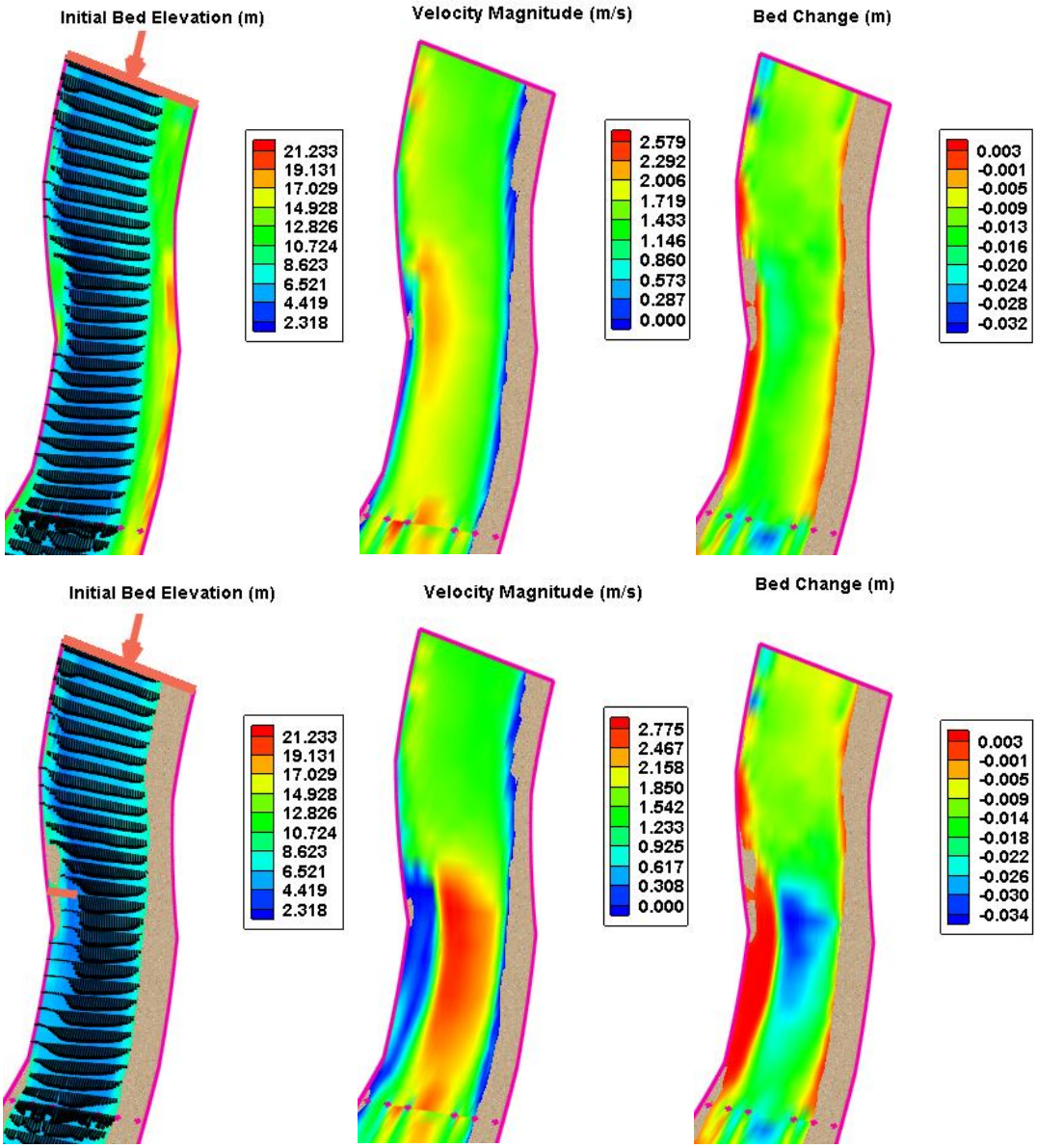

Time=0(d): 0(h): 0(s) Time=4(d): 3(h): 0(s) Time=11(d): 0(h): 0(s)

Figure 120. Hydraulic Characteristics without Dike (up) and with Dike (down)

6.2 Recommendations

To examine the effect of gate operation on the riverbed change, long-term riverbed change was analyzed using planned cross section data by a 1-D model. But compared with echo sounding measuring data, there are some differences between both cross section data sets. Assuming any sediment discharge did not enter downstream from Daechung Regulation Dam and sediment entering from tributary was used as suspended sediment load data measured in 2010. When the 1-D model was simulated, all gates were assumed to move simultaneously, though actually the gates would be operated one by one in turn. Therefore, continuous monitoring and observation are needed to examine the impact of gate on the ecofriendly surroundings.

Long-term riverbed change was simulated by HEC-RAS model. But there are limitations to analyze sediment movement by gate operation, because it assumes the equilibrium state and quasi-unsteady flow, and we cannot distinguish suspended load and bed load from bed material load. To overcome this weakness, CCHE2D model, treating non-equilibrium state under unsteady flow, is meaningful for examining how much abrupt hydraulic characteristics through gate operation affect sediment movement. Therefore, it is desirable to at first conduct the 1-D model (HEC-RAS) in respect to macro scale and then work the 2-D model (CCHE2D) about local scale. In future, the water quality and habitat assessment, according to gate operation, need to be studied for scientific river control.

REFERENCES

ASCE task committee on relations between morphology of small streams and sediment yield of the committee on sedimentation of the hydraulics division (1982), Relationships between morphology of small streams and sediment yields, Hydraulics Division, ASCE, 108(HY11), 1328-1365.

Armanini, A. and Silvio, G. D. (1988), A one-dimensional model for the transport of a sediment mixture in non-equilibrium conditions, Hydraulic Research, 26(3), 275-292.

Bhuiyan, F., Hey, R. and Wormleaton, P. (2007), Hydraulic evaluation of w-weir for river restoration, Hydraulic Engineering, 133 (6), 596-609.

Bilotta, G.S and Brazier, R.E. (2008), Understanding the influence of suspended solids on water quality and aquatic biota, Water Research, 42 (12), 2849-2861.

Duan, J. G. and Nanda, S.K. (2006), Two-dimensional depth-averaged model simulation of suspend sediment concentration distribution in a groyne field, Hydrology, 327 (3-4), 426-437.

Dargahi, B. (2008), Mitigation of sedimentation problems in the lower reach of the River Klarälven, Hydraulic Research, 46(2), 224-236.

Daejeon Regional Construction Management Administration (2009), Geum River management basic plan.

Ding, Y. and Wang. S. (2012), Optimal control of flood water with sediment transport in alluvial channel, Separation and Purification Technology, 84, 85-94.

Ercan, A., Younis, B. A. (2009), Prediction of bank erosion in a reach of the Sacramento River and its mitigation with groynes, Water Resources Management, 23 (15), 3121-3147.

He, Z., Wu, W. and Douglas Shields, F. (2009), Numerical analysis of effects of large wood structures on channel morphology and fish habitat suitability in a Southern US sandy creek, Echohydrology, 2 (3), 370-380.

Hwang, S. B. (2010), Flood analysis in Namhan River using rule operation techniques. M.S., Thesis Dissertation, The Sangi University.

Hummel, R. and Duan, J. G. (2011), Modeling sediment transport in the Pantano Wash, Tucson, World Environmental and Water Resources Congress 2011, 4246-4254.

Jia, Y. and Wang, S. (2001), CCHE2D: two-dimensional hydrodynamic and sediment transport model for unsteady open channel flows over loose bed, Technical Report No. NCCHE-TR-2001-1, National Center for Computational Hydroscience and Engineering, The University of Mississippi.

Jones, J. I., Murphy, J. F., Collins, A.L., Sear, D.A., Naden, P.S. and Armitage P.D. (2012), The Impact of fine sediment on macro-invertebrates, River Research and Applications, 28 (6), 1055-1071, doi: 10.1002/rra. 1516.

Khan, A. A. (2003), CCHE2D-GUI-Graphical user interface for the CCHE2D model user's manual, Technical Report, National Center for Computational Hydroscience and Engineering, The University of Mississippi.

Ministry of Construction & Transportation (2006), Annual hydrological report on Korea, No. 11-1500000-000580-10.

Ministry of Construction & Transportation (2007), Annual hydrological report on Korea, No. 11-1500000-000580-10.

Ministry of Land, Transport and Maritime Affairs (2009), The four major rivers restoration master plan.

Ministry of Land, Transport and Maritime Affairs (2010), Water resources investigation Report, No. 11-1611000-001505-10.

Nicklow, J. and Mays, L. (2000), Optimization of multiple reservoir networks for sedimentation control, Hydraulic Engineering, 126 (4), 232-242.

New Jersey Department of Environmental Protection (2012), Pompton Lake Dam floodgate operations study, Final report.

Papanicolaou, A., Elhakeem, M., Krallis, G., Prakash, S., and Edinger, J. (2008), Sediment transport modeling review – current and future development, Hydraulic Engineering, 134 (1), 1-14.

Pereira, J. F., McCorquodale, J.A., Meselhe, E.A., Georgiou, I.Y., and Allison, M.A. (2009), Numerical simulation of bed material transport in the lower Mississippi River, Coastal Research, Special Issue 56, 1449-1453.

Scott, S. H. and Jia, Y (2006), Simulation of sediment transport and channel morphology change in large river systems, US-CHINA Workshop on advanced computational modeling in hydroscience & engineering, Oxford, Mississippi, USA.

Schwendel, A. C., Death, R. G. and Fuller, I. C. (2010), The assessment of shear stress and bed stability in stream ecology, Freshwater Biology, 55 (2), 261-281.

Sánchez, A., Wu, W. (2011), A non-equilibrium sediment transport model for coastal inlets and navigation channels, Coastal Research, Special Issue No. 59, 39~48.

Tena, A., Książek, L., Vericat, D. and Batalla, R. J. (2012), Assessing the geomorphic effects of a flushing flow in a large regulated river, River Research And Applications, 28, doi: 10.1002/rra.2572.

U.S. Army Corps of Engineers (2010), HEC-RAS river analysis system user's manual ver. 4.1, Hydrologic Engineering Center.

U.S. Army Corps of Engineers (2010), HEC-RAS river analysis system hydraulic reference manual ver.4.1, Hydrologic Engineering Center.

Walker, K. F. and Thoms, M. C. (1993), Environmental effects on flow regulation on the lower River Murray, Australia, Regulated Rivers: Research & Management, 8 (1-2), 103-119.

Wu, W. (2001), CCHE2D sediment transport model, Technical Report No. NCCHE-TR-2001-3, National Center for Computational Hydroscience and Engineering, The University of Mississippi.

Wu, W. (2004), Depth-averaged two-dimensional numerical modeling of unsteady flow and nonuniform sediment transport in open channels, Hydraulic Engineering, 130(10), 1013-1024.

Zhang, Y. (2006), CCHE-GUI-Graphical users interface for NCCHE model user's manual, Technical Report No. NCCHE-TR-2006-02, National Center for Computational Hydroscience and Engineering, The University of Mississippi.

Zhang, Y. and Jia, Y. (2009), CCHE-MESH: 2d structured mesh generator user's manual, Technical Report No. NCCHE-TR-2009-01, National Center for Computational Hydroscience and Engineering, The University of Mississippi.